

**IMPROVING THE COLLECTION AND CALIBRATION OF VOLTAMMETRIC MEASUREMENTS OF  
STRIATAL DOPAMINE RELEASE**

Nathan Thomas Rodeberg

A dissertation submitted to the faculty at the University of North Carolina at Chapel Hill in partial fulfillment  
of the requirements for the degree of Doctor of Philosophy in the Department of Chemistry.

Chapel Hill  
2017

Approved by:

R. Mark Wightman

Matthew R. Lockett

James W. Jorgenson

Regina M. Carelli

Garret D. Stuber

© 2017  
Nathan Thomas Rodeberg  
ALL RIGHTS RESERVED

## ABSTRACT

Nathan Thomas Rodeberg: Improving the Collection and Calibration of Voltammetric Measurements of Striatal Dopamine Release  
(Under the direction of R. Mark Wightman)

Fast-scan cyclic voltammetry (FSCV) enables rapid and sensitive measurements of electroactive neurochemicals in a variety of organisms, including rodents, non-human primates, and most recently, humans. Many FSCV recordings have focused on the role of the neurotransmitter dopamine, which is implicated in a wide host of different behavioral and pathological states. Experiments using FSCV in conscious rodents have corroborated previous electrophysiology studies that demonstrated dopamine plays a key role in learning, reward-seeking behavior, and the actions of drugs of abuse.

The first half of this dissertation concerns studies delving into the role of phasic dopamine release during intracranial self-stimulation (ICSS). In ICSS, subjects are trained to self-administer electrical stimulation of the brain in a manner akin to self-administration of drugs of abuse. Unsurprisingly, given the established role of dopamine in reward-seeking, histological and pharmacological studies have implicated dopamine as a key mediator of this task. However, direct measurements of dopamine release on a timescale relevant to behavior were elusive until the development of FSCV. Early FSCV studies suggested a dissociation between phasic dopamine release and ICSS responding, which stood in stark contrast to evidence from previous reports. Chapter 2 revisits this original finding with the use of more sensitive FSCV measurements and improved calibration methodology, while Chapter 3 extends the study with behavioral and pharmacological manipulations to further probe the relationship between dopamine release and ICSS.

The second half of this dissertation pertains to the recent development of chronically-implanted fused-silica microelectrodes (CFMs) for longitudinal FSCV measurements. While these electrodes permit recordings over unprecedented timescales in single recording locations, experimental and practical limitations have required changes in calibration compared to previously established techniques with acutely-implanted glass CFMs. Chapter 4 investigates the potential pitfalls of one approach to calibration, which uses universal models to analyze collected data. Chapter 5 is a collaborative review written with the developers of these electrodes, which addresses similarities and differences between experiments using acutely- or chronically- implanted CFMs, while Chapter 6 describes further characterization and comparison of these two electrode designs. Altogether, the studies in this dissertation suggest improvements for the collection, interpretation, and calibration of FSCV data.

## ACKNOWLEDGEMENTS

While it takes a village to raise a child, it took a small army to develop me as a scientist. First, I would like to thank my advisor Dr. Mark Wightman for his steadfast support during graduate school. You taught me that strong science can tell compelling stories, and much of my development as a scientist and as a scientific communicator has been through your mentorship. I would also like to acknowledge several people at Concordia College that set me on my current path. Dr. Chopper Krogstad first introduced me to scientific research, and though I'm sure he would hardly call anything I describe in this dissertation as *chemistry*, he was invaluable in setting off the spark that keeps the cogs turning through the day-to-day ups and downs of academic research. Dr. Darin Ulness and Dr. Julie Mach first introduced me to neuroscience and its deep ties to chemistry and, along with Dr. Mark Jensen's teaching of analytical chemistry (which I originally thought would be tremendously boring), I'm not sure where I would be without them.

The work presented in this dissertation is the end product of collaboration with several lab mates and a couple different research groups. Chapter 2 involved collaboration with Dr. Beth Bucher and Justin Johnson. Dr. Michael Sadoris, Dr. Courtney Cameron, and Justin Johnson contributed data and/or data analysis to Chapter 4, which also included important intellectual contributions from Dr. Gina Carelli. Chapter 5 was a highly collaborative work, with major input and guidance from Dr. Paul Phillips and Dr. Stefan Sandberg at the University of Washington – Seattle, in addition to discussion and editing by Justin Johnson. Lastly, Chapter 6 is the culmination of a project originally headed by Dr. Beth Bucher that has received

contributions from several motivated undergraduate students over the years, including Laura Kim, Isaac Studebaker, Nathaniel Swofford, Marc Gonzalez, Devon Martin, and Aki Min.

Lastly, I would like to give personal thanks to several people who have made graduate school as bearable as possible. Dr. Beth Bucher taught me nearly everything I know about voltammetry and *in vivo* experiments, and was one of the earliest and strongest driving forces behind me feeling at home in my new environment at UNC. Now that I'm older than you were when I started, I mildly regret all of my jokes about your advanced age. Dr. Nina Owesson-White helped me keep my sanity during freely-moving experiments, and her unexpected gifts of sour patch kids fueled many needed revitalizations. Several close friends in my department, including Robert Soto, Mac Gilliland, and (now labmate) Caddy Hobbs helped me get through the first year(s) of course work, both in and outside of the classroom. Justin Johnson, my electronics TA turned good lab mate and friend, was a great collaborator and sounding board, even when my questions only became slightly less obnoxious after electronics had ended. The 'Rodeberg-Johnson' series certainly got much further than I thought it would.

Outside of the lab, I was lucky to have a great support system, spearheaded by my loving parents and family. Thank you for unconditionally supporting me throughout my education, as well as reading and passing along my work even when it must have sounded like complete gibberish. I was fortunate to move to Chapel Hill with a familiar face, my long time buddy and (former) roommate Taylor. Thank you for all of the memories formed in Chapel Hill (and elsewhere), and making graduate school much less bleak than it could have been. And last, but not at all least, I would like to acknowledge my soon-to-be-wife Deirdre. I am incredibly lucky you swapped seats at TRU, and I look forward to sharing a long life and career in science with you.

## TABLE OF CONTENTS

LIST OF TABLES.....	xii
LIST OF FIGURES .....	xiii
LIST OF ABBREVIATIONS AND SYMBOLS .....	xv
CHAPTER 1: FAST-SCAN CYCLIC VOLTAMMOMETRY FOR THE MONITORING OF ELECTROACTIVE NEUROCHEMICALS .....	1
Introduction .....	1
Fast-scan cyclic voltammetry: the basics.....	3
Electrochemical measurements.....	3
Carbon-based microelectrodes.....	5
Analytical merits of fast-scan cyclic voltammetry .....	7
Sensitivity .....	7
Temporal resolution.....	13
Chemical selectivity & resolution .....	14
Accuracy .....	19
Conclusions & future directions .....	23
References.....	24
CHAPTER 2: DOPAMINE DYNAMICS DURING CONTINUOUS INTRACRANIAL SELF-STIMULATION: EFFECT OF WAVEFORM ON FSCV DATA.....	34
Introduction .....	34
Experimental .....	36
Animals .....	36
Surgery.....	37
Behavior .....	37

FSCV.....	38
Data analysis.....	39
Statistical analysis .....	40
Flow Cell analysis.....	40
Results .....	41
Anodic limit and stimulated release in anesthetized animals.....	41
Phasic dopamine concentrations during continuous ICSS .....	45
Sensitivity determines ability to consistently monitor dopamine .....	50
Effect of biofouling on continuous measurements.....	52
Temporal resolution determines ability to reliably quantitate rapidly spaced transients.....	53
Balance of temporal resolution and sensitivity determine ability to monitor dopamine dynamics.....	57
Discussion.....	60
References.....	64
<b>CHAPTER 3: DEPLETION OF RELEASABLE DOPAMINE DRIVES DISSOCIATION BETWEEN PHASIC DOPAMINE RELEASE AND CONTINUOUS ICSS.....</b>	<b>68</b>
Introduction .....	68
Experimental .....	71
Animals .....	71
Surgery.....	71
Behavior .....	72
FSCV recordings .....	73
Drug administration .....	74
Data analysis.....	74
Statistics.....	75
Results .....	76
Yoked ICSS.....	76
Fixed-interval ICSS.....	78

Cocaine and amphetamine administration.....	82
Correlation of behavior and dopamine levels.....	88
Discussion.....	91
References.....	96
CHAPTER 4: CONSTRUCTION OF TRAINING SETS FOR VALID CALIBRATION OF <i>IN VIVO</i> FSCV DATA BY PRINCIPAL COMPONENT ANALYSIS.....	100
Introduction .....	100
Experimental .....	102
Animals .....	102
Surgery.....	103
Behavior .....	103
ICSS.....	104
FSCV.....	105
Data analysis.....	105
Results & discussion .....	107
FSCV measurements during behavior consist of multiple physiologically relevant components .....	107
Training sets from natural rewards .....	109
PCR and training sets from separate electrodes.....	112
Residual analysis .....	118
Standard training sets constructed from multiple electrodes.....	121
Conclusions .....	125
References.....	128
CHAPTER 5: HITCHHIKER'S GUIDE TO VOLTAMMETRY: ACUTE AND CHRONIC ELECTRODES FOR <i>IN VIVO</i> FAST-SCAN CYCLIC VOLTAMMETRY.....	131
Techniques for monitoring molecules in neuroscience .....	131
Development of FSCV for freely-moving animals .....	133
Experimental considerations .....	135
Electrode materials and design .....	135

Experimental design for FSCV recordings in freely-moving animals .....	138
<i>In vivo</i> electrode positioning .....	139
Reference electrodes .....	143
Signal stability .....	143
Chemometric data analysis .....	147
Principal Component Regression .....	148
Additional diagnostics to test the quality of training sets .....	155
PCR with residual analysis in practice .....	156
Conclusions and perspectives .....	162
References.....	165
<b>CHAPTER 6: CHARACTERIZATION OF FUSED-SILICA ELECTRODES FOR LONGITUDINAL MEASUREMENTS OF STRIATAL DOPAMINE RELEASE .....</b>	<b>177</b>
Introduction .....	177
Experimental .....	180
Animals .....	180
Electrode Construction .....	180
FSCV.....	182
Flow-Cell Analysis .....	182
Surgery.....	183
<i>In vivo</i> recordings .....	184
Data analysis.....	185
Statistics.....	186
Results .....	186
<i>In vitro</i> comparison of electrode designs.....	186
Acute <i>in vivo</i> comparison of electrode designs .....	191
Effect of prolonged use of carbon-fibers on electrode sensitivity.....	194
Failure of electrical stimulation to track potential sensitivity changes <i>in vivo</i> .....	197
Alternate methods for tracking sensitivity of chronically implanted CFMs .....	200

Changes in background current following long-term implantation .....	202
Discussion.....	205
References.....	209

## LIST OF TABLES

Table 2.1. Comparisons of $[DA]_{\max}$ , rise time, and $t_{1/2}$ between different waveforms.....	42
Table 2.2. The post-implantation sensitivity for different implantation durations .....	54
Table 2.3. The total number (and percentage) of transients that were quantifiable across waveforms .....	59
Table 3.1. Comparison of dopamine profiles during dual session ICSS on FR1 and FI5 paradigms.....	81
Table 4.1. Characteristics of dopamine K-matrices for various subjects for two different training set construction methods .....	111
Table 4.2. Training sets built in different subjects predict different peak dopamine concentrations than training sets built within subject .....	116
Table 4.3. Key parameters from the K-matrices for dopamine and pH changes.....	117
Table 4.4. The number of transients that failed residual analysis during various training set misapplications .....	120
Table 6.1. The sensitivity, noise levels, and temporal response over repeated cycling of FS CFMs.....	196
Table 6.2. The background amplitudes at chronically-implanted CFMs before and after long-term implantation.....	203
Table 6.3. Changes in background amplitude over repeated cycling of FS CFMs <i>in vitro</i> .....	204

## LIST OF FIGURES

Figure 1.1. Background subtraction with fast-scan cyclic voltammetry. ....	4
Figure 1.2. Diagram of carbon paste and carbon fiber microelectrodes.....	6
Figure 1.3. Electrode modifications for FSCV measurements .....	11
Figure 1.4. Principal component regression to remove influence of pH from dopamine concentration predictions.....	16
Figure 2.1. Differences in cyclic voltammogram characteristics across waveforms .....	44
Figure 2.2. Depiction of ICSS data analysis .....	46
Figure 2.3. The amplitude of individual dopamine transients during and across ICSS sessions with different waveforms.....	48
Figure 2.4. Dopamine concentration versus time traces for representative measurements on each waveform before, during, and after the first intracranial self- stimulation session.....	51
Figure 2.5. Temporal resolution is diminished with extended anodic limits .....	56
Figure 2.6. Temporal resolution and its dependence on pressing rate differ across waveforms .....	58
Figure 3.1. Electrically-evoked dopamine release during yoked-ICSS (FR1) stimulation pattern.....	77
Figure 3.2. Fixed-interval 5 (FI5) paradigm for ICSS. ....	79
Figure 3.3. Comparison of the decline in electrically-evoked dopamine release between FR1 and FI5 ICSS .....	80
Figure 3.4. The effects of cocaine and amphetamine on electrically-evoked dopamine release. ....	84
Figure 3.5. The effect of cocaine and amphetamine on dopamine release during FI5 ICSS. ....	86
Figure 3.6. Phasic dopamine release patterns during drug-treated FI5 ICSS.....	87
Figure 3.7. Comparison of response rates and dopamine concentrations between and across treatments.....	89
Figure 4.1. pH changes depend on reinforcer identity and order .....	108
Figure 4.2. Training set construction with naturally evoked transients .....	110
Figure 4.3. The use of principal component analysis to predict analyte concentrations.....	113

Figure 4.4. Training sets built in different subjects predict different dopamine transient concentrations .....	115
Figure 4.5. Residual analysis with different training sets .....	119
Figure 4.6. K-Matrices from composite training sets built with standards collected at different carbon-fiber microelectrodes .....	122
Figure 4.7. Parameters of interest for composite generalized training sets.....	123
Figure 4.8. K-matrices for composite training sets constrained to two principal components .....	124
Figure 5.1. The designs of borosilicate glass and fused silica CFMs.....	137
Figure 5.2. Comparison of concentrations measured at acute and chronic CFMs without optimization for dopamine release sites .....	141
Figure 5.3. Dopamine transients at chronically implanted CFMs .....	142
Figure 5.4. An example of the use of principal component analysis to analyze cocaine-induced dopamine transients .....	149
Figure 5.5. Training sets built with data from separate electrodes could capture qualitative information .....	160
Figure 6.1. Environmental scanning electron micrographs of fused-silica and borosilicate glass carbon-fiber microelectrodes.....	187
Figure 6.2. <i>In vitro</i> characterization of FS and BSG electrodes .....	189
Figure 6.3. Acute <i>in vivo</i> comparison of BSG and FS electrodes .....	193
Figure 6.4. The effect of prolonged cycling of CFMs on sensitivity towards dopamine .....	195
Figure 6.5. Temporal distortion in the electrically-evoked dopamine signal at chronically-implanted CFMs .....	199
Figure 6.6. The amplitude and frequency of drug-evoked dopamine transients before and after CFM implantation .....	201

## LIST OF ABBREVIATIONS AND SYMBOLS

*	probability less than 0.05
**	probability less than 0.01
***	probability less than 0.001
[X]	concentration of analyte X
[DA] <sub>max</sub>	peak concentration of dopamine transients
°C	degrees Celsius
α	confidence interval
AA	ascorbic acid
Ag/AgCl	silver/silver chloride
AMPA	α-amino-3-hydroxy-5-methyl-4-isoxazolepropionic acid
AP	anterior-posterior
ATP	adenosine triphosphate
BSG	borosilicate glass
CaCl <sub>2</sub>	calcium chloride
CFM	carbon-fiber microelectrode
CNT	carbon nanotube
CS	conditioned stimuli
CV	cyclic voltammogram
DA	dopamine
dB	decibels
DOQ	dopamine-ortho-quinone
DV	dorsal-ventral
E <sub>app</sub>	applied potential
E <sub>x</sub>	potential at which peak current occurs for denoted species x

ECP	electrochemical pretreatment
ET	electron-transfer
FI5	fixed-interval 5
FR1	fixed-ratio 1
FS	fused silica
FSCV	fast-scan cyclic voltammetry
g	grams
HCl	hydrochloric acid
H <sub>2</sub> O <sub>2</sub>	hydrogen peroxide
HDCV	High-Definition Cyclic Voltammetry
hr	hours
Hz	Hertz
i.p.	intraperitoneal injection
IACUC	Institutional Animal Care and Use Committee
ICSS	intracranial self-stimulation
$i_{p,a}$	peak anodic current
$i_{p,c}$	peak cathodic current
KCl	potassium chloride
kg	kilograms
KHz	kilohertz
L	liters
LOD	limit of detection
$\mu$ A	microamperes
$\mu$ m	micrometer
$\mu$ M	micromolar

$\mu\text{s}$	microseconds
mA	milliamperes
M-ENK	met-enkephalin
MFB	medial forebrain bundle
mg	milligrams
$\text{MgCl}_2$	magnesium chloride
min	minutes
ML	medial-lateral
mL	milliliters
mm	millimeters
mM	millimolar
ms	milliseconds
MSN	medium spiny neuron
mV	millivolts
n	number of samples
$\text{N}_2$	molecular nitrogen
nA	nanoamperes
$\text{Na}_2\text{SO}_4$	sodium sulfate
NAc	nucleus accumbens
NaCl	sodium chloride
$\text{NaH}_2\text{PO}_4$	monobasic sodium phosphate
NaOH	sodium hydroxide
nm	nanometer
nM	nanomolar
NR	no reward
$\text{O}_2$	molecular oxygen

$p$	probability
PC	principal component
PCA	principal component analysis
PCR	principal component regression
PEDOT	polyethylenedioxythiophene
$Q_\alpha$	residual threshold at significance interval $\alpha$
$Q_t$	sum of the squares residual at time $t$
$r^2$	coefficient of determination
RMS	root mean square
$\sigma$	standard deviation
s	second
SEM	standard error of the mean
SN	substantia nigra
$t$	time
$t_{1/2}$	decay time from 100-50% max value
TRIS	tris(hydroxymethyl)aminomethane
UEI	universal electrochemical instrument
UNC	University of North Carolina at Chapel Hill
V	volts
VTA	ventral tegmental area

## **CHAPTER 1: FAST-SCAN CYCLIC VOLTAMMETRY FOR THE MONITORING OF ELECTROACTIVE NEUROCHEMICALS**

### **INTRODUCTION**

The existence of chemical signaling between nerves was first proposed by Otto Loewi following experiments in beating heart muscle of anesthetized frogs (Loewi, 1921). Later investigation, largely by Henry Dale and colleagues, validated this theory for much of the peripheral nervous system (Dale et al., 1936). However, this hypothesis emerged amid controversy, as it was at odds with the prevailing theory that signal transduction occurred solely via electrical impulses across gap junctions between cells. As such, it took decades of experiments and debates between neurophysiologists and pharmacologists before chemical transmission was accepted as standard for communication within both the peripheral and central nervous system (Valenstein, 2002).

While much information regarding neurotransmission has been elucidated since these original discoveries, chemical signaling within the brain still appears to be extremely complex. In addition to the large number of molecules that have been proposed to act as neurotransmitters or neuromodulators, it is common for each species to act at a wide host of receptors that can differ both in their substrate affinities and downstream consequences following activation (Beaulieu & Gainetdinov, 2011; Monaghan et al., 1989; Waldhoer et al., 2004). Moreover, neurotransmitters can exert different effects by signaling at different time scales. For example, dopamine neurons have been shown to exhibit two patterns of cellular activity: “tonic firing”, which is characterized by slow, rhythmic firing, and “phasic firing”, which consists of irregular, high frequency bursts (Schultz, 1998). The former is thought to produce low ambient concentrations of dopamine, while the latter produces high concentration release events,

termed 'transients', that can temporarily activate high affinity receptors. These two modes of transmission have been demonstrated to carry different neurobiological and behavioral signals (Floresco et al., 2003; Grace, 1991; Schultz, 1998). Therefore, development of techniques that can accurately monitor these molecules for physiologically relevant concentrations and time scales is an important endeavor. Moreover, these techniques should be compatible with experiments in conscious subjects so that relationships between neurotransmitter signaling and behavior can be revealed.

While there have been several techniques used to measure neurochemicals in real time (Bucher & Wightman, 2015; Robinson et al., 2008), there are two main methods used today. The most established procedure is microdialysis, which utilizes a probe enclosed in a permeable membrane that interfaces with the surrounding brain tissue. Any molecule that can diffuse across this membrane, in accordance to its concentration gradient with respect to the dialysate, can be collected for downstream analysis. Thus, the sensitivity and selectivity of this technique are predominately determined by the detection method employed (Kennedy, 2013). However, the time needed for adequate equilibrium of analytes across the membrane, as well as the minimum sample volume needed for detection, limit its temporal resolution to the order of tens of seconds to minutes.

The focus of this chapter will be on an alternative technique, fast-scan cyclic voltammetry (FSCV), which uses an applied potential at an electrode to oxidize and reduce analytes of interest. Though limited to electroactive molecules, the high temporal resolution of FSCV permits measurements of rapid release events on a behaviorally relevant time scale. The development, analytical merits, and limitations of FSCV will be discussed.

## FAST-SCAN CYCLIC VOLTAMMETRY: THE BASICS

### Electrochemical measurements

The first electrochemical techniques for monitoring neurochemicals in brain tissue included linear sweep voltammetry (Kissinger et al., 1973; Wightman et al., 1976), differential pulse voltammetry (Ewing et al., 1983; Gonon et al., 1980), and chronoamperometry (Ewing, et al., 1983; Gerhardt et al., 1984). While these techniques were sufficient to detect faradaic currents corresponding to electroactive molecules *in vivo*, they were seldom able to see through the 'mud' to detect their neurotransmitters of interest due to the comparatively large ambient concentrations of other easily oxidized species in the brain, such as ascorbic acid (AA) and neurotransmitter metabolites (Parsons & Justice, 1992). Indeed, it has been demonstrated that the electrochemical signal arising from slow voltage sweeps in brain tissue is dominated by AA (Ewing et al., 1981). Moreover, these techniques lacked adequate sensitivity to measure smaller, but physiologically relevant, neurotransmitter concentrations.

A significant step forward came with the development of FSCV, in which potentials are swept at high scan rates (>100 V/s) in triangular ramps to oxidize and reduce electroactive analytes within a given potential window (Armstrong-James et al., 1980; Millar et al., 1985; Stamford et al., 1984). High scan rates have two primary benefits. First, this process increases the redox current, which enables higher sensitivity (Bard & Faulkner, 2001). Second, this allows each sweep to be completed on the order of milliseconds, which permits sub-second measurements of neurotransmitter release. These advances enabled the first chemically-resolved, real-time measurements of electrically-evoked dopamine transients (Kuhr & Wightman, 1986; Stamford et al., 1986).

Traditional electrochemists avoid rapid scan rates for a good reason; non-faradaic current arising from charging of the double layer scales proportionally with scan rate, and easily dwarfs out the analytical signal. As a result, rapid voltage sweeps in the brain do not produce cyclic voltammograms (CVs) that resemble any particular analyte (Figure 1.1a). However, if this

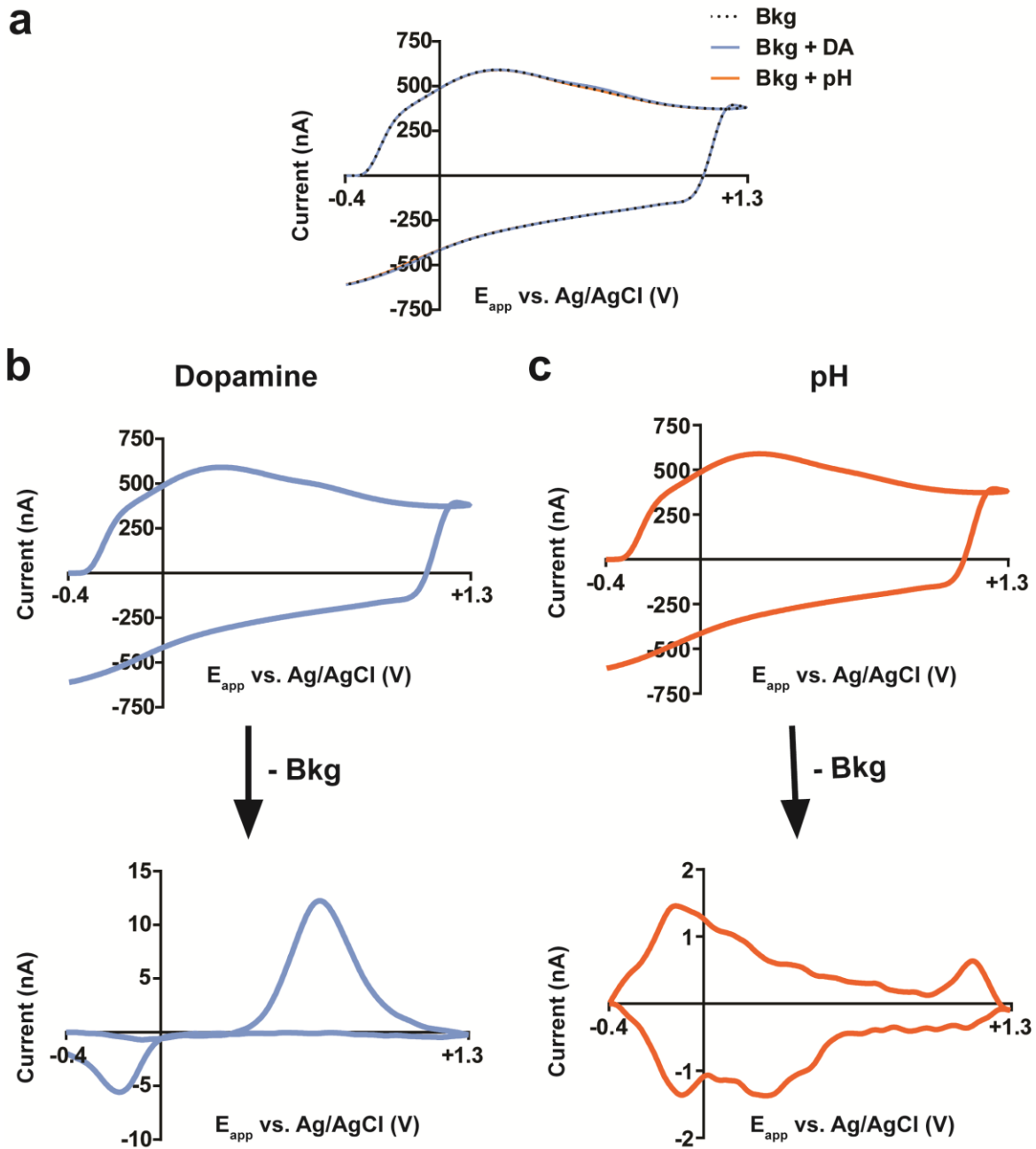


**Figure 1.1.** Background subtraction with fast-scan cyclic voltammetry. a) Rapid potential sweeps (400 V/s) in brain tissue produce large background currents (black dotted line) that result from charging of the double layer and redox of electroactive groups on the electrode surface and in the surrounding environment. Superimposition of CVs for analytes of interest (dopamine, blue, and pH changes, orange) does not appreciably alter the background current. However, if the background current is relatively stable over the recording window, it can be digitally subtracted from experimentally relevant CVs to produce analyte-specific CVs for dopamine (b) and pH changes (c).

background signal is relatively stable over the course of the measurement window, background CVs preceding the 'event' of interest can be digitally subtracted out, with any remaining signal reflecting changes in the surrounding environment (e.g. release of neurotransmitters, pH changes) (Howell et al., 1986; Millar, et al., 1985) (Figure 1.1b-c). Unfortunately, this renders FSCV a differential technique that is unsuitable for measurements of ambient levels of neurochemicals in the brain.

### **Carbon-based microelectrodes**

A technique can be only as good as its tools. The development of *in vivo* electrochemistry was made possible by the simultaneous development of microelectrodes, which were so small compared to their macroelectrode predecessors that detailed characterization was necessary (Cheng et al., 1979). This characterization revealed that these miniature probes have a number of electrochemical advantages. First, their small dimensions enhance mass transfer to electrode surface via radial diffusion, which allows steady-state measurements at sufficiently slow scan rates (Wightman, 1981). Second, the low area, and thus capacitance, of these electrodes allows them to respond rapidly to changes in potential; scan rates up to  $10^6$  V/s have been used, with the fastest speeds ultimately determined by the bandwidth of instrumentation (Amatore et al., 1987; Wipf & Wightman, 1988). Third, microelectrodes generate sufficiently small currents that any distortion that arises from ohmic drop is minimal, which enables measurements in resistive media (Howell & Wightman, 1984). Fourth, these small currents introduce minimal polarization of the reference electrode, which supports the use of two electrode designs (Fitch & Evans, 1986). Last, these small currents reduce concern with toxicity of electrogenerated products *in vivo*, particularly with the use of cyclic voltammetry (Wightman, 1981).

While several different electrode materials have been used to construct microelectrodes, carbon in particular has a number of advantages (McCreery, 2008). Compared to metal

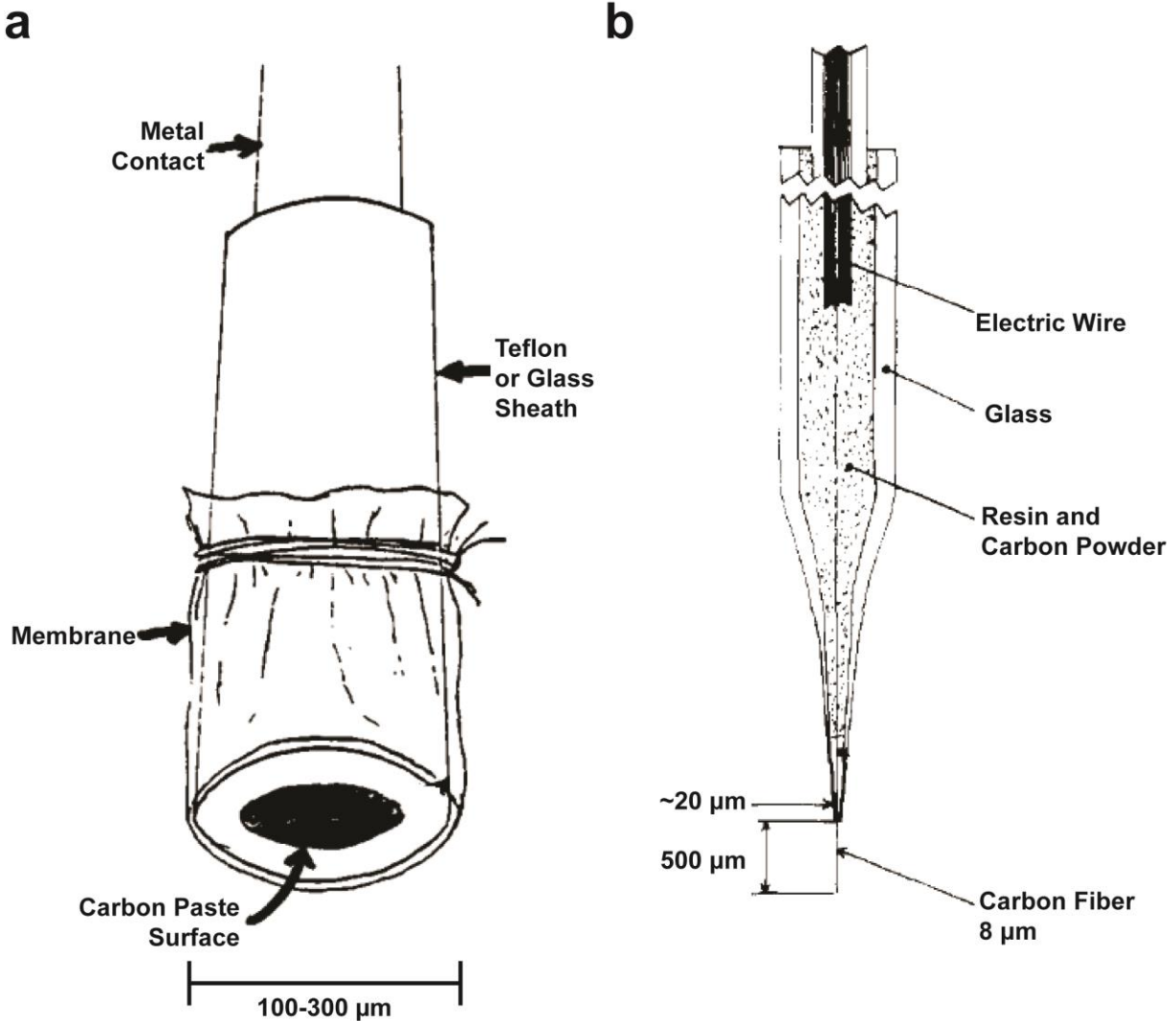


**Figure 1.2.** Diagram of carbon paste and carbon fiber microelectrodes. a) Schematic for a carbon paste microelectrode. Glass or Teflon capillaries are filled with graphite-Nujol-epoxy mixtures and allowed to harden. The outer diameter of the electrode is determined by the size of the sheath (typically 100-300 μm). Figure was adapted from (Nagy et al., 1982). b) Schematic for a carbon fiber microelectrode. The sensing element of the electrode (the carbon fiber) is much smaller in diameter than carbon paste electrodes. The taper in the insulating glass capillary allows its diameter to remain small above the electrode surface, which minimizes tissue damage. Electrical contact is established here through resin and carbon powder, which has largely been replaced with the use of conductive silver paint or electrolyte solution for modern experiments. Figure was adapted from (Ponchon et al., 1979).

substrates, such as gold, carbon has a wider potential window and exhibits less biofouling, though it displays slower electron-transfer (ET) kinetics (Zachek et al., 2008). Carbon microelectrodes are also inexpensive and easy to fabricate, and are amenable to a wide number of surface modifications for tunable electrochemistry. The first types of microelectrodes used *in vivo* were constructed with carbon paste and were 100 to 300  $\mu\text{m}$  in diameter (Figure 1.2a) (Cheng, et al., 1979; Conti et al., 1978; Kissinger, et al., 1973). While these probes were much smaller than standard macroelectrodes, they did not provide advantages over microdialysis in either spatial resolution or avoidance of tissue damage. An attractive alternative emerged with the development of carbon-fiber microelectrodes (CFMs) (Figure 1.2b) (Armstrong-James & Millar, 1979; Gonon et al., 1978). These probes vary from 5 to 15  $\mu\text{m}$  in diameter, and are therefore capable of making highly localized measurements in the brain. For example, spacing between dopamine terminals in the striatum has been estimated to be around  $\sim 1 \mu\text{m}$  (Wightman, 1981), which allows these sensors to sample heterogeneity in this brain region (Wightman et al., 2007; Wightman et al., 1988). Moreover, it has shown that acute implantation of these sensors does not significantly damage the surrounding tissue (Peters et al., 2004), especially compared to microdialysis probes (Jaquins-Gerstl & Michael, 2009).

## **ANALYTICAL MERITS OF FAST-SCAN CYCLIC VOLTAMMETRY**

### **Sensitivity**

An important aim for *in vivo* measurements is the ability to monitor physiologically relevant concentrations of neurotransmitters. Strategies for enhancing sensitivity for FSCV at CFMs generally fall into three camps: waveform modifications, electrode pre-treatment and electrode coatings. While the focus of this section will be on promoting sensitivity towards dopamine, the most commonly measured analyte with FSCV, many of the same principles in theory could be extended to similar neurochemicals.

### *Waveform Modification*

The first waveforms used for *in vivo* FSCV had potential limits of  $\pm 700$ - $1000$  mV and holding potentials of  $0$  V, with 1.5 cycles of each potential sweep carried out at  $300$  V/s (Armstrong-James, et al., 1980; Millar, et al., 1985). While this waveform was sufficient to detect dopamine concentrations approaching  $10^{-6}$  M, prolonged electrical stimulation ( $10$  s) was required to evoke measurable concentrations *in vivo* (Millar, et al., 1985). Therefore, improvements in sensitivity were essential to make measurements under more physiological conditions.

Waveform modifications to enhance sensitivity towards dopamine rely on the fact that dopamine adsorbs to the electrode surface (Bath et al., 2000; Baur et al., 1988). Adsorption of dopamine appears to be necessary for both reliable detection (Bath et al., 2001; DuVall & McCreery, 1999) and fast ET kinetics (DuVall & McCreery, 2000). The amine side chain, which is protonated at physiological pH, appears to be critically important for adsorption (Baur, et al., 1988; Michael & Justice, 1987). Consequently, holding at negative potentials between scans promotes electrostatic attraction of dopamine to the electrode surface. This introduces a dependency of sensitivity on the waveform application frequency, as higher repetition rates provide less time for dopamine to accumulate at the surface between measurements (Bath, et al., 2000; Kile et al., 2012). While the use of a negative holding potential is a simple and widely used approach, it has limitations; holding potentials lower than  $-600$  mV can result in unstable results (Heien et al., 2003), and negative holding potentials may promote the generation of hydrogen peroxide (Dengler et al., 2015), which could have deleterious effects in brain tissue. Modification of the anodic limit of the waveform, specifically its extension to more positive potentials, can also increase sensitivity towards dopamine (Hafizi et al., 1990; Heien, et al., 2003; Rodeberg et al., 2016). This process generates surface oxide groups on the carbon surface (Roberts et al., 2010) that are critically important for adsorption of dopamine (Bath, et al., 2001). Furthermore, this process continually regenerates the electrode surface, which allows

enhanced sensitivity to be maintained over the course of measurements (Takmakov et al., 2010b). Routine measurements using negative holding potentials and extended anodic limits at untreated CFMs have an *in vivo* limit of detection around 20 nM (Heien, et al., 2003; Rodeberg, et al., 2016).

The current for adsorbing species, including dopamine, is directly proportional to the scan rate (Bard & Faulkner, 2001; Bath, et al., 2000). Therefore, increasing the scan rate is another viable tactic for increasing sensitivity. Scan rates in excess of 2,000 V/s have been used for measurements of dopamine, with a corresponding *in vitro* limit of detection around 1 nM (Keithley et al., 2011). The use of large scan rates also amplifies non-faradaic current, as well as current arising from redox of surface moieties on the CFM surface. While these contributions can be removed digitally through background subtraction, sufficiently high scan rates can generate background currents that saturate the digital-to-analog converter. In these cases, analog background subtraction can be used to eliminate its contribution (Hermans et al., 2008; Keithley, et al., 2011).

### *Electrode pre-treatment*

Pre-treatment of the electrode surface generally serves three goals: increasing surface oxide content (Alsmeyer & McCreery, 1991), cleaning the electrode surface (Bath, et al., 2000), and/or enhancing the edge/basal plane ratio (Wightman et al., 1984), as edge planes have been demonstrated to be the most reactive sites for electron transfer on carbon surfaces (Banks et al., 2005). The first widespread approach for CFMs was electrochemical pre-treatment (ECP) (Feng et al., 1987; Gonon et al., 1981), which facilitates adsorption and 'cracks' the electrode surface, increasing the effective surface area for electron transfer (Kovach et al., 1986; Swain & Kuwana, 1991). Though ECP enhances sensitivity, it has a limited lifespan *in vivo* and can induce temporal distortion during measurements (Feng, et al., 1987; Marcenac & Gonon, 1985). An alternative treatment to ECP is flame etching, which decreases the surface area of CFMs

while simultaneously increasing the sensitivity per unit area (Strand & Venton, 2008). In contrast to ECP, the temporal response at these electrodes appears faster compared to untreated carbon fibers. Flame-etched CFMs have an *in vivo* limit of detection around 10 nM, and are sufficient to detect dopamine release following single pulse electrical stimulation. However, it is unknown whether flame etching suffers from the same short lifespan *in vivo* as ECP. Another, more simple approach is soaking the CFM in isopropyl alcohol spiked with activated carbon (Bath, et al., 2000). This likely serves the dual purpose of cleaning the surface and facilitating the formation of surface oxides. This treatment increases sensitivity approximately four fold at cylindrical CFMs for measurements with a modest (+1.0 V) anodic limit. However, it is unclear whether these significant advantages hold with extended waveforms that naturally renew the electrode surface and generate oxygen-containing functional groups.

### *Electrode coatings*

The development of electrode coatings for microelectrodes has often been tackled with the primary goal of enhancing electrode selectivity towards particular analytes (see **Chemical Selectivity & Resolution** section below). However, these coatings often provide the added benefit of enhanced sensitivity due to preconcentration of analytes at the electrode surface. The first common electrode coating for *in vivo* electrochemistry was the perfluorinated polymer Nafion (Gerhardt, et al., 1984; Kristensen et al., 1987). The negative charge within the Nafion structure promotes accumulation of cationic species, such as dopamine, resulting in a roughly two to five fold enhancement of sensitivity (Gerhardt, et al., 1984). However, this increase in sensitivity comes at the expense of temporal resolution, as Nafion coatings can cause noticeable distortion of the FSCV signal (Kristensen, et al., 1987). Nafion can be either dip-coated or electrodeposited on the electrode surface, though the latter approach is preferred for carbon fibers due to reproducibility concerns with the former (Brazell et al., 1987).

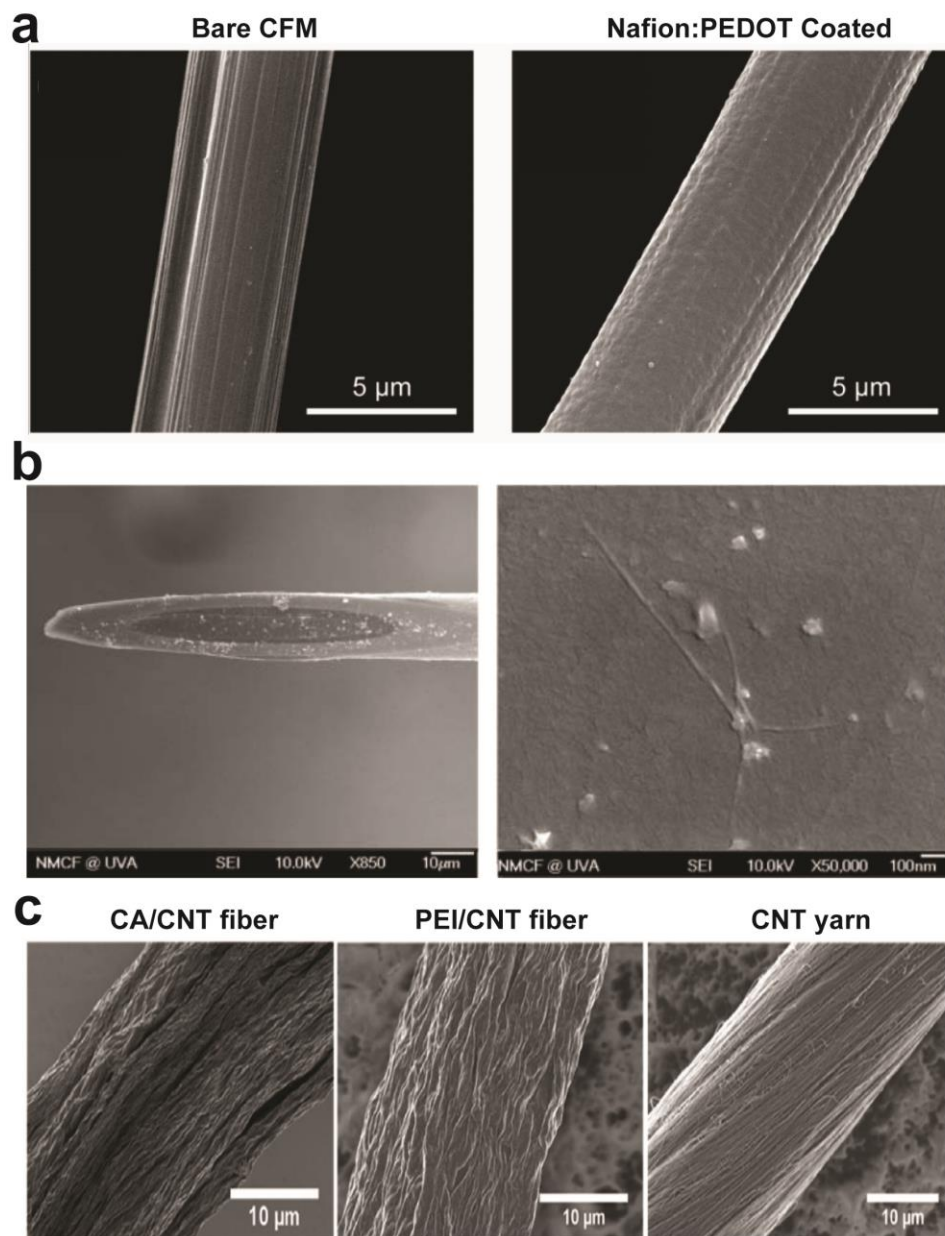


**Figure 1.3.** Electrode modifications for FSCV measurements. a) Electrodeposition of composite Nafion:PEDOT coatings on CFMs results in smoother electrode surfaces, in addition to more sensitive and selective FSCV measurements towards dopamine. Figure adapted from (Vreeland et al., 2015). b) CNTs can be directly deposited on carbon-fiber disk electrodes (left panel) to enhance sensitivity. Enhanced magnification reveals nanotube structures on the electrode surface (right panel). Figure adapted from (Swamy & Venton, 2007a). c) CNT electrodes can be fabricated with wet-spinning procedures with different substrates (chlorosulfonic acid, CA, left; polyethylenimine, PEI, middle) or pulled from aligned CNT arrays (right) to produces electrodes with different microscopic and electrochemical properties. Figure adapted from (Yang et al., 2017).

A recently developed coating uses the conductive polymer polyethylenedioxythiophene (PEDOT) as a component in stable electrode films (Figure 1.3a) (Vreeland, et al., 2015) (The positive charge of PEDOT acts with Nafion as a counterion for stable deposition of films on CFM surfaces via (slow-scan) cyclic voltammetry, obviating the concern of irreproducibility with regular Nafion coatings. The chemistry of this polymer pairing was found to be tunable; low density PEDOT:Nafion (i.e. low [PEDOT]) doubled sensitivity towards dopamine, while high density coatings quadrupled sensitivity at the expense of temporal resolution. Both preparations resulted in limits of detection around 5 nM. PEDOT has also been combined with graphene oxide (GO) in lieu of Nafion for FSCV measurements (Taylor et al., 2017). Electrodeposition of PEDOT:GO for 50 s was sufficient for a 10-fold enhancement of sensitivity. Unfortunately, PEDOT:GO is vulnerable to overoxidation, so this film is only compatible with waveforms without extended anodic limits.

Carbon nanotubes (CNT) have also been used to modify CFMs for more sensitive measurements (Jacobs et al., 2010; Swamy & Venton, 2007a; Xiao & Venton, 2012) (Figure 1.3b). Electrode modifications with CNTs differ in a few distinct ways from other coatings. First, CNT-modified CFMs do not appear to suffer from the same temporal distortion as polymer-coated electrodes (Xiao & Venton, 2012), which allows more sensitive measurements to be made more rapidly. Second, CNT deposition can enhance ET kinetics towards dopamine and other analytes (Jacobs, et al., 2010). Third, CNT modification tends to increase redox current for all measured species, rather than solely cationic species (Xiao & Venton, 2012). This renders CNT-CFMs less selective than other coated electrodes. Similar to other electrode modifications, reproducibility of fabrication can be an issue (Swamy & Venton, 2007a), though improvements have been made via self-assembly (Xiao & Venton, 2012). An alternative use of CNTs is its direct use as the electrode substrate (Figure 1.3c). CNT electrodes display the same advantages as CNT-modified CFMs and have limits of detection approaching 10 nM (Jacobs et al., 2014; Schmidt et al., 2013; Yang et al., 2016). Furthermore, CNT yarn electrodes can be

combined with other electrode pretreatments to augment results (Yang, et al., 2016) and engineered using different substrates to produce different electrochemical characteristics (Yang, et al., 2017).

### **Temporal resolution**

In addition to the requirement for adequate sensitivity, a reliable technique for monitoring neurotransmission *in vivo* must have sufficient temporal resolution to resolve rapid neurotransmitter release events. Due to the small area, and thus capacitance, of CFMs, FSCV is capable of voltage sweeps at high scan rates ( $>100$  V/s), which enables subsecond measurements (Wightman, 1981). The main determinant of the temporal resolution is the application frequency of the voltammetric waveform. To allow the diffusion layer to settle between measurements, a holding time of ten times the length of the voltage sweep is suggested (Howell, et al., 1986; Kawagoe et al., 1993). For standard *in vivo* measurements with scans between  $-0.4$  V and  $+1.3$  V at  $400$  V/s, this amounts to  $\sim 85$  ms between scans, which results in a desirable application frequency of  $\sim 10$  Hz. While measurements at higher sampling frequencies are possible at bare CFMs, they have reduced sensitivity towards dopamine, likely due to less time for adsorption between scans (Kile, et al., 2012). Curiously, this effect is not seen at CNT yarn electrodes, which has been attributed to slower desorption kinetics for the oxidized form of dopamine, dopamine-ortho-quinone (DOQ) (Jacobs, et al., 2014). This enables measurements at up to  $500$  Hz without significant loss of sensitivity.

Adsorption and desorption kinetics also affect the temporal response of CFMs. Voltammetric measurements exhibit slower responses to dopamine boluses than constant potential amperometry (Venton et al., 2002) and respond more quickly to freely diffusing species (e.g. AA) than predominately adsorbing species (e.g. dopamine) (Bath, et al., 2000). Correspondingly, electrode treatments that facilitate adsorption (and thus sensitivity) tend to

come at the expense of temporal resolution. In particular, extended anodic limits dramatically increase adsorption of dopamine to the CFM surface while blunting the temporal response (Heien, et al., 2003), which can impact interpretation of data collected in freely-moving animals with narrowly-spaced stimuli (Rodeberg, et al., 2016). It has been demonstrated that these effects can be removed via deconvolution (Venton, et al., 2002). However, care must be taken to delineate the effects of adsorption on the signal to separate it from other effects that could alter signal duration, including proximity to dopamine terminals (Venton et al., 2003b), long-term implantation (Clark et al., 2010), and overfiltering (Atcherley et al., 2013).

### **Chemical selectivity & resolution**

In the words of Ralph Adams, ‘no amount of instrumental cajoling can provide discrimination between competing oxidation reactions at the electrode surface’ (Adams, 1990). Indeed, a major limitation of electrochemistry is its relatively poor resolving power. Early measurements with *in vivo* electrochemistry were plagued with uncertainty of signal identity; particularly, dopamine was difficult to resolve from other easily oxidizable species present in brain tissue (Adams, 1976; Kovach et al., 1984). This ambiguity often led to discrepancies between research reports, including contrasting results during amphetamine (Wightman, 1981) and cocaine administration (Garris & Wightman, 1995; Gratton & Wise, 1994). Two of the principal interfering species *in vivo*, AA and dopamine metabolite dihydroxyphenylacetic acid (DOPAC) are anionic at physiological pH. Therefore, the first step to enhance selectivity was the use of anion-excluding polymers (Gerhardt, et al., 1984; Kristensen, et al., 1987). Coating electrodes with Nafion results in the signal from AA and DOPAC contributing <1% of the signal from equivalent concentrations of dopamine (Gerhardt, et al., 1984).

The use of FSCV provides an additional level of selectivity over slow-scan techniques, as molecules can be separated by their ET kinetics in addition to their half-wave potentials. For example, ascorbic acid has more sluggish ET kinetics at CFMs than dopamine, leading to its

oxidation wave occurring at more positive potentials (Baur, et al., 1988). The use of electrode coatings with FSCV further enhances selectivity (Baur, et al., 1988; Kristensen, et al., 1987), which is particularly important for measurements of serotonin, which competes with substantial interference from its metabolite 5-hydroxyindoleacetic acid (5-HIAA) (Dankoski & Wightman, 2013; Jackson et al., 1995). Recent improvements to electrode coatings include PEDOT:Nafion composite films that measure over 1500-fold higher current for dopamine over AA, an order of magnitude enhancement over dip-coated Nafion (Vreeland, et al., 2015).

The main interference in typical *in vivo* measurements of dopamine arises from pH changes, which occur in the brain as an effect of metabolism and blood flow during cellular activity (Venton, et al., 2003b). pH changes in the environment surrounding CFMs can alter redox of pH-sensitive surface functionalities, such as quinone groups, and modify the background current; therefore, as a consequence of background subtraction, pH changes produce distinctive CVs (Dengler, et al., 2015; Takmakov et al., 2010a). These CVs can overlap with dopamine CVs; therefore, the use of univariate analysis (i.e. direct conversion of current at the peak oxidation potential of dopamine to concentration) can allow pH changes to interfere with reliable assignment of faradaic current (Jones et al., 1994). One approach to minimize this effect is to alter the surface of the electrode to reduce sensitivity to pH (Runnels et al., 1999). Another approach is to use the current arising from pH changes at potentials with minimal dopamine contribution (e.g.  $\sim +0.2$  V on the anodic scan) to extrapolate the pH contribution at the peak potential for dopamine ( $\sim +0.6$  V) (Cheer et al., 2004). In this way, the contribution from pH can be manually subtracted out to reduce interference.

A more rigorous practice is the use the multivariate calibration techniques, such as principal component regression (PCR), to analyze data with overlapping currents from multiple analytes (Figure 1.4) (Heien et al., 2004; Heien et al., 2005). With this technique, the calibration model is built using a collection of CVs, termed a 'training set', that represents individual neurochemicals (e.g. dopamine and pH CVs). PCR separates experimental current into

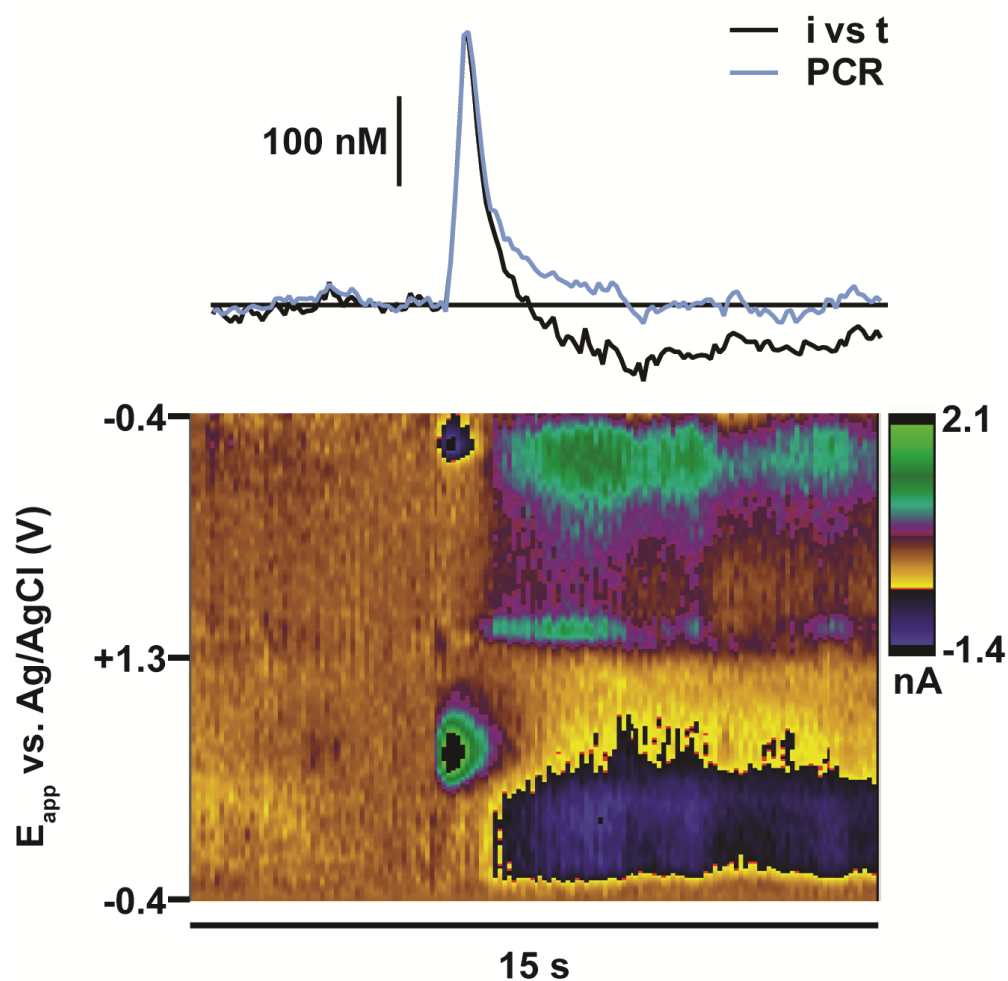


**Figure 1.4.** Principal component regression to remove influence of pH from dopamine concentration predictions. Electrical stimulation of the ventral tegmental area evoked both dopamine release and pH changes in the nucleus accumbens. Raw voltammetric data is depicted with a color plot (applied potential along the y-axis, time along the x-axis, and current amplitude plotted in false color). Because CVs for dopamine and basic pH changes overlap, simple concentration prediction using the current at the peak oxidation potential for dopamine predicted a ~50 nM decrease in dopamine levels below baseline following the electrically-evoked release event. However, the use of principal component regression with a model that included both dopamine and pH changes predicted dopamine levels returned to baseline shortly after stimulation.

contributions from each species contained in the training set. The applicability of the model can be tested through residual analysis in which current uncaptured by the model ('residual') is compared to a tolerance level specific to each training set, which is based on estimations of noise levels (Keithley et al., 2009). Failure of residual analysis indicates that the model is insufficient for calibration, and the corresponding data is discarded. While PCR cannot provide chemical identification (i.e. it does not alter selectivity at the electrode surface), its ability to monitor multiple analytes, as well as its ability to statistically validate the reliability of the model, gives it a substantial advantage over univariate techniques.

### *Waveform modifications*

Modifications to the voltammetric waveform can also alter selectivity between different species at bare CFMs. Indeed, waveform customization has long been used to expand the chemical toolbox of FSCV. The first notable instance of this was the development of a waveform for monitoring O<sub>2</sub> changes *in vivo*, which sweeps to a negative potential (-1.4 V) to reduce oxygen to hydrogen peroxide (Zimmerman & Wightman, 1991). The concurrent use of positive anodic limits (+0.8 V) also permits detection of catecholamines, and simultaneous measurements of norepinephrine, O<sub>2</sub>, and pH changes have been conducted *in vivo* (Bucher et al., 2014).

Waveforms have been adapted to detect other non-traditional analytes with FSCV. One example is adenosine, which exhibits redox properties at high overpotentials (>1.2 V vs. Ag/AgCl) (Swamy & Venton, 2007b). Because these potentials approach the limit of the potential window *in vivo*, redox peaks for adenosine typically occur near the switching potential, where there are significant contributions from non-faradaic currents, in addition to faradaic currents from other analytes. As a result, specificity is a major issue for these measurements. Venton and coworkers have demonstrated that a brief holding time (1 ms) at the switching potential can result in moderate differences in current-potential relationships between

adenosine, adenosine triphosphate (ATP), and hydrogen peroxide (Ross & Venton, 2014). With PCR, these dissimilarities were sufficient to allow the three analytes to be resolved, though some misassigned current persisted *in vitro*.

Another target molecule that requires waveform modification for detection is met-enkephalin (M-ENK), a peptide involved in the endogenous opioid system in the brain (Schmidt et al., 2014). The electrochemical properties of M-ENK primarily arise from its electroactive amino acid residues, tyrosine and methionine. Measurements with a standard voltammetric waveform, sweeping between -0.4 V and +1.4 V, are inadequate to monitor M-ENK reliably, as there is significant contribution from other species (e.g. dopamine) and M-ENK tends to foul the electrode surface over successive measurements. Sombers and colleagues addressed these problems in two distinct ways. First, a lower scan rate (100 V/s) was used from -0.2 V to +0.6 V in regions to reduce sensitivity towards dopamine and AA. Second, a holding time (3 ms) at the switching potential (+1.2 V) was used to weaken adsorption of M-ENK products to the electrode surface, thereby reducing subsequent biofouling. While these measurements of M-ENK appear to have sufficient chemical resolution from dopamine and AA, a systematic comparison of M-ENK signals to other analytes that contribute near +1.2 V (e.g. adenosine, ATP, hydrogen peroxide) has yet to be attempted. Moreover, other tyrosine-containing peptides have peaks similar to M-ENK, which could make separation of different peptides a difficult task (Schmidt, et al., 2014).

#### *Additional criteria for chemical specificity*

Ultimately, some species cannot be efficiently resolved with FSCV, even with the use of PCR. For example, dopamine and norepinephrine have nearly identical CVs when employing traditional voltammetric waveforms (Heien, et al., 2003). Therefore, careful practice of FSCV requires the use of additional identification criteria *in vivo* (Millar, et al., 1985; Phillips & Wightman, 2003). The two most common approaches are pharmacological and anatomical

verification. First, pharmacological manipulation with analyte-specific drugs can confirm signal identity. In particular, routine norepinephrine measurements utilize both dopamine- and norepinephrine-specific drugs to ensure the measurements do not arise from mixed catecholamine signals (Fox et al., 2017; Park et al., 2011). Second, different brain regions express different neurotransmitter content and release (Fox & Wightman, 2017; Nicola & Malenka, 1998); therefore, anatomical specificity can be provided when measurements are made in regions where one neurotransmitter dominates (Park et al., 2010; Park et al., 2013).

### **Accuracy**

Phasic dopamine signals measured with FSCV have been shown to be dependent on burst firing of dopaminergic neurons (Somers et al., 2009). During impulse-dependent release, more than 90% of dopamine spills out of the synapse within  $<100 \mu\text{s}$  (Garris et al., 1994). Correspondingly, measurements in the extracellular space depend on a balance of dopamine release, diffusion, and uptake, rather than directly representing synaptic concentrations (which are three to six orders of magnitude higher) (Cragg & Rice, 2004; Garris, et al., 1994). However, these signals have functional relevance, as a significant population of dopamine receptors and transporters is found outside of the synaptic cleft, supporting the role of dopamine as a 'volume neurotransmitter' (Caille et al., 1996; Levey et al., 1993; Sesack et al., 1994). Therefore, the chemoanalytical power of FSCV to transduce neurochemical measurements into analyte concentrations is valuable, and the determination of accurate concentrations with FSCV is an important experimental aim.

The accuracy of determined concentrations depends primarily on two factors: 1) the ability of PCR to extract analyte current reliably from complex data and 2) the suitability of the external calibration factor that relates the measured current to concentrations.

### *Accuracy of PCR signal extraction*

Before concentrations of neurotransmitter can be reliably estimated, its faradaic current must be separating from other interferents in the signal (e.g. pH, noise). The standard means of achieving this is through the use of PCR (Heien, et al., 2005; Rodeberg et al., 2017). PCR requires accurate knowledge of the CV characteristics for each analyte in the training set. Therefore, 'pure' analyte CVs are typically collected post-experiment with electrical stimulation, a process known to evoke both neurotransmitter release and pH changes. (Fox, et al., 2017; Heien, et al., 2005; Venton et al., 2003a). Moreover, the use of CVs from the same recording environment (i.e. same electrode, brain environment, and equipment) allows reasonable estimations of noise levels for the recording session, which is an important parameter for model validation (Johnson et al., 2016; Keithley, et al., 2009).

However, there are a few limitations to the use of PCR. Training sets may vary between experimenters and labs, as the selection of CV standards for the training set involves a degree of subjectivity (Keithley et al., 2010). Additionally, the use of 'unrepresentative' CVs in the training set can impede model performance. The development of chronically-implanted microelectrodes, with the aim of longitudinal measurements over weeks to months of recording, has required modifications to PCR use due to experimental limitations (Clark, et al., 2010; Rodeberg, et al., 2017). Post-experiment electrical stimulation is not typically feasible at these electrodes, due to both concerns with long-term functionality of the stimulating electrode and the potential impact of electrical stimulation on sustained behavior (Rodeberg, et al., 2017). The most widely used solution is to build 'standard' training sets at separate electrodes to analyze all subsequent data. However, the application of these types of training sets appears to systematically underestimate concentrations, which suggests that signal extraction (and thus concentration estimation) is impaired with these models (Johnson, et al., 2016; Keithley & Wightman, 2011; Rodeberg et al., 2015). Current investigations are underway to improve multivariate calibration and address these concerns.

### *Accuracy of external calibration factors*

After analyte concentrations are extracted, they are converted to concentrations using a calibration factor obtained *in vitro* (i.e. a flow cell); therefore, the accuracy of FSCV measurements is also tied to the similarity of *in vivo* and *in vitro* conditions. In comparison to constant-potential amperometry, the diffusion layer of FSCV measurements is very small (~3 µm) due to its rapid scan rates. As a result, measurements in flow cell are flow-rate independent, which permits *in vitro* measurements to be representative of efflux *in vivo* (Kawagoe, et al., 1993; Venton, et al., 2002).

Nonetheless, there are other issues with estimation of calibration factors. CFMs have been demonstrated to lose sensitivity after implantation into brain tissue (Logman et al., 2000). Consequently, postcalibration (i.e. generation of calibration curves following implantation) is standard for *in vivo* measurements. Ideally, this calibration is done for each individual CFM to capture variability between different electrodes. However, in some cases the CFM is deliberately destroyed with a high electrolytic current to create lesions for precise marking of the recording location (Bucher, et al., 2014; Fox, et al., 2017). In these cases, an average postcalibration factor obtained from several electrodes is used, with the assumption that it is representative of all *in vivo* measurements. While this undoubtedly adds imprecision in comparisons between different electrodes, it is unlikely to affect interpretation of measurements made within single recording sessions, as previous work has suggested that the majority of this sensitivity loss occurs immediately upon insertion into tissue (Capella et al., 1990; Ewing, et al., 1981; Michael et al., 1987) with no significant differences in sensitivity seen between subsequent implant durations (Clark, et al., 2010; Rodeberg, et al., 2016; Singh et al., 2011). Notably, electrode coatings measurements have been suggested to prevent this loss of sensitivity *in vivo* (Cahill et al., 1996; Singh, et al., 2011; Vreeland, et al., 2015). In either case, postcalibration sensitivity also depends on treatment of the electrode post-removal from the brain (e.g. cleaning and rinsing) (Cahill, et al., 1996). Removal of adhered material enhances

sensitivity, but likely makes these measurements less representative of the tissue environment in which measurements were made.

Fouling of the electrode surface is not the only factor that can alter sensitivity at CFMs. Application of voltammetric waveforms, particularly ones with high anodic limits, has been shown to generate surface oxide groups that augment sensitivity towards dopamine and other species (Hafizi, et al., 1990; Heien, et al., 2003; Roberts, et al., 2010). Common practice is to therefore 'cycle' waveforms at high repetition frequencies to hasten the conditioning of the electrode surface to promote CFM stability over the course of subsequent measurements. Long-term stability of the CFM sensitivity is of particular concern for chronically-implanted CFMs, which are used for weeks to months of recordings (Clark, et al., 2010; Rodeberg, et al., 2017). Extended anodic limits have been shown to regenerate the CFM surface (Takmakov, et al., 2010b). While this process should maintain sensitivity by replacing damaged surface functional groups, this process is concomitant with loss of carbon from the surface. Therefore, surface area is deteriorated over prolonged use; for the standard *in vivo* dopamine waveform (-0.4 V to +1.3 V), the carbon fiber completely disappears after approximately  $1.4 \times 10^7$  scans (Takmakov, et al., 2010b). Assuming one hour of cycling (60 Hz) before measurements and 90 min of recording (10 Hz) for each CFM measurement, this means approximately 52 sessions can be carried out before complete CFM degradation. While standard measurements with chronic CFMs seldom approach this limit, it is probable that a gradient of sensitivity loss exists as the CFM is etched away. Therefore, methods to track sensitivity over time at a CFM *in vivo* would be extremely valuable. The two contemporary methods that attempt to address this concern involve tracking the magnitude of the background current, which is also proportional the surface area of the CFM (Roberts et al., 2013), and using a proven stimulus (e.g. unexpected food reward) to evoke dopamine release and track its magnitude over time, which rests on the assumption that this reward-evoked release remains relatively stable (Clark et al., 2013;

Rodeberg, et al., 2017). Future studies using more rigorously controlled stimuli (i.e. optogenetic stimulation) could test the stability of CFMs over prolonged use more meticulously.

## **CONCLUSIONS & FUTURE DIRECTIONS**

Fast-scan cyclic voltammetry is an attractive tool for the real-time monitoring of neurochemicals *in vivo*. It has been demonstrated to have sufficient sensitivity and temporal resolution to track rapid signaling events on a timescale relevant to behavior. Moreover, the technique is flexible, due to the ease of CFM modification and the ability to customize voltammetric waveforms for enhanced sensitivity and/or selectivity. Nonetheless, the resolving power and accuracy of this technique are areas for continued improvement.

A few current and future innovations may increase the widespread use of FSCV. The introduction of chronically implanted CFMs has allowed measurements of dopamine over previously unattainable timescales during behavioral and disease-based models (Clark, et al., 2013; Clark, et al., 2010; Covey et al., 2016). Multimodal measurements that combine FSCV with iontophoresis and electrophysiology recordings at the same CFM have permitted unprecedented insights into dopamine signaling (Belle et al., 2013; Kirkpatrick et al., 2016; Owesson-White et al., 2016). Lastly, past and current development of carbon-based arrays permits multiplexed FSCV recordings collection from several sites *in vivo*, which could cultivate unique knowledge regarding signaling and pharmacological heterogeneity in single brain structures (Parent et al., 2017; Schwerdt et al., 2017; Zachek et al., 2010). These advances will lead to increasingly versatile use of FSCV in future research.

## REFERENCES

- Adams, R. N. (1976). Probing brain chemistry with electroanalytical techniques. *Anal Chem*, 48(14), 1126A-1138A.
- Adams, R. N. (1990). In vivo electrochemical measurements in the CNS. *Prog Neurobiol*, 35(4), 297-311.
- Alsmeyer, Y. W., & McCreery, R. L. (1991). Surface enhanced Raman examination of carbon electrodes: effects of laser activation and electrochemical pretreatment. *Langmuir*, 7(10), 2370-2375.
- Amatore, C., Jutand, A., & Pflüger, F. (1987). Nanosecond time resolved cyclic voltammetry: Direct observation of electrogenerated intermediates with bimolecular diffusion controlled decay using scan rates in the megavolt per second range. *J Electroanal Chem*, 218(1-2), 361-365.
- Armstrong-James, M., & Millar, J. (1979). Carbon fibre microelectrodes. *J Neurosci Methods*, 1(3), 279-287.
- Armstrong-James, M., Millar, J., & Kruk, Z. (1980). Quantification of noradrenaline iontophoresis. *Nature*, 288(5787), 181-183.
- Atcherley, C. W., Vreeland, R. F., Monroe, E. B., Sanchez-Gomez, E., & Heien, M. L. (2013). Rethinking data collection and signal processing. 2. Preserving the temporal fidelity of electrochemical measurements. *Anal Chem*, 85(16), 7654-7658.
- Banks, C. E., Davies, T. J., Wildgoose, G. G., & Compton, R. G. (2005). Electrocatalysis at graphite and carbon nanotube modified electrodes: edge-plane sites and tube ends are the reactive sites. *Chem Commun (Camb)*(7), 829-841.
- Bard, A. J., & Faulkner, L. R. (2001). *Electrochemical methods: Fundamentals and applications* (2nd ed.). New York: Wiley.
- Bath, B. D., Martin, H. B., Wightman, R. M., & Anderson, M. R. (2001). Dopamine Adsorption at Surface Modified Carbon-Fiber Electrodes. *Langmuir*, 17(22), 7032-7039.
- Bath, B. D., Michael, D. J., Trafton, B. J., Joseph, J. D., Runnels, P. L., & Wightman, R. M. (2000). Subsecond adsorption and desorption of dopamine at carbon-fiber microelectrodes. *Anal Chem*, 72(24), 5994-6002.
- Baur, J. E., Kristensen, E. W., May, L. J., Wiedemann, D. J., & Wightman, R. M. (1988). Fast-scan voltammetry of biogenic amines. *Anal Chem*, 60(13), 1268-1272.
- Beaulieu, J.-M., & Gainetdinov, R. R. (2011). The physiology, signaling, and pharmacology of dopamine receptors. *Pharmacol Rev*, 63(1), 182-217.
- Belle, A. M., Owesson-White, C., Herr, N. R., Carelli, R. M., & Wightman, R. M. (2013). Controlled iontophoresis coupled with fast-scan cyclic voltammetry/electrophysiology in awake, freely moving animals. *ACS Chem Neurosci*, 4(5), 761-771.

- Brazell, M. P., Kasser, R. J., Renner, K. J., Feng, J., Moghaddam, B., & Adams, R. N. (1987). Electrocoating carbon fiber microelectrodes with Nafion improves selectivity for electroactive neurotransmitters. *J Neurosci Methods*, *22*(2), 167-172.
- Bucher, E. S., et al. (2014). Medullary norepinephrine neurons modulate local oxygen concentrations in the bed nucleus of the stria terminalis. *J Cereb Blood Flow Metab*, *34*(7), 1128-1137.
- Bucher, E. S., & Wightman, R. M. (2015). Electrochemical analysis of neurotransmitters. *Annu Rev Anal Chem*, *8*, 239-261.
- Cahill, P. S., Walker, Q. D., Finnegan, J. M., Mickelson, G. E., Travis, E. R., & Wightman, R. M. (1996). Microelectrodes for the measurement of catecholamines in biological systems. *Anal Chem*, *68*(18), 3180-3186.
- Caille, I., Dumartin, B., & Bloch, B. (1996). Ultrastructural localization of D1 dopamine receptor immunoreactivity in rat striatonigral neurons and its relation with dopaminergic innervation. *Brain Res*, *730*(1-2), 17-31.
- Capella, P., Ghasemzadeh, B., Mitchell, K., & Adams, R. N. (1990). Nafion-coated carbon fiber electrodes for neurochemical studies in brain tissue. *Electroanalysis*, *2*(3), 175-182.
- Cheer, J. F., Wassum, K. M., Heien, M. L., Phillips, P. E., & Wightman, R. M. (2004). Cannabinoids enhance subsecond dopamine release in the nucleus accumbens of awake rats. *J Neurosci*, *24*(18), 4393-4400.
- Cheng, H.-Y., Schenk, J., Huff, R., & Adams, R. (1979). In vivo electrochemistry: behavior of micro electrodes in brain tissue. *J Electroanal Chem*, *100*(1-2), 23-31.
- Clark, J. J., Collins, A. L., Sanford, C. A., & Phillips, P. E. (2013). Dopamine encoding of Pavlovian incentive stimuli diminishes with extended training. *J Neurosci*, *33*(8), 3526-3532.
- Clark, J. J., et al. (2010). Chronic microsensors for longitudinal, subsecond dopamine detection in behaving animals. *Nat Methods*, *7*(2), 126-129.
- Conti, J., Strope, E., Adams, R., & Marsden, C. (1978). Voltammetry in brain tissue: chronic recording of stimulated dopamine and 5-hydroxytryptamine release. *Life Sci*, *23*(27-28), 2705-2715.
- Covey, D. P., Dantrassy, H. M., Zlebnik, N. E., Gildish, I., & Cheer, J. F. (2016). Compromised Dopaminergic Encoding of Reward Accompanying Suppressed Willingness to Overcome High Effort Costs Is a Prominent Prodromal Characteristic of the Q175 Mouse Model of Huntington's Disease. *J Neurosci*, *36*(18), 4993-5002.
- Cragg, S. J., & Rice, M. E. (2004). DANCING past the DAT at a DA synapse. *Trends Neurosci*, *27*(5), 270-277.
- Dale, H. H., Feldberg, W., & Vogt, M. (1936). Release of acetylcholine at voluntary motor nerve endings. *J Physiol*, *86*(4), 353.

- Dankoski, E. C., & Wightman, R. M. (2013). Monitoring serotonin signaling on a subsecond time scale. *Front Integr Neurosci*, 7, 44.
- Dengler, A. K., Wightman, R. M., & McCarty, G. S. (2015). Microfabricated Collector-Generator Electrode Sensor for Measuring Absolute pH and Oxygen Concentrations. *Anal Chem*, 87(20), 10556-10564.
- DuVall, S. H., & McCreery, R. L. (1999). Control of Catechol and Hydroquinone Electron-Transfer Kinetics on Native and Modified Glassy Carbon Electrodes. *Anal Chem*, 71(20), 4594-4602.
- DuVall, S. H., & McCreery, R. L. (2000). Self-catalysis by Catechols and Quinones during Heterogeneous Electron Transfer at Carbon Electrodes. *J Am Chem Soc*, 122(28), 6759-6764.
- Ewing, A. G., Bigelow, J. C., & Wightman, R. M. (1983). Direct in vivo monitoring of dopamine released from two striatal compartments in the rat. *Science*, 221(4606), 169-171.
- Ewing, A. G., Dayton, M. A., & Wightman, R. M. (1981). Pulse voltammetry with microvoltammetric electrodes. *Anal Chem*, 53(12), 1842-1847.
- Feng, J. X., Brazell, M., Renner, K., Kasser, R., & Adams, R. N. (1987). Electrochemical pretreatment of carbon fibers for in vivo electrochemistry: effects on sensitivity and response time. *Anal Chem*, 59(14), 1863-1867.
- Fitch, A., & Evans, D. H. (1986). Use of microelectrodes for the study of a fast chemical step in an electrode reaction. *J Electroanal Chem*, 202(1-2), 83-92.
- Floresco, S. B., West, A. R., Ash, B., Moore, H., & Grace, A. A. (2003). Afferent modulation of dopamine neuron firing differentially regulates tonic and phasic dopamine transmission. *Nat Neurosci*, 6(9), 968-973.
- Fox, M. E., Rodeberg, N. T., & Wightman, R. M. (2017). Reciprocal Catecholamine Changes during Opiate Exposure and Withdrawal. *Neuropsychopharmacology*, 42(3), 671-681.
- Fox, M. E., & Wightman, R. M. (2017). Contrasting Regulation of Catecholamine Neurotransmission in the Behaving Brain: Pharmacological Insights from an Electrochemical Perspective. *Pharmacol Rev*, 69(1), 12-32.
- Garris, P. A., Ciolkowski, E. L., Pastore, P., & Wightman, R. M. (1994). Efflux of dopamine from the synaptic cleft in the nucleus accumbens of the rat brain. *J Neurosci*, 14(10), 6084-6093.
- Garris, P. A., & Wightman, R. M. (1995). Distinct pharmacological regulation of evoked dopamine efflux in the amygdala and striatum of the rat in vivo. *Synapse*, 20(3), 269-279.
- Gerhardt, G. A., Oke, A. F., Nagy, G., Moghaddam, B., & Adams, R. N. (1984). Nafion-coated electrodes with high selectivity for CNS electrochemistry. *Brain Res*, 290(2), 390-395.

- Gonon, F., Buda, M., Cespuglio, R., Jouvet, M., & Pujol, J.-F. (1980). In vivo electrochemical detection of catechols in the neostriatum of anaesthetized rats: dopamine or DOPAC? *Nature*, 286(5776), 902-904.
- Gonon, F., et al. (1978). Mesure électrochimique continue de la libération de dopamine réalisée in vivo dans le néostriatum du rat. *CR Acad. Sci. Paris*, 286, 1203-1206.
- Gonon, F., Fombarlet, C., Buda, M., & Pujol, J. F. (1981). Electrochemical treatment of pyrolytic carbon fiber electrodes. *Anal Chem*, 53(9), 1386-1389.
- Grace, A. (1991). Phasic versus tonic dopamine release and the modulation of dopamine system responsivity: a hypothesis for the etiology of schizophrenia. *Neuroscience*, 41(1), 1-24.
- Gratton, A., & Wise, R. A. (1994). Drug- and behavior-associated changes in dopamine-related electrochemical signals during intravenous cocaine self-administration in rats. *J Neurosci*, 14(7), 4130-4146.
- Hafizi, S., Kruk, Z. L., & Stamford, J. A. (1990). Fast cyclic voltammetry: improved sensitivity to dopamine with extended oxidation scan limits. *J Neurosci Methods*, 33(1), 41-49.
- Heien, M. L., Johnson, M. A., & Wightman, R. M. (2004). Resolving neurotransmitters detected by fast-scan cyclic voltammetry. *Anal Chem*, 76(19), 5697-5704.
- Heien, M. L., et al. (2005). Real-time measurement of dopamine fluctuations after cocaine in the brain of behaving rats. *Proc Natl Acad Sci U S A*, 102(29), 10023-10028.
- Heien, M. L., Phillips, P. E., Stuber, G. D., Seipel, A. T., & Wightman, R. M. (2003). Overoxidation of carbon-fiber microelectrodes enhances dopamine adsorption and increases sensitivity. *Analyst*, 128(12), 1413-1419.
- Hermans, A., Keithley, R. B., Kita, J. M., Sombers, L. A., & Wightman, R. M. (2008). Dopamine detection with fast-scan cyclic voltammetry used with analog background subtraction. *Anal Chem*, 80(11), 4040-4048.
- Howell, J. O., Kuhr, W. G., Ensman, R. E., & Wightman, R. M. (1986). Background subtraction for rapid scan voltammetry. *J Electroanal Chem*, 209(1), 77-90.
- Howell, J. O., & Wightman, R. M. (1984). Ultrafast voltammetry and voltammetry in highly resistive solutions with microvoltammetric electrodes. *Anal Chem*, 56(3), 524-529.
- Jackson, B. P., Dietz, S. M., & Wightman, R. M. (1995). Fast-scan cyclic voltammetry of 5-hydroxytryptamine. *Anal Chem*, 67(6), 1115-1120.
- Jacobs, C. B., Ivanov, I. N., Nguyen, M. D., Zestos, A. G., & Venton, B. J. (2014). High temporal resolution measurements of dopamine with carbon nanotube yarn microelectrodes. *Anal Chem*, 86(12), 5721-5727.
- Jacobs, C. B., Peairs, M. J., & Venton, B. J. (2010). Review: Carbon nanotube based electrochemical sensors for biomolecules. *Analytica Chimica Acta*, 662(2), 105-127.

- Jaquins-Gerstl, A., & Michael, A. C. (2009). Comparison of the brain penetration injury associated with microdialysis and voltammetry. *J Neurosci Methods*, 183(2), 127-135.
- Johnson, J. A., Rodeberg, N. T., & Wightman, R. M. (2016). Failure of Standard Training Sets in the Analysis of Fast-Scan Cyclic Voltammetry Data. *ACS Chem Neurosci*, 7(3), 349-359.
- Jones, S. R., Mickelson, G. E., Collins, L. B., Kawagoe, K. T., & Wightman, R. M. (1994). Interference by pH and Ca<sup>2+</sup> ions during measurements of catecholamine release in slices of rat amygdala with fast-scan cyclic voltammetry. *J Neurosci Methods*, 52(1), 1-10.
- Kawagoe, K. T., Zimmerman, J. B., & Wightman, R. M. (1993). Principles of voltammetry and microelectrode surface states. *J Neurosci Methods*, 48(3), 225-240.
- Keithley, R. B., Carelli, R. M., & Wightman, R. M. (2010). Rank estimation and the multivariate analysis of in vivo fast-scan cyclic voltammetric data. *Anal Chem*, 82(13), 5541-5551.
- Keithley, R. B., Heien, M. L., & Wightman, R. M. (2009). Multivariate concentration determination using principal component regression with residual analysis. *Trends Analyt Chem*, 28(9), 1127-1136.
- Keithley, R. B., et al. (2011). Higher sensitivity dopamine measurements with faster-scan cyclic voltammetry. *Anal Chem*, 83(9), 3563-3571.
- Keithley, R. B., & Wightman, R. M. (2011). Assessing principal component regression prediction of neurochemicals detected with fast-scan cyclic voltammetry. *ACS Chem Neurosci*, 2(9), 514-525.
- Kennedy, R. T. (2013). Emerging Trends in in Vivo Neurochemical Monitoring by Microdialysis. *Curr Opin Chem Biol*, 17(5), 10.1016/j.cbpa.2013.1006.1012.
- Kile, B. M., et al. (2012). Optimizing the Temporal Resolution of Fast-Scan Cyclic Voltammetry. *ACS Chem Neurosci*, 3(4), 285-292.
- Kirkpatrick, D. C., McKinney, C. J., Manis, P. B., & Wightman, R. M. (2016). Expanding neurochemical investigations with multi-modal recording: simultaneous fast-scan cyclic voltammetry, iontophoresis, and patch clamp measurements. *Analyst*, 141(16), 4902-4911.
- Kissinger, P. T., Hart, J. B., & Adams, R. N. (1973). Voltammetry in brain tissue—a new neurophysiological measurement. *Brain Res*, 55(1), 209-213.
- Kovach, P. M., Deakin, M. R., & Wightman, R. M. (1986). Electrochemistry at partially blocked carbon-fiber microcylinder electrodes. *J Phys Chem*, 90(19), 4612-4617.
- Kovach, P. M., Ewing, A. G., Wilson, R. L., & Wightman, R. M. (1984). In vitro comparison of the selectivity of electrodes for in vivo electrochemistry. *J Neurosci Methods*, 10(3), 215-227.
- Kristensen, E. W., Kuhr, W. G., & Wightman, R. M. (1987). Temporal characterization of perfluorinated ion exchange coated microvoltammetric electrodes for in vivo use. *Analytical Chemistry*, 59(14), 1752-1757.

- Kuhr, W. G., & Wightman, R. M. (1986). Real-time measurement of dopamine release in rat brain. *Brain Res*, 381(1), 168-171.
- Levey, A. I., et al. (1993). Localization of D1 and D2 dopamine receptors in brain with subtype-specific antibodies. *Proc Natl Acad Sci U S A*, 90(19), 8861-8865.
- Loewi, O. (1921). Über humorale übertragbarkeit der herznervenwirkung. *Pflüger, Arch*, 189(1), 239-242.
- Logman, M. J., Budygin, E. A., Gainetdinov, R. R., & Wightman, R. M. (2000). Quantitation of in vivo measurements with carbon fiber microelectrodes. *J Neurosci Methods*, 95(2), 95-102.
- Marcenac, F., & Gonon, F. (1985). Fast in vivo monitoring of dopamine release in the rat brain with differential pulse amperometry. *Anal Chem*, 57(8), 1778-1779.
- McCreery, R. L. (2008). Advanced carbon electrode materials for molecular electrochemistry. *Chem Rev*, 108(7), 2646-2687.
- Michael, A. C., Ikeda, M., & Justice, J. B., Jr. (1987). Mechanisms contributing to the recovery of striatal releasable dopamine following MFB stimulation. *Brain Res*, 421(1-2), 325-335.
- Michael, A. C., & Justice, J. B., Jr. (1987). Oxidation of dopamine and 4-methylcatechol at carbon fiber disk electrodes. *Anal Chem*, 59(3), 405-410.
- Millar, J., Stamford, J. A., Kruk, Z. L., & Wightman, R. M. (1985). Electrochemical, pharmacological and electrophysiological evidence of rapid dopamine release and removal in the rat caudate nucleus following electrical stimulation of the median forebrain bundle. *Eur J Pharmacol*, 109(3), 341-348.
- Monaghan, D. T., Bridges, R. J., & Cotman, C. W. (1989). The excitatory amino acid receptors: their classes, pharmacology, and distinct properties in the function of the central nervous system. *Annu Rev Pharmacol Toxicol*, 29(1), 365-402.
- Nagy, G., Rice, M. E., & Adams, R. N. (1982). A new type of enzyme electrode: the ascorbic acid eliminator electrode. *Life Sci*, 31(23), 2611-2616.
- Nicola, S. M., & Malenka, R. C. (1998). Modulation of synaptic transmission by dopamine and norepinephrine in ventral but not dorsal striatum. *J Neurophysiol*, 79(4), 1768-1776.
- Owesson-White, C., et al. (2016). Cue-Evoked Dopamine Release Rapidly Modulates D2 Neurons in the Nucleus Accumbens During Motivated Behavior. *J Neurosci*, 36(22), 6011-6021.
- Parent, K. L., et al. (2017). Platform to Enable Combined Measurement of Dopamine and Neural Activity. *Anal Chem*, 89(5), 2790-2799.
- Park, J., Aragona, B. J., Kile, B. M., Carelli, R. M., & Wightman, R. M. (2010). In vivo voltammetric monitoring of catecholamine release in subterritories of the nucleus accumbens shell. *Neuroscience*, 169(1), 132-142.

- Park, J., et al. (2013). Opposing catecholamine changes in the bed nucleus of the stria terminalis during intracranial self-stimulation and its extinction. *Biol Psychiatry*, 74(1), 69-76.
- Park, J., Takmakov, P., & Wightman, R. M. (2011). In vivo comparison of norepinephrine and dopamine release in rat brain by simultaneous measurements with fast-scan cyclic voltammetry. *J Neurochem*, 119(5), 932-944.
- Parsons, L. H., & Justice, J. B., Jr. (1992). Extracellular concentration and in vivo recovery of dopamine in the nucleus accumbens using microdialysis. *J Neurochem*, 58(1), 212-218.
- Peters, J. L., Miner, L. H., Michael, A. C., & Sesack, S. R. (2004). Ultrastructure at carbon fiber microelectrode implantation sites after acute voltammetric measurements in the striatum of anesthetized rats. *J Neurosci Methods*, 137(1), 9-23.
- Phillips, P. E., & Wightman, R. M. (2003). Critical guidelines for validation of the selectivity of in vivo chemical microsensors. *Trends Analyt Chem*, 22(8), 509-514.
- Ponchon, J. L., Cespuglio, R., Gonon, F., Jouvot, M., & Pujol, J. F. (1979). Normal pulse polarography with carbon fiber electrodes for in vitro and in vivo determination of catecholamines. *Anal Chem*, 51(9), 1483-1486.
- Roberts, J. G., Moody, B. P., McCarty, G. S., & Sombers, L. A. (2010). Specific oxygen-containing functional groups on the carbon surface underlie an enhanced sensitivity to dopamine at electrochemically pretreated carbon fiber microelectrodes. *Langmuir*, 26(11), 9116-9122.
- Roberts, J. G., Toups, J. V., Eyuaem, E., McCarty, G. S., & Sombers, L. A. (2013). In situ electrode calibration strategy for voltammetric measurements in vivo. *Anal Chem*, 85(23), 11568-11575.
- Robinson, D. L., Hermans, A., Seipel, A. T., & Wightman, R. M. (2008). Monitoring rapid chemical communication in the brain. *Chem Rev*, 108(7), 2554-2584.
- Rodeberg, N. T., Johnson, J. A., Bucher, E. S., & Wightman, R. M. (2016). Dopamine Dynamics during Continuous Intracranial Self-Stimulation: Effect of Waveform on Fast-Scan Cyclic Voltammetry Data. *ACS Chem Neurosci*, 7(11), 1508-1518.
- Rodeberg, N. T., Johnson, J. A., Cameron, C. M., Saddoris, M. P., Carelli, R. M., & Wightman, R. M. (2015). Construction of Training Sets for Valid Calibration of in Vivo Cyclic Voltammetric Data by Principal Component Analysis. *Anal Chem*, 87(22), 11484-11491.
- Rodeberg, N. T., Sandberg, S. G., Johnson, J. A., Phillips, P. E., & Wightman, R. M. (2017). Hitchhiker's Guide to Voltammetry: Acute and Chronic Electrodes for in Vivo Fast-Scan Cyclic Voltammetry. *ACS Chem Neurosci*, 8(2), 221-234.
- Ross, A. E., & Venton, B. J. (2014). Sawhorse waveform voltammetry for selective detection of adenosine, ATP, and hydrogen peroxide. *Anal Chem*, 86(15), 7486-7493.

- Runnels, P. L., Joseph, J. D., Logman, M. J., & Wightman, R. M. (1999). Effect of pH and surface functionalities on the cyclic voltammetric responses of carbon-fiber microelectrodes. *Anal Chem*, 71(14), 2782-2789.
- Schmidt, A. C., Dunaway, L. E., Roberts, J. G., McCarty, G. S., & Sombers, L. A. (2014). Multiple scan rate voltammetry for selective quantification of real-time enkephalin dynamics. *Anal Chem*, 86(15), 7806-7812.
- Schmidt, A. C., Wang, X., Zhu, Y., & Sombers, L. A. (2013). Carbon Nanotube Yarn Electrodes for Enhanced Detection of Neurotransmitter Dynamics in Live Brain Tissue. *ACS Nano*, 7(9), 7864-7873.
- Schultz, W. (1998). Predictive reward signal of dopamine neurons. *J Neurophysiol*, 80(1), 1-27.
- Schwerdt, H. N., et al. (2017). Subcellular probes for neurochemical recording from multiple brain sites. *Lab Chip*, 17(6), 1104-1115.
- Sesack, S. R., Aoki, C., & Pickel, V. M. (1994). Ultrastructural localization of D2 receptor-like immunoreactivity in midbrain dopamine neurons and their striatal targets. *J Neurosci*, 14(1), 88-106.
- Singh, Y. S., Sawarynski, L. E., Dabiri, P. D., Choi, W. R., & Andrews, A. M. (2011). Head-to-head comparisons of carbon fiber microelectrode coatings for sensitive and selective neurotransmitter detection by voltammetry. *Anal Chem*, 83(17), 6658-6666.
- Somers, L. A., Beyene, M., Carelli, R. M., & Wightman, R. M. (2009). Synaptic overflow of dopamine in the nucleus accumbens arises from neuronal activity in the ventral tegmental area. *J Neurosci*, 29(6), 1735-1742.
- Stamford, J. A., Kruk, Z. L., & Millar, J. (1986). Sub-second striatal dopamine release measured by in vivo voltammetry. *Brain Res*, 381(2), 351-355.
- Stamford, J. A., Kruk, Z. L., Millar, J., & Wightman, R. M. (1984). Striatal dopamine uptake in the rat: in vivo analysis by fast cyclic voltammetry. *Neurosci Lett*, 51(1), 133-138.
- Strand, A. M., & Venton, B. J. (2008). Flame etching enhances the sensitivity of carbon-fiber microelectrodes. *Anal Chem*, 80(10), 3708-3715.
- Swain, G. M., & Kuwana, T. (1991). Electrochemical formation of high surface area carbon fibers. *Analytical Chemistry*, 63(5), 517-519.
- Swamy, B. E., & Venton, B. J. (2007a). Carbon nanotube-modified microelectrodes for simultaneous detection of dopamine and serotonin in vivo. *Analyst*, 132(9), 876-884.
- Swamy, B. E., & Venton, B. J. (2007b). Subsecond detection of physiological adenosine concentrations using fast-scan cyclic voltammetry. *Anal Chem*, 79(2), 744-750.
- Takmakov, P., Zachek, M., Keithley, R., Bucher, E., McCarty, G., & Wightman, R. (2010a). Characterization of local pH changes in brain using fast-scan cyclic voltammetry with carbon microelectrodes. *Anal Chem*, 82(23), 9892-9900.

- Takmakov, P., et al. (2010b). Carbon microelectrodes with a renewable surface. *Anal Chem*, 82(5), 2020-2028.
- Taylor, I. M., Robbins, E. M., Catt, K. A., Cody, P. A., Happe, C. L., & Cui, X. T. (2017). Enhanced dopamine detection sensitivity by PEDOT/graphene oxide coating on in vivo carbon fiber electrodes. *Biosens Bioelectron*, 89(Pt 1), 400-410.
- Valenstein, E. S. (2002). The discovery of chemical neurotransmitters. *Brain Cogn*, 49(1), 73-95.
- Venton, B. J., Michael, D. J., & Wightman, R. M. (2003a). Correlation of local changes in extracellular oxygen and pH that accompany dopaminergic terminal activity in the rat caudate-putamen. *J Neurochem*, 84(2), 373-381.
- Venton, B. J., Troyer, K. P., & Wightman, R. M. (2002). Response times of carbon fiber microelectrodes to dynamic changes in catecholamine concentration. *Anal Chem*, 74(3), 539-546.
- Venton, B. J., Zhang, H., Garris, P. A., Phillips, P. E., Sulzer, D., & Wightman, R. M. (2003b). Real-time decoding of dopamine concentration changes in the caudate-putamen during tonic and phasic firing. *J Neurochem*, 87(5), 1284-1295.
- Vreeland, R. F., et al. (2015). Biocompatible PEDOT:Nafion composite electrode coatings for selective detection of neurotransmitters in vivo. *Anal Chem*, 87(5), 2600-2607.
- Waldhoer, M., Bartlett, S. E., & Whistler, J. L. (2004). Opioid receptors. *Annu Rev Biochem*, 73(1), 953-990.
- Wightman, R., et al. (2007). Dopamine release is heterogeneous within microenvironments of the rat nucleus accumbens. *Eur J Neurosci*, 26(7), 2046-2054.
- Wightman, R. M. (1981). Microvoltammetric electrodes. *Anal Chem*, 53(9), 1125A-1134A.
- Wightman, R. M., et al. (1988). Real-time characterization of dopamine overflow and uptake in the rat striatum. *Neuroscience*, 25(2), 513-523.
- Wightman, R. M., Deakin, M. R., Kovach, P. M., Kuhr, W. G., & Stutts, K. J. (1984). Methods to improve electrochemical reversibility at carbon electrodes. *J Electrochem Soc*, 131(7), 1578-1583.
- Wightman, R. M., Strope, E., Plotsky, P. M., & Adams, R. N. (1976). Monitoring of transmitter metabolites by voltammetry in cerebrospinal fluid following neural pathway stimulation. *Nature*, 262(5564), 145-146.
- Wipf, D. O., & Wightman, R. M. (1988). Submicrosecond measurements with cyclic voltammetry. *Anal Chem*, 60(22), 2460-2464.
- Xiao, N., & Venton, B. J. (2012). Rapid, sensitive detection of neurotransmitters at microelectrodes modified with self-assembled SWCNT forests. *Anal Chem*, 84(18), 7816-7822.

- Yang, C., Trikantopoulos, E., Jacobs, C. B., & Venton, B. J. (2017). Evaluation of carbon nanotube fiber microelectrodes for neurotransmitter detection: Correlation of electrochemical performance and surface properties. *Anal Chim Acta*, 965, 1-8.
- Yang, C., et al. (2016). Laser Treated Carbon Nanotube Yarn Microelectrodes for Rapid and Sensitive Detection of Dopamine in Vivo. *ACS sensors*, 1(5), 508-515.
- Zachek, M. K., Hermans, A., Wightman, R. M., & McCarty, G. S. (2008). Electrochemical dopamine detection: comparing gold and carbon fiber microelectrodes using background subtracted fast scan cyclic voltammetry. *J Electroanal Chem (Lausanne)*, 614(1), 113-120.
- Zachek, M. K., Park, J., Takmakov, P., Wightman, R. M., & McCarty, G. S. (2010). Microfabricated FSCV-compatible microelectrode array for real-time monitoring of heterogeneous dopamine release. *Analyst*, 135(7), 1556-1563.
- Zimmerman, J. B., & Wightman, R. M. (1991). Simultaneous electrochemical measurements of oxygen and dopamine in vivo. *Anal Chem*, 63(1), 24-28.

## CHAPTER 2: DOPAMINE DYNAMICS DURING CONTINUOUS INTRACRANIAL SELF-STIMULATION: EFFECT OF WAVEFORM ON FSCV DATA<sup>1</sup>

### INTRODUCTION

Intracranial self-stimulation (ICSS), in which animals are trained to respond for electrical stimulation of the brain, is a central paradigm for investigating brain reward pathways that are activated by drugs of abuse and natural reward-seeking behavior (Carlezon & Chartoff, 2007; Fulton et al., 2000; Olds & Milner, 1954). The neurotransmitter dopamine has long been associated with this task in anatomical (Fibiger et al., 1987; Phillips & Fibiger, 1978) and pharmacological (Carlezon & Chartoff, 2007; Wise, 1996) studies. For instance, drugs that target the dopaminergic system, such as amphetamine, cocaine, and other dopamine receptor-specific ligands, alter ICSS behavior even in well-trained animals (Carlezon & Chartoff, 2007; Steinberg et al., 2014; Wise, 1996). Furthermore, regions that promote the strongest ICSS responding when stimulated contain dopaminergic neurons (Corbett & Wise, 1980). However, the role of direct activation of these neurons has been controversial (Gallistel et al., 1981). Paired-pulse collision studies of the medial forebrain bundle (MFB) have implicated large, myelinated descending fibers to the ventral tegmental area (VTA) as the principal neuronal population activated with typical electrical stimulation parameters, while suggesting that direct activation of small, unmyelinated dopamine neurons makes only a minor contribution (Bielajew & Shizgal, 1986; Yeomans et al., 1988). Instead, separate neurons are thought to activate dopamine cells trans-synaptically during ICSS through the release of excitatory

---

<sup>1</sup> This chapter previously appeared as an article in ACS Chemical Neuroscience. The original citation is as follows: Rodeberg, N.T., Johnson, J.A., Bucher, E.S., & Wightman, R.M. "Dopamine Dynamics during Continuous Intracranial Self-Stimulation: Effect of Waveform on Fast-Scan Cyclic Voltammetry Data," *ACS Chemical Neuroscience* 7, no. 11 (2016): 1508.

neurotransmitters, such as acetylcholine (Yeomans & Baptista, 1997) and glutamate (Sombers et al., 2009). Nevertheless, selective activation of dopaminergic neurons using optogenetics is sufficient to drive self-stimulation behavior (Berrios et al., 2016; Steinberg, et al., 2014; Witten et al., 2011).

Direct measurements of dopamine release during ICSS were first made using microdialysis, which monitors gradual changes in tonic extracellular dopamine levels. This technique typically displays increased dopamine concentrations during ICSS followed by a decline to basal levels following trial termination (Fiorino et al., 1993; Hernandez et al., 2006; You et al., 2001). The development of fast-scan cyclic voltammetry (FSCV) permitted the measurement of dopamine dynamics on a time scale relevant to behavioral responding (i.e. phasic dopamine release) (Garris et al., 1999; Kilpatrick et al., 2000; Owesson-White et al., 2008). In contrast to microdialysis measurements, FSCV measurements in the nucleus accumbens (NAc) have revealed a progressive decline in electrically-evoked release during continuous ICSS, with no detectable dopamine release present in later periods of ICSS behavior despite long timeouts between behavioral sessions (Garris, et al., 1999). This led to the conclusion that phasic dopamine release was not necessary for the maintenance of ICSS behavior, an unexpected finding given previous pharmacological evidence.

However, it remains unclear whether phasic dopamine release was fully abolished or rather fell to undetectable levels. Advances in the field of FSCV have improved the technique's limit of detection (LOD). In the original study, dopamine concentrations were evaluated using univariate analysis, which did not account for contributions from pH or noise present in the experimental CV. Since then, multivariate calibration has become standard for analyzing voltammetric data collected in awake animals (Heien et al., 2004; Heien et al., 2005; Kishida et al., 2016; Yorgason et al., 2011). One such technique, principal component regression (PCR), has been extensively characterized and validated for FSCV (Heien, et al., 2004; Heien, et al., 2005; Keithley et al., 2010; Keithley et al., 2009) and is able to separate and quantitate multiple

electroactive species of interest whilst diminishing noise contributions, allowing for more effective isolation of the dopamine signal (Keithley, et al., 2010).

The original measurements made with carbon-fiber microelectrodes used a voltammetric waveform with an anodic limit of +1.0 V. Subsequent studies have shown that the use of a higher anodic limit promotes the generation of surface oxides that facilitate the adsorption of dopamine, enhancing sensitivity (Heien et al., 2003; Takmakov et al., 2010). Additionally, extended anodic limits also provide active and continuous regeneration of the carbon-fiber surface (Takmakov, et al., 2010), which permits the maintenance of high sensitivity throughout the measurement period. When PCR and extended waveforms are combined, the consequent decrease in the LOD may allow the monitoring of smaller dopamine transients previously unobservable with the use of the +1.0 V waveform and univariate analyses.

In this study, dopamine fluctuations during continuous ICSS were re-evaluated using three voltammetric waveforms commonly employed *in vivo* (anodic limits of +1.0 V, +1.3 V, and +1.4 V vs. Ag/AgCl) and PCR. This approach reveals that phasic dopamine release is not abolished during ICSS, but rather decays to smaller, steady-state levels previously undetectable with less sensitive methods. However, higher anodic limits result in diminished temporal resolution that precludes the ability to separate individual transients during rapid responding, and subsequently, the delineation of how dopamine release changes during this task. Therefore, the waveform utilized considerably impacts the amplitude and time course of voltammetric data collected in freely-moving animals. Failure to recognize these differences could lead to a misinterpretation of the role of dopamine in this reward-based behavior.

## **EXPERIMENTAL**

### **Animals**

Male Sprague-Dawley rats (250-450 g) from Charles River (Wilmington, MA, USA) were housed individually on a 12/12 h light/dark cycle. Rats were given access to water and foods

chow *ad libitum*. Animal procedures were approved by the UNC-Chapel Hill Institutional Animal Care and Use Committee (IACUC).

## **Surgery**

Animals were anesthetized using isoflurane (1.5-4%). Guide cannulas for the working electrode (Bioanalytical Systems, West Lafayette, IN) were implanted above the NAc shell using stereotaxic coordinates (AP +1.7 mm, ML +0.8 mm, DV 2.5 mm). A separate guide cannula was implanted in the contralateral hemisphere to allow experiment-day lowering of a fresh Ag/AgCl reference electrode. A bipolar stimulating electrode (Plastics One, Roanoke, VA) was positioned above the ipsilateral VTA (AP -5.2 mm, ML +1.0 mm, DV -8.4-8.8 mm ventral from skull surface). Stainless steel screws and dental cement were used to secure the cannulas and stimulating electrode to the skull surface. Animals were given a minimum of three days of post-surgery recovery before behavioral training.

For biofouling experiments, surgical preparation differed slightly. Animals were anesthetized with urethane, and no stimulating electrode or guide cannulas were used. Fresh carbon-fiber and Ag/AgCl electrodes were used for implantation.

## **Behavior**

Rats were trained in intracranial self-stimulation following protocol described previously (Garris, et al., 1999). Rats were placed in plexiglass operant chambers (Med Associates Inc., St. Albans, VT, USA) and connected to head-mounted voltammetric amplifier attached to a commutator (Crist Instrument Co., Hagerstown, MD, USA) that permitted movement within the behavioral chamber. Stimulation current was applied through a optically isolated current source (NeuroLog NL-800, Medical Systems, Greenvale, NY, USA) and adjusted to the maximal current that did not evoke strong motor responses that would prevent reliable behavior (24 biphasic pulses, 60 Hz, 2 ms pulses, 75-175  $\mu$ A). Following current adjustment, the behavioral

session was initiated with the onset of white noise, cue light illumination, and lever extension into the chamber. All behavioral events were controlled with a MedAssociates system. Rats were primed with electrical stimulation as they approached the lever until they learned to respond (lever press; fixed-ratio 1, FR1) for self-administered electrical stimulation. Care was taken to minimize the number of non-contingent stimulations, and non-contingent stimulation was not administered during training once rats had acquired ICSS (i.e. spend entirety of training session responding for ICSS). Rats were trained for a minimum of two sessions per day for a minimum of three days (maximum of five). Occasionally, rats were trained for a third session during the first two days of training. The lever was retracted for 30 min between behavioral sessions. All rats used for voltammetric recordings acquired and maintained ICSS (i.e. pressed for the entire duration of lever presentation) for the final two testing days without need for non-contingent stimulations.

## **FSCV**

Glass-sealed carbon-fiber microelectrodes (90-110  $\mu\text{m}$  in length) were lowered into the nucleus accumbens through micromanipulators placed in the implanted guide cannula. On experiment day, freshly coated Ag/AgCl reference electrodes were implanted into the contralateral hemisphere. Electrodes were cycled (approximately 15 min at 60 Hz, 15 min at 10 Hz) before electrochemical measurements to minimize the contribution of electrode drift to the signal. All waveforms employed the same scan rate (400 V/s) and holding potential (-0.4 V), while anodic limits varied (+1.0, +1.3, and +1.4 V). Dopamine release was monitored for a minimum of fifty electrical stimulations per ICSS session in all animals. The session duration required to meet this criteria varied, depending on press rate (mean: 167 seconds, range from 89 to 318 seconds).

For FSCV recordings in anesthetized animals ( $n = 8$ ), stimulated release events (300  $\mu\text{A}$ , 24 pulses) were measured in the NAc. For within-subject comparisons, stimulated release

was measured with all three waveforms (+1.0, +1.3, and +1.4 V; n = 6 stimulations per waveform) in a sequential manner. The electrode was cycled (15 min at 60 Hz, 15 min at 10 Hz) each time a new waveform was employed.

Data was collected using HDCV programming (UNC-Chapel Hill, NC, USA) (Bucher et al., 2013) built in LabView (National Instruments, Austin, TX, USA). Voltammetric current was transduced through locally constructed UEI potentiostat instrumentation (UNC Electronics Facility). Data was digitally filtered (4<sup>th</sup> order low pass Bessel, 2 KHz cutoff).

### **Data analysis**

Dopamine concentrations were predicted using principal component regression (PCR) using residual analysis following previously established protocol and software (Bucher, et al., 2013; Heien, et al., 2004; Keithley, et al., 2009). Training sets were built using dopamine and pH standards recorded *in vivo* post-experiment from the same electrode and recording location as the collected data (Rodeberg et al., 2015). Dopamine transients for which  $Q_t$  exceeded  $Q_a$  at  $[DA]_{max}$  were excluded from data analysis. Individual release events were analyzed by aligning the voltammetric background to the time of stimulation (preceding the stimulation by 0-2 s) for each individual event, minimizing the interference from electrode drift or additive pH changes from successive stimulation that would exceed the training set range. In a few longer behavioral trials, the number of transients of analyzed was limited to the first 70 electrical stimulations to keep data set sizes comparable.

To ensure measurement of low concentration dopamine transients was reliable, a limit of detection (LOD) was calculated for each separate electrode. Data were collected at the same recording site as ICSS measurements, but without electrical stimulation, to estimate noise levels. The LOD was established as 3\*RMS in the chemometrized dopamine signal.

## Statistical analysis

Results are presented as mean  $\pm$  SEM. Statistical tests were performed in GraphPad Software, with results considered significant if  $p < 0.05$ . One-way ANOVAs were used for comparisons between the three different waveforms. Repeated measures one-way ANOVAs were used when the outcomes were quantitative, independent variables were nominal, and multiple observations were made with each unit. Two-way repeated measures ANOVAs were conducted to test the effect of two independent variables on a single dependent variable. If significant differences were found for any ANOVA test, Tukey's multiple comparisons *post hoc* test was used to make pairwise comparisons. A two-tailed t-test was used to compare the average concentrations between the two ICSS sessions.

## Flow Cell analysis

External calibration factors were determined using flow injection analysis. All dopamine solutions were prepared in TRIS buffer (3.25 mM KCl, 1.2 mM  $\text{CaCl}_2 \cdot 2\text{H}_2\text{O}$ , 1.2 mM  $\text{MgCl}_2 \cdot 6\text{H}_2\text{O}$ , 2.0 mM  $\text{Na}_2\text{SO}_4$ , 1.25 mM  $\text{NaH}_2\text{PO}_4 \cdot \text{H}_2\text{O}$ , 140 mM NaCl, 15 mM Trizma HCl) adjusted to pH 7.4 with NaOH. Dopamine solutions were bubbled under  $\text{N}_2$  to prevent oxidative degradation of dopamine during successive calibrations. For sensitivity factor measurements between waveforms, a physiological range of dopamine concentrations (50 nM - 2  $\mu\text{M}$ ) was used. For biofouling measurements, point calibrations at 1  $\mu\text{M}$  for both pre- and post-calibration were used. All calibration currents were normalized by electrode length to 100  $\mu\text{m}$ .

## RESULTS

### Anodic limit and stimulated release in anesthetized animals

Early FSCV measurements of dopamine release in awake animals were made using a voltammetric waveform scanning from a holding potential of -0.4 V to an anodic limit of +1.0 V (Garris et al., 1997; Rebec et al., 1997). While the resulting sensitivity was adequate to measure real-time dopamine release during initial ICSS responding (Garris, et al., 1999), the dopamine signal disappeared after multiple lever presses and did not reappear even following a 30 min timeout. It was unclear whether this was due to insufficient sensitivity or the absence of dopamine release at these later times. Subsequent investigation into the effect of the anodic waveform limit showed increased sensitivity using an anodic limit of +1.4 V (Heien, et al., 2003), with an anodic limit of +1.3 V later subsequently taken as optimal for dopamine measurements. The relative sensitivities to dopamine of these waveforms are evident in their *post vivo* calibration factors (normalized to 100  $\mu\text{m}$  fiber lengths; +1.0 V waveform,  $3.9 \pm 0.2 \text{ nA}/\mu\text{M}$ ; +1.3 V waveform,  $11.8 \pm 0.8 \text{ nA}/\mu\text{M}$ ; +1.4 V waveform,  $28.8 \pm 3.3 \text{ nA}/\mu\text{M}$ ).

While the effect of the anodic limit on dopamine sensitivity has been well characterized *in vitro* (Heien, et al., 2003; Keithley et al., 2011), its effect on temporal responses during measurements of dopamine release events *in vivo* is less clear. To investigate this, measurements of electrically stimulated (24 pulses, 300  $\mu\text{A}$ , 60 Hz,  $n = 6$  for each waveform at each electrode) dopamine release were made in the NAc shell of anesthetized rats ( $n = 8$ ). Due to the heterogeneity of dopamine release kinetics in the NAc (Wightman et al., 2007), measurements were made using all three waveforms at each recording site to enable within-subject comparisons (Figure 2.1a). Because the more positive anodic limits alter the electrode surface (Takmakov, et al., 2010), measurements were made in ascending order of anodic limit to prevent effects of prior history on electrode responses. Peak evoked dopamine concentrations ( $[\text{DA}]_{\text{max}}$ ), rise time (10-90% max signal), and  $t_{1/2}$  values (100-50%) were

Waveform	[DA] <sub>max</sub>	Rise Time (10-90%)	t <sub>1/2</sub> (100-50%)
+1.0 V	267 ± 64 nM	0.3 ± 0.05 s	0.5 ± 0.05 s
+1.3 V	321 ± 78 nM	0.3 ± 0.02 s	0.7 ± 0.05 s
+1.4 V	244 ± 56 nM	0.3 ± 0.02 s	1.1 ± 0.08 s

**Table 2.1.** Comparisons of [DA]<sub>max</sub>, rise time, and t<sub>1/2</sub> between different waveforms. Data is expressed as mean ± SEM (n = 8 for each data set).

compared across waveforms (Table 2.1). No significant differences in  $[DA]_{\max}$  were seen between waveform (repeated measures one-way ANOVA,  $F_{2,14} = 3.814$ ,  $p > 0.05$ ). While differences were not observed in the rise time (10-90% max signal) for electrically evoked transients across waveforms (repeated measures one-way ANOVA,  $F_{2,14} = 0.1273$ ,  $p > 0.05$ ), there were significant differences in  $t_{1/2}$  values (100-50%) (repeated measures one-way ANOVA,  $F_{(2,14)} = 39.94$ ,  $p < 0.0001$ ). Tukey's multiple comparisons post hoc test revealed significant differences between the +1.4 V waveform and both the +1.0 V and +1.3 V waveforms ( $p < 0.001$ ) but not between the +1.0 V and +1.3 waveform ( $p > 0.05$ ). The falling portion of the dopamine signal is a measure of the response time of the electrode as well as an index of the uptake rate mediated by the dopamine transporter. The results here demonstrate that the diminished temporal response of higher anodic limit waveforms preferentially affects the uptake-dominated region of electrically-stimulated release events, while minimally affecting the region dominated by release.

Differences in the voltammetric characteristics of dopamine across waveforms are also evident. More negative anodic peak locations (Figure 2.1b), more positive cathodic peak locations (Figure 2.1c), and smaller anodic peak widths (Figure 2.1d) were seen with extended waveforms compared to the +1.0 V waveform. These observations are consistent with enhanced electron transfer kinetics (Bard & Faulkner, 2001), likely due to generation of surface oxide groups. Consistent with a previous study showing differences in voltammetric characteristics across electrodes (Rodeberg, et al., 2015), the potential of the anodic peak for dopamine on the +1.3 V waveform varied over a range of 40 mV. Significant differences were also seen in the peak current ratios between waveforms (Figure 2.1e). This is likely due to a greater contribution of adsorption to the signal on extended waveforms. As the oxidized form of dopamine (dopamine-o-quinone) adsorbs less strongly than dopamine, it is more likely to desorb before its subsequent reduction (Bath et al., 2000), resulting in an enhanced  $i_{p,a}/i_{p,c}$  ratio.

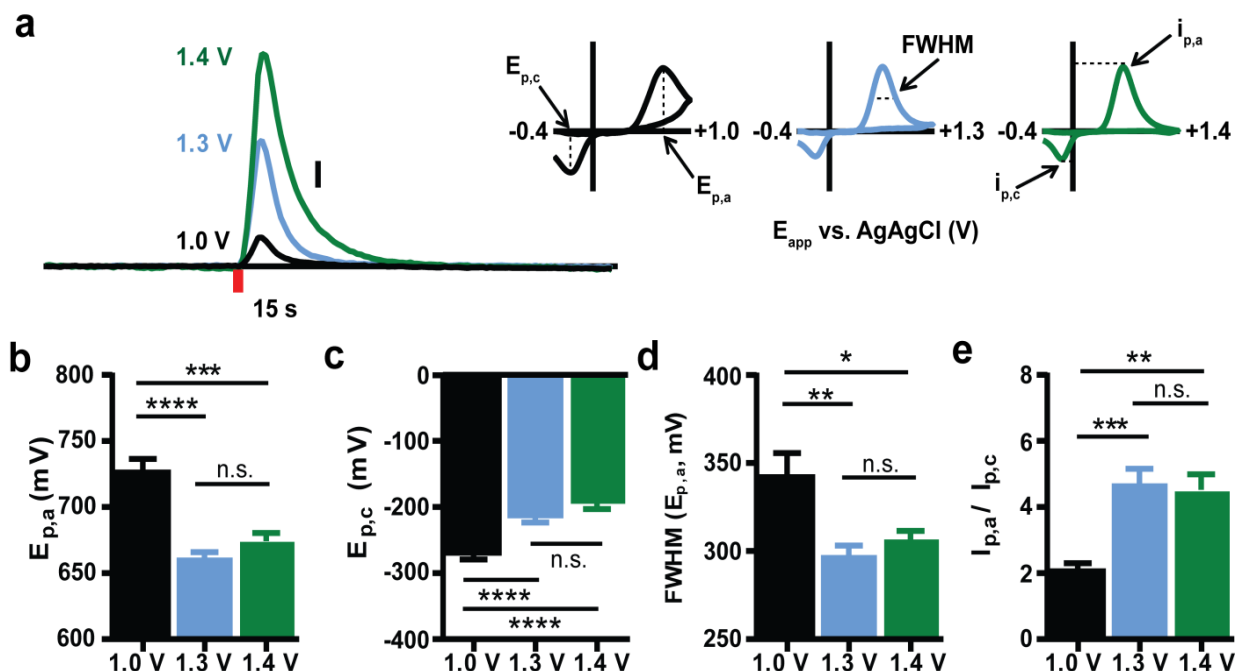


**Figure 2.1.** Differences in cyclic voltammogram characteristics across waveforms. a) Electrically evoked dopamine release measured with each waveform in an anesthetized rat, with inset cyclic voltammograms displayed for each waveform. Voltammogram characteristics of interest are labeled. b) Anodic peak potentials ( $E_{p,a}$ ) varied significantly across separate waveform anodic limits at the same electrode (+1.0 V waveform,  $728 \pm 9$  mV; +1.3 V waveform,  $662 \pm 4$  mV; +1.4 V waveform,  $674 \pm 6$  mV),  $***p < 0.001$ ,  $****p < 0.0001$ . c) Cathodic peak potentials significantly varied across waveforms (+1.0 V waveform,  $-273 \pm 6$  mV; +1.3 V waveform,  $-217 \pm 6$  mV; +1.4 V waveform,  $-194 \pm 9$  mV),  $*p < 0.05$ . d) The full-width at half maximum (FWHM) for the anodic peak varied significantly across waveforms (+1.0 V waveform,  $344 \pm 12$  mV; +1.3 V waveform,  $298 \pm 5$  mV; +1.4 V waveform,  $307 \pm 5$  mV),  $**p < 0.01$ . e) The ratio of the peak anodic current to the magnitude of the peak cathodic current varied significantly across waveforms (+1.0 V waveform,  $2.15 \pm 0.15$ ; +1.3 V waveform,  $4.72 \pm 0.4$ ; +1.4 V waveform,  $4.53 \pm 0.5$ ). Error bars reflect standard error, based on the number of electrodes.

## Phasic dopamine concentrations during continuous ICSS

To address whether the sustained absence of the dopamine signal in early studies was due to insufficient sensitivity, ICSS measurements were repeated with the original +1.0 V waveform and compared to measurements with more sensitive voltammetric waveforms (+1.3 V and +1.4 V). Rats were trained to respond on a fixed-ratio 1 (FR1, lever press) schedule for electrical stimulation of the substantia nigra/ventral tegmental area (SN/VTA) region following previous protocol (Garris, et al., 1999). To prevent severe motor responses associated with the large current intensities used in anesthetized animals (300  $\mu$ A), smaller current intensities were used for ICSS training and recordings (75-175  $\mu$ A). Once trained, each rat was assigned one of the three waveform variations for data acquisition. Stimulation currents were not significantly different between waveforms (one-way ANOVA,  $F_{2,9} = 1.499$   $p > 0.05$ ). A carbon-fiber microelectrode was lowered into the NAc shell in 150  $\mu$ m increments until electrically-evoked dopamine release was detected and optimized (Wightman, et al., 2007), after which experimenter-delivered ('non-contingent') stimulations were administered to establish baseline DA release in the final recording location. Next, rats were allowed to press a lever continuously for a minimum of 50 electrical stimulations. This process was subsequently repeated 30 min later in a separate behavioral session.

For each ICSS session in each animal, dopamine maximal concentrations following each lever press (evoked by the electrical stimulation,  $[DA]_{\max}$ ) were determined by PCR and monitored as a function of stimulation number (Figure 2.2). Transients that failed residual analysis at  $[DA]_{\max}$  were considered 'invalid', and concentration values were not recorded (+1.0 V waveform, 17% of electrically-evoked transients; +1.3 V waveform, 2%; +1.4 V waveform, 2%).

While PCA reduces noise (Keithley, et al., 2010; Keithley, et al., 2009), some noise remains in the concentration traces. To ensure that dopamine was being measured at lower

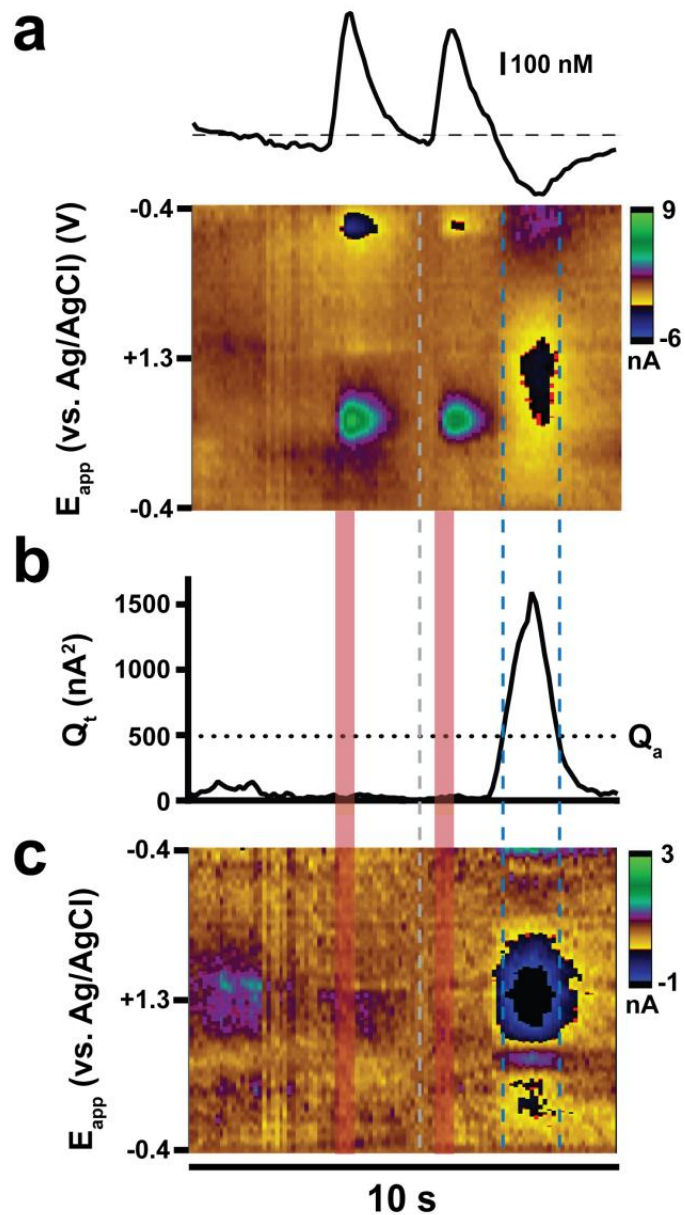


**Figure 2.2.** Depiction of ICSS data analysis. a) Ten second segments of data were aligned to the digital events representing electrical stimulation (red bars). Background was taken 0-2 seconds preceding electrical stimulation (grey dotted line), minimizing the contribution of drift or overlapping pH changes to concentration prediction. b) The residual trace for the corresponding ten second data segment in part (a). During data analysis,  $Q_t$  occasionally crossed  $Q_\alpha$  either during dopamine transients or during periods without electrical stimulation (ex. area between the two blue dotted lines). Data was discarded if these residual failures occurred at  $[DA]_{max}$ , while residual crosses during other time points did not impede concentration prediction. As shown by the dashed black line, the validity of the DA peak was maintained. c) Residual color plots exhibited which currents were not captured by the within-subject training set.

concentrations, we evaluated the limit of detection (LOD) for each voltammetric recording session. This was done with the electrode implanted in the brain at the recording locations where ICSS data was collected, but in the absence of electrical stimulation, to ensure that noise levels were similar to those during ICSS. To minimize the effects of short-term electrode drift, data was analyzed in 10 s intervals for LOD determination. Segments in which spontaneous dopamine transients were apparent in the color plot, or which failed residual analysis, were excluded from these LOD determinations. The apparent 'dopamine concentration' for each segment was extracted with PCR and the average noise of these segments (taken as three times the root mean square noise,  $n \geq 5$  separate replicates for each subject) was taken as the LOD of the data set. There were significant differences in LODs between waveforms (+1.0 V waveform,  $92 \pm 8$  nM; +1.3 V waveform,  $31 \pm 4$  nM; +1.4 V waveform,  $17 \pm 2$  nM,  $n=4$  respectively; one-way ANOVA,  $F_{2,9} = 17.21$ ,  $p < 0.001$ ). Tukey's multiple comparisons *post hoc* analysis revealed significant differences between +1.0 vs +1.3 and +1.4 ( $p < 0.01$  and  $0.001$ , respectively) but not +1.3 vs. +1.4 ( $p > 0.05$ ).

Concentrations evoked by electrical stimulation differed between animals, most likely due to differences in placements of the stimulating and working electrodes (concentration of first lever-press induced transient;  $355 \pm 66$  nM, range from 60 to 832 nM). These concentrations were not significantly correlated with stimulation current ( $r^2 = 0.236$ ,  $p > 0.05$ ). To make reliable comparisons across animals, concentrations and LOD values were normalized for each animal to the concentration of the first electrically-evoked ICSS transient in the first behavioral session.

Transients that fell below the within-subject LOD were discarded from analysis (+1.0 V waveform, 69% of valid transients; +1.3 V waveform, 0.02%; +1.4 V waveform, 0%). While  $[DA]_{\max}$  decreased with stimulation number with each waveform, the profile of dopamine release differed across waveforms (Figure 2.3). Measurements with an anodic limit of +1.0 V revealed a similar pattern to those seen in the original study (Figure 2.3a). Dopamine release was initially observed early in the first ICSS session; however, the transients quickly decreased to smaller

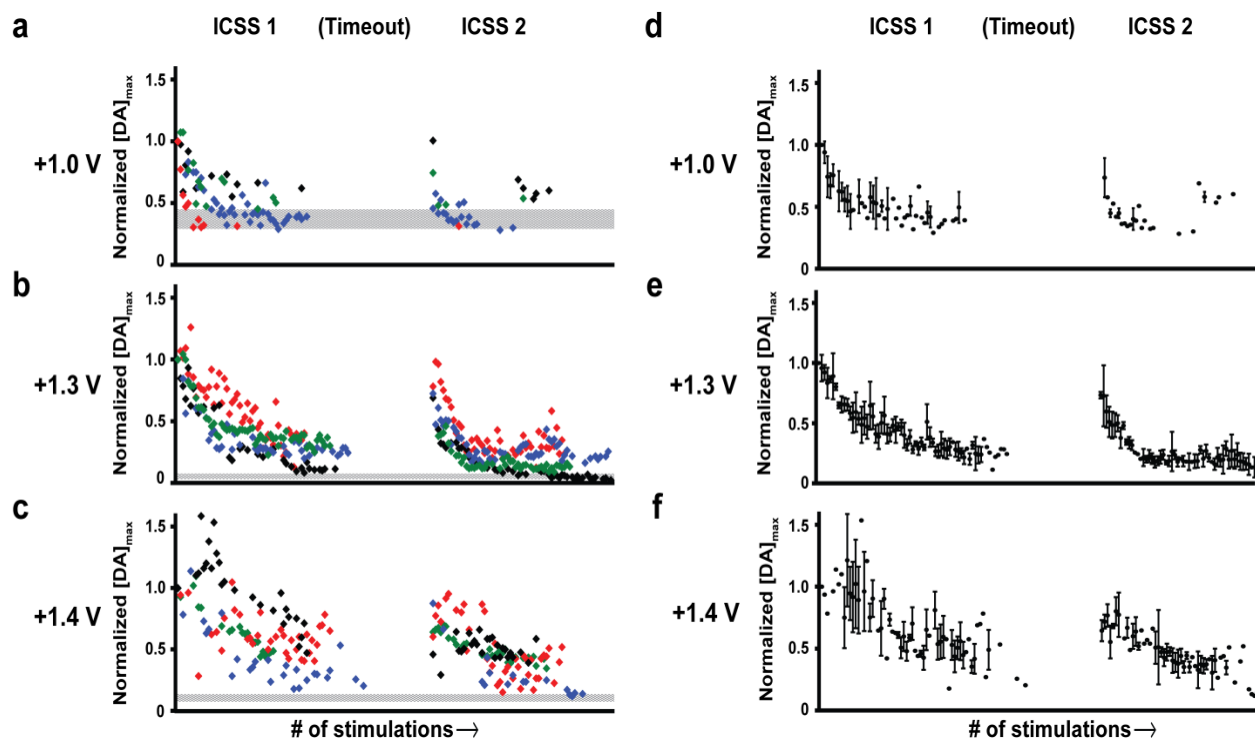


**Figure 2.3.** The amplitude of individual dopamine transients during and across ICSS sessions with different waveforms. Dopamine concentrations were normalized to the concentration of the first electrically-evoked transient of the first ICSS session for each separate subject. Transients that fell below the within-subject LOD (depicted by grey bar, mean  $\pm$  SEM) were discarded. Each waveform had four separate subjects, represented by the four different colors. a) Measurements on the +1.0 V waveform revealed a decrease in dopamine during the first ICSS session and few detectable transients in the subsequent session. b) Measurements on the +1.3 V waveform reveal decreases in dopamine in both ICSS sessions, with the majority of transients detected and quantifiable. c) Measurements on the +1.4 V waveform reveal decreases in dopamine in both ICSS sessions, but less consistency between recordings than measurements on the +1.3 V waveform. d-f) Average concentration profile for (d) the +1.0 V waveform, (e) +1.3 V waveform, and (f) +1.4 V waveform. Data points depict mean  $\pm$  SEM at each stimulation.

amplitudes, with most stimulations failing to produce dopamine transients exceeding the within-subject LOD (mean  $\pm$  SEM represented by grey bar). After a 30 min timeout, in which the lever and electrical stimulation were unavailable, dopamine release was only observed early in the subsequent ICSS session, while the vast majority of stimulations did not result in observable dopamine release. Due to the paucity of observable dopamine transients, it is difficult to determine a consistent trend for dopamine release during ICSS with this waveform across subjects (Figure 2.3d). The enhanced sensitivity of the +1.3 V waveform captured dopamine release throughout the entire ICSS recording session, with nearly all electrical stimulations evoking observable events (Figure 2.3b). Thus, more reliable comparisons of dopamine concentration values both within and across ICSS sessions could be made. The average dopamine concentrations across lever presses between animals exhibit a more rapid decay of dopamine during the second ICSS session (Figure 2.3e). Regression using a single-phase exponential decay ( $r^2 = 0.713$  and  $0.533$  for the two sessions, respectively) revealed a significantly larger rate constant for the second ICSS session, indicating a faster decline ( $p < 0.0001$ ). Correspondingly, the average (normalized) dopamine transient concentration was lower in the second session than in the first (ICSS 1:  $0.436 \pm 0.025$ , ICSS 2:  $0.231 \pm 0.017$ , two-tailed  $t$ -test,  $t_{135} = 6.753$ ,  $p < 0.0001$ ). Taken together, these data could explain the rapid disappearance of the dopamine signal measured on the +1.0 V waveform during the second ICSS session, with the transients more rapidly approaching undetectable values.

Measurements with the +1.4 V waveform also consistently resulted in observable dopamine signals release during ICSS (Figure 2.3c). In all rats ( $n = 4$ ), each electrical stimulation resulted in a detectable dopamine transient, partially due to the lower LODs observed with the +1.4 V waveform (average  $\sim 17$  nM). However, compared to measurements on the +1.3 V waveform, the concentration profile across stimulations differed. The average profiles (Figure 2.3f) fit a single-phase decay ( $r^2 = 0.408$  and  $0.478$  for the two sessions, respectively), but did not have significantly different rate constants ( $p > 0.05$ ). Nonetheless, the

average normalized concentration values were lower in the second ICSS session compared to the first (ICSS 1:  $0.684 \pm 0.034$ , ICSS 2:  $0.457 \pm 0.022$ , two-tailed  $t$ -test,  $t_{111} = 5.174$ ,  $p < 0.0001$ ).

A repeated-measures two-way ANOVA was performed to test for differences in press rate between waveform groups and ICSS sessions. No interaction was found between waveform and ICSS session ( $F_{2,9} = 0.690$ ,  $p > 0.05$ ). No main effect of waveform ( $F_{2,9} = 1.008$ ,  $p > 0.05$ ) or ICSS session ( $F_{1,9} = 1.733$ ,  $p > 0.05$ ) was observed. Therefore, the lower dopamine concentrations during the second ICSS session were not associated with changes in press rates. This is consistent with recent evidence that the amplitude of phasic dopamine release can be dissociated from pressing rate (Cossette et al., 2016).

### **Sensitivity determines ability to consistently monitor dopamine**

To understand why different voltammetric waveforms provide drastically different dopamine release profiles during ICSS, it is necessary to recognize the benefits and limitations of each. Representative traces for the first ICSS session are shown for three separate subjects measured with different waveforms (Figure 2.4). Representative data indicate the most common features with measurements using the +1.0 V waveform (Figure 2.4a). Non-contingent stimulation ('pre-ICSS') and the first lever press-induced stimulations during ICSS ('early ICSS') evoke sharp dopamine transients that surpass the LOD (red dotted line). However, electrical stimulations near the end of the ICSS session ('late ICSS') do not evoke observable dopamine signals. The inability to detect dopamine release is not due to complete dopamine depletion or electrode failure, as non-contingent stimulation following ICSS ('post-ICSS') resulted in observable dopamine transients (normalized concentration: ICSS 1,  $0.708 \pm 0.112$ ; ICSS 2,  $0.457 \pm 0.070$ ). Nonetheless, the smaller concentration of dopamine transients after prolonged stimulation prevents this waveform from providing a reliable measurement of dopamine release during this task.

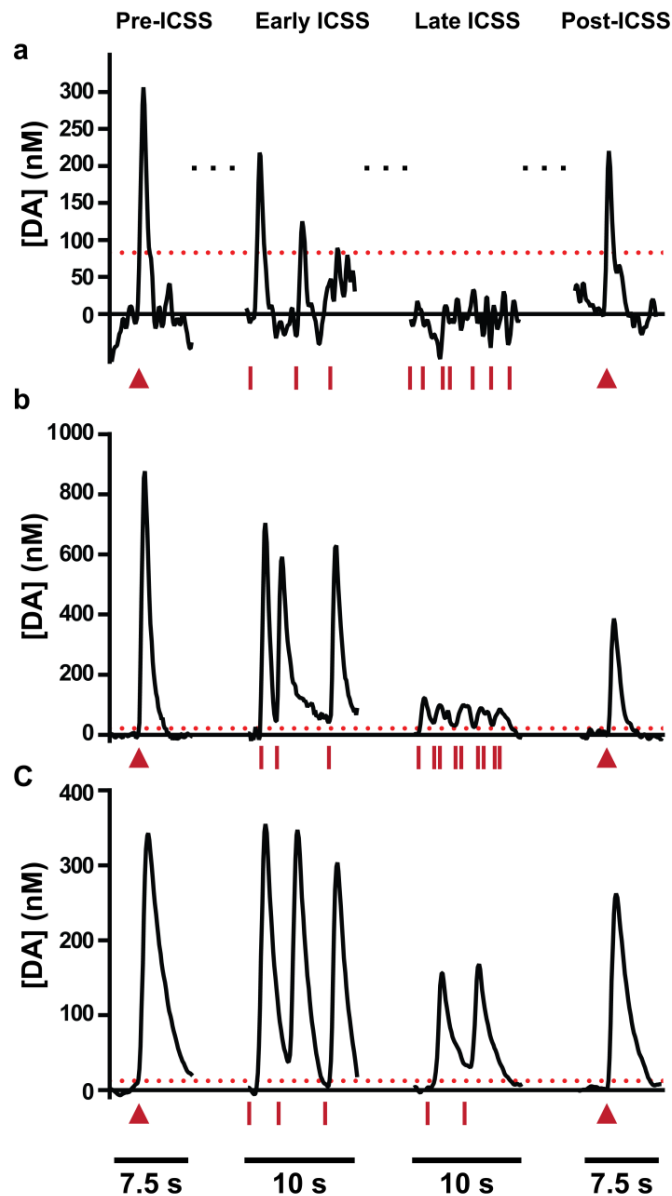


**Figure 2.4.** Dopamine concentration versus time traces for representative measurements on each waveform before, during, and after the first intracranial self-stimulation session. Red triangles and red bars represent non-contingent and operant-delivered electrical stimulation, respectively. Red dotted lines indicate LOD for each data set. a) Measurements on the +1.0 V waveform reveal electrically evoked dopamine transients above the LOD (85 nM) before and immediately after ICSS. During early ICSS, dopamine release exceeds the LOD but falls to undetectable levels later in the behavioral session. b) Measurements on the +1.3 V waveform consistently reveal dopamine release above the LOD (21 nM) before, during, and immediately after ICSS. Notably, dopamine release falls to much smaller levels late in the ICSS session after prolonged stimulation. c) Measurements on the +1.4 V waveform reveal electrically evoked dopamine transients above the LOD (12 nM) before, during, and immediately following ICSS.

Measurements with the +1.3 V and +1.4 V waveforms, however, were able to consistently monitor dopamine release (Figure 2.4b-c). While dopamine transients diminish in amplitude during ICSS, the enhanced sensitivity permits the measurement of dopamine transients that would be near or below the LOD on the +1.0 V waveform. The wider time course of the transients with these two waveforms compared to the +1.0 V waveform is consistent with the observations made in anesthetized animals.

No significant differences were seen between the concentrations evoked by the first-lever press during ICSS and non-contingent stimulation preceding the session (paired two-tailed t-test,  $t_{23} = 0.7367$ ,  $p > 0.05$ ). However, these two signals were significantly correlated across animals and sessions ( $r^2 = 0.804$ ,  $p < 0.0001$ ), with larger release to non-contingent stimulation predicting higher concentrations during ICSS.

### **Effect of biofouling on continuous measurements**

The diminished ability to detect dopamine on the +1.0 V waveform during the second ICSS session could be related to progressive biofouling of the carbon-fiber microelectrode. The sensitivity of carbon-fiber microelectrodes have been demonstrated previously to decrease upon implantation in the brain (Logman et al., 2000; Singh et al., 2011). Notably, waveforms with extended anodic limits have been shown be more resistant to biofouling due to active regeneration of the carbon-fiber surface (Takmakov, et al., 2010), which could explain their comparative success in monitoring dopamine during later time points. To investigate this issue, the relative concentration values of the non-contingent stimulations preceding each ICSS session were first compared. On all three waveforms, the electrically evoked signals preceding the second ICSS session were generally lower in amplitude than non-contingent stimulations preceding the first ICSS session (+1.0 V waveform,  $62.7 \pm 14.8\%$ ; +1.3 V waveform,  $68.3 \pm 10.3\%$ ; +1.4 V waveform,  $81.9 \pm 5\%$ ). While a general trend was observed across anodic limits, no systematic difference was seen between signal recovery and waveform (one-way ANOVA,

$F_{2,11} = 0.815, p > 0.05$ ). Furthermore, the magnitude of signal depression was not significantly correlated with the time between the two sets of non-contingent stimulations ( $43 \pm 2$  min;  $r^2 = 0.217, p > 0.05$ ) or stimulation current ( $r^2 = 0.082, p > 0.05$ ).

Despite the lacks of correlation between the timing of non-contingent stimulation and signal depression, the results could be confounded by the variation in implantation time between subjects. Therefore, further biofouling experiments were performed to test the effect of precise implantation times on the sensitivity loss due to *in vivo* biofouling for each waveform. Carbon-fiber microelectrodes were calibrated before and after 60 or 90 min of implantation in anesthetized rat brain (Table 2.2). A two-way ANOVA revealed no interaction between implantation duration and waveform ( $F_{2,24} = 0.1936 p > 0.05$ ) or main effect of implant duration ( $F_{1,24} = 0.0621, p > 0.05$ ) on post-calibration sensitivity. However, there was a main effect of waveform ( $F_{1,24} = 46.37, p < 0.0001$ ). Tukey's multiple comparisons post hoc revealed significant differences between the +1.4 V waveform signal recovery and both the +1.0 V and +1.3 V waveform at both implant durations ( $p > 0.0001$ ) but not between the +1.0 V and +1.3 V waveform ( $p > 0.05$ ). Interestingly, the +1.4 V waveform maintained pre-implantation sensitivity for both implant durations, likely due to continued conditioning of the electrode surface during *in vivo* implantation. Consequently, while the trend in post-calibration sensitivity across waveforms is similar to the trends in restoration of the dopamine signal, the failure to completely restore the signal when measuring with the +1.4 V waveform suggests that biofouling is not the sole determinant of the decay in the dopamine signal.

### **Temporal resolution determines ability to reliably quantitate rapidly spaced transients**

It has been previously demonstrated that temporal resolution is reduced at extended anodic limits (Heien, et al., 2003). Indeed, this is apparent in Figure 2.4, as electrically evoked dopamine transients measured on extended waveforms, particularly with the +1.4 V waveform, are broader than those measured on the +1.0 V waveform. This is of particular concern for the

Waveform	1 hr	1.5 hr
+1.0 V	44.5 ± 6.1%	37.9 ± 5.8%
+1.3 V	51.4 ± 4.2%	51.4 ± 5.8%
+1.4 V	106.4 ± 12.1%	108.5 ± 7.7%

**Table 2.2.** The post-implantation sensitivity for different implantation durations (1 hour, 1.5 hours) and waveforms. Values expressed as mean ± SEM. n = 5 for all pairs of waveform-duration.

continuous ICSS paradigm, which permits the rat to press the lever for electrical stimulation *ad libitum*, receiving a maximum of one stimulation every 400 ms (i.e. the duration of electrical stimulus). Thus, it is possible in this paradigm for rats to undergo rapid bouts of pressing in which dopamine transients become difficult to resolve due to the finite response time of the carbon-fiber microelectrodes.

To demonstrate how this effect varies across waveforms, three representative thirty second segments of similar pressing rates collected on different waveforms are shown in Figure 2.5. Lever presses generally induce transients that rapidly return to baseline when measured with the +1.0 V waveform (Figure 2.5a). With a similar press rate, measurements on the +1.3 V waveform also result in resolvable transients, but baseline is not always reached between each transient (Figure 2.5b). When baseline is not reached, an apparent ‘facilitation’ in the signal occurs as previous transients contribute to  $[DA]_{\max}$  for subsequent events (see transients 3-4, Figure 2.5b). Similar results can be seen for measurements with the +1.4 V waveform (data not shown); however, moderate pressing rates occasionally resulted in a rising envelope of dopamine signal with superimposed individual transients (Figure 2.5c). While digital background subtraction immediately before each transient can partially diminish the contribution of this ‘envelope’ to  $[DA]_{\max}$ , it cannot eliminate background rises occurring during the dopamine transients themselves. As a result, these temporally distorted signals can lead to overestimations of  $[DA]_{\max}$ , and can make it difficult to ascertain how electrically evoked release is changing on a stimulation-by-stimulation basis.

In addition to rising ‘envelopes’ interfering with quantitation of  $[DA]_{\max}$ , the rapid nature of continuous ICSS can lead to individual transients becoming unresolvable when stimulations are too narrowly spaced (see presses 6-7 in Figure 2.5a, presses 9-11 in Figure 2.5c). The diminished temporal resolution of extended waveforms exacerbates this problem. To investigate this, the percentage of observable transients (i.e. those above the LOD and passing residual analysis) resolved at half-maximum from the preceding transient was determined for each ICSS

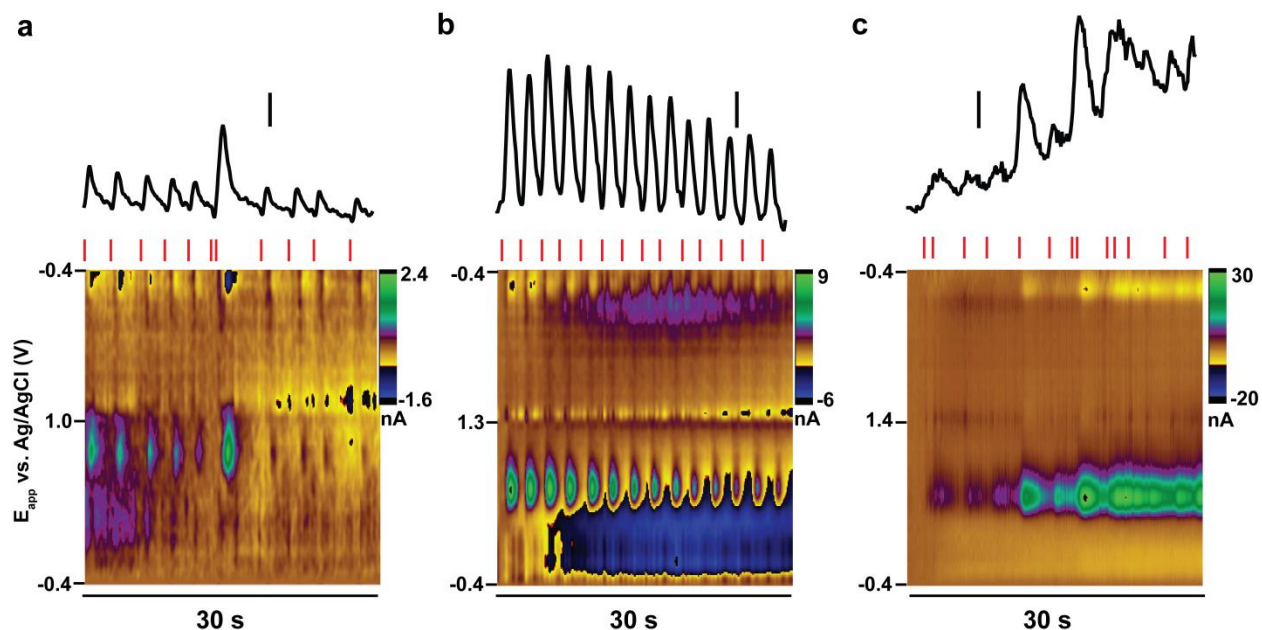


**Figure 2.5.** Temporal resolution is diminished with extended anodic limits. a) Measurements on the +1.0 V waveform reveal that electrical stimulation evokes transient increases in dopamine concentration that rapidly return to baseline before subsequent transients. b) Measurements on the +1.3 V waveform typically reveal resolved transients at moderate pressing frequencies, though dopamine concentrations do not always return to baseline before onset of subsequent transients, leading to apparent ‘facilitations’ in the DA signal. c) Measurements on the +1.4 V waveform suffer from drastically diminished temporal resolution. Some cases of moderate pressing rates revealed rising envelopes of DA signal with superimposed transients, making it difficult to ascertain how dopamine dynamics were changing on a stimulation-by-stimulation basis.

session on each waveform. If resolved at half-maximum it was assumed that the preceding transient will minimally contribute to  $[DA]_{\max}$  of the subsequent transient. Transients that did not meet this criteria were excluded from Figure 2.2. The ability to resolve transients significantly decreased at extended anodic limits (Figure 2.6a). (one-way ANOVA,  $F_{2,21} = 15.95$ ,  $p < 0.0001$ ). Tukey's multiple comparisons post hoc test revealed significant differences in the percent resolution between anodic limits of +1.0 V and +1.4 V ( $p < 0.0001$ ) and between +1.3 V and +1.4 V ( $p < 0.01$ ) but not between +1.0 V and +1.3 V ( $p > 0.05$ ).

However, the resolution of adjacent transients is also impacted by the pressing rate of the animal, as higher pressing rates will result in more narrowly separated dopamine events. Therefore, the percent resolution was compared to the pressing rate for each corresponding ICSS session for each waveform (Figure 2.6b). Linear fits to the data show a relatively flat profile for data collected on the +1.0 V waveform, indicating detectable transients are readily resolved at moderate to high pressing rates. The +1.3 V waveform performs well at lower pressing rates, but higher press rates result in diminished ability to resolve, and subsequently quantitate, adjacent dopamine transients. This effect is even more pronounced on the +1.4 V waveform, where temporal resolution suffers even at slower press rates and fails dramatically at higher pressing rates, where approximately half of transients were unable to be adequately resolved.

### **Balance of temporal resolution and sensitivity determine ability to monitor dopamine dynamics**

Taken together, these data suggest the ability to reliably determine the shape of the dopamine concentration profile during ICSS depends on the tradeoff between enhanced sensitivity and diminished temporal resolution. Only 23% of dopamine transients could be reliably quantified with the +1.0 V waveform, with a large percentage of presses (56%) resulting in unobservable events (Figure 2.3, Table 2.3). Conversely, measurements on the +1.3 V V

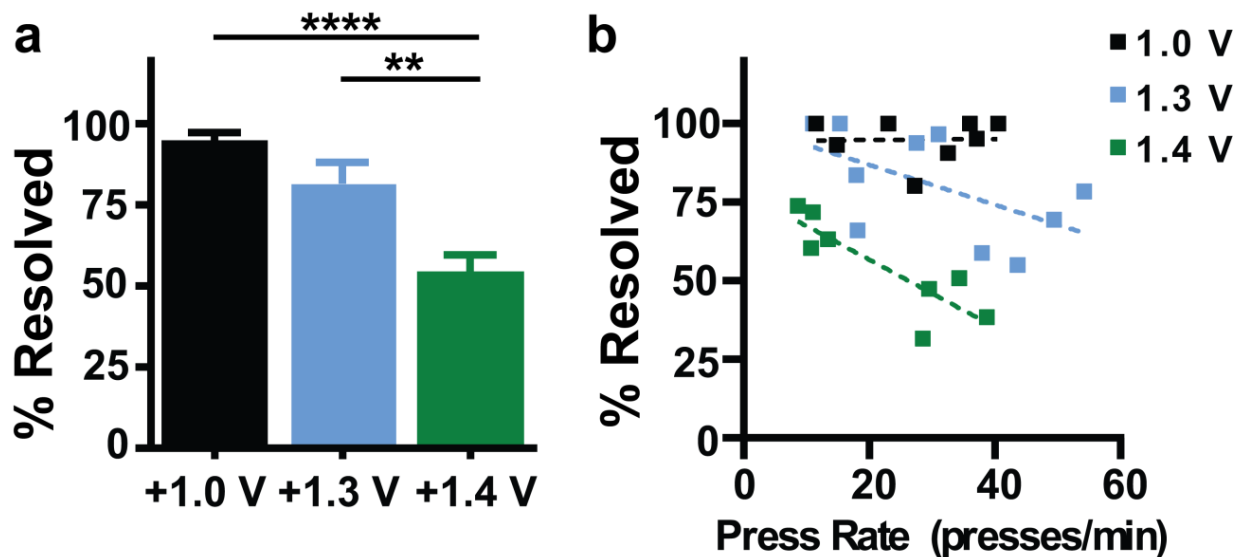


**Figure 2.6.** Temporal resolution and its dependence on pressing rate differ across waveforms. a) The percentage of transients that were resolved at half-maximum from the preceding transient differed amongst waveforms (+1.0 V waveform,  $95.0 \pm 2.5$  %; +1.3 V waveform,  $81.6 \pm 6.6$  %; +1.4 V waveform,  $54.8 \pm 5.4$  %). One way ANOVA with Tukey's multiple comparisons,  $**p < 0.01$ ,  $****p < 0.001$ . b) The effect of press rate on temporal resolution varied across waveforms. The temporal resolution of detectable transients on the +1.0 V waveform was relatively insensitive to the range of observed pressing rates. Measurements at higher pressing rates suffered from diminished temporal resolution on the +1.3 V waveform, while temporal resolution on the +1.4 V waveform was diminished at all pressing rates.

Waveform	# quantifiable	# undetected	# unresolved	# failed residual
<b>+1.0 V (n = 467)</b>	107 (23%)	262 (56%)	17 (4%)	81 (17%)
<b>+1.3 V (n = 448)</b>	381 (78%)	1 (0.02%)	96 (20%)	10 (2%)
<b>+1.4 V (n = 441)</b>	236 (54%)	0 (0%)	198 (45%)	7 (2%)

**Table 2.3.** The total number (and percentage) of transients that were quantifiable across waveforms. The number of transients below the LOD, unresolved from preceding transients, or failed residual analysis varied across waveforms are included. n = total number of transients for all ICSS sessions measured with each waveform.

waveform resulted in only one transient that fell below the LOD across all subjects and ICSS sessions. However, a higher percentage of transients (20%) were unresolvable from preceding transients. This problem was exacerbated on the +1.4 V waveform, where nearly half (45%) of transients were unable to be resolved. Ultimately, of the three waveforms investigated, the +1.3 V waveform was able to provide the best balance of enhanced sensitivity and temporal resolution, quantifying the greatest percentage (78%) of electrically-evoked transients.

## **DISCUSSION**

This study supports the previous conclusion that continuously elevated phasic dopamine release is not required for maintenance of ICSS behavior (Garris, et al., 1999). However, in contrast to the original findings, the use of more sensitive waveforms revealed that dopamine transients do not completely disappear during this task, but rather diminish to smaller values undetectable in previous investigations. Notably, continuous ICSS is a unique behavioral paradigm in which the ability to resolve narrowly spaced events is crucial. Thus, the enhanced ability of the +1.3 V waveform to detect electrically-evoked transients throughout ICSS while maintaining moderate temporal resolution supports its use as the standard waveform for measurements in awake animals with narrowly spaced dopamine events. However, the enhanced sensitivity of +1.4 V waveform may be useful for studying behavioral paradigms in which temporal resolution is unnecessary for understanding the voltammetric data (e.g. studies without narrowly spaced cues and/or behavioral responses). Nonetheless, its use to study rapid behaviors like ICSS could lead to erroneous conclusions about dopamine dynamics; indeed, the +1.4 V waveform revealed 'rises' in dopamine concentrations during ICSS (Figure 2.5c) similar to those seen in microdialysis experiments, rather than a decay in dopamine release as suggested by the other waveforms. This reduced temporal resolution could alter concentration prediction for moderately resolved release events (i.e. resolved at half maximum), with tailing currents from preceding transients augmenting concentration values for subsequent events.

Potential offsets are often used in voltammetric recordings in awake animals because of biofouling of chronically-implanted reference electrodes that results in an altered potential. The offsets are often quite large, typically ~200 mV (Heien, et al., 2005). The use of offsets can lead to an unwanted extended anodic limit, resulting in altered electrode performance. Accordingly, acute reference electrodes were used in this study to reliably compare waveforms. As shown here and elsewhere, the voltammetric waveform, including any offsets, is an important experimental consideration that can affect sensitivity, temporal resolution, and electrode stability (Keithley, et al., 2011).

A difference between this study and *Garris et. al.* is the stimulus pulse duration (2 ms and 1 ms pulses respectively). Longer pulse widths promote slightly greater dopamine release when stimulation current remains constant (Park et al., 2011). However, longer pulse widths have more pronounced motor effects during electrical stimulation, which can limit rapid response rates during ICSS. The moderate press rates in this study with longer pulse widths made it possible to resolve individual transients and study changes in phasic dopamine release over time. Shorter pulse widths could permit more rapid pressing; however, this may result in unresolved transients, particularly with extended waveforms. It has been hypothesized that extracellular dopaminergic tone is a function of summated phasic dopamine transients (Owesson-White et al., 2012). Thus, it is possible that these signals (i.e. unresolved dopamine transients) would begin to resemble microdialysis signals for rapid pressing (Hernandez, et al., 2006), in which a gradual rise in dopamine is succeeded by a fall in dopamine levels during continuous pressing as the summated transients begin to decay in amplitude (see Figure 5c). In previous work a three component model (short-term facilitation, short-term depression, and long-term depression) was developed that predicts dopamine concentrations during isolated and rapid stimulation patterns (Kita et al., 2007; Montague et al., 2004). The time constant for recovery from long-term depression was predicted to be 12-15 min, and studies in anesthetized rats show full recovery on the order of 30 min (Michael et al., 1987). However, the 30 min

timeout in this study was insufficient for dopamine to return to pre-ICSS levels. Indeed, dopamine release often remained attenuated, which could not be solely attributed to biofouling of the electrode, suggesting this model has not captured all long term factors controlling dopamine release. This could be due to depletion of releasable vesicles or a decreased rate of dopamine synthesis. Alternatively, because dopamine VTA neurons are thought to be activated transsynaptically during electrical stimulation via ionotropic glutamate receptors (Sombers, et al., 2009), this mechanism could be altered. For example, it has been shown that the subunit composition of AMPA receptors in the VTA can change after repetitive brain stimulation (Carlezon et al., 2001). Recent studies have shown that optogenetic stimulation of glutamatergic neurons that form synapses on dopamine neurons within the VTA is sufficient to promote ICSS (Wang et al., 2015) and evoke dopamine release in the NAc (Qi et al., 2014).

ICSS can be learned very quickly. In fact, we have previously shown that dopamine release and ICSS behavior are acquired and reach stable responding within 200 lever presses (Owesson-White, et al., 2008). Therefore, it is unlikely that differences in training history between subjects were a significant source of variability in the decay of dopamine release between and across sessions. However, future longitudinal studies of dopamine release during ICSS could investigate whether these dopamine profiles change over extended training.

While this study did not manipulate phasic dopamine release to test its effect on behavior, it was found that even as the concentration of dopamine transients in the NAc fell across ICSS sessions, subjects continued to respond for ICSS at similar rates. Therefore, the original assertion that consistently elevated phasic dopamine release is unnecessary for the maintenance of ICSS remains valid. Nevertheless, a full dissociation of dopamine release from ICSS behavior seems unlikely. A few possibilities for the role of electrically-evoked dopamine release in ICSS remain. First, the high dopamine concentrations evoked by early stimulation may be required for acquisition of this task via corticostriatal synaptic plasticity that promotes learning (Reynolds et al., 2001), but is unnecessary for maintenance. However, this

pharmacological manipulations in well-trained animals can still alter behavior (Carlezon & Chartoff, 2007; Steinberg, et al., 2014; Wise, 1996), which contradicts this view. Second, the low steady-state dopamine concentrations seen after repeated responding in this study, as well as the slower increases in dopaminergic tone demonstrated with microdialysis (Fiorino, et al., 1993; Hernandez, et al., 2006; You, et al., 2001), may be sufficient to activate high-affinity D2 receptors on striatal medium spiny neurons, which inhibits their activity (Calipari et al., 2016). Activation of D2-expressing medium spiny neurons can be aversive (Kravitz et al., 2012). Therefore, it is possible that the relatively low dopamine concentrations after continuous pressing remain vital for inhibiting these cells to prevent activation of circuitry that could compete with the primary reward pathway activated by ICSS. The mechanism we prefer is that dopamine mediates responses to cues predicting reward availability. Although the visual cue and lever were both continually present, making it impossible to separate their contributions, elsewhere, using a delayed lever availability paradigm, we have shown that dopamine responses to cues during ICSS modulate D2-containing medium spiny neurons (Owesson-White et al., 2016). Indeed, we found that D1-mediated responses occurred near the time of the stimulation, whereas responses after the cue were mediated by D2 receptors. Therefore, there is evidence that dopamine is important for both cue and operant responses. Ultimately, future studies involving pharmacological manipulations of dopamine during ICSS with FSCV measurements will further elucidate the relationship between phasic dopamine release and ICSS behavior.

## REFERENCES

- Bard, A. J., & Faulkner, L. R. (2001). *Electrochemical methods: Fundamentals and applications* (2nd ed.). New York: Wiley.
- Bath, B. D., Michael, D. J., Trafton, B. J., Joseph, J. D., Runnels, P. L., & Wightman, R. M. (2000). Subsecond adsorption and desorption of dopamine at carbon-fiber microelectrodes. *Anal Chem*, *72*(24), 5994-6002.
- Berrios, J., et al. (2016). Loss of UBE3A from TH-expressing neurons suppresses GABA co-release and enhances VTA-NAc optical self-stimulation. *Nat Commun*, *7*, 10702.
- Bielajew, C., & Shizgal, P. (1986). Evidence implicating descending fibers in self-stimulation of the medial forebrain bundle. *J Neurosci*, *6*(4), 919-929.
- Bucher, E. S., et al. (2013). Flexible software platform for fast-scan cyclic voltammetry data acquisition and analysis. *Anal Chem*, *85*(21), 10344-10353.
- Calipari, E. S., et al. (2016). In vivo imaging identifies temporal signature of D1 and D2 medium spiny neurons in cocaine reward. *Proc Natl Acad Sci U S A*, *113*(10), 2726-2731.
- Carlezon, W. A., Jr., & Chartoff, E. H. (2007). Intracranial self-stimulation (ICSS) in rodents to study the neurobiology of motivation. *Nat Protoc*, *2*(11), 2987-2995.
- Carlezon, W. A., Jr., et al. (2001). Repeated exposure to rewarding brain stimulation downregulates GluR1 expression in the ventral tegmental area. *Neuropsychopharmacology*, *25*(2), 234-241.
- Corbett, D., & Wise, R. A. (1980). Intracranial self-stimulation in relation to the ascending dopaminergic systems of the midbrain: a moveable electrode mapping study. *Brain Res*, *185*(1), 1-15.
- Cossette, M. P., Conover, K., & Shizgal, P. (2016). The neural substrates for the rewarding and dopamine-releasing effects of medial forebrain bundle stimulation have partially discrepant frequency responses. *Behav Brain Res*, *297*, 345-358.
- Fibiger, H. C., LePiane, F. G., Jakubovic, A., & Phillips, A. G. (1987). The role of dopamine in intracranial self-stimulation of the ventral tegmental area. *J Neurosci*, *7*(12), 3888-3896.
- Fiorino, D. F., Coury, A., Fibiger, H. C., & Phillips, A. G. (1993). Electrical stimulation of reward sites in the ventral tegmental area increases dopamine transmission in the nucleus accumbens of the rat. *Behav Brain Res*, *55*(2), 131-141.
- Fulton, S., Woodside, B., & Shizgal, P. (2000). Modulation of brain reward circuitry by leptin. *Science*, *287*(5450), 125-128.
- Gallistel, C. R., Shizgal, P., & Yeomans, J. S. (1981). A portrait of the substrate for self-stimulation. *Psychol Rev*, *88*(3), 228-273.

- Garris, P. A., Christensen, J. R., Rebec, G. V., & Wightman, R. M. (1997). Real-time measurement of electrically evoked extracellular dopamine in the striatum of freely moving rats. *J Neurochem*, *68*(1), 152-161.
- Garris, P. A., Kilpatrick, M., Bunin, M. A., Michael, D., Walker, Q. D., & Wightman, R. M. (1999). Dissociation of dopamine release in the nucleus accumbens from intracranial self-stimulation. *Nature*, *398*(6722), 67-69.
- Heien, M. L., Johnson, M. A., & Wightman, R. M. (2004). Resolving neurotransmitters detected by fast-scan cyclic voltammetry. *Anal Chem*, *76*(19), 5697-5704.
- Heien, M. L., et al. (2005). Real-time measurement of dopamine fluctuations after cocaine in the brain of behaving rats. *Proc Natl Acad Sci U S A*, *102*(29), 10023-10028.
- Heien, M. L., Phillips, P. E., Stuber, G. D., Seipel, A. T., & Wightman, R. M. (2003). Overoxidation of carbon-fiber microelectrodes enhances dopamine adsorption and increases sensitivity. *Analyst*, *128*(12), 1413-1419.
- Hernandez, G., et al. (2006). Prolonged rewarding stimulation of the rat medial forebrain bundle: neurochemical and behavioral consequences. *Behav Neurosci*, *120*(4), 888-904.
- Keithley, R. B., Carelli, R. M., & Wightman, R. M. (2010). Rank estimation and the multivariate analysis of in vivo fast-scan cyclic voltammetric data. *Anal Chem*, *82*(13), 5541-5551.
- Keithley, R. B., Heien, M. L., & Wightman, R. M. (2009). Multivariate concentration determination using principal component regression with residual analysis. *Trends Anal Chem*, *28*(9), 1127-1136.
- Keithley, R. B., et al. (2011). Higher sensitivity dopamine measurements with faster-scan cyclic voltammetry. *Anal Chem*, *83*(9), 3563-3571.
- Kilpatrick, M. R., Rooney, M. B., Michael, D. J., & Wightman, R. M. (2000). Extracellular dopamine dynamics in rat caudate-putamen during experimenter-delivered and intracranial self-stimulation. *Neuroscience*, *96*(4), 697-706.
- Kishida, K. T., et al. (2016). Subsecond dopamine fluctuations in human striatum encode superposed error signals about actual and counterfactual reward. *Proc Natl Acad Sci U S A*, *113*(1), 200-205.
- Kita, J. M., Parker, L. E., Phillips, P. E., Garris, P. A., & Wightman, R. M. (2007). Paradoxical modulation of short-term facilitation of dopamine release by dopamine autoreceptors. *J Neurochem*, *102*(4), 1115-1124.
- Kravitz, A. V., Tye, L. D., & Kreitzer, A. C. (2012). Distinct roles for direct and indirect pathway striatal neurons in reinforcement. *Nat Neurosci*, *15*(6), 816-818.
- Logman, M. J., Budygin, E. A., Gainetdinov, R. R., & Wightman, R. M. (2000). Quantitation of in vivo measurements with carbon fiber microelectrodes. *J Neurosci Methods*, *95*(2), 95-102.

- Michael, A. C., Ikeda, M., & Justice, J. B., Jr. (1987). Mechanisms contributing to the recovery of striatal releasable dopamine following MFB stimulation. *Brain Res*, 421(1-2), 325-335.
- Montague, P. R., et al. (2004). Dynamic gain control of dopamine delivery in freely moving animals. *J Neurosci*, 24(7), 1754-1759.
- Olds, J., & Milner, P. (1954). Positive reinforcement produced by electrical stimulation of septal area and other regions of rat brain. *J Comp Physiol Psychol*, 47(6), 419-427.
- Owesson-White, C., et al. (2016). Cue-Evoked Dopamine Release Rapidly Modulates D2 Neurons in the Nucleus Accumbens During Motivated Behavior. *J Neurosci*, 36(22), 6011-6021.
- Owesson-White, C. A., Cheer, J. F., Beyene, M., Carelli, R. M., & Wightman, R. M. (2008). Dynamic changes in accumbens dopamine correlate with learning during intracranial self-stimulation. *Proc Natl Acad Sci U S A*, 105(33), 11957-11962.
- Owesson-White, C. A., et al. (2012). Sources contributing to the average extracellular concentration of dopamine in the nucleus accumbens. *J Neurochem*, 121(2), 252-262.
- Park, J., Takmakov, P., & Wightman, R. M. (2011). In vivo comparison of norepinephrine and dopamine release in rat brain by simultaneous measurements with fast-scan cyclic voltammetry. *J Neurochem*, 119(5), 932-944.
- Phillips, A. G., & Fibiger, H. C. (1978). The role of dopamine in maintaining intracranial self-stimulation in the ventral tegmentum, nucleus accumbens, and medial prefrontal cortex. *Can J Psychol*, 32(2), 58-66.
- Qi, J., et al. (2014). A glutamatergic reward input from the dorsal raphe to ventral tegmental area dopamine neurons. *Nat Commun*, 5, 5390.
- Rebec, G. V., Christensen, J. R., Guerra, C., & Bardo, M. T. (1997). Regional and temporal differences in real-time dopamine efflux in the nucleus accumbens during free-choice novelty. *Brain Res*, 776(1-2), 61-67.
- Reynolds, J. N., Hyland, B. I., & Wickens, J. R. (2001). A cellular mechanism of reward-related learning. *Nature*, 413(6851), 67-70.
- Rodeberg, N. T., Johnson, J. A., Cameron, C. M., Saddoris, M. P., Carelli, R. M., & Wightman, R. M. (2015). Construction of Training Sets for Valid Calibration of in Vivo Cyclic Voltammetric Data by Principal Component Analysis. *Anal Chem*, 87(22), 11484-11491.
- Singh, Y. S., Sawarynski, L. E., Dabiri, P. D., Choi, W. R., & Andrews, A. M. (2011). Head-to-head comparisons of carbon fiber microelectrode coatings for sensitive and selective neurotransmitter detection by voltammetry. *Anal Chem*, 83(17), 6658-6666.
- Somers, L. A., Beyene, M., Carelli, R. M., & Wightman, R. M. (2009). Synaptic overflow of dopamine in the nucleus accumbens arises from neuronal activity in the ventral tegmental area. *J Neurosci*, 29(6), 1735-1742.

- Steinberg, E. E., Boivin, J. R., Saunders, B. T., Witten, I. B., Deisseroth, K., & Janak, P. H. (2014). Positive reinforcement mediated by midbrain dopamine neurons requires D1 and D2 receptor activation in the nucleus accumbens. *PLoS One*, *9*(4), e94771.
- Takmakov, P., et al. (2010). Carbon microelectrodes with a renewable surface. *Anal Chem*, *82*(5), 2020-2028.
- Wang, H. L., Qi, J., Zhang, S., Wang, H., & Morales, M. (2015). Rewarding Effects of Optical Stimulation of Ventral Tegmental Area Glutamatergic Neurons. *J Neurosci*, *35*(48), 15948-15954.
- Wightman, R., et al. (2007). Dopamine release is heterogeneous within microenvironments of the rat nucleus accumbens. *Eur J Neurosci*, *26*(7), 2046-2054.
- Wise, R. A. (1996). Addictive drugs and brain stimulation reward. *Annu Rev Neurosci*, *19*, 319-340.
- Witten, I. B., et al. (2011). Recombinase-driver rat lines: tools, techniques, and optogenetic application to dopamine-mediated reinforcement. *Neuron*, *72*(5), 721-733.
- Yeomans, J., & Baptista, M. (1997). Both nicotinic and muscarinic receptors in ventral tegmental area contribute to brain-stimulation reward. *Pharmacol Biochem Behav*, *57*(4), 915-921.
- Yeomans, J. S., Maidment, N. T., & Bunney, B. S. (1988). Excitability properties of medial forebrain bundle axons of A9 and A10 dopamine cells. *Brain Res*, *450*(1-2), 86-93.
- Yorgason, J. T., Espana, R. A., & Jones, S. R. (2011). Demon voltammetry and analysis software: analysis of cocaine-induced alterations in dopamine signaling using multiple kinetic measures. *J Neurosci Methods*, *202*(2), 158-164.
- You, Z. B., Chen, Y. Q., & Wise, R. A. (2001). Dopamine and glutamate release in the nucleus accumbens and ventral tegmental area of rat following lateral hypothalamic self-stimulation. *Neuroscience*, *107*(4), 629-639.

## **CHAPTER 3: DEPLETION OF RELEASABLE DOPAMINE DRIVES DISSOCIATION BETWEEN PHASIC DOPAMINE RELEASE AND CONTINUOUS ICSS**

### **INTRODUCTION**

The crucial role of dopamine in reward-seeking behavior is well established through a host of different behavioral paradigms and experimental techniques (Adamantidis et al., 2011; Ikemoto & Panksepp, 1999; Schultz, 1998; Wise, 2002). One popular method for studying reward pursuit is intracranial self-stimulation (ICSS), in which subjects are trained to self-administer brain stimulation (Carlezon & Chartoff, 2007; Olds & Milner, 1954). With ICSS, the direct nature of the stimulus (e.g. electrical or optical stimulation) bypasses peripheral inputs and avoids satiety, which can affect self-administration of drugs of abuse and food reward (Wise, 1996). Furthermore, ICSS can be readily combined with behavioral or pharmacological manipulations to test their effect on reward (Fulton et al., 2000; Markou & Koob, 1991; Negus & Miller, 2014). Unsurprisingly, given its importance in other reward-seeking paradigms, there is strong evidence that dopamine release is critical for ICSS behavior. Brain regions that support vigorous ICSS responses have high densities of dopamine cells (Corbett & Wise, 1980) or their projections, and drugs that manipulate dopamine levels tend to alter ICSS in a predictable manner (Carlezon & Chartoff, 2007; Negus & Miller, 2014; Wise, 1996). Perhaps the most incontrovertible evidence for the role of dopamine in ICSS comes from optogenetic studies, in which selective optical stimulation of dopamine neurons is necessary and sufficient to promote this behavior (Adamantidis, et al., 2011; Ilango et al., 2014; Steinberg et al., 2014; Witten et al., 2011).

While accumulated evidence has made it clear that dopamine is a key mediator of ICSS, there have been relatively few investigations into how dopamine release is related to ongoing

ICSS behavior. Microdialysis measurements reveal increased dopamine overflow in the nucleus accumbens (NAc) over the order of minutes to hours during ICSS responding (Fiorino et al., 1993; Hernandez et al., 2006; Hernandez et al., 2012). However, this technique is insufficient to measure phasic dopamine release events on a time scale relevant to individual responses. In contrast, measurements using fast-scan cyclic voltammetry (FSCV) have revealed that phasic dopamine release appears to be dissociated from ICSS behavior. While early studies suggested a complete loss of dopamine release during ICSS (Garris et al., 1999; Kruk et al., 1998), more recent investigation has suggested that these results were an effect of inadequate sensitivity, though more sensitive FSCV measurements still revealed a decrease in dopamine release during continuous responding (Rodeberg et al., 2016). The source of this decay in electrically-evoked dopamine release remains unclear. One proposed theory has been that the decline in the phasic dopamine signal is an effect of reward predictability; stimulation patterns acquired in behaving rats appeared to evoke more consistent dopamine release in 'yoked' controls (Garris, et al., 1999), which corroborates previous electrophysiological studies that suggested unexpected reward elicit greater dopamine activity than fully expected rewards (Mirenowicz & Schultz, 1996; Schultz, 1998). Conversely, the diminishing dopamine signal during ICSS could result from depletion of releasable dopamine due to excessive stimulation (Michael et al., 1987; Montague et al., 2004). Consistent with this hypothesis, longer timeouts between stimulations (5 – 25 s) permit continual monitoring of dopamine release (Owesson-White et al., 2008).

Two of the most frequently tested drugs with ICSS, amphetamine and cocaine, are well established to augment ICSS behavior (Elmer et al., 2010; Gilliss et al., 2002; Negus & Miller, 2014). In addition to their role as blockers of the dopamine transporter (DAT), both drugs facilitate electrically-evoked dopamine release. Cocaine promotes dopamine release through the recruitment of reserve pools of vesicles in a synapsin-dependent process (Kile et al., 2010; Venton et al., 2006). The mechanism for amphetamine-induced augmentation of dopamine release is less clear. Early investigations in brain slices and anesthetized rodents suggested

amphetamine *decreases* electrically-evoked dopamine release in response to prolonged (~10 s) stimulation; this effect of amphetamine was attributed to depletion of synaptic dopamine vesicles via actions at the vesicular monoamine transporter, and subsequent efflux of cytosolic dopamine through DAT (Jones et al., 1998; Kuhr et al., 1985; Schmitz et al., 2001). However, more recent studies have demonstrated that amphetamine augments dopamine release in the NAc in response to shorter stimulation durations (0.4 s) (Avelar et al., 2013; Covey et al., 2013; Daberkow et al., 2013). This cannot be solely attributed to uptake inhibition, as the magnitude of dopamine transients is relatively insensitive to changes in uptake (Howard et al., 2013). Interestingly, the ability of amphetamine to enhance electrically-evoked release depends critically on the stimulus duration and brain region, as long-train (10 s) and short-train (0.4 – 2 s) stimulation decrease and increase electrically-evoked release in the dorsal striatum following amphetamine, respectively, while decreases are not typically seen in the NAc (Covey, et al., 2013). These effects have been attributed to the ability of amphetamine to boost the readily releasable pool of dopamine vesicles while simultaneously depleting the reserve pool. ICSS stimulation patterns represent interplay between these two stimulus durations and their corresponding vesicular pools, as ICSS consists of short but rapidly-repeated stimulation trains. Therefore, it is unclear how amphetamine alters dopamine release in the NAc during repeated ICSS responding.

This study further investigates the relationship between phasic dopamine release and ICSS behavior by testing the effect of reward expectancy and drugs of abuse (i.e. cocaine and amphetamine) on dopamine release patterns during continued responding. These experiments reveal that the expectancy of stimulation plays a minimal role in the decay of the dopamine signal. Moreover, while cocaine and amphetamine both boost electrically-evoked release during ICSS in a similar manner, their maximal effects are relatively short-lived compared to sustained increases in ICSS responding. In support of previous studies, these results do not support a key role of dopamine release magnitude in ongoing ICSS behavior.

## **EXPERIMENTAL**

### **Animals**

Male Sprague-Dawley rats (250-450 g) were purchased from Charles River (Wilmington, MA, USA). Subjects were housed individually following surgery on a 12/12 hr light/dark cycle with *ad libitum* access to both food and water. All *in vivo* procedures were approved by the Institutional Animal Care and Use Committee (IACUC) at the University of North Carolina at Chapel Hill.

### **Surgery**

Animals were anesthetized with isoflurane (induction 4%; maintenance 1.5%-2.5%) and prepared for FSCV recordings in the NAc as previously described (Rodeberg, et al., 2016). All stereotactic measurements were made with respect to the skull landmark bregma. A guide cannula (Bioanalytical Systems, West Lafayette, IN) for the glass-encased carbon-fiber microelectrode was placed in the right hemisphere above the NAc (AP +1.7 mm, ML +0.8 mm, DV 2.5 mm from skull surface), with a cannula placed in the contralateral hemisphere for implantation of a fresh reference electrode on the day of the experiment. A bipolar stimulating electrode (Plastics One, Roanoke, VA) was targeted at the ventral tegmental area (VTA) (AP - 5.2 mm, ML +1.0 mm, DV -8.6 mm). Cannulas and stainless steel screws were affixed to the skull surface with acrylic dental cement. Each animal was allowed a minimum of three days to recover post-surgery before ICSS training.

## **Behavior**

### *Fixed-interval ICSS*

Rats were first trained in fixed-ratio 1 (FR1) ICSS following previous protocol (Garris, et al., 1999; Rodeberg, et al., 2016). Briefly, subjects were placed in operant chambers (MedAssociates Inc., St. Albans, VT, USA) and tethered to a head-mounted amplifier attached to a swiveled commutator (Crist Instrument Co., Hagerstown, MD, USA) that allowed movement around the chamber. First, electrical stimulation (60 Hz, 24 biphasic pulses, 2 ms pulse width) was given to each subject and adjusted to the maximal in-range current (75-175  $\mu$ A) that induced appetitive behavior (e.g. rearing, sniffing, exploring) without evoking substantial motor effects (e.g. circling, bucking) that would interfere with acquisition of ICSS behavior. Next, ICSS was initiated with the onset of white noise and extension of a lever into the chamber, which was positioned beneath an illuminated cue light. Each subject was primed with electrical stimulation as it approached the lever until animals acquired ICSS (i.e. pressed the lever on an FR1 schedule without interruption).

Following acquisition of FR1 ICSS, animals were trained on a fixed-interval (FI) schedule of ICSS. In this paradigm, each stimulation-reinforced lever press was followed by a timeout in which electrical stimulation was unavailable. During this timeout, the lever remained extended so that unreinforced responses could be recorded as time-locked, digital events. The minimum time between stimulations was gradually increased from 1 s (FI1) to 5 s (FI5) over successive sessions. Animals were trained for a maximum of three sessions per day, separated by thirty minute timeouts, with a maximum of 150 stimulations per day. Animals were considered sufficiently trained for voltammetric recordings once the press rate was stable ( $\pm 10$  % for three consecutive sessions). On recording day, animals pressed on a FI5 schedule for two separate sessions separated by a 30 min timeout.

### *'Yoked' controls*

Yoked control animals (n = 5) were surgically prepared as described above, but were not trained in ICSS before FSCV recordings. Instead, stimulation current was adjusted on the day of measurements. All subjects received an identical stimulation pattern that was obtained in a separate rat in a previous study using an FR1 stimulus pattern (Rodeberg, et al., 2016). This stimulation record was chosen because it resulted in FSCV data with minimal overlap of electrically-evoked dopamine transients, which can interfere with quantitation and subsequent comparisons between animals. During yoked stimulation, the behavioral chamber was adjusted similarly (i.e. white noise, cue light) but without lever extension.

### **FSCV recordings**

#### *Electrode construction*

Carbon fibers (T-650, Thornel, Amoco Corporation, Greenville, SC) were aspirated into 600  $\mu\text{m}$  outer diameter borosilicate glass capillaries, sealed using a heat-puller (Narishige, Tokyo, Japan), and trimmed to 100  $\mu\text{m}$  in length. To solidify the seal, each electrode was dipped in heated epoxy resin (Epon 828, Miller Stephenson Chemical Co., Inc., Danbury, CT) mixed with 15% hardener m/m (*m*-phenylenediamine, Sigma, St. Louis, MO) for 30 s followed by a brief rinse in warm acetone. Following one night of drying at air temperature, the electrodes were cured at high temperatures (100° C for 4 hr, 150° C overnight) before use.

#### *FSCV Measurements*

All FSCV measurements were made with a waveform that swept from a holding potential of -0.4 V to +1.3 V and back at 400 V/s against a freshly implanted Ag/AgCl reference electrode; this waveform was demonstrated previously to provide a favorable balance of sensitivity and temporal resolution for recordings during continuous ICSS (Rodeberg, et al., 2016). Each electrode was cycled in the brain for a minimum of 30 minutes at a high frequency (60 Hz)

followed by 15 min at the recording frequency (10 Hz) before dopamine measurements to allow conditioning of the electrode surface to stabilize. FSCV data was collected using HDCV software (Bucher et al., 2013) built in LabView (National Instruments, Austin, TX), with a locally designed potentiostat (UEI, UNC Electronics Facility).

On the day of the experiment for both yoked and ICSS-trained animals, a micromanipulator was used to drive the working electrode along the dorsal-ventral axis in 75  $\mu\text{m}$  increments through the implanted guide cannula. Once a site supporting robust dopamine release was found, behavior (yoked or ICSS) was initiated.

### **Drug administration**

Cocaine (20 mg/kg, RTI International, Raleigh, NC), d-amphetamine (2.5 mg/kg, Sigma, St. Louis, MO), or vehicle (0.9% saline, Hospira, Rocky Mount, NC) ( $n = 5$  for all groups) were administered via intraperitoneal injection (1 mL/kg) 10 min into the 30 min timeout between FI5 ICSS sessions. These doses were chosen to ensure robust changes in phasic dopamine release that could be tracked over time. Successful drug delivery was confirmed with measurement of increased spontaneous transients and altered electrically-evoked release (i.e. increased amplitude and width compared to pre-drug recordings).

### **Data analysis**

Voltammetric data was analyzed using HDCV Analysis software. Principal component regression with residual analysis was used to extract dopamine concentrations as described previously (Heien et al., 2005; Keithley et al., 2009; Rodeberg et al., 2015). Briefly, electrical stimulation was varied in intensity (i.e. current amplitude, pulse number) post-experiment to evoke dopamine and pH changes that spanned the ranges of current seen during recordings. Residual analysis was used to confirm PCR model validity for all predicted transients; any

transient for which  $Q_t$  passed the within-subject training set  $Q_\alpha$  at peak dopamine concentration was discarded.

ICSS and yoked stimulation data were broken into 10 s segments centered  $\pm 5$  s around each electrical stimulation. Each segment was digitally background subtracted preceding the electrically-evoked dopamine transient. As observed with previous measurements using the +1.3 V waveform, dopamine transients were detected for every stimulation. However, due to heterogeneity of release sites in the NAc (Wightman et al., 2007) and between-subject differences in current intensity that supported ICSS, average electrically-evoked dopamine concentrations varied between subjects. Therefore, to make more reliable comparisons, dopamine concentrations were normalized against the magnitude of the first electrically-evoked dopamine transient during ICSS, as done previously (Rodeberg, et al., 2016).

## **Statistics**

Data is expressed as mean  $\pm$  standard error. All statistical analyses were made using GraphPad Prism software, with a significance threshold of  $p < 0.05$ . Two-tailed t-tests were used to compare (normalized) electrically-evoked dopamine amplitudes before and after treatment for both non-contingent stimulation and the first stimulation during ICSS 2 (i.e. post-treatment). For each FI5 ICSS session within each treatment group, paired two-tailed t-tests were used to compare within-session changes in average press rate and average dopamine concentrations between the two halves of the session. A repeated-measures two-way ANOVA was used to test the effect of two independent variables (ICSS session, drug treatment) on a dependent variable (press rate). Single-phase decays were fit with the least squares fitting method, and extra sum-of-squares F tests were used to compare parameters (rate of decay ( $k$ ) and plateau) between ICSS paradigms (i.e. FR1 vs. FI5 ICSS) and sessions (i.e. before and after drug treatment).

## RESULTS

### Yoked ICSS

Previous investigations have reported that electrically-evoked dopamine transients appeared more frequently during unexpected, 'yoked' stimulation patterns than in subjects responding for ICSS with an FR1 stimulus pattern (Garris, et al., 1999). This was partially attributed to the unexpected nature of the stimulus, as unexpected rewards are demonstrated to activate dopamine neurons more potently than fully expected rewards (Mirenowicz & Schultz, 1996; Schultz, 1998). However, a systematic comparison of dopamine concentrations between these two groups has not been attempted, partially due to limited sensitivity in previous experiments. With this aim, rats ( $n = 5$ ) with no previous exposure to electrical stimulation ('yoked' controls) were subjected to an ICSS stimulation pattern acquired from a trained animal in a previous study (Rodeberg, et al., 2016). The particular pattern used was selected because it resulted in minimal overlap of electrically-evoked dopamine transients, which can impede reliable quantitation and subsequent comparisons. A voltammetric waveform with an anodic limit of +1.3 V was used due to previous demonstration that this waveform had the best balance of sensitivity and temporal resolution for measurements during FR1 ICSS (Rodeberg, et al., 2016). During yoked stimulation, dopamine release was monitored in the NAc using FSCV (Figure 3.1a). Following extraction of dopamine concentrations using PCR, the dopamine profiles (i.e. normalized dopamine transient magnitude vs. stimulation number) collected in yoked animals were compared to data from the original, behaving animal (Figure 3.1b). Similar to measurements in the original animal (black squares), electrically-evoked dopamine release in yoked controls (blue circles) declined in magnitude over the 50 successive stimulations. The decline in dopamine concentrations in each naïve animal was significantly correlated with the decline in the behaving animal for all subjects ( $0.562 < r^2 < 0.721$ ,  $p < 0.0001$  for each subject). The behaving and yoked data both fit single-phase decays ( $r^2 = 0.810$  and  $0.964$ , respectively); notably, there was no significant difference between the decay rates ( $K$ ) of the two fits ( $K_{\text{beh}} =$

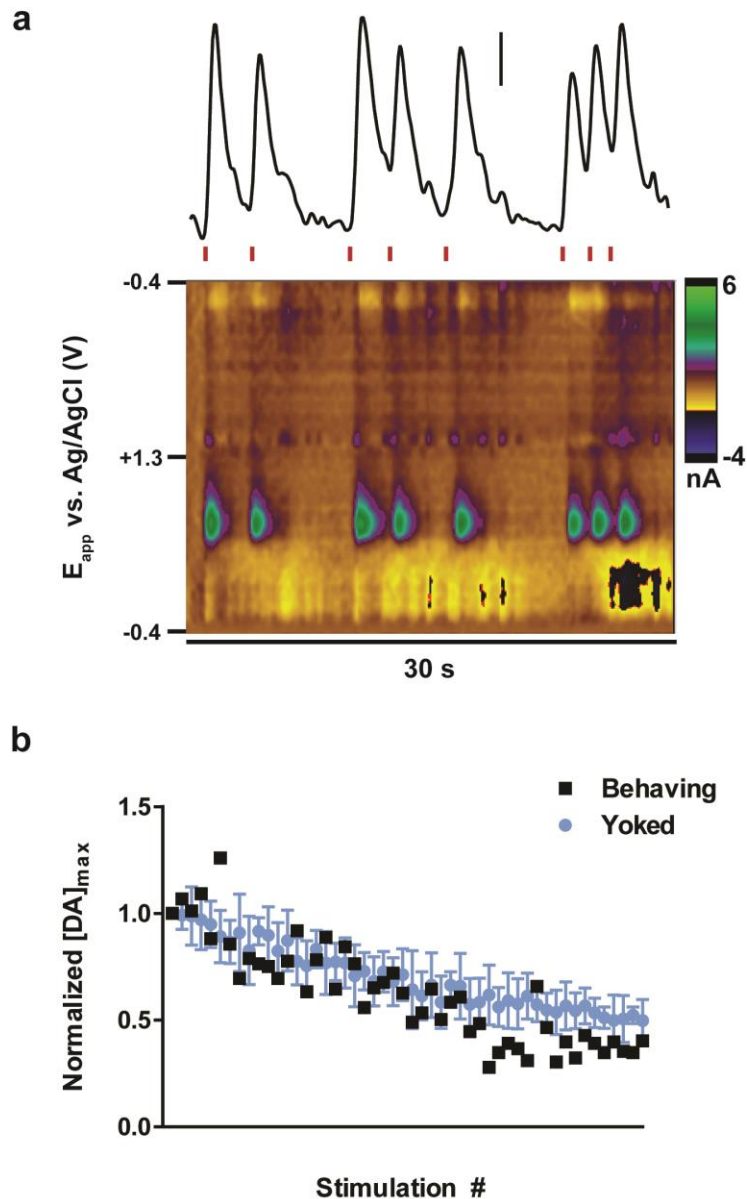


**Figure 3.1.** Electrically-evoked dopamine release during yoked-ICSS (FR1) stimulation pattern. a) Representative voltammetric data from a subject receiving a yoked stimulation pattern acquired in a previous subject. The concentration vs time trace (black, scale bar = 100 nM) extracted with principal component regression reveals dopamine transients evoked by each electrical stimulation (red bars) in the 30 second trace. The peak value for each evoked transient ( $[DA]_{max}$ ) was determined for every corresponding electrical stimulation. The color plot beneath the concentration trace serves as a qualitative representation of this 30 s segment. b) Comparison of  $[DA]_{max}$  between the behaving animal (black squares) and yoked controls (blue circles, mean  $\pm$  SEM,  $n = 4$ ). Peak evoked release over successive stimulations ( $n = 50$ ) declined in a highly similar fashion between the behaving and non-behaving subjects.

0.0257,  $K_{yoke} = 0.0270$ ,  $p = 0.964$ ). This suggests that the expectancy of electrical stimulation plays a minimal role in the decay of dopamine release during ICSS.

### **Fixed-interval ICSS**

As the expectancy of the reward does not seem to drive the decay of phasic dopamine release during prolonged ICSS, the most plausible hypothesis remains to be depletion of releasable dopamine. If this is the case, slower stimulation patterns should result in less attenuation of the dopamine signal. With this aim, we used a fixed-interval 5 (FI5) schedule of ICSS responding, which limits the rate of stimulations each subject can receive. However, in contrast to previous ICSS studies with fixed- and variable-time outs (Cheer et al., 2005; Owesson-White, et al., 2008), the lever remained extended event when stimulation was unavailable, so that ICSS behavior could be continually monitored (i.e. unreinforced responses were recorded) (Figure 3.2). Stimulations were administered following each 5 s interval if the subject pressed the lever within the relevant window. Therefore, while each rat received a nearly identical stimulation rate (12 stim/min), differences in ICSS behavior between subjects could be delineated from overall press rates, which included unreinforced responses. A previous ICSS protocol was used in which each subject performed two self-stimulation sessions separated by a 30 min timeout (Garris, et al., 1999; Rodeberg, et al., 2016). We compared the FI5 response rates to the average response rates from all tested animals ( $n = 12$ ) from a previous FR1 study (Rodeberg, et al., 2016), which used the same stimulation parameters and range of stimulation currents. Though the rate of electrical stimulation was lower on an FI5 schedule (i.e. limited to 12 stim/min), animals were found to press at a similar rate for both ICSS 1 (FR1:  $26.3 \pm 3.3$  response/min; FI5:  $31.7 \pm 5.2$  response/min) and ICSS 2 (FR1:  $29.0 \pm 4.1$  response/min; FI5:  $29.4 \pm 5.0$  response/min). This indicates that, with the stimulation parameters employed, changing FR1 to FI5 did not appreciably alter ICSS behavior.

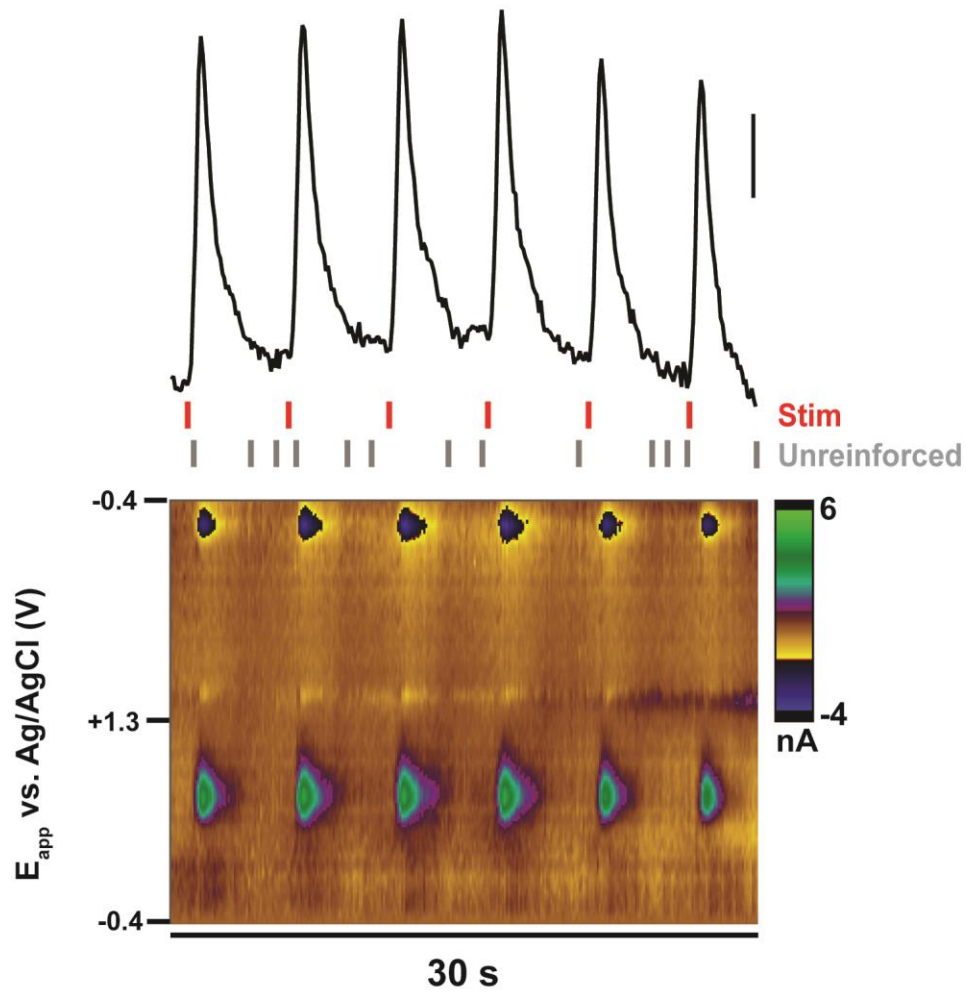


**Figure 3.2.** Fixed-interval 5 (FI5) paradigm for ICSS. Within each 5 s window, the animal must respond to receive a stimulation (red bars) following expiration of the timeout. However, in contrast to other timeout paradigms, the lever remains extended between stimulations, which permits free responses on the lever (grey bars) which have no programmed consequence, but are recorded for overall metrics of response rate. Electrical stimulation of the VTA evokes dopamine transients, which are well resolved due to spacing between adjacent stimulation. Scale bar: 100 nM.

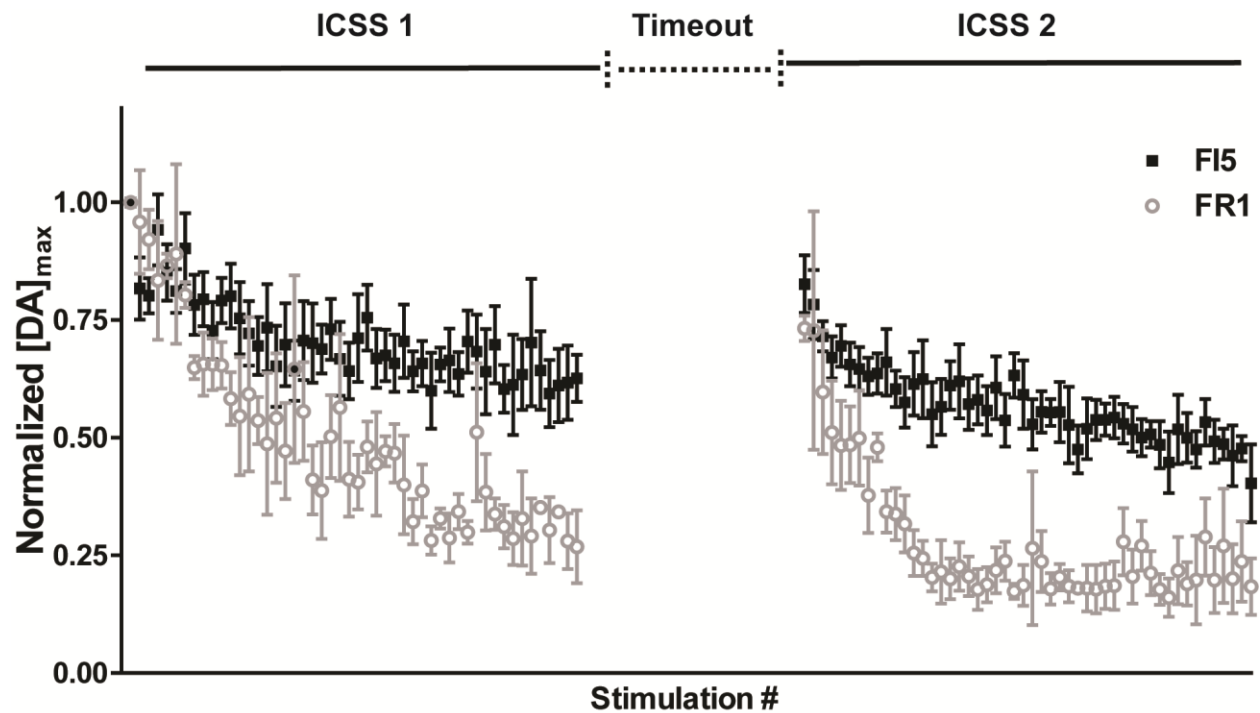


**Figure 3.3.** Comparison of the decline in electrically-evoked dopamine release between FR1 ( $n = 4$ ) and FI5 ( $n = 5$ ) ICSS measured on the +1.3 V waveform. Dopamine concentrations were normalized against the first electrically-evoked dopamine transient in the first ICSS session to control for differences in transient magnitudes and provide more reliable comparisons between subjects. Exponential fits to each set of data revealed that dopamine release plateaued at a higher concentration in both ICSS sessions for FI5 responding compared to an FR1 schedule. Moreover, while dopamine declined at a quicker rate in ICSS 2 compared to ICSS 1 on an FR1 schedule, there was no significant difference in decay rate between sessions for FI5 responding. This data demonstrates that increased spacing between stimulations lessens attenuation of the dopamine signal, consistent with the dopamine depletion hypothesis for phasic dopamine release during ICSS.

	ICSS 1			ICSS 2		
	k	Plateau	r <sup>2</sup>	k	Plateau	r <sup>2</sup>
FR1	0.0654	0.285	0.915	0.157	0.199	0.919
FI5	0.0781	0.633	0.782	0.0497	0.458	0.844

**Table 3.1.** Comparison of dopamine profiles during dual session ICSS on FR1 and FI5 paradigms. The best fit values for the first-order rate of decay (k) and plateau, as well as the coefficients of correlation, are displayed for each ICSS paradigm and ICSS session.

We compared the dopamine profiles during FI5 ICSS to FR1 ICSS data collected with the same waveform ( $n = 4$ ) (Rodeberg, et al., 2016) (Figure 3.3). Notably, the x-axis in this plot represents stimulation number, so that comparisons in the dopamine concentration profile can be made; however, it should be understood that FI5 sessions were longer in duration than FR1 sessions, in which stimulation was freely available. In both paradigms, dopamine release was detected reliably throughout both sessions using a waveform with an anodic limit of +1.3 V. Each ICSS session for each respective paradigm (FR1, FI5) was fit with a single-phase decay, and best-fit values for the rate of decay ( $k$ ) and the plateau were compared (Table 3.1). The FR1 schedule resulted in a statistically significant increase in  $k$  ( $p < 0.0001$ ) and a lower plateau ( $p = 0.0109$ ) for the second ICSS session compared to the first. In contrast,  $k$  was not significantly different between sessions on a FI5 schedule ( $p = 0.198$ ), though the plateau was significantly lower for the second session ( $p < 0.0001$ ). Comparisons between FR1 and FI5 paradigms revealed that the FI5 schedule resulted in higher plateaus for both sessions (ICSS 1,  $p = 0.0004$ ; ICSS 2,  $p = 0.0124$ ), and a lower  $k$  for the second ICSS session ( $p < 0.0001$ ) but not the first ( $p = 0.5525$ ). Altogether, this data indicates that a FI5 schedule lessens the attenuation of the dopamine signal compared to a continuous FR1 schedule, which is in line with previous studies that demonstrated more stable dopamine release with fixed- and variable-timeout paradigms (Cheer, et al., 2005; Owesson-White, et al., 2008).

### **Cocaine and amphetamine administration**

Next, we tested the effects of two drugs known to facilitate ICSS behavior, cocaine and amphetamine (Elmer, et al., 2010; Gilliss, et al., 2002; Negus & Miller, 2014), on dopamine release during ICSS. Interestingly, cocaine has been demonstrated to facilitate phasic dopamine release via recruitment of reserve pools of vesicles in a synapsin-dependent process (Venton, et al., 2006). Therefore, it is possible that some of the success of cocaine in facilitation of ICSS behavior is due to its ability to augment and/or maintain electrically-evoked dopamine

release. In a similar fashion, amphetamine, has been demonstrated to augment electrically-evoked dopamine release with the short stimulation trains used here for ICSS (Avelar, et al., 2013; Covey, et al., 2013; Daberkow, et al., 2013), though decreases in electrically-evoked release *in vivo* have been reported for long train (~10 s) stimulation (Kuhr, et al., 1985). However, all of these studies were done with well-separated electrical stimulations, and it is unknown how these drugs affect phasic dopamine release during ICSS-like stimulation. However, both cocaine and amphetamine act as potent DAT blockers (Giros et al., 1996) which, in combination with potential increases in pressing rate, would lead to unresolved dopamine transients on an FR1 schedule; this would prevent reliable tracking of phasic dopamine dynamics during ICSS following administration of either drug. Thus, the effects of both drugs were tested on an FI5 ICSS schedule.

The two tested drugs, cocaine and amphetamine, were administered between sessions (20 min preceding the second ICSS session) so that their effects on dopamine release during ICSS could be compared to within-subject, pre-drug data. To ensure this dose timing was adequate for full onset of each drug, the two drug doses used for ICSS studies (cocaine, 20 mg/kg i.p.; amphetamine, 2.5 mg/kg i.p.) were tested for their effects of electrically-evoked release in urethane-anesthetized animals ( $n = 5$  for each group) (Figure 3.4a-b). Both drugs increased the amplitude ( $[DA]_{max}$ ) and duration ( $t_{1/2}$ ) of dopamine transients compared to pre-drug values, which was consistent with previous reports on their effects on electrical stimulation (Daberkow, et al., 2013; Venton, et al., 2006). The maximal effect of cocaine on  $[DA]_{max}$  ( $176 \pm 16\%$  of pre-drug values, 6 min) was more rapidly reached than the effect of amphetamine ( $183 \pm 23\%$ , 14 min). However, both drugs had stable augmentation of release within the time window in which FI5 ICSS was performed (range between animals indicated for both drugs by vertical dashed bars). Furthermore, non-contingent electrical stimulation was given before each FI5 ICSS session in each tested subject to verify onset of the drug (Figure 3.4c-d). Cocaine and amphetamine both augmented electrically-evoked release compared to pre-drug amplitude

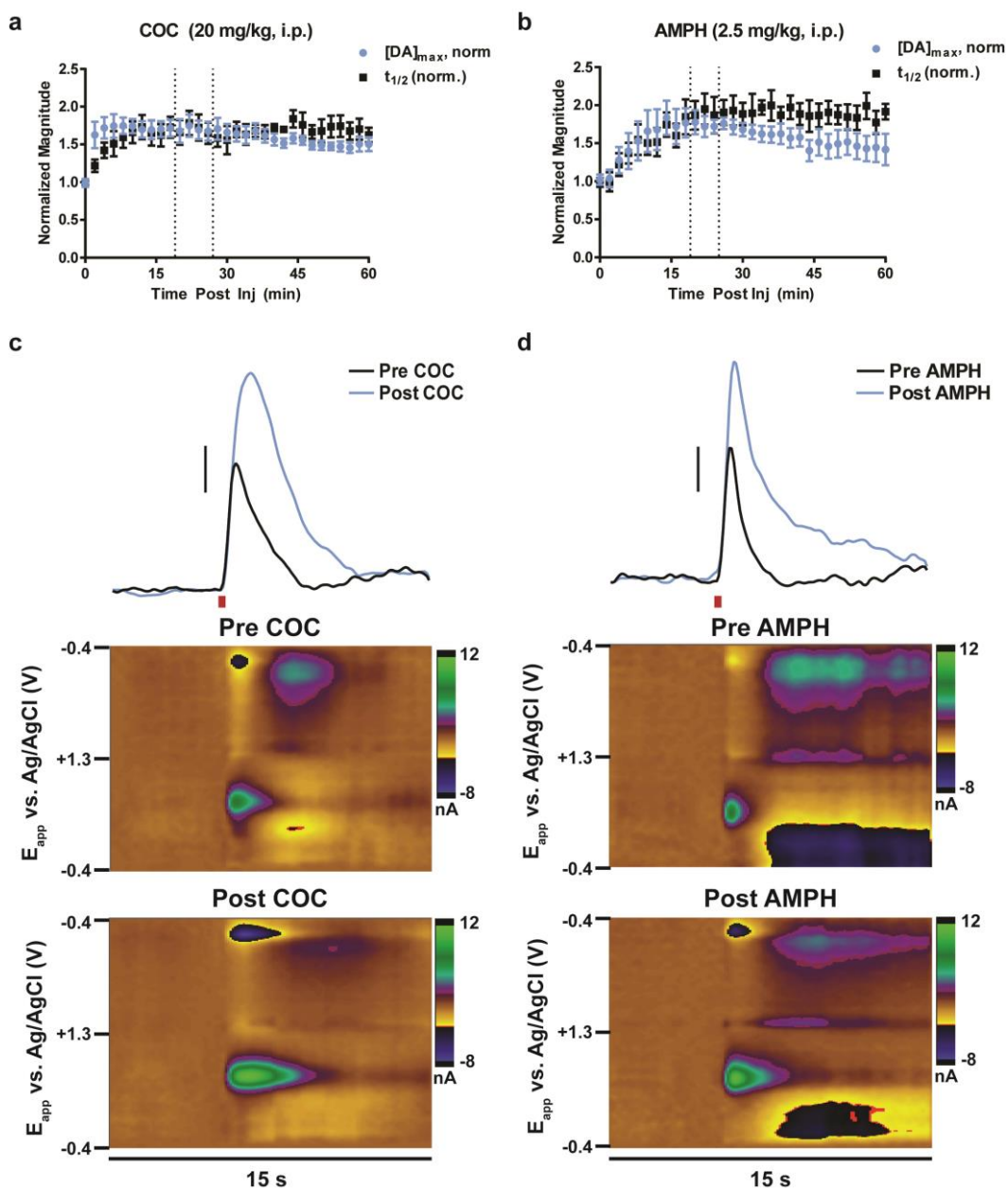


**Figure 3.4.** The effects of cocaine (20 mg/kg) and amphetamine (2.5 mg/kg) on electrically-evoked (60 Hz, 24 pulses) dopamine release. a-b) Dose-timing curves for the effects of cocaine (a) and amphetamine (b) in urethane-anesthetized animals on peak dopamine transient magnitude ( $[DA]_{max}$ ) and the decay rate ( $t_{1/2}$ ). These data reveal that the effect of these drug doses on electrically-evoked dopamine release is stable during the time period following treatment that was assayed in subjects performing FI5 ICSS (range depicted with vertical dashed black bars). Electrical stimulations were spaced at 2 min intervals to prevent stimulated-induced attenuation of the dopamine signal. c-d) Electrically-evoked dopamine release before and after cocaine (c) and amphetamine (d) administration in awake animals. Consistent with the data in anesthetized animals, cocaine and amphetamine increased both release magnitude and duration. Scale bars: 200 nM.

(post cocaine:  $169 \pm 5\%$  of pre-drug amplitude,  $t_8 = 12.48$ ,  $p < 0.0001$ ); post amphetamine:  $158 \pm 11\%$ ,  $t_8 = 5.161$ ,  $p = 0.0009$ ), while saline injection produced no significant changes (post saline:  $86 \pm 7\%$ ,  $t_8 = 2.063$ ,  $p = 0.073$ ).

Representative color plots, in addition to current versus time traces at the peak oxidation potential for dopamine, are shown for two minutes of FI5 ICSS responding following cocaine (Figure 3.5a) and amphetamine (Figure 3.5b) administration. The current versus time traces suggest raised 'baseline' levels of dopamine during pressing; this is likely the effect of DAT inhibition for both drug treatments. However this information is only qualitative, as PCR failed residual analysis over these extended time windows, preventing reliable long-term quantitation of dopamine levels. Instead, we monitored average dopamine release over a 30 s interval during initiation of ICSS session following each treatment. Dopamine concentrations were normalized against the magnitude of the first electrically-evoked transient within each trace to control for differences in concentrations between recording sites (Figure 3.5c). On this time interval, electrically-evoked dopamine release following saline treatment was stable, and returned to baseline between each successive stimulation (Figure 3.5c, left panel). In contrast, cocaine (middle panel) and amphetamine (right panel) administration resulted in transients superimposed on a rising envelope of dopamine levels (~40% of the electrically-evoked magnitude of dopamine transients). This is consistent with the actions of both drugs at the DAT transporter, which prevents reuptake of dopamine between stimulations and thus raises extracellular dopamine levels.

However, to monitor dopamine release over the entirety of the ICSS session, background subtraction was used prior to each electrically-evoked transient to isolate phasic changes in dopamine. This process eliminated information regarding tonic changes in dopamine during ICSS. Isolation and quantitation of dopamine transients in the second ICSS session revealed that both cocaine and amphetamine augmented phasic release compared to saline

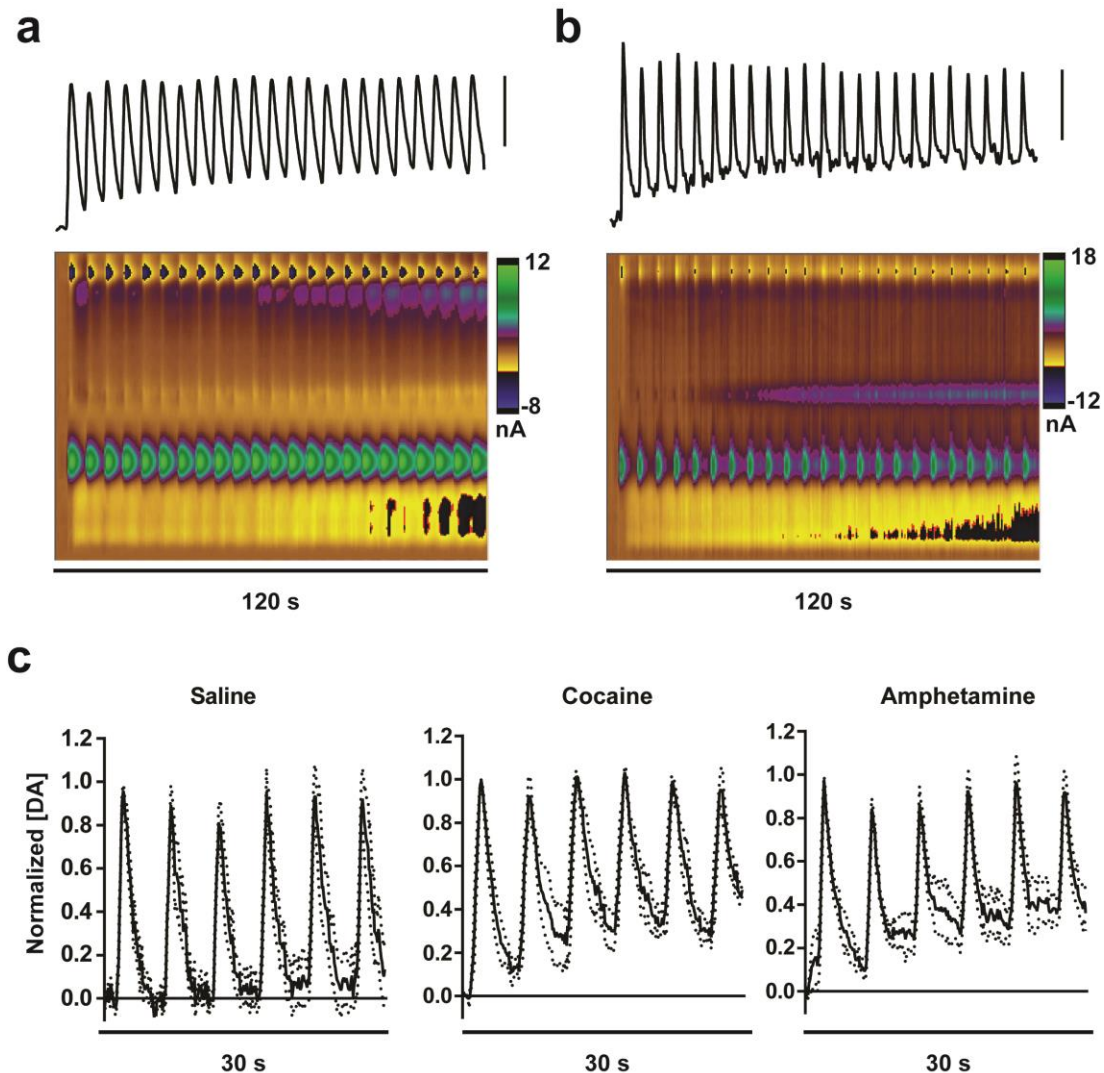


**Figure 3.5.** The effect of cocaine and amphetamine on dopamine release during FI5 ICSS. a) Representative trace of dopamine release during FI5 ICSS responding following cocaine administration. The current at the dopamine peak potential reveals a gradual rise in the baseline signal, likely an effect of uptake inhibition. Due to failure of PCR with residual analysis over long time periods, each transient was analyzed with local background subtraction to track changes in phasic signaling over time; however, these measurements preclude statements about changes in tonic dopamine levels using FSCV. Scale bar: 5 nA. b) A representative trace for dopamine release during FI5 ICSS following amphetamine administration, which exhibits similar trends to cocaine treatment. Scale bar: 5 nA. c) The effect of saline (left), cocaine (middle), and amphetamine (right) on rising dopamine baseline during early FI5 ICSS. 30 s intervals during early FI5 ICSS for each subject were normalized against the magnitude of the first electrically-evoked dopamine transient in the trace to control for differences in concentrations between subjects. Average traces reveal that dopamine transients are superimposed on a rising baseline in dopamine signal following cocaine and amphetamine treatment, but not saline.

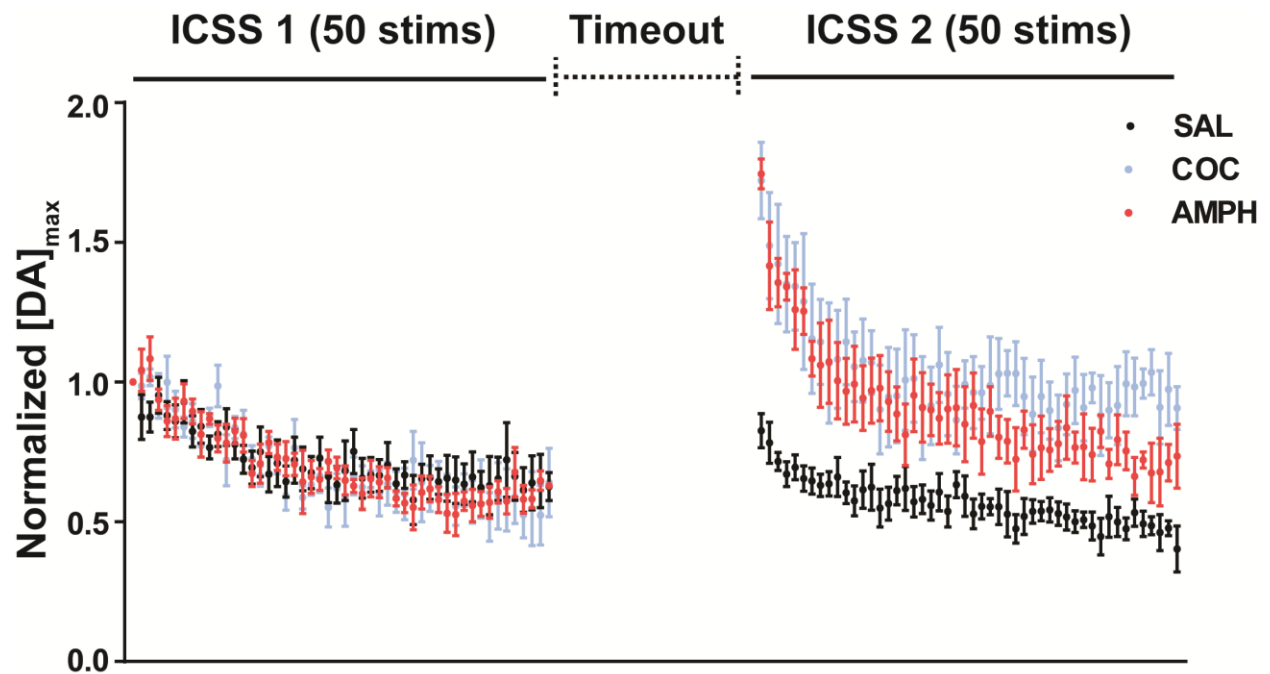


**Figure 3.6.** Phasic dopamine release patterns during drug-treated FI5 ICSS. The effects of cocaine (blue) and amphetamine (red) on the dopamine profile during ICSS 2 compared to vehicle/saline control (black). The maximal effects of cocaine and amphetamine on augmenting phasic dopamine release were short-lived, as evidenced by greater decay rates ( $K$ ) of exponential fits for ICSS 2 compared to ICSS 1 for cocaine and amphetamine, but not saline. Exponential fits plateaued at significantly different concentrations for each treatment.

controls (Figure 3.6). This was particularly evident for the first electrically-evoked transient during the second FI5 ICSS session, which was significantly greater in magnitude than the first stimulation of the first FI5 ICSS session for both cocaine ( $171 \pm 14\%$ ,  $t_8 = 5.191$ ,  $p = 0.0008$ ) and amphetamine ( $175 \pm 5\%$ ,  $t_8 = 13.86$ ,  $p < 0.0001$ ). Interestingly, saline controls showed a significant decrease in the amplitude of non-contingent stimulation preceding the second ICSS session ( $83 \pm 6\%$ ,  $t_8 = 2.819$ ,  $p = 0.0225$ ), which is consistent with previous reports that a 30 minute time out is insufficient to fully restore electrically-evoked dopamine release (Rodeberg, et al., 2016). However, the maximal effects of both amphetamine and cocaine wore off more quickly; the decay rate was larger following treatment for both cocaine ( $k_1 = 0.0674$ ,  $k_2 = 0.184$ ,  $p = 0.0021$ ) and amphetamine ( $k_1 = 0.0665$ ,  $k_2 = 0.115$ ,  $p = 0.044$ ), while there was no significant difference in  $k$  between sessions for saline ( $k_1 = 0.078$ ,  $k_2 = 0.0497$ ,  $p = 0.198$ ). Nonetheless, electrically-evoked dopamine release following both cocaine and amphetamine treatment remained elevated compared to vehicle controls, as evidenced by significantly higher exponential plateaus for cocaine ( $0.935$ ,  $p = 0.0003$ ) and amphetamine ( $0.763$ ,  $p = 0.0067$ ) compared to vehicle ( $0.478$ ). The plateau for cocaine was significantly higher than amphetamine ( $p = 0.0281$ ), which indicates the effects for cocaine may be more prolonged than amphetamine at these respective doses. Ultimately, both cocaine and amphetamine augment phasic dopamine release during FI5 ICSS in a similar manner, with maximal effects occurring for early electrical stimulations.

### **Correlation of behavior and dopamine levels**

Both amphetamine and cocaine have been reported to augment ICSS behavior (Elmer, et al., 2010; Gilliss, et al., 2002; Negus & Miller, 2014). Therefore, it is possible that there is a relationship between the ability to augment dopamine release and the vigor of ICSS behavior. First, the press rates for the two sessions of FI5 ICSS were investigated as a function of treatment (Figure 3.7a). Four of six subjects for both drug treatments had increased response

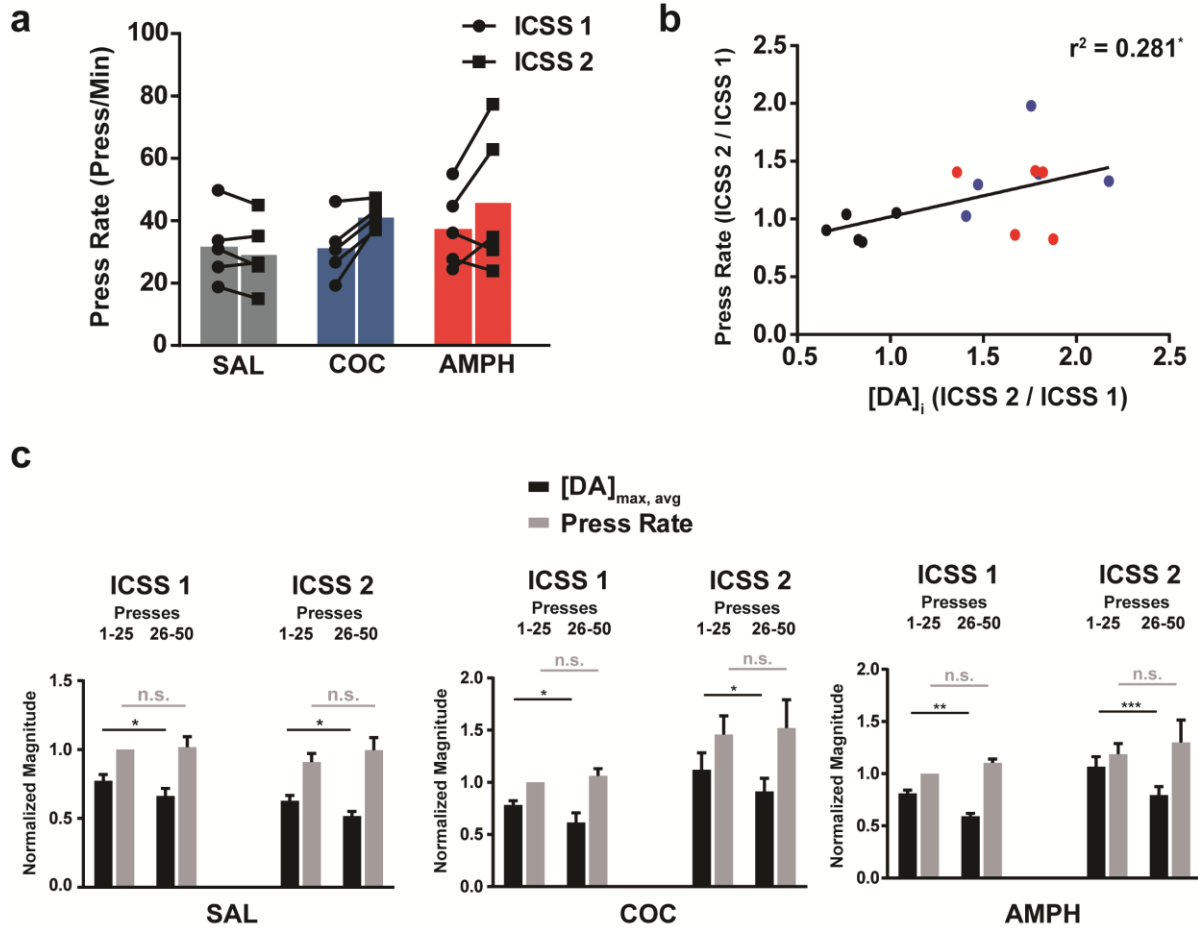


**Figure 3.7.** Comparison of response rates and dopamine concentrations between and across treatments. a) Press rates for subjects administered saline, cocaine, or amphetamine between sessions ( $n = 5$  for each group). While the press rate increased in all 5 subjects for cocaine and 3 out of 5 subjects for amphetamine, a repeated measures two-way ANOVA revealed only a main effect of ICSS session ( $p = 0.0278$ ), with no interaction ( $p = 0.0755$ ) or main effect of treatment ( $p = 0.4013$ ). b) Correlation between the ratio of press rates between sessions (y-axis) to the initially evoked dopamine transient ( $[DA]_i$ , top) and average dopamine concentrations ( $[DA]_{avg}$  bottom) during ICSS 2 across treatments (saline: black, cocaine: blue, amphetamine: red). A significant trend was seen between the change in press rate and changes in initial phasic dopamine release levels ( $p = 0.042$ ) c) Comparison of changes in dopamine and press rate within session. While dopamine decreased significantly between the two halves of the ICSS session for both ICSS sessions within all treatments, no significant differences were seen in press rates within session for any group.

rates in the second ICSS session. A repeated-measures two-way ANOVA was used to test for differences in response rate (press/min) between treatment groups (SAL, COC, AMPH) and ICSS session. There was a significant main effect of ICSS session ( $F_{1,12} = 6.257, p = 0.0278$ ), but no interaction ( $F_{2,12} = 3.229, p = 0.073$ ) or main effect of drug ( $F_{2,12} = 0.9861, p = 0.401$ ). Therefore, it cannot be stated definitively whether the tested drugs increased ICSS responding in this paradigm. Notably, the procedure for selecting the stimulation current was designed to maximize stimulated dopamine release for ease of FSCV measurements, rather than being optimized for stimulation currents that would favor changes in ICSS responding (i.e. determination of current intensity – rate curves). As a result, the two subjects that failed to press faster following amphetamine treatment may have been pressing near max threshold rates, preventing further augmentation of ICSS behavior.

Next, it was tested whether changes (or lack thereof) of response rates following drug administration were correlated with changes in electrically-evoked dopamine release. Within treatments, there was no significant correlation between changes in the magnitude of the first electrically-evoked transient during ICSS 2 ( $[DA]_i$ ) and changes in press rates for saline ( $r^2 = 0.089, p = 0.626$ ), cocaine ( $r^2 = 0.093, p = 0.618$ ), or amphetamine ( $r^2 = 0.457, p = 0.210$ ). However, when all treatments were grouped, there was a significant correlation between changes in  $[DA]_i$  and press rate (Figure 3.7b) ( $r^2 = 0.281, p = 0.042$ ). Notably, this correlation includes the two subjects that did not respond faster following amphetamine treatment.

Lastly, comparisons were made to determine whether changes in evoked dopamine release within session were correlated with changes in response rates (Figure 3.7c). Each trial was split into two phases (first 25 presses, last 25 presses), with the average normalized  $[DA]$  calculated for each bin. Similarly, the press rate was normalized against the first half of the first ICSS session to control for differences in response rate magnitudes between animals. For saline-treated animals, there was a significant difference in  $[DA]_{avg}$  between bins for ICSS 1 ( $t_4 = 4.351, p = 0.0121$ ) and ICSS 2 ( $t_4 = 4.139, p = 0.0144$ ); however, there were no difference in

press rate between bins for either session (ICSS 1,  $t_4 = 0.236$ ,  $p = 0.825$ ; ICSS 2,  $t_4 = 0.681$ ,  $p = 0.534$ ). Similar trends occurred for both tested drugs. For cocaine,  $[DA]_{avg}$  was significantly lower for the second half within both sessions (ICSS 1,  $t_4 = 4.233$ ,  $p = 0.0133$ ; ICSS 2,  $t_4 = 4.078$ ,  $p = 0.151$ ), but there were no differences in press rate within-session (ICSS 1,  $t_4 = 0.909$ ,  $p = 0.4146$ ; ICSS 2,  $t_4 = 0.850$ ,  $p = 0.443$ ). These trends were mirrored within amphetamine-treated animals, as dopamine significantly changed within session (ICSS 1,  $t_4 = 5.452$ ,  $p = 0.0055$ ; ICSS 2,  $t_4 = 10.84$ ,  $p = 0.0004$ ) but press rate did not (ICSS 1,  $t_4 = 2.135$ ,  $p = 0.0997$ ; ICSS 2,  $t_4 = 0.892$ ,  $p = 0.423$ ). Altogether, this data suggests that for all treatments,  $[DA]$  significantly decreased between the first and second half of each ICSS session (i.e. both before and after treatment). However, this change in average dopamine transient magnitude was not accompanied by significant changes in responding. This data suggests that the changes in phasic dopamine release within session do not play a significant role in the modulation of press rate.

## DISCUSSION

This study expands and supports previous FSCV studies during ICSS in multiple ways. First, this study revealed that the expectancy of ICSS stimulation patterns plays a negligible role in the depreciation of electrically-evoked transients during ICSS, which suggests that the pattern of stimulation, rather than its expectancy, is the major determinant of the pattern of phasic dopamine release during continuous ICSS. Second, this study supports previous findings that timeouts between stimulations result in more gradual attenuation of the dopamine signal (Cheer et al., 2007; Cheer, et al., 2005; Owesson-White, et al., 2008), consistent with depletion-driven attenuation of dopamine release during ICSS. To further test this, two drugs shown to augment phasic dopamine release and ICSS behavior, cocaine and amphetamine, were tested on a FI5 schedule for their effects on behavior and dopamine profiles. While both drugs significantly increased phasic dopamine release during early ICSS, their maximal effects wore off rapidly

and changes in dopamine release within session were not mirrored by dynamic changes in behavior. Ultimately, this data supports previous evidence that dopamine release does not act as the ultimate reward mediator of ICSS.

The first finding of this study was that the expectancy of brain stimulation reward played a minimal role in phasic dopamine dynamics during repeated stimulation. This finding supports a previous microdialysis study that measured similar changes in tonic dopamine levels during fixed- and variable-interval stimulation (Hernandez et al., 2007). These findings are not altogether surprising, as electrical stimulation involves more direct activation of dopamine neurons than natural (i.e. food, sucrose) rewards, and thus brain stimulation reward may be more difficult to 'predict away' than other stimuli. Notably, due to the heterogeneity in the density of release sites in the NAc (Wightman, et al., 2007), it is difficult to assess with FSCV whether the absolute magnitude of dopamine transients (rather than changes over successive stimulation) is larger for unexpected over expected stimulation, as suggested in a previous study (Garris, et al., 1999). Repetitive stimulation, even in FI5 paradigms, results in significant attenuation of electrically-evoked stimulation even following a thirty minute time out. Therefore, administration of both operant- and yoked-ICSS stimulation patterns during the same recording session in the same animal would likely be confounded by the impact of repeated stimulation. However, chronically-implanted CFMs (Clark et al., 2010) would permit recordings on separate days in the same animal, and could therefore test this theory without these concerns.

Cocaine and amphetamine both augmented phasic dopamine release in a similar fashion during FI5 ICSS, despite their typical grouping into different drug classes when assessed with ICSS (i.e. amphetamine as a 'monoamine releaser', cocaine as a uptake inhibitor) (Negus & Miller, 2014), in a manner consistent with augmentation of the readily releasable pool of dopamine. This is in agreement with recent studies that demonstrated amphetamine-induced increases in electrically-evoked dopamine release for short-train stimulations in the NAc (Avelar, et al., 2013; Covey, et al., 2013; Daberkow, et al., 2013).

However, amphetamine is also thought to deplete reserve pools of dopamine vesicles via liberation of dopamine from synaptic vesicles via weak base action at the vesicular monoamine transporter and subsequent facilitation of reverse transport of dopamine through DAT. In the current study, the phasic dopamine profile following amphetamine plateaued at a significantly lower magnitude than cocaine, which is thought to have similar actions on the readily releasable pool (Venton, et al., 2006); this may be due to amphetamine's depleting actions on the reserve pools of vesicles, which are likely increasingly interrogated during repeated stimulation.

With the current ICSS schedule and drug dose paradigm, there was no significant main effect of drug on response rates, though there was a main effect of ICSS session. Manipulations of ICSS behavior are typically assessed with curve-sweep paradigms, which systematically test behavioral responses as a function of stimulation frequency before and after treatment to test for effects (Carlezon & Chartoff, 2007; Negus & Miller, 2014). However, with voltammetry, irregular stimulation frequencies can result in artifacts in the voltammetric signal, particularly in awake animals (Cossette et al., 2016), which can interfere with the success of multivariate calibration. As a result, a consistent stimulation frequency of 60 Hz was used, which has been shown in this lab to facilitate ICSS with FSCV recordings (Beyene et al., 2010; Cheer, et al., 2007; Garris, et al., 1999; Owesson-White, et al., 2008). Consequently, changes in behavior following treatment were assessed at the same stimulation frequency and current as the subsequent ICSS session (and previous training). A notable limitation of this method is that the effect of drugs may vary as a function of baseline responding (Negus & Miller, 2014), which could explain why no statistically significant trends in behavior between drug treatments were seen with the current experimental approach, which was instead optimized for fidelity of FSCV recordings to track changes in dopamine release.

Nonetheless, a significant correlation was found between the augmentation of the initial evoked dopamine transient during ICSS following treatment ( $[DA]_i$ ) and the change in press rate across animals. This demonstrates that augmented dopamine release is correlated with

increased ICSS responding. Examination of within-session dopamine release and response rates revealed that, despite significant within-session decreases in electrically evoked dopamine both before and after treatment, no significant changes in responding were seen within session. This suggests that sustained magnitude of dopamine transients is unimportant for ongoing ICSS behavior. This is consistent with the hypothesis that dopamine release in the NAc is important for initiation, but not maintenance, of reward-seeking behavior (Cheer, et al., 2007; Nicola, 2010; Nicola et al., 2005). It also supports previous assertions that dopamine release is unlikely to serve as the final stage in brain stimulation reward (Cossette, et al., 2016). Instead, other neurotransmitters are necessary for the 'final stage' of neurotransmission that supports continuous ICSS responding. Indeed, the effect of dopamine on MSNs appears to require concomitant local changes in glutamate (Yagishita et al., 2014), and other neurotransmitters, such as GABA (Cheer, et al., 2005; Steffensen et al., 2001) and acetylcholine (Yeomans & Baptista, 1997), have been shown to play important roles in ICSS behavior. Notably, selective optogenetic stimulation of VTA dopamine neurons evokes glutamate release in the NAc even when glutamate co-transmission is abolished (Wang et al., 2017). Therefore, even in conditions that highly favor selective activation of dopamine neurons (in contrast to electrical stimulation), other transmitters such as glutamate may be necessary for the manifestation of dopamine's role in mediating ICSS behavior. Ultimately, while not assessed in this study due to the use of an ICSS paradigm with a continually available lever, the most important role of phasic dopamine release may be mediating responses to cues predicting reward availability (Cheer, et al., 2007; du Hoffmann & Nicola, 2014; Owesson-White et al., 2016), which represents a key factor in the initiation of reward-seeking behavior.

While our data demonstrates that sustained phasic dopamine release is not critical for maintenance of ICSS behavior, it is possible that underlying 'tonic' changes in dopamine levels play an important role. Previous work has shown that elevations in tonic dopamine persist for two hours of well-spaced (12 s inter-stimulation intervals) electrical stimulation patterns

(Hernandez, et al., 2006). In contrast, more rapid stimulation (~1.5 s inter-stimulation intervals) patterns result in higher peak changes in dopamine levels followed by decreased tone, which indicate depletion may alter tonic dopamine levels in a similar fashion to phasic dopamine release, though on different timescales. Interestingly, this depletion is followed by diminished ICSS responding, which indicates dopamine tone may indeed track ICSS behavior. This is in contrast to our findings for phasic dopamine release, which significantly attenuates within a single ICSS session without paired changes in behavior. Notably, amphetamine and cocaine both elevate tonic dopamine levels, through DAT blockade and, in the case of amphetamine, efflux of cytosolic dopamine into extracellular space. The subsequent elevations in tonic levels of dopamine, rather than their effects on phasic release, may underlie their ability to facilitate ICSS. Consistent with this finding, we found rising baselines in dopamine signal during early ICSS following amphetamine and cocaine, but not saline, treatment. Further microdialysis measurements during prolonged ICSS could reveal whether significant changes in tonic dopamine levels are tracked by dynamic changes in behavior.

## REFERENCES

- Adamantidis, A. R., et al. (2011). Optogenetic interrogation of dopaminergic modulation of the multiple phases of reward-seeking behavior. *J Neurosci*, 31(30), 10829-10835.
- Avelar, A. J., Juliano, S. A., & Garris, P. A. (2013). Amphetamine augments vesicular dopamine release in the dorsal and ventral striatum through different mechanisms. *J Neurochem*, 125(3), 373-385.
- Beyene, M., Carelli, R. M., & Wightman, R. M. (2010). Cue-evoked dopamine release in the nucleus accumbens shell tracks reinforcer magnitude during intracranial self-stimulation. *Neuroscience*, 169(4), 1682-1688.
- Bucher, E. S., et al. (2013). Flexible software platform for fast-scan cyclic voltammetry data acquisition and analysis. *Anal Chem*, 85(21), 10344-10353.
- Carlezon, W. A., Jr., & Chartoff, E. H. (2007). Intracranial self-stimulation (ICSS) in rodents to study the neurobiology of motivation. *Nat Protoc*, 2(11), 2987-2995.
- Cheer, J. F., Aragona, B. J., Heien, M. L., Seipel, A. T., Carelli, R. M., & Wightman, R. M. (2007). Coordinated accumbal dopamine release and neural activity drive goal-directed behavior. *Neuron*, 54(2), 237-244.
- Cheer, J. F., Heien, M. L., Garris, P. A., Carelli, R. M., & Wightman, R. M. (2005). Simultaneous dopamine and single-unit recordings reveal accumbens GABAergic responses: implications for intracranial self-stimulation. *Proc Natl Acad Sci U S A*, 102(52), 19150-19155.
- Clark, J. J., et al. (2010). Chronic microsensors for longitudinal, subsecond dopamine detection in behaving animals. *Nat Methods*, 7(2), 126-129.
- Corbett, D., & Wise, R. A. (1980). Intracranial self-stimulation in relation to the ascending dopaminergic systems of the midbrain: a moveable electrode mapping study. *Brain Res*, 185(1), 1-15.
- Cossette, M. P., Conover, K., & Shizgal, P. (2016). The neural substrates for the rewarding and dopamine-releasing effects of medial forebrain bundle stimulation have partially discrepant frequency responses. *Behav Brain Res*, 297, 345-358.
- Covey, D. P., Juliano, S. A., & Garris, P. A. (2013). Amphetamine elicits opposing actions on readily releasable and reserve pools for dopamine. *PLoS One*, 8(5), e60763.
- Daberkow, D. P., et al. (2013). Amphetamine paradoxically augments exocytotic dopamine release and phasic dopamine signals. *J Neurosci*, 33(2), 452-463.
- du Hoffmann, J., & Nicola, S. M. (2014). Dopamine invigorates reward seeking by promoting cue-evoked excitation in the nucleus accumbens. *J Neurosci*, 34(43), 14349-14364.

- Elmer, G. I., Pieper, J. O., Hamilton, L. R., & Wise, R. A. (2010). Qualitative differences between C57BL/6J and DBA/2J mice in morphine potentiation of brain stimulation reward and intravenous self-administration. *Psychopharmacology (Berl)*, *208*(2), 309-321.
- Fiorino, D. F., Coury, A., Fibiger, H. C., & Phillips, A. G. (1993). Electrical stimulation of reward sites in the ventral tegmental area increases dopamine transmission in the nucleus accumbens of the rat. *Behav Brain Res*, *55*(2), 131-141.
- Fulton, S., Woodside, B., & Shizgal, P. (2000). Modulation of brain reward circuitry by leptin. *Science*, *287*(5450), 125-128.
- Garris, P. A., Kilpatrick, M., Bunin, M. A., Michael, D., Walker, Q. D., & Wightman, R. M. (1999). Dissociation of dopamine release in the nucleus accumbens from intracranial self-stimulation. *Nature*, *398*(6722), 67-69.
- Gilliss, B., Malanga, C. J., Pieper, J. O., & Carlezon, W. A., Jr. (2002). Cocaine and SKF-82958 potentiate brain stimulation reward in Swiss-Webster mice. *Psychopharmacology (Berl)*, *163*(2), 238-248.
- Giros, B., Jaber, M., Jones, S. R., Wightman, R. M., & Caron, M. G. (1996). Hyperlocomotion and indifference to cocaine and amphetamine in mice lacking the dopamine transporter. *Nature*, *379*(6566), 606-612.
- Heien, M. L., et al. (2005). Real-time measurement of dopamine fluctuations after cocaine in the brain of behaving rats. *Proc Natl Acad Sci U S A*, *102*(29), 10023-10028.
- Hernandez, G., Haines, E., Rajabi, H., Stewart, J., Arvanitogiannis, A., & Shizgal, P. (2007). Predictable and unpredictable rewards produce similar changes in dopamine tone. *Behav Neurosci*, *121*(5), 887-895.
- Hernandez, G., et al. (2006). Prolonged rewarding stimulation of the rat medial forebrain bundle: neurochemical and behavioral consequences. *Behav Neurosci*, *120*(4), 888-904.
- Hernandez, G., Trujillo-Pisanty, I., Cossette, M.-P., Conover, K., & Shizgal, P. (2012). Role of dopamine tone in the pursuit of brain stimulation reward. *J Neurosci*, *32*(32), 11032-11041.
- Howard, C. D., Daberkow, D. P., Ramsson, E. S., Keefe, K. A., & Garris, P. A. (2013). Methamphetamine-induced neurotoxicity disrupts naturally occurring phasic dopamine signaling. *Eur J Neurosci*, *38*(1), 2078-2088.
- Ikemoto, S., & Panksepp, J. (1999). The role of nucleus accumbens dopamine in motivated behavior: a unifying interpretation with special reference to reward-seeking. *Brain Res Rev*, *31*(1), 6-41.
- Ilango, A., Kesner, A. J., Broker, C. J., Wang, D. V., & Ikemoto, S. (2014). Phasic excitation of ventral tegmental dopamine neurons potentiates the initiation of conditioned approach behavior: parametric and reinforcement-schedule analyses. *Front Behav Neurosci*, *8*, 155.

- Jones, S. R., Gainetdinov, R. R., Wightman, R. M., & Caron, M. G. (1998). Mechanisms of amphetamine action revealed in mice lacking the dopamine transporter. *J Neurosci*, *18*(6), 1979-1986.
- Keithley, R. B., Heien, M. L., & Wightman, R. M. (2009). Multivariate concentration determination using principal component regression with residual analysis. *Trends Analyt Chem*, *28*(9), 1127-1136.
- Kile, B. M., Guillot, T. S., Venton, B. J., Wetsel, W. C., Augustine, G. J., & Wightman, R. M. (2010). Synapsins differentially control dopamine and serotonin release. *J Neurosci*, *30*(29), 9762-9770.
- Kruk, Z. L., Cheeta, S., Milla, J., Muscat, R., Williams, J. E., & Willner, P. (1998). Real time measurement of stimulated dopamine release in the conscious rat using fast cyclic voltammetry: dopamine release is not observed during intracranial self stimulation. *J Neurosci Methods*, *79*(1), 9-19.
- Kuhr, W. G., Ewing, A. G., Near, J. A., & Wightman, R. M. (1985). Amphetamine attenuates the stimulated release of dopamine in vivo. *J Pharmacol Exp Ther*, *232*(2), 388-394.
- Markou, A., & Koob, G. F. (1991). Postcocaine anhedonia. An animal model of cocaine withdrawal. *Neuropsychopharmacology*, *4*(1), 17-26.
- Michael, A. C., Ikeda, M., & Justice, J. B., Jr. (1987). Mechanisms contributing to the recovery of striatal releasable dopamine following MFB stimulation. *Brain Res*, *421*(1-2), 325-335.
- Mirenowicz, J., & Schultz, W. (1996). Preferential activation of midbrain dopamine neurons by appetitive rather than aversive stimuli. *Nature*, *379*(6564), 449-451.
- Montague, P. R., et al. (2004). Dynamic gain control of dopamine delivery in freely moving animals. *J Neurosci*, *24*(7), 1754-1759.
- Negus, S. S., & Miller, L. L. (2014). Intracranial self-stimulation to evaluate abuse potential of drugs. *Pharmacol Rev*, *66*(3), 869-917.
- Nicola, S. M. (2010). The flexible approach hypothesis: unification of effort and cue-responding hypotheses for the role of nucleus accumbens dopamine in the activation of reward-seeking behavior. *J Neurosci*, *30*(49), 16585-16600.
- Nicola, S. M., Taha, S. A., Kim, S. W., & Fields, H. L. (2005). Nucleus accumbens dopamine release is necessary and sufficient to promote the behavioral response to reward-predictive cues. *Neuroscience*, *135*(4), 1025-1033.
- Olds, J., & Milner, P. (1954). Positive reinforcement produced by electrical stimulation of septal area and other regions of rat brain. *J Comp Physiol Psychol*, *47*(6), 419-427.
- Owesson-White, C., et al. (2016). Cue-Evoked Dopamine Release Rapidly Modulates D2 Neurons in the Nucleus Accumbens During Motivated Behavior. *J Neurosci*, *36*(22), 6011-6021.

- Owesson-White, C. A., Cheer, J. F., Beyene, M., Carelli, R. M., & Wightman, R. M. (2008). Dynamic changes in accumbens dopamine correlate with learning during intracranial self-stimulation. *Proc Natl Acad Sci U S A*, *105*(33), 11957-11962.
- Rodeberg, N. T., Johnson, J. A., Bucher, E. S., & Wightman, R. M. (2016). Dopamine Dynamics during Continuous Intracranial Self-Stimulation: Effect of Waveform on Fast-Scan Cyclic Voltammetry Data. *ACS Chem Neurosci*, *7*(11), 1508-1518.
- Rodeberg, N. T., Johnson, J. A., Cameron, C. M., Saddoris, M. P., Carelli, R. M., & Wightman, R. M. (2015). Construction of Training Sets for Valid Calibration of in Vivo Cyclic Voltammetric Data by Principal Component Analysis. *Anal Chem*, *87*(22), 11484-11491.
- Schmitz, Y., Lee, C. J., Schmauss, C., Gonon, F., & Sulzer, D. (2001). Amphetamine distorts stimulation-dependent dopamine overflow: effects on D2 autoreceptors, transporters, and synaptic vesicle stores. *J Neurosci*, *21*(16), 5916-5924.
- Schultz, W. (1998). Predictive reward signal of dopamine neurons. *J Neurophysiol*, *80*(1), 1-27.
- Steffensen, S. C., Lee, R. S., Stobbs, S. H., & Henriksen, S. J. (2001). Responses of ventral tegmental area GABA neurons to brain stimulation reward. *Brain Res*, *906*(1-2), 190-197.
- Steinberg, E. E., Boivin, J. R., Saunders, B. T., Witten, I. B., Deisseroth, K., & Janak, P. H. (2014). Positive reinforcement mediated by midbrain dopamine neurons requires D1 and D2 receptor activation in the nucleus accumbens. *PLoS One*, *9*(4), e94771.
- Venton, B. J., et al. (2006). Cocaine increases dopamine release by mobilization of a synapsin-dependent reserve pool. *J Neurosci*, *26*(12), 3206-3209.
- Wang, D. V., et al. (2017). Disrupting Glutamate Co-transmission Does Not Affect Acquisition of Conditioned Behavior Reinforced by Dopamine Neuron Activation. *Cell Rep*, *18*(11), 2584-2591.
- Wightman, R., et al. (2007). Dopamine release is heterogeneous within microenvironments of the rat nucleus accumbens. *Eur J Neurosci*, *26*(7), 2046-2054.
- Wise, R. A. (1996). Addictive drugs and brain stimulation reward. *Annu Rev Neurosci*, *19*, 319-340.
- Wise, R. A. (2002). Brain reward circuitry: insights from unsensed incentives. *Neuron*, *36*(2), 229-240.
- Witten, I. B., et al. (2011). Recombinase-driver rat lines: tools, techniques, and optogenetic application to dopamine-mediated reinforcement. *Neuron*, *72*(5), 721-733.
- Yagishita, S., Hayashi-Takagi, A., Ellis-Davies, G. C., Urakubo, H., Ishii, S., & Kasai, H. (2014). A critical time window for dopamine actions on the structural plasticity of dendritic spines. *Science*, *345*(6204), 1616-1620.
- Yeomans, J., & Baptista, M. (1997). Both nicotinic and muscarinic receptors in ventral tegmental area contribute to brain-stimulation reward. *Pharmacol Biochem Behav*, *57*(4), 915-921.

## CHAPTER 4: CONSTRUCTION OF TRAINING SETS FOR VALID CALIBRATION OF *IN VIVO* FSCV DATA BY PRINCIPAL COMPONENT ANALYSIS<sup>1</sup>

### INTRODUCTION

*In vivo* measurement techniques such as microdialysis and electrochemical methods have enhanced understanding of the roles of neurotransmitters during behavior (Bucher & Wightman, 2015). One electrochemical technique, fast-scan cyclic voltammetry (FSCV), is particularly useful to detect subsecond dopamine release in behaving animals. The cyclic voltammograms (CVs) provided by this technique give chemically specific information for identification of measured species. Most FSCV applications have utilized acutely implanted carbon-fiber microelectrodes, but chronically-implanted electrodes have also been used (Clark et al., 2010). Chronically-implanted electrodes are advantageous because they permit longitudinal recordings at the same location in the brain.

Calibration is a major concern with all *in vivo* techniques. Originally, the peak oxidation current in CVs for dopamine was scaled to concentration with a calibration factor obtained *in vitro*. However, this technique fails when multiple species overlap, as when pH and dopamine changes occur simultaneously (Day et al., 2007; Phillips et al., 2003; Roitman et al., 2004; Roitman et al., 2008), and are inappropriate for long-term dopamine measurements, such as slow basal level increases in response to cocaine (Heien et al., 2005; Willuhn et al., 2014a) and other prolonged responses (Hollon et al., 2014; Howe et al., 2013) where current contributions from interferences are more likely to play a role. Comparison of CVs with templates for

---

<sup>1</sup> This chapter previously appeared as an article in *Analytical Chemistry*. The original citation is as follows: Rodeberg, N.T., Johnson, J.A., Cameron, C.M., Saddoris, M.P., Carelli, R.M., & Wightman, R.M. "Construction of Training Sets for Valid Calibration of *In Vivo* Cyclic Voltammetric Data by Principal Component Analysis," *Analytical Chemistry* 87, no. 22: 11484.

dopamine, utilizing the correlation coefficient to confirm analyte identity, has also been used (Clark, et al., 2010; Robinson et al., 2003). More recently, principal component analysis in tandem with inverse least-squares regression (PCR) (Heien et al., 2004; Kramer, 1998) has been introduced for resolving and quantifying overlapping compounds in FSCV data (Heien, et al., 2005; Keithley et al., 2009). PCR models use training sets containing CVs from multiple electroactive analytes for calibration (Heien, et al., 2004). As a multivariate analysis technique, PCR uses the entire CV for concentration prediction. When used with acutely implanted electrodes, training sets can be constructed at the same brain location where behaviorally evoked chemical measurements were made using electrical stimulation to evoke defined chemical changes. Detailed description of the use of PCR with FSCV can be found elsewhere (Heien, et al., 2004; Heien, et al., 2005; Keithley et al., 2010; Keithley, et al., 2009; Keithley & Wightman, 2011; Kramer, 1998).

Chronically-implanted microelectrodes (Clark, et al., 2010) pose unique calibration problems. Longitudinal experiments need to demonstrate both electrode stability and reliable concentration calibration over successive recording sessions. The short durations of acute implantation studies minimizes the neuroimmunological response and adhesion of biomolecules to the electrode, thus making post-experiment calibration factors obtained *in vitro* relevant to *in vivo* data (Peters et al., 2004). However, this may not be true for the extensive implantation times used in chronic recordings. The temporal distortion seen with chronically implanted microelectrodes (Clark, et al., 2010) suggests tissue encapsulation and/or biofouling, each of which represents a much different environment from those seen in *post vivo* calibration. Recent measurements with chronically implanted electrodes have found peak dopamine concentrations of 5 nM or less (Hollon, et al., 2014), which represents an order-of-magnitude deviation from dopamine concentrations measured with acutely-implanted microelectrodes during natural reward (Roitman, et al., 2004; Roitman, et al., 2008). The chemoanalytical power of FSCV to determine concentrations is important because the affinity of receptors varies significantly

between subtype, as highlighted for dopamine (Tritsch & Sabatini, 2012). Thus, these differences are concerning and may reflect problems with current calibration methodology for these sensors.

Because stimulating electrodes are rarely implanted with chronically implanted microelectrode, robust dopamine and pH training sets are rarely obtained in the same location as behavioral measurements. To circumvent this problem, one approach has utilized unexpected sucrose delivery, a procedure that evokes dopamine transients (Day, et al., 2007) for within-subject analyte verification (Gan et al., 2010; Wanat et al., 2010). Another calibration attempt has been the use of 'standard training sets' built from electrically-stimulated dopamine transients acquired in separate subjects (Clark et al., 2013; Flagel et al., 2011; Goertz et al., 2015; Hart et al., 2014; Hollon, et al., 2014; Howe, et al., 2013; Wanat et al., 2013; Willuhn, et al., 2014a; Willuhn et al., 2014b). Here, we compare these techniques at acutely-implanted electrodes to previously established protocols for PCR using data from behaving animals. The results reveal that large concentration errors are introduced with these approaches to PCR, which indicate deficits in signal extraction. Furthermore, the standard training set approach nullifies the use of residual analysis for model validation.

## **EXPERIMENTAL**

### **Animals**

Male Sprague-Dawley rats (250-400 g) from Charles River (Wilmington, MA, USA, n = 6) and Harlan Sprague Dawley (Indianapolis, IN, USA, n = 19) were housed individually on a 12/12 h light/dark cycle. Rats were given access to water *ad libitum*. For behavioral paradigms utilizing sucrose rewards, animals were food-restricted as described previously (Cameron et al., 2014). Animal procedures were approved by the UNC-Chapel Hill Institutional Animal Care and Use Committee (IACUC).

## **Surgery**

Rats in the multiple schedule reinforcement and cue discrimination task were surgically implanted with jugular vein catheters (Cameron, et al., 2014). For subjects participating in multiple schedule reinforcement (n = 8) and Pavlovian conditioning (n = 4), rats were anesthetized with a mixture of ketamine hydrochloride (100 mg/kg) and xylazine hydrochloride (10 mg/kg i.m.) and a guide cannula (Bioanalytical Systems, West Lafayette, IN) for the working electrode was implanted above the nucleus accumbens (NAc) core (+1.3 mm anterior, +1.3 mm lateral, all measurements from bregma). A Ag/AgCl reference electrode was implanted in the contralateral hemisphere. A bipolar stimulating electrode (Plastics One, Roanoke, VA) was positioned above the ventral tegmental area (VTA) (-5.2 mm posterior, +1.0 mm lateral, -7 mm ventral from brain surface). The stimulating electrode was lowered in 0.2 mm increments until electrical stimulation resulted in diminished physical response, suggesting proximity to the desired stimulation site. Stainless steel screws and dental cement were used to secure all items to the skull surface.

Rats for intracranial self-stimulation (ICSS, n = 5) underwent similar surgery, with minor differences. They were anesthetized with isoflurane (1.5-4%). The guide cannula (Bioanalytical Systems, West Lafayette, IN) was implanted above the NAc shell (+1.7 mm anterior, +0.8 mm lateral). Another guide cannula was implanted in the contralateral hemisphere for experiment-day implantation of the reference electrode. The bipolar stimulating electrode (Plastics One, Roanoke, VA) was implanted 8.4-8.6 mm ventral from skull surface.

## **Behavior**

Three separate behavioral paradigms were investigated in this study. All training and experiments were conducted in plexiglass operant chambers housed in sound- and noise-attenuated cubicles (Med Associates Inc., St. Albans, VT. USA).

### *Multiple schedule reinforcement*

The multiple schedule reinforcement paradigm was described previously (Cameron, et al., 2014). Prior to surgery, rats ( $n = 8$ ) were trained to press a lever for sucrose (45 mg pellet; TestDiet, St. Louis, MO, USA) on a fixed-ratio 1 (FR1) schedule. A cue light above the lever was illuminated with lever extension. Each lever press was followed by the onset of a tone (65 dB, 2900 Hz, 20 s) and a timeout (20 s). Rats were trained until stable responding of at least 50 presses per behavioral session. Rats were subsequently trained to lever press for cocaine (0.33 mg/infusion, approximately 1 mg/kg/infusion, 6 s) at a separate lever; each lever press was followed by a different tone (65 dB, 800 Hz, 20 s) and a timeout (20 s).

Following behavioral training, rats underwent voltammetric surgery. After recovery, rats were retrained for two consecutive days in separate sessions for both sucrose and cocaine responding. Rats subsequently underwent a multiple schedule of reinforcement for sucrose and cocaine, in which rats had access to the lever paired with sucrose (15 min) or cocaine (2 h), followed by a timeout (20 s) and availability of the other reinforcer. The order of the reinforcers was pseudo-randomized across animals to ensure an equal number of subjects ( $n=4$ ) underwent each reinforcer order.

### *Pavlovian conditioning*

The second behavioral paradigm involved Pavlovian conditioning for sucrose reward, as described previously (Saddoris & Carelli, 2014). Rats ( $n = 4$ ) underwent extensive training (9 d) to discriminate between a cue that predicted sucrose delivery (CS+), a cue paired with reward omission (CS-), and two separate CS+ presentations without reward presentation (CS+NR). Voltammetric recordings of cue responses were made on the tenth day of training.

## **ICSS**

Following surgery, rats ( $n = 5$ ) were trained in ICSS as previously described (Garris et al., 1999). Each training session began with white noise, house and cue lights, and lever

extension. Rats were primed with electrical stimulation (24 biphasic pulses, 60 Hz, 75-150  $\mu$ A) as they approached the lever until the rat acquired ICSS (FR1 schedule continuous reinforcement). Rats underwent two separate training sessions (2 min) on a minimum of three days before voltammetric recordings.

On the recording day, freshly prepared Ag/AgCl reference and carbon-fiber microelectrode were inserted and voltammetric recordings were begun. Subjects were allowed to press a lever continually for electrical stimulation, for two minutes or a minimum of 50 presses. Subject C experienced an electrode break during behavior, preventing full collection of this data set. However, sufficient data was collected in subject C to build a training set for PCR.

## **FSCV**

Glass-sealed carbon-fiber microelectrodes, 90-110  $\mu$ m exposed length, were inserted into micromanipulators that was placed in the implanted guide cannula. The microelectrode was lowered to the brain region of interest where robust dopamine release was identified. The microelectrode and reference electrode were connected to a head-mounted amplifier attached to a commutator (Med-Associates, St. Albans, VT) allowing unrestricted movement. Behavioral events (cues, lever extension) were controlled with a MedAssociates system. FSCV data was displayed as two-dimensional color plots with time as the abscissa, the applied potential as the ordinate, and the current in false color.

## **Data analysis**

Statistical tests were conducted using commercial software (Statistica, Tulsa, OK; GraphPad Software, La Jolla, CA). Significance was tested at  $\alpha = 0.05$ . Training sets for dopamine and pH were built according to guidelines described previously (Heien, et al., 2004; Keithley, et al., 2010; Keithley, et al., 2009; Keithley & Wightman, 2011). Training sets consisted of five cyclic voltammograms for both dopamine and pH changes that spanned the amplitudes

obtained during behavioral experiments. Normally, the sets were from the same animal with the same electrode and instrumentation as the behavioral data to ensure they included noise typical of each electrode and recording site. The CVs were collected during electrical stimulations that were not part of the behavioral data. K-matrices (see supplementary material) for dopamine and pH were calculated for each set to aid in qualitative analyte identification. Currents were converted to concentrations using external calibration factors (10 nA/ $\mu$ m at the peak oxidation potential for dopamine, -40 nA/pH unit at  $E_{QH}$  for pH) (Tadmakov et al., 2010).

To characterize pH changes during each lever press for sucrose and cocaine, voltammetric data was divided into 20-s snippets surrounding lever presses. pH changes were calculated every 100 ms, and averaged into 500 ms bins during statistical analysis. If animals responded more for one reinforcer than another, data was truncated to provide an equal number of trials for each reinforcer for each subject.

For rats undergoing Pavlovian conditioning, two training sets were built for each subject: one using CVs for dopamine and pH obtained during electrical stimulation, and a second set using CVs from naturally occurring transients. Time blocks (centered  $\pm$  5 s surrounding cue onset) were constructed and peak dopamine concentrations at cue onset or delivery of unexpected sucrose were obtained from local maxima in the dopamine concentration versus time traces in each time block taken 0-3 s following cue onset. The time point of each transient was recorded to ensure both training sets were analyzing the same event. Dopamine transients that fell below the limit of detection ( $3 \times \text{RMS}$ ) during analysis with the electrical stimulation training set were excluded from data analysis.

For ICSS, data were analyzed in 10-s blocks ( $\pm$  5 s around each lever press) and the peak concentrations were recorded. Each snippet was digitally background subtracted at local minima in the current versus time trace at the peak oxidation potential for dopamine, usually two to three seconds before each lever press. In cases where several presses were in rapid succession, the same local minima were used for the adjacent dopamine transients. Composite

training sets were constructed using a locally written program using LabVIEW (National Instruments, Austin, TX). CVs for both dopamine and pH were selected at random from each training sets A-E. Due to the large number of possible composite training sets ( $5^{10}$ ), the number of training sets was limited to 10,000. This process was repeated with larger training set sizes ( $n = 2, 3, \text{ and } 4$  CV standards from each training set for both DA and pH). Resulting K-matrices and  $Q_{\alpha}$  values were recorded and averaged for each training set size.

## RESULTS & DISCUSSION

### **FSCV measurements during behavior consist of multiple physiologically relevant components**

FSCV data recorded *in vivo* contains contributions from numerous substances. Signals in dopamine rich regions often include pH changes that occur not only during electrical stimulation of dopaminergic pathways (Venton et al., 2003) but also during unconditioned (Ariansen et al., 2012; Heien, et al., 2005; Roitman, et al., 2008) and Pavlovian (Ariansen, et al., 2012) behaviors. We illustrate these changes here with CVs obtained during a behavioral task for which we previously showed evoked fluctuations in dopamine (Cameron, et al., 2014). Rats were initially trained to press a lever for sucrose reward; each press resulted in one pellet (FR1) delivered into a nearby food receptacle. Rats were then trained to press a spatially separate lever (FR1) for intravenous infusions of cocaine. On test day, FSCV recordings were made during a multiple schedule, wherein rats responded for one reinforcer (FR1; sucrose, 15 min; or cocaine, 2 hr) followed by a 20 s timeout period (no lever extended, dark chamber), and finally extension of the other reinforcer-paired lever. Reinforcer order was varied across animals. Dopamine increases following lever presses (peak, 0.6 V) and is accompanied by a basic pH shift (peak, 0.2 V) (Takmakov, et al., 2010) (Figure 4.1a). These signals were resolved by PCR using a training set obtained at the same location via electrical stimulation of the SN/VTA.

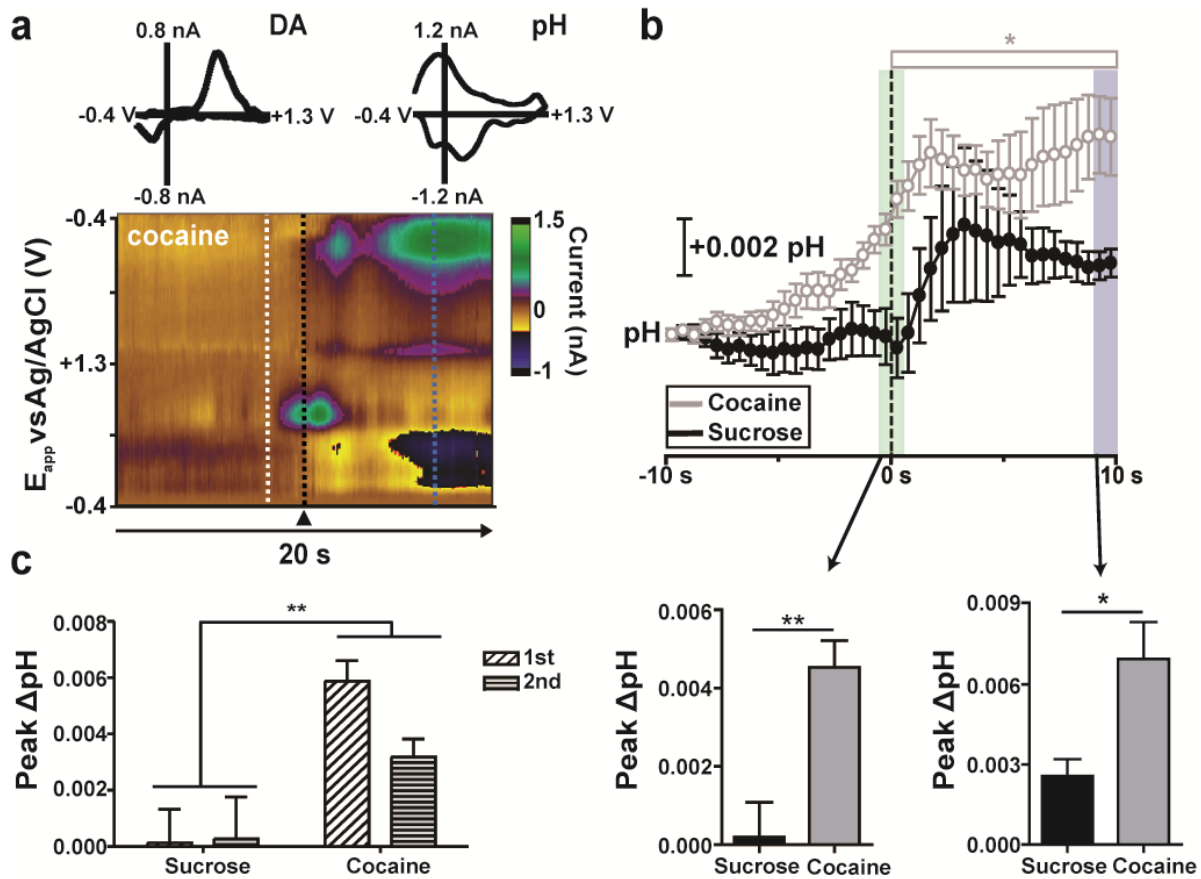


**Figure 4.1.** pH changes depend on reinforcer identity and order. a) Example of dopamine and basic pH shifts for one animal during performance of the sucrose/cocaine multiple schedule. A three-dimensional color plot is obtained by plotting time as the abscissa, the applied potential as the ordinate, and the current in false color. Insets: cyclic voltammograms (CVs) immediately surrounding lever press reflect dopamine (black dotted line), while CVs averaged at 7 s following lever press indicate basic shifts in pH (blue dotted line). Background subtraction at white dotted line. b) (Top) Changes in pH in the NAC core during sucrose and cocaine self-administration. pH is averaged into 500 ms bins (mean  $\pm$  SEM) and aligned to lever press (dotted line, time 0 s) for cocaine (gray) and sucrose (black). Open bar indicates bins significantly higher than baseline for cocaine (Newman-Keuls post hoc test,  $*p < 0.05$ ). (Bottom) Comparison of peak pH within a 1 s window surrounding lever press (left, green column,  $p < 0.005$ ) and 9-10 s later right, blue column,  $p < 0.5$ ) for sucrose (black) versus cocaine (gray),  $p < 0.005$ . c) Comparison of peak pH within a 1 s window surrounding lever press for sucrose and cocaine when self-administered first (white bars) versus second (gray bars) in the multiple schedule,  $p < 0.005$ .

The average time course and amplitude of pH changes to sucrose and cocaine were found to be significantly different (Figure 4.1b), and both time courses differed from those seen with dopamine (Cameron, et al., 2014). The onset of pH changes preceded lever responding for cocaine, but not for sucrose. Cocaine-reinforced pH responses were larger than sucrose-reinforced responses, regardless of reinforcer order (two-way mixed design ANOVA [sucrose vs. cocaine, within subjects factors; reinforcer order, between subject factor];  $F_{1,6}=22.12$ ,  $p < 0.005$ ) (Figure 4.1c). This example critically illustrates the necessity for multivariate analysis when monitoring with FSCV, as each analyte carries distinct information.

### **Training sets from natural rewards**

In experiments where it is inconvenient to implant stimulating electrodes, naturally occurring transients, such as those evoked with unexpected sucrose delivery (Day, et al., 2007), have been used for analyte verification. An example is shown in Figure 4.2a, where cue-, sucrose-, and electrically-evoked dopamine CVs collected at the same electrode and recording location maintain a high correlation ( $0.91 < r^2 < 0.99$ ). However, this procedure provides only qualitative information. Instead, the naturally evoked transients could be used to build a PCR model that permits multivariate concentration prediction. To evaluate this approach, data was collected in four subjects that performed a behavioral discrimination task described previously (Saddoris & Carelli, 2014). The signals here were dopamine transients in response to cues. Two training sets were built in each subject at the same electrode: one using transients evoked from sucrose delivery and the other from electrically evoked transients (Table 4.1). The food pellets tended to give a narrower range of amplitudes than the electrical stimulations (Figure 4.2b). For each animal, the dopamine concentrations obtained with the training set employing electrical stimulation in the same animal were first determined. Next, the dopamine concentrations computed with the sucrose-evoked training set were determined, and the percent difference to the values obtained with electrically-evoked training sets was found

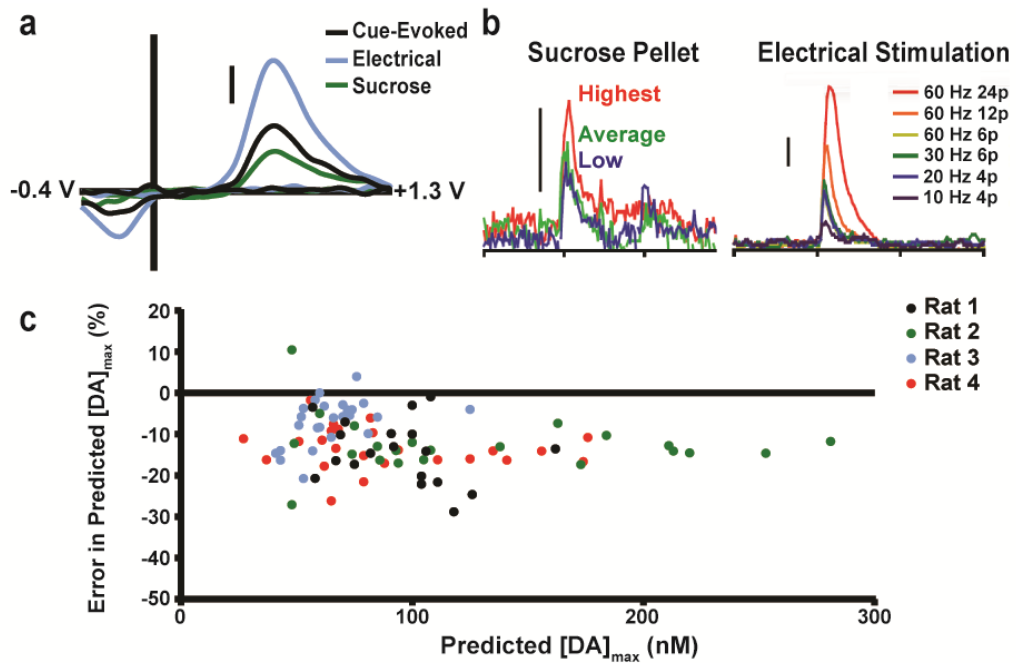


**Figure 4.2.** Training set construction with naturally evoked transients. a) Dopamine CVs evoked by cues, electrical stimulation, and unexpected sucrose delivery share high correlation. b) Dopamine transients evoked by unexpected delivery of sucrose pellets (left) post-experiment have a relatively small (maximum ~ 150 nM) and narrow (~60-70 nM) range. Varying stimulation parameters (right) enables generation of dopamine transients over a wide range. c) Peak dopamine concentration values obtained using training sets built with only naturally occurring transients post-experiment compared to values obtained with training sets built with electrical stimulation in the same subject. Sucrose-constructed training sets consistently predicted lower dopamine concentrations than electrical stimulation training sets.

Subject	Training Set	$r^2$	$Q_\alpha$ (nA <sup>2</sup> )	$E_{p,a}$ (V)	$E_{p,c}$ (V)	$I_{p,a}/I_{p,c}$
SOCC1	Electrical	0.882	199.8	0.63	-0.26	2.3
	Sucrose		191.9	0.64	-0.26	6.3
SOCC2	Electrical	0.883	473.1	0.66	-0.19	3.2
	Sucrose		413.1	0.66	-0.32	3.5
SOCC3	Electrical	0.957	289.2	0.59	-0.25	3.9
	Sucrose		144.6	0.60	-0.23	2.1
SOCC4	Electrical	0.923	311.6	0.58	-0.18	5.9
	Sucrose		127.4	0.59	-0.20	3.2

**Table 4.1.** Characteristics of dopamine K-matrices for various subjects for two different training set construction methods: electrically-evoked or naturally occurring dopamine transients. Minor differences were seen in the peak potentials, while notable differences observed in the peak current ratio. The most significant difference between constructed training sets were  $Q_\alpha$  values, which were systematically lower for transients constructed only with naturally occurring transients. Relatively low correlation coefficients for SOCC1 and SOCC3 were due to difficulty in obtaining clean cyclic voltammograms from naturally occurring transients, leading to broader oxidation peaks (SOCC1) and minor ionic fluctuations on the anodic scan (SOCC2).

(Figure 4.2c). Generally, the dopamine concentrations predicted by sucrose-evoked training sets were considerably lower despite using the same electrode and sensitivity factor (ratio paired t-test,  $p < 0.0001$  for all subjects). The large majority of transients (96.1%) were underestimated with few overestimations (2.3%). These differences are likely due to the narrow range of concentrations obtained with the sucrose-evoked transients compared to those obtained with electrical stimulations. Post-experiment transients evoked with unexpected sucrose delivery can fail to span the concentration range of transients seen during behavior, which has been stated previously to be an important facet of training set construction (Keithley, et al., 2009). Moreover, it is more difficult to separate sucrose-evoked dopamine transients from other chemical events, such as overlapping pH and ionic fluctuations, than it is for time-locked electrical stimulations, resulting in the use of impure training set standards for model construction. With a narrow calibration range, impure standards will have an undue influence on the extrapolation of the calibration curve to higher concentrations.

### **PCR and training sets from separate electrodes**

An alternate approach has been the use of training sets built with electrodes from other experiments to predict concentrations. To further investigate this approach, we used data from rats executing ICSS (Garris, et al., 1999). The data sets from each of the five animals were designated by the letters A-E. Animals pressed a lever repetitively for approximately two minutes, and each lever press evoked electrical stimulation of the SN/VTA. Voltammetric responses were measured in the NAc with acutely implanted carbon-fiber microelectrodes. A representative color plot (Figure 4.3) indicates both dopamine and pH changes, observed in all animals. Interestingly, the individual voltammogram shown (top left) was highly correlated with an isolated, electrically evoked dopamine CV ( $r^2 = 0.851$ ) despite clearly containing pH contributions, illustrating that the template approach (Clark, et al., 2010; Robinson, et al., 2003) is insufficient for species resolution.

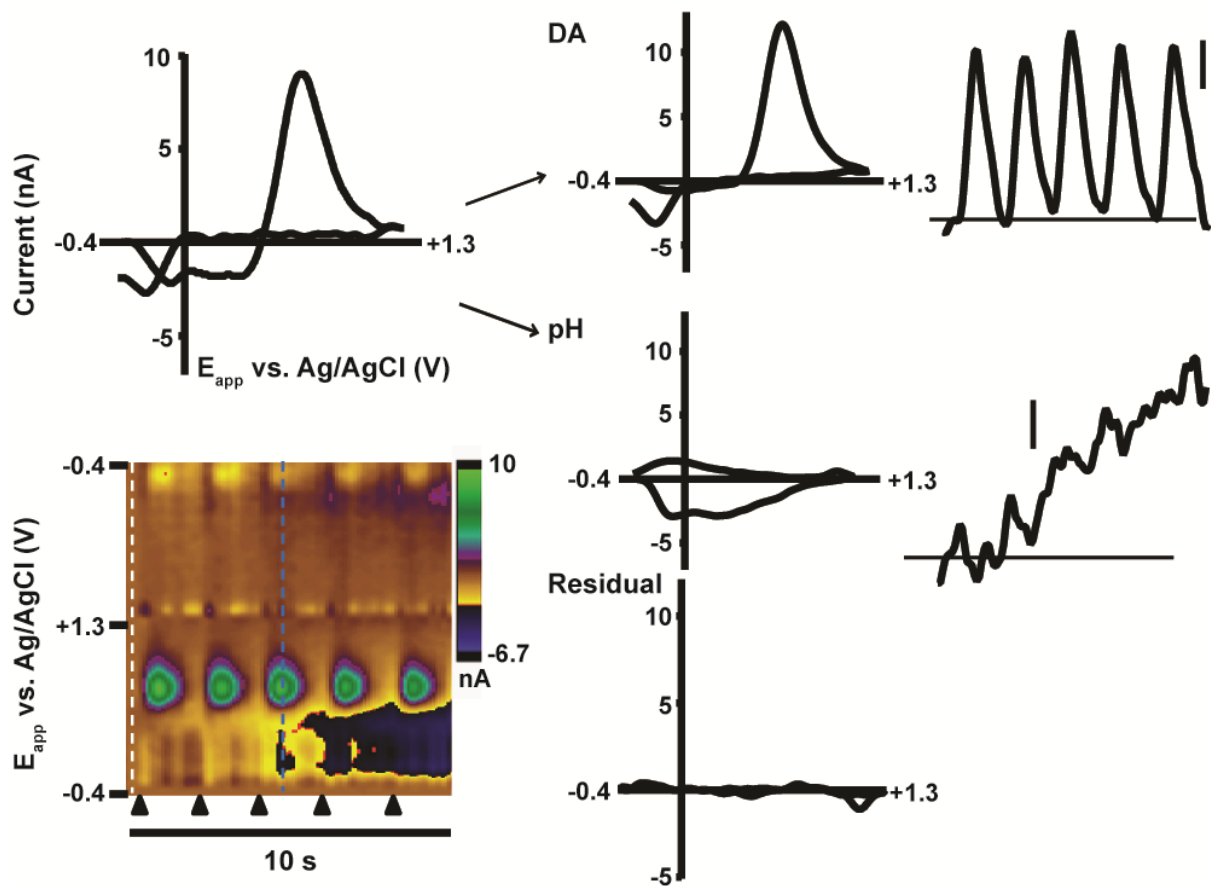


**Figure 4.3.** The use of principal component analysis to predict analyte concentrations. The white dotted line represents the cyclic voltammogram used for digital background subtraction. Each black triangle indicates a lever press-induced electrical stimulation, resulting in dopamine release. The inset cyclic voltammogram (top left) was collected at the blue dotted line. Principal component analysis allows separation of the total current into contributions from dopamine and pH, with any remaining current contained in a residual voltammogram (bottom right). Using this method, concentration versus time traces are acquired for both analytes (top right, DA and middle right, pH).

Training sets for dopamine and pH changes were constructed from data obtained during experimenter-delivered electrical stimulation in each animal. Five CVs were used for each analyte. The K-matrices from these data (Figure 4.4a-b) serve as graphical representations of the general shape of the CVs for each particular analyte. The overall shapes of dopamine and pH K-matrices were similar across subjects, as evidenced by high correlation coefficients between K-matrices (Pearson's  $r$ ,  $0.953 < r < 0.992$  for dopamine,  $0.950 < r < 0.985$  for pH). First, we calculated the concentrations of dopamine transients ( $[DA]_{\max}$ ) during ICSS for each animal using the training set obtained within-subject. Next, we evaluated dopamine concentrations using training sets obtained with different microelectrodes and subjects, and these concentration predictions were compared to those predicted by the within-subject training set (Figure 4.4c). Significant differences were found (repeated measures one-way ANOVA with Dunnett's multiple comparisons, Table 4.2). Application of training sets from other animals tended to underestimate  $[DA]_{\max}$  (78.4% peaks), though overestimations also occurred (20.3%). Percent deviations widely varied over a physiological range of transients (~50-300 nM), with deviations approaching 50% for some transients.

Inspection of the CVs comprising the training sets reveals the origin of these errors (Table 4.3). Despite the high correlation between K-matrices, differences in peak locations, peak separations, and ratios of peak currents exist between training sets at separate electrodes. Because PCR utilizes the entire CV for concentration prediction, variation in these key CV characteristics between electrodes causes PCR models using different training sets to predict different responses when applied to the same data set. Because training sets generated from recordings with the same electrode and recording session contain features similar to experimental CVs, they provide the best estimate of actual analyte responses. Thus, the variability in Figure 4.4c reveals the failure of calibration with alternate (between-subject) training sets that will ultimately lead to erroneous data interpretation.

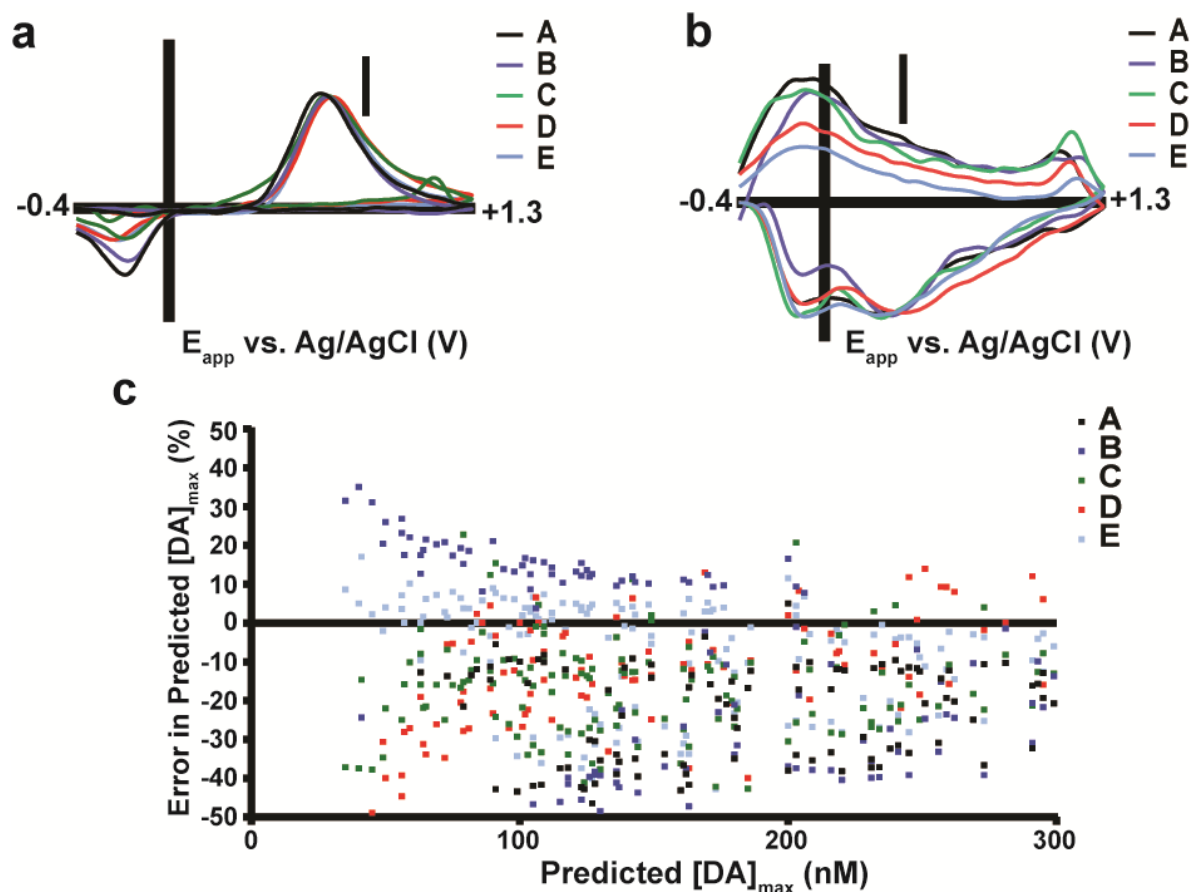


**Figure 4.4.** Training sets built in different subjects predict different dopamine transient concentrations. a) Dopamine K-matrices for five different training sets (A-E). Each K-matrix is normalized to the external calibration factor (10 nA/ $\mu$ M) measured at the peak anodic potential ( $E_{p,a}$ ). Differences are seen in the ratio of peak currents, peak location, and separation between the anodic and cathodic peaks. b) pH K-matrices from training sets A-E. Each K-matrix is normalized to the external calibration factor (-40 nA/pH unit) at  $E_{Q,H}$ . c) Dopamine transients seen during ICSS were first analyzed with the training set built in the same subject as the unknown data set. These transients were subsequently analyzed with training sets built in other subjects, and these values were compared to the original predicted concentration.

<i>Data Set</i> →	A (n = 52)	B (n = 57)	C (n = 17)	D (n = 65)	E (n = 60)
T.S. A	<b>103 ± 6</b>	264 ± 26 ****	224 ± 11 ****	177 ± 18 ****	107 ± 6 ****
T.S. B	117 ± 6 ****	<b>296 ± 28</b>	224 ± 12 ****	184 ± 21 ****	286 ± 28 ****
T.S. C	89 ± 6 ****	257 ± 24 ****	<b>269 ± 13</b>	194 ± 19 ****	242 ± 11 ****
T.S. D	87 ± 6 ****	262 ± 26 ****	282 ± 13 **	<b>237 ± 19</b>	203 ± 21 ****
T.S. E	107 ± 6 ****	286 ± 28 ****	242 ± 11 ***	203 ± 21 ****	<b>578 ± 34</b>
No PCR	130 ± 6 ****	296 ± 27	204 ± 20 ****	154 ± 21 ****	524 ± 36 ****

**Table 4.2.** Training sets (T.S.) built in different subjects predict different peak dopamine concentrations than training sets built within subject. Five different data sets (n = # of electrically evoked dopamine transients) were analyzed with five different training sets (including the training set built within subject, in bold). The mean maximum concentration ± SEM of the dopamine transients are expressed in nM. Asterisks denote significance level from control within-subject training set (Repeated measures one-way ANOVA, Dunnet's multiple comparisons, \*  $p < 0.05$ , \*\*  $p < 0.01$ , \*\*\*  $p < 0.001$ , \*\*\*\*  $p < 0.0001$ ). The average absolute percent difference in predicted concentration compared to the prediction with the correct training set for each individual transient is included in parentheses (mean ± SEM). These values contain both overestimations and underestimations in predicted peak dopamine concentration.

Dopamine						
T.S.	$E_{p,a}$ (V)	$E_{p,c}$ (V)	$\Delta E_p$ (V)	$I_{p,a}/I_{p,c}$	$I_{p,a}$ Range (nA)	$Q_\alpha$ (nA <sup>2</sup> )
A	0.65	-0.19	0.84	1.74	0.37 → 2.74	217.6
B	0.68	-0.18	0.86	2.14	1.00 → 11.14	492.5
C	0.67	-0.19	0.86	3.80	0.71 → 4.17	312.0
D	0.70	-0.24	0.94	3.57	0.57 → 7.87	571.7
E	0.69	-0.22	0.91	3.54	1.44 → 15.3	858.8
pH						
T.S.	$E_c$ (V)	$E_{QH}$ (V)	$E_Q$ (V)	$I_{QH}/I_Q$	$I_{QH}$ Range (nA)	$Q_\alpha$ (nA <sup>2</sup> )
A	-0.11	0.22	-0.06	0.90	-0.57 → -1.72	217.6
B	-0.10	0.30	-0.07	1.02	-1.20 → -2.52	492.5
C	-0.13	0.26	-0.09	1.02	-0.81 → -1.72	312.0
D	-0.10	0.37	-0.10	1.39	-1.34 → -3.96	571.7
E	-0.09	0.25	-0.10	2.04	-2.02 → -6.58	858.8

**Table 4.3.** Key parameters from the K-matrices for dopamine (top) and pH changes (bottom), collected in five separate animals. Differences in peak locations, relative peak amplitudes, the range of measured currents, and residual thresholds were seen between animals.  $Q_\alpha$  are specific to overall training sets, and are therefore the same for both analytes within each individual training set. The importance of these parameters in cyclic voltammetry is highlighted in “Electrochemical Methods: Fundamentals and Applications” by Bard & Faulkner, Chapter 6 (Bard & Faulkner, 2001). The relevance and origin of the peak parameters for pH changes has been described previously (Takmakov, et al., 2010).

## Residual analysis

While the preceding results show that use of inappropriate training sets leads to significant errors in concentration prediction, an even larger problem is that model validation is precluded. For training sets established within the same animal and same electrode, we have used residual analysis for validation (Keithley, et al., 2009), in which a residual is calculated from the voltammetric currents unaccounted for by the training sets. If the squared sum of residual current at each applied potential for a particular CV ( $Q_t$ ) exceeds a training set-specific threshold value ( $Q_\alpha$ ), then, according to previously established guidelines (Jackson & Mudholkar, 1979), a source of variance not accounted for in the PCR model is significantly contributing to the signal, indicating the model is invalid to analyze the data.

As an example, the ten-second trace in Figure 4.3 was analyzed with both the training set built in the same subject (E), the appropriate training set, as well as a training set built from data obtained in another animal (C). Training set C yielded a relatively small (~17%) error in concentration prediction (compared to E) due to a notably high signal-to-noise ratio (S/N) of this data trace. The  $Q_t$  values obtained with the appropriate training set (E) did not exceed its  $Q_\alpha$ , indicating a valid analysis (Figure 4.5a). In contrast,  $Q_t$  values for training set C frequently exceeded its  $Q_\alpha$  value (Figure 4.5b), indicating that large parts of this analysis are invalid. Color plots of the residuals allow these unassigned currents to be evaluated as a function of potential. The invalid analysis (training set C, Figure 4.5b) reveals considerable unassigned current near the peak locations for dopamine and pH, features not present for the valid training set E (Figure 5a).

The number of residual threshold crosses at  $[DA]_{\max}$  varied between applied training sets for each data set (Table 4.4). Data sets with low noise result in few to no residual crosses across training sets (ex. data set A). However, alternative training sets can produce more residual threshold crosses than analysis with within-subject training sets, rejecting experimental

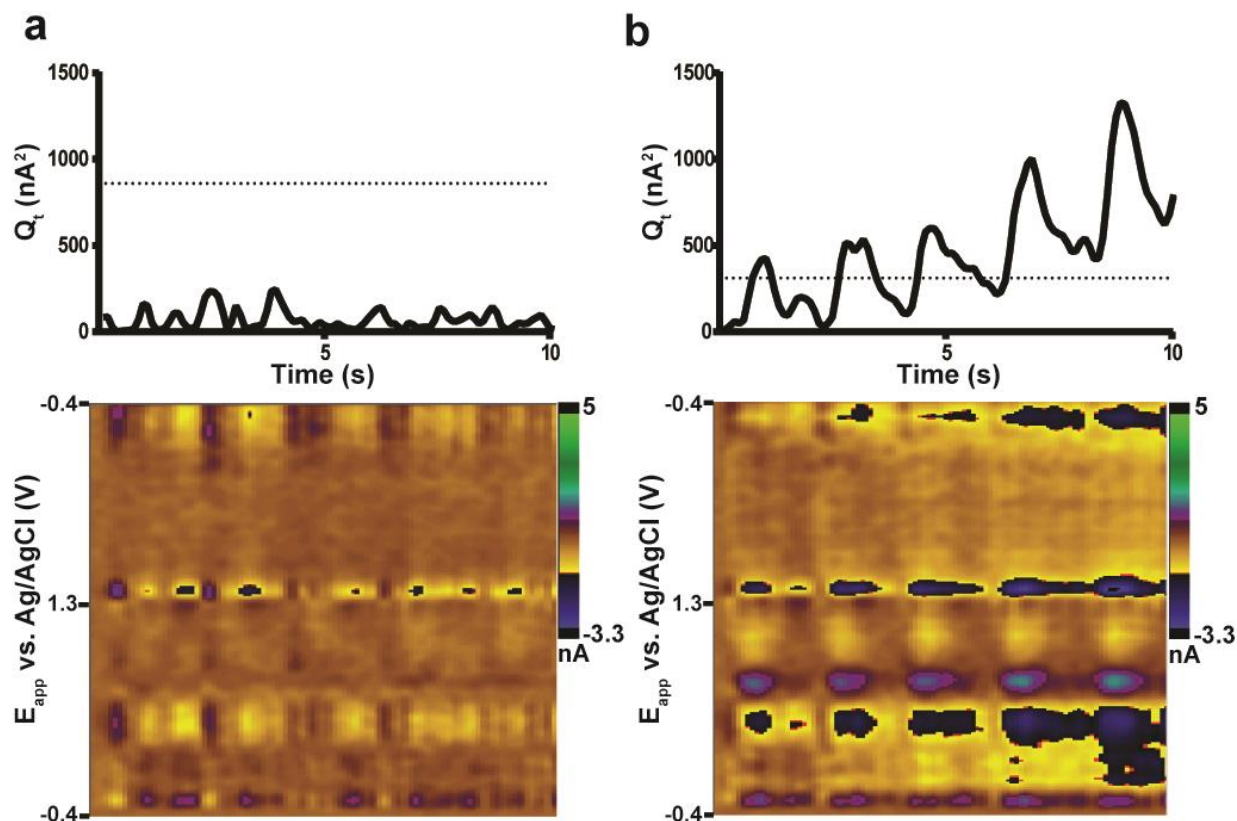


**Figure 4.5.** Residual analysis with different training sets. a) The residual trace and color plot from a training set built in the same subject (E). The residual trace remains below the residual threshold (dotted line,  $Q_\alpha = 858.8$ ). The residual plot contains little unaccounted current at potentials where dopamine and pH contribute. b) The residual trace and color plot from a training set built in a different animal (C) applied to these data. The residual trace rises throughout the trace and crosses the residual threshold ( $Q_\alpha = 312.0$ ). The residual color plot reveals large sources of discarded current near potentials for dopamine and pH.

Data Set →	A (n =52)	B (n=64)	C (n=22)	D (n=65)	E (n=60)
Training Set A ( $Q_a=217.6$ )	0	18	17	10	53
Training Set B ( $Q_a=492.5$ )	0	7	14	8	43
Training Set C ( $Q_a=312.0$ )	0	18	5	0	10
Training Set D ( $Q_a=571.7$ )	0	4	0	0	1
Training Set E ( $Q_a=858.8$ )	0	3	10	0	0

**Table 4.4.** The number of transients for which  $Q_t$  (at  $[DA]_{max}$ ) exceeded the  $Q_a$  threshold during various training set misapplications. Analysis with the appropriate training set is highlighted in bold, with the number of residual crosses shown for alternate training sets shown for each data set. n = the number of electrically evoked transients in each data set.

data that would be retained using proper PCR protocol (ex. data set C, E). Conversely, alternative training sets can result in fewer residual crosses than the within-subject training set, as is the case with training sets with larger  $Q_\alpha$  (ex. training set E). This leads to the retention of questionable data that should have been discarded. The inappropriate inclusion of false data or exclusion of accurate data illustrates the failure of model validation when using generalized training sets.

### **Standard training sets constructed from multiple electrodes**

Recently, some have adopted a PCR approach that analyzes data using a “standard training set” built from CVs collected in multiple subjects (Howe, et al., 2013). Ideally, the generality of this training set would allow it to be more applicable across data sets than alternate training sets built from single, electrodes.

To evaluate this approach, composite training sets containing 10 CVs were made using one dopamine and one pH CV selected at random from each training set (A-E) shown above. Due to the large number of possible training sets ( $5^{10}$ ), the number of training sets constructed was limited to 10,000, and the resulting K-matrices for each training set were averaged. While the average K-matrices for DA and pH exhibit standard shapes for these analytes, variability was seen between training sets, particularly between pH K-matrices (Figure 4.6a). Furthermore, a wide range of  $Q_\alpha$  values is seen between composite training sets (Figure 4.7a), indicating an inconsistent treatment of noise.

If this variability reflects bias based on the random selection of CV standards, increasing the number of standards could provide more consistent K-matrices. However, increasing the number of CV standards selected from each training set resulted in K-matrices that no longer resemble the represented analytes (Figure 4.6b-d). This reduced ability of PCR to reliably identify dopamine and pH stems from the increased rank of these training sets (Figure 4.7b).

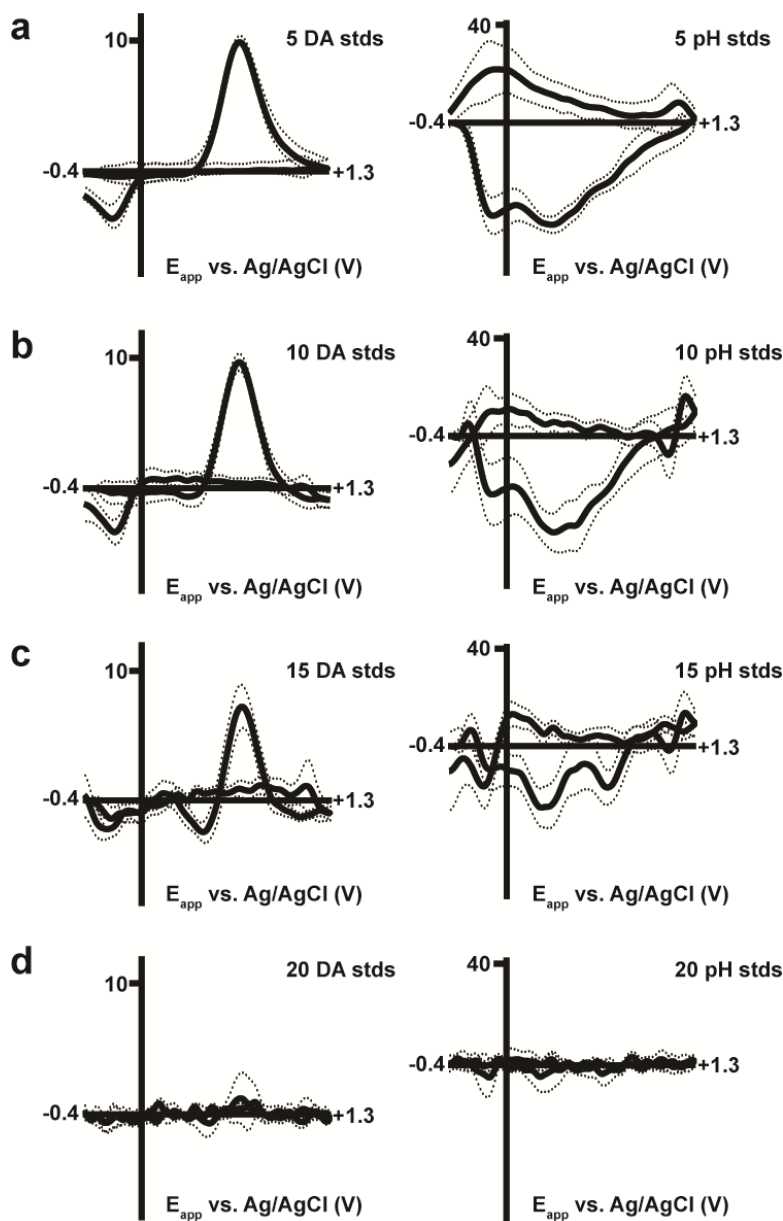


**Figure 4.6.** K-Matrices from composite training sets built with standards collected at different carbon-fiber microelectrodes. a) Composite training sets containing 10 CVs were made using one dopamine and one pH CV selected at random from each training set (A-E). b) As in a) but made with 20 CVs using two dopamine and two pH CVs selected randomly from each training set. c) As in a) but made with 30 CVs using three dopamine and three pH CVs randomly selected from each training set. d) As in a) but made with 40 CVs using four dopamine and four pH CVs randomly selected from each training set. Average (solid line) and 95% confidence limits (dotted line) for both DA and pH K-matrices ( $n=10,000$ ) are shown for each training set size.

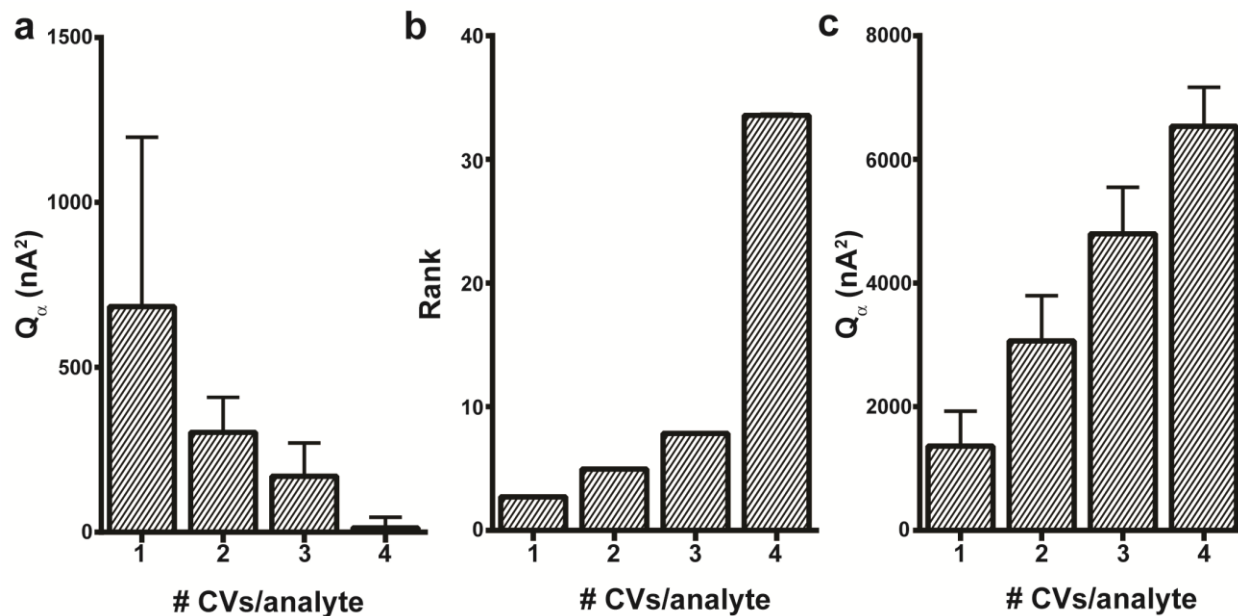


**Figure 4.7.** Parameters of interest for composite generalized training sets. a) As the rank increases, the  $Q_{\alpha}$  value decreases ( $684.1 \pm 513.5$ ,  $303.6 \pm 106.2$ ,  $170.1 \pm 101.0$ , and  $13.5 \pm 32.3$  nA<sup>2</sup> for one through four CVs/analyte from each training set respectively.) b) As the number of CVs/analyte incorporated from electrode is increased, the rank (or number of primary components) increases ( $2.7 \pm 0.7$ ,  $5.0 \pm 0.7$ ,  $7.8 \pm 1.3$ , and  $33.5 \pm 10.2$  for one through four CVs/analyte respectively.) c) If the number of principal components retained is restricted to two, the  $Q_{\alpha}$  values increase dramatically as more CVs/analyte from each electrode (e.g. larger number of total standards) are used ( $1366.6 \pm 563.8$ ,  $3065.5 \pm 732.0$ ,  $4798.8 \pm 750.0$ ,  $6535.1 \pm 634.3$  for one through four CVs/analyte respectively). Numbers expressed as mean  $\pm$  standard deviation ( $n=10,000$  for each training set size).

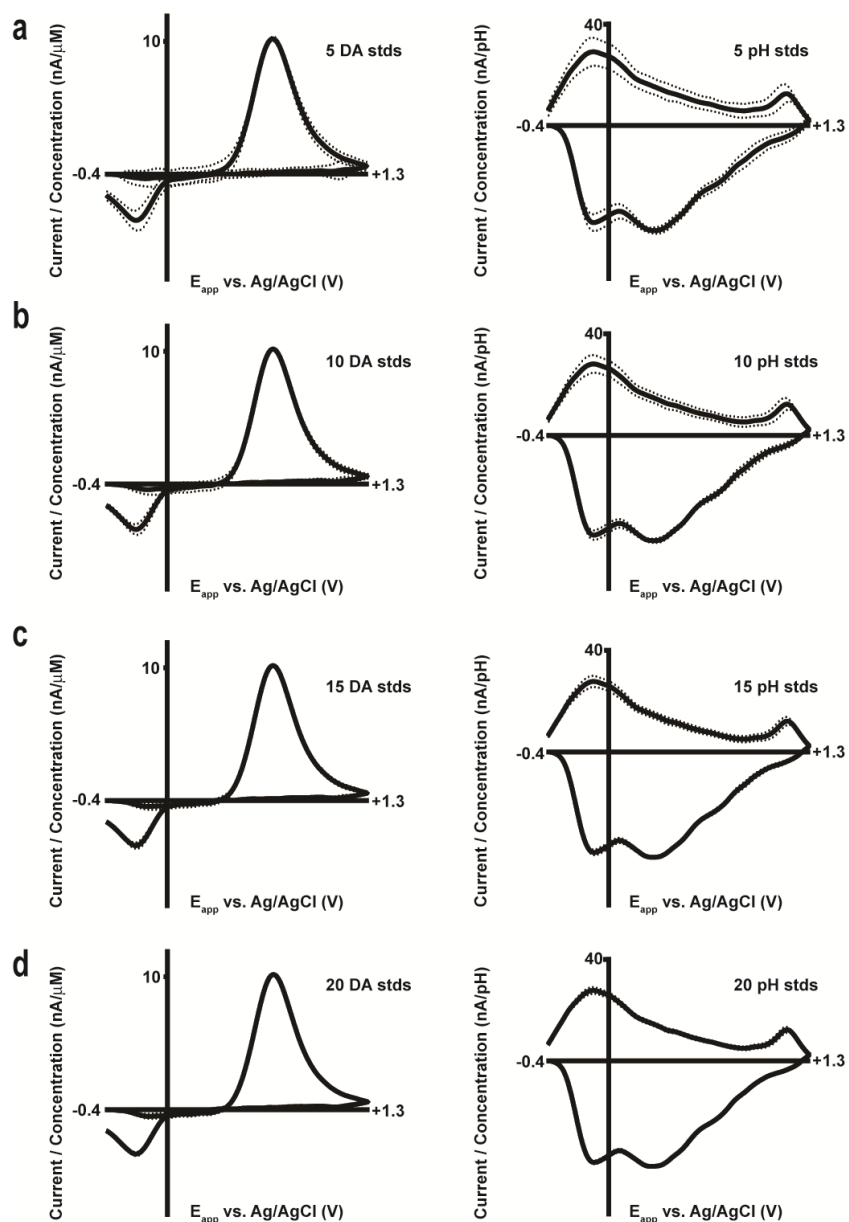


**Figure 4.8.** K-matrices for composite training sets constrained to two principal components. Composite training sets containing one (a), two (b), three (c), and four (d) cyclic voltammogram standards per analyte (dopamine and pH) from each individual training set (A-E) were constructed. Instead of determining the rank of each training set with Malinowski's F-test, the number of principal components for each composite training set was constrained to two. The average (solid line) and 95% confidence limits (dotted line) for both DA and pH K-matrices ( $N=10,000$ ) are displayed for each training set size. The shape of the average K-matrices for dopamine and pH were independent of training set size. (Pearson's correlation,  $0.999 \leq r \leq 1.000$  for DA,  $0.999 \leq r \leq 1.000$  for pH).

PCR calculates a number of principal components (PCs) equal to the number of standards in the training set. These PCs are separated into PCs that describe significant sources of variance (primary PCs) and those that do not (secondary PCs). Rank, the number of retained primary PCs, is an important parameter in PCR that we determine using Malinowski's F-test (Keithley, et al., 2010). With this approach, each individual training set (A-E) had two primary PCs, reflecting features for both dopamine and pH changes. However, in composite training sets built from multiple electrodes, standard CVs have a wider range of key characteristics (Table 4.3) and different sources of deterministic current. This requires more primary PCs (e.g. higher rank) to describe the sources of variance. As a result, the signal for the analytes is spread amongst several PCs, leading to K-matrices without clear depictions of each analyte. In this case, the calibration model will overfit the data, causing a diminished tolerance for uncaptured variance and a reduction in the  $Q_\alpha$  values (Figure 4.7a). These problems are common to PCR and are well characterized in the literature (Kramer, 1998).

In principle, one could restrain the number of primary PCs to two, reflecting only variance within dopamine and pH signals. This leads to much cleaner K-matrices for dopamine and pH for all training set sizes (Figure 4.8). However, because  $Q_\alpha$  values are largely determined by information in secondary PCs (Keithley, et al., 2009), the forced removal of PCs that Malinowski's F-test would retain results in very large  $Q_\alpha$  values (Figure 4.7c) precluding model validation.

## **CONCLUSIONS**

When used correctly, PCR is a powerful tool to unravel overlapping signals, particularly for CVs in awake, behaving animals. As shown here and elsewhere, pH changes serve as an intriguing indirect marker for local activity (Ariansen, et al., 2012; Roitman, et al., 2008) in various behavioral paradigms, carrying its own unique signal. However, despite its advantages,

PCR can only provide meaningful results with training sets obtained by appropriate protocols. Calibration sets need to span the concentration range that occurs during behavior.

Furthermore, they should be generated using the same equipment used to collect the experimental data. Indeed, the transfer of multivariate calibration models between instrumentation is a well-documented problem in the literature (Feudale et al., 2002). The generalized training sets do not provide a suitable PCR model for two major reasons. First, their application leads to significant underestimations of concentrations, effectively diminishing the signal-to-noise ratio, masking small, yet biologically relevant signals. Second, generalized training sets violate the theory behind residual analysis, which is important for model validation.

For FSCV, these problems arise from differences in CVs between electrodes, which can arise from multiple sources. Reference electrodes have been known to drift during chronic implantation (Heien, et al., 2005) (Zhang et al., 1999), leading to voltage offsets in the CVs. Voltage distortion may be particularly problematic when using chronically implanted microelectrodes, because impedance changes following implantation (Williams et al., 2007) could cause CVs to vary across recording sessions. Nonetheless, the use of acutely implanted working and reference electrodes in this study did not prevent differences between electrodes. This reflects a fundamental limitation in comparing CVs across different carbon-fiber microelectrodes: carbon surfaces are complex and heterogeneous (McCreery, 2008; Takmakov, et al., 2010), which leads to differences in electron-transfer and adsorption kinetics. Particularly, the pH signal was shown to vary widely across electrodes in this study, a perhaps unsurprising finding due to the strong dependence of the pH response on the surface state of the electrode (Takmakov, et al., 2010). Thus, building separate training sets for each carbon-fiber electrode becomes essential to convert experimental data into meaningful chemical information. The unpredictable deviations in dopamine concentrations across training sets (Figure 4.4c) make it unlikely that a standard training set could be constructed that would be consistent to all experiments. Indeed, PCR has been used to demonstrate systematic differences between

instruments, rather than reconcile data between them (Rao, 1964). Furthermore, a principal advantage of PCR is its ability to separate sources of variance into distinct contributions from signal and noise (Keithley, et al., 2009). This advantage is violated twofold with generalized training sets, as standards from different electrodes will not reflect noise in the experimental data set and will introduce unrepresentative noise.

A principal advantage of using chronically implanted microelectrodes is to monitor changes in dopamine over time at the same electrode and recording site. For such trends across recording sessions to be considered reliable, it must be established that concentration calibration methods can act consistently across recording days. In light of the variability in training sets from different electrodes, improved calibration methodology for these sensors is crucial. . Otherwise, improper PCR protocols could mask true longitudinal trends in dopamine release. Thus, as the original developers of PCA stated (Jolliffe, 2002; Kramer, 1998), the PCR model must be generated under the same experimental conditions as the data to be analyzed.

## REFERENCES

- Ariansen, J. L., et al. (2012). Monitoring extracellular pH, oxygen, and dopamine during reward delivery in the striatum of primates. *Front Behav Neurosci*, 6, 36.
- Bard, A. J., & Faulkner, L. R. (2001). *Electrochemical methods: fundamentals and applications* (2nd ed.). New York: Wiley.
- Bucher, E. S., & Wightman, R. M. (2015). Electrochemical analysis of neurotransmitters. *Annu Rev Anal Chem*, 8, 239-261.
- Cameron, C. M., Wightman, R. M., & Carelli, R. M. (2014). Dynamics of rapid dopamine release in the nucleus accumbens during goal-directed behaviors for cocaine versus natural rewards. *Neuropharmacology*, 86, 319-328.
- Clark, J. J., Collins, A. L., Sanford, C. A., & Phillips, P. E. (2013). Dopamine encoding of Pavlovian incentive stimuli diminishes with extended training. *J Neurosci*, 33(8), 3526-3532.
- Clark, J. J., et al. (2010). Chronic microsensors for longitudinal, subsecond dopamine detection in behaving animals. *Nat Methods*, 7(2), 126-129.
- Day, J. J., Roitman, M. F., Wightman, R. M., & Carelli, R. M. (2007). Associative learning mediates dynamic shifts in dopamine signaling in the nucleus accumbens. *Nat Neurosci*, 10(8), 1020-1028.
- Feudale, R. N., Woody, N. A., Tan, H., Myles, A. J., Brown, S. D., & Ferré, J. (2002). Transfer of multivariate calibration models: a review. *Chemometrics and Intelligent Laboratory Systems*, 64(2), 181-192.
- Flagel, S. B., et al. (2011). A selective role for dopamine in stimulus-reward learning. *Nature*, 469(7328), 53-57.
- Gan, J. O., Walton, M. E., & Phillips, P. E. (2010). Dissociable cost and benefit encoding of future rewards by mesolimbic dopamine. *Nat Neurosci*, 13(1), 25-27.
- Garris, P. A., Kilpatrick, M., Bunin, M. A., Michael, D., Walker, Q. D., & Wightman, R. M. (1999). Dissociation of dopamine release in the nucleus accumbens from intracranial self-stimulation. *Nature*, 398(6722), 67-69.
- Goertz, R. B., Wanat, M. J., Gomez, J. A., Brown, Z. J., Phillips, P. E., & Paladini, C. A. (2015). Cocaine increases dopaminergic neuron and motor activity via midbrain alpha1 adrenergic signaling. *Neuropsychopharmacology*, 40(5), 1151-1162.
- Hart, A. S., Rutledge, R. B., Glimcher, P. W., & Phillips, P. E. (2014). Phasic dopamine release in the rat nucleus accumbens symmetrically encodes a reward prediction error term. *J Neurosci*, 34(3), 698-704.
- Heien, M. L., Johnson, M. A., & Wightman, R. M. (2004). Resolving neurotransmitters detected by fast-scan cyclic voltammetry. *Anal Chem*, 76(19), 5697-5704.

- Heien, M. L., et al. (2005). Real-time measurement of dopamine fluctuations after cocaine in the brain of behaving rats. *Proc Natl Acad Sci U S A*, 102(29), 10023-10028.
- Hollon, N. G., Arnold, M. M., Gan, J. O., Walton, M. E., & Phillips, P. E. (2014). Dopamine-associated cached values are not sufficient as the basis for action selection. *Proc Natl Acad Sci U S A*, 111(51), 18357-18362.
- Howe, M. W., Tierney, P. L., Sandberg, S. G., Phillips, P. E., & Graybiel, A. M. (2013). Prolonged dopamine signalling in striatum signals proximity and value of distant rewards. *Nature*, 500(7464), 575-579.
- Jackson, J. E., & Mudholkar, G. S. (1979). Control procedures for residuals associated with principal component analysis. *Technometrics*, 21(3), 341-349.
- Jolliffe, I. (2002). *Principal component analysis* (2nd ed.). New York: Springer.
- Keithley, R. B., Carelli, R. M., & Wightman, R. M. (2010). Rank estimation and the multivariate analysis of in vivo fast-scan cyclic voltammetric data. *Anal Chem*, 82(13), 5541-5551.
- Keithley, R. B., Heien, M. L., & Wightman, R. M. (2009). Multivariate concentration determination using principal component regression with residual analysis. *Trends Analyt Chem*, 28(9), 1127-1136.
- Keithley, R. B., & Wightman, R. M. (2011). Assessing principal component regression prediction of neurochemicals detected with fast-scan cyclic voltammetry. *ACS Chem Neurosci*, 2(9), 514-525.
- Kramer, R. (1998). *Chemometric techniques for quantitative analysis*. New York: Marcel Dekker, Inc.
- McCreery, R. L. (2008). Advanced carbon electrode materials for molecular electrochemistry. *Chem Rev*, 108(7), 2646-2687.
- Peters, J. L., Miner, L. H., Michael, A. C., & Sesack, S. R. (2004). Ultrastructure at carbon fiber microelectrode implantation sites after acute voltammetric measurements in the striatum of anesthetized rats. *J Neurosci Methods*, 137(1), 9-23.
- Phillips, P. E., Stuber, G. D., Heien, M. L., Wightman, R. M., & Carelli, R. M. (2003). Subsecond dopamine release promotes cocaine seeking. *Nature*, 422(6932), 614-618.
- Rao, C. R. (1964). The use and interpretation of principal component analysis in applied research. *Sankhyā A*, 329-358.
- Robinson, D. L., Venton, B. J., Heien, M. L., & Wightman, R. M. (2003). Detecting subsecond dopamine release with fast-scan cyclic voltammetry in vivo. *Clin Chem*, 49(10), 1763-1773.
- Roitman, M. F., Stuber, G. D., Phillips, P. E., Wightman, R. M., & Carelli, R. M. (2004). Dopamine operates as a subsecond modulator of food seeking. *J Neurosci*, 24(6), 1265-1271.

- Roitman, M. F., Wheeler, R. A., Wightman, R. M., & Carelli, R. M. (2008). Real-time chemical responses in the nucleus accumbens differentiate rewarding and aversive stimuli. *Nat Neurosci*, *11*(12), 1376-1377.
- Saddoris, M. P., & Carelli, R. M. (2014). Cocaine self-administration abolishes associative neural encoding in the nucleus accumbens necessary for higher-order learning. *Biol Psychiatry*, *75*(2), 156-164.
- Takmakov, P., Zachek, M., Keithley, R., Bucher, E., McCarty, G., & Wightman, R. (2010). Characterization of local pH changes in brain using fast-scan cyclic voltammetry with carbon microelectrodes. *Anal Chem*, *82*(23), 9892-9900.
- Tritsch, N. X., & Sabatini, B. L. (2012). Dopaminergic modulation of synaptic transmission in cortex and striatum. *Neuron*, *76*(1), 33-50.
- Venton, B. J., Michael, D. J., & Wightman, R. M. (2003). Correlation of local changes in extracellular oxygen and pH that accompany dopaminergic terminal activity in the rat caudate-putamen. *J Neurochem*, *84*(2), 373-381.
- Wanat, M. J., Bonci, A., & Phillips, P. E. (2013). CRF acts in the midbrain to attenuate accumbens dopamine release to rewards but not their predictors. *Nat Neurosci*, *16*(4), 383-385.
- Wanat, M. J., Kuhnen, C. M., & Phillips, P. E. (2010). Delays conferred by escalating costs modulate dopamine release to rewards but not their predictors. *J Neurosci*, *30*(36), 12020-12027.
- Williams, J. C., Hippensteel, J. A., Dilgen, J., Shain, W., & Kipke, D. R. (2007). Complex impedance spectroscopy for monitoring tissue responses to inserted neural implants. *J Neural Eng*, *4*(4), 410-423.
- Willuhn, I., Burgeno, L. M., Groblewski, P. A., & Phillips, P. E. (2014a). Excessive cocaine use results from decreased phasic dopamine signaling in the striatum. *Nat Neurosci*, *17*(5), 704-709.
- Willuhn, I., et al. (2014b). Phasic dopamine release in the nucleus accumbens in response to pro-social 50 kHz ultrasonic vocalizations in rats. *J Neurosci*, *34*(32), 10616-10623.
- Zhang, X., Wang, J., Ogorevc, B., & Spichiger, U. E. (1999). Glucose Nanosensor Based on Prussian-Blue Modified Carbon-Fiber Cone Nanoelectrode and an Integrated Reference Electrode. *Electroanalysis*, *11*(13), 945-949.

## CHAPTER 5: HITCHHIKER'S GUIDE TO VOLTAMMETRY: ACUTE AND CHRONIC ELECTRODES FOR IN VIVO FAST-SCAN CYCLIC VOLTAMMETRY<sup>1</sup>

### TECHNIQUES FOR MONITORING MOLECULES IN NEUROSCIENCE

Monitoring of molecules in the brain has undergone significant advances in the past four decades. One of the earliest techniques for measuring neurotransmitter release was push-pull perfusion, a method that uses a cannula for sample collection prior to downstream analysis (Cheramy et al., 1981; Nieoullon et al., 1977). However, the direct interface of the perfusate with brain tissue raised concerns with sample contamination and flow-induced damage to the surrounding environment. To address these issues, this procedure was later adapted to incorporate a dialysis membrane, creating the technique known as microdialysis (Delgado et al., 1972; Sharp et al., 1986; Ungerstedt & Pycock, 1974; Zetterstrom et al., 1983). Microdialysis restricts flow to the probe, which minimizes brain damage and maintains sample purity. Equilibration of analytes across the membrane according to their concentration gradients results in concentration changes in the dialysate reflective of fluctuations in the brain. Microdialysis is highly versatile, with its sensitivity, selectivity, and number of analytes that can be monitored simultaneously dependent on the detection method employed. Its main limitation is spatiotemporal resolution, as microdialysis probes are typically at least 200  $\mu\text{m}$  in diameter, and samples are historically collected approximately every 5-20 min to allow sufficient sample volume accumulation at low flow rates (Pettit & Justice, 1989; Sharp, et al., 1986; Zetterstrom et al., 1986; Zetterstrom, et al., 1983). Recent improvements, largely due to reduction in the

---

<sup>1</sup> This chapter previously appeared as an article in the journal of ACS Chemical Neuroscience. The original citation is as follows: Rodeberg, N.T., Sandberg, S.G., Johnson, J.J., Phillips, P.E.M., & Wightman, R.M. "Hitchhiker's Guide to Voltammetry: Acute and Chronic Electrodes for in Vivo Fast-Scan Cyclic Voltammetry." *ACS Chemical Neuroscience* 8, no. 2 (2017): 221.

minimum volume needed for sample analysis, have permitted microdialysis measurements on a sub-minute time scale (Harstad & Bowser, 2016; Saylor & Lunte, 2015; Wang et al., 2008; Wang et al., 2010).

For the subset of brain molecules that are electroactive, particularly biogenic amines, electrochemical monitoring has flourished as an alternative methodology (Hawley et al., 1967; Refshauge et al., 1974). This approach was first attempted in the Ralph Adams lab with a carbon paste electrode implanted in the striatum of an anesthetized rat (Kissinger et al., 1973). Slow potential sweeps between -0.2 to +0.6 V vs. Ag/AgCl revealed peaks in current corresponding to the oxidation and reduction of electroactive substances; however, the identity of the molecule(s) producing the signal was unclear, with the authors suggesting it could arise from dopamine, norepinephrine, or ascorbic acid. Indeed, early voltammetric measurements suffered from poor chemical resolution between catecholamines and other easily oxidized species, often present in the brain at higher concentrations (Gonon et al., 1980; Gratton & Wise, 1994; Huff et al., 1979; Kissinger, et al., 1973; Schenk et al., 1983; Wightman et al., 1988b). In response to these problems, criteria were developed to ensure that intended analytes were indeed the source of recorded signals, including electrochemical, anatomical, pharmacological, and independent verification (Kuhr et al., 1984; Marsden et al., 1988; Phillips & Wightman, 2003). A major advance to the field came with the development of fast-scan cyclic voltammetry (FSCV), a technique that utilizes rapid potential sweeps to oxidize and reduce analytes of interest (Baur et al., 1988; Ewing et al., 1983; Stamford et al., 1984). This process produces cyclic voltammograms, which display measured current as a function of the applied potential, that serve as 'fingerprints' for compound identification, providing an advantage over single potential techniques (Baur, et al., 1988; Heien et al., 2004; Heien et al., 2003). This moderate chemical selectivity allows the use of chemometric methods to separate, and subsequently quantitate, analytes with different current-potential characteristics (see **Data Analysis** section below) (Heien, et al., 2004; Heien et al., 2005).

The development of carbon-fiber microelectrodes (CFMs) has aided the FSCV field in multiple ways (Armstrong-James & Millar, 1979; Ponchon et al., 1979; Wightman, 1981). The small size, and thus reduced capacitance and time constant, of these electrodes permits rapid scan rates ( $>100$  V/s), which enables measurements on a sub-second time scale. Additionally, this relatively small size compared to traditional probes increases spatial resolution and permits localized measurements in discrete brain regions. Moreover, in contrast to tissue damage observed near microdialysis probes, minimal damage is seen surrounding fiber implantation sites (Kozai et al., 2015; Peters et al., 2004). These probes are also easily modified with a variety of surface coatings, which can improve chemical selectivity, electron transfer kinetics, and sensitivity (Gerhardt et al., 1984; Schmidt et al., 2013; Singh et al., 2011; Swamy & Venton, 2007a; Vreeland et al., 2015). Lastly, carbon-based electrodes demonstrate strong biocompatibility, and are more resistant to biofouling than metal electrodes. These advantages make FSCV with CFMs an attractive measurement technique for rapid neurotransmitter dynamics.

## **DEVELOPMENT OF FSCV FOR FREELY-MOVING ANIMALS**

Measurements using FSCV with CFMs were originally conducted in anesthetized animals (Baur, et al., 1988; Kuhr et al., 1987; Stamford, et al., 1984; Wightman et al., 1988a). However, these studies could not reveal direct information about neurotransmission during behavior. The first FSCV measurements in freely moving animals detected dopamine release in terminal regions, evoked by electrical stimulation of afferent axonal pathways in rats. These experiments used acutely implanted glass-encased CFMs lowered into the brain using head-mounted microdrives (Garris et al., 1997; Rebec et al., 1997; Rebec et al., 1993). Later, behavioral evoked dopamine was detected by this approach (Robinson et al., 2001), and these types of recordings became routine, primarily due to improved sensitivity obtained by increasing the anodic limit of the waveform (Hafizi et al., 1990; Rodeberg et al., 2016) to maintain oxygen-

containing moieties on the electrode surface which enhance adsorption of positively charged analytes (such as dopamine) (Heien, et al., 2003). FSCV has been adapted for multimodal recordings with simultaneous extracellular electrophysiological recordings (Armstrong-James et al., 1980; Cheer et al., 2005; Owesson-White et al., 2016; Stamford et al., 1993) and iontophoresis (Belle et al., 2013; Herr et al., 2010; Kirkpatrick et al., 2016; Owesson-White, et al., 2016) at the same probe.

The most recent generation of FSCV use in freely behaving animals has been to adapt CFMs for chronic implantation, permitting longitudinal measurements over an extended timescale in the same animal. This is not a novel direction for electrochemical monitoring, as earlier methodologies had adopted such an approach (Conti et al., 1978; O'Neill et al., 1983; Yamamoto & Spanos, 1988). Notably, these early studies, which utilize amperometry, clearly show the need for more chemical specificity in the measurements due to difficulty assigning the source of the signal. The standard fabrication of CFMs for FSCV using a glass-encased design had limited success when chronically implanted (Kruk et al., 1998). However, the chronic CFMs used today employ a basic design where a carbon fiber is sealed in a small diameter fused-silica tube (Clark et al., 2010). Similar to results at acutely implanted CFMs (Peters, et al., 2004) and other miniaturized devices (Kozai et al., 2012), these electrodes were demonstrated to avoid the progressive immune response and cell death that can impair measurements at larger probes (Kozai, et al., 2015).

With the improved sensitivity (Heien, et al., 2003) and low-noise (Michael et al., 1999) of modern approaches to using FSCV *in vivo*, recordings in striatal regions permit detection of dopamine elicited by task-related events such as the delivery of primary rewards (Day et al., 2007; Hart et al., 2014), including pharmacological rewards (Aragona et al., 2008; Cheer et al., 2007b; Fox et al., 2017; Heien, et al., 2005; Vander Weele et al., 2014) or reward-associated stimuli (Day, et al., 2007; Flagel et al., 2011; Owesson-White, et al., 2016; Phillips et al., 2003b; Roitman et al., 2004). In addition, spontaneous dopamine 'transients' (i.e. brief elevations in

extracellular dopamine concentration above the ambient level, produced by release events) can be observed which do not appear to be time locked to overt stimuli (Flagel et al., 2010; Robinson et al., 2002; Stuber et al., 2005) but are dependent upon activity in the ventral tegmental area (Sompers et al., 2009), and have been suggested to be a contributor to ambient extracellular dopamine levels in the nucleus accumbens (Owesson-White et al., 2012). While the function of these dopamine transients has not been fully characterized, their activity can be altered by behavioral context (Robinson, et al., 2002) as well as pharmacological agents including drugs of abuse (Cheer, et al., 2007b; Stuber, et al., 2005).

The objective of this paper is to discuss the nuances of using FSCV in behaving animals, based primarily on experience on measuring striatal dopamine. We will attempt to discuss the potential pitfalls that can make the use of FSCV or related approaches challenging, and then summarize how these caveats differentially affect alternative approaches, with a particular focus on the use of acute or chronic electrode.

## **EXPERIMENTAL CONSIDERATIONS**

### **Electrode materials and design**

The most common construction of recording electrodes for FSCV in behaving animals uses carbon fibers housed in glass or fused-silica capillaries. These carbon fibers host surface moieties, such as carbonyl, hydroxyl, or more complex groups (McCreery, 1995; Roberts et al., 2010), which can alter the electrochemical properties of the carbon fiber by changing its surface charge and steric properties. The constellation of functional groups on the carbon surface can be tuned with electrochemical (Suaud-Chagny et al., 1986), thermal (Strand & Venton, 2008), or chemical (Runnels et al., 1999) pretreatment, and will determine the selectivity of the adsorption of molecules to the surface, including fouling agents and electrochemical analytes. A popular approach using FSCV at CFMs is to use the applied waveform on each FSCV scan to electrochemically condition the electrode, essentially 'pretreating' the electrode surface each

time a measurement is made (Hafizi, et al., 1990). Specifically, increasing the anodic limit of the waveform above 1.0 V versus Ag/AgCl substantially enhances the sensitivity to dopamine by increasing dopamine-adsorbing oxide groups on the carbon surface and slowly etching the fiber surface to mitigate the effects of irreversible fouling (Hafizi, et al., 1990; Heien, et al., 2003; Roberts, et al., 2010). This approach has the advantage over traditional pretreatment strategies in that equilibrium is maintained throughout the experiment, providing stable sensitivity.

Construction of CFMs involves housing a carbon fiber in a capillary insulator with an exposed length at one end (the sensor) and an electrical connection at the other. For glass-based electrodes, a single carbon fiber is aspirated into a borosilicate glass capillary (600-1,000- $\mu\text{m}$  outer diameter, 400-500- $\mu\text{m}$  inner diameter) (Figure 5.1a, left panel). The capillary is then pulled on a commercial glass-electrode puller (either vertical or horizontal) to produce a tapered seal onto the carbon fiber. Sometimes the glass seal is then deliberately broken and resealed using epoxy (Epon 828 with 14% m-phenylenediamine by weight), which is more robust (i.e. prevents unintentionally exposed carbon-fiber from providing a low resistance path for current) and reduces the shunt capacitance of the electrode taper by providing a thicker insulating layer between the carbon-fiber and the extracellular fluid. For fused-silica-based electrodes, a single carbon fiber is loaded into a polyimide-coated fused-silica tube (90- $\mu\text{m}$  outer diameter, 20- $\mu\text{m}$  inner diameter, 8-12-mm length) submerged in isopropyl alcohol (Figure 5.1b). With the carbon fiber protruding, one end of the tube is sealed with epoxy (Devcon 20845). For either electrode type, the carbon fiber protruding from the seal is then trimmed to the desired length, and an electrical connection is made at the other end. Typical lengths of the trimmed carbon fiber range from 50 to 200  $\mu\text{m}$ , where longer exposed fibers are more sensitive, but have lower spatial resolution. Typically, glass-based electrodes have been used for acute implantation, while fused-silica-based electrodes are favored for chronic implantation due to

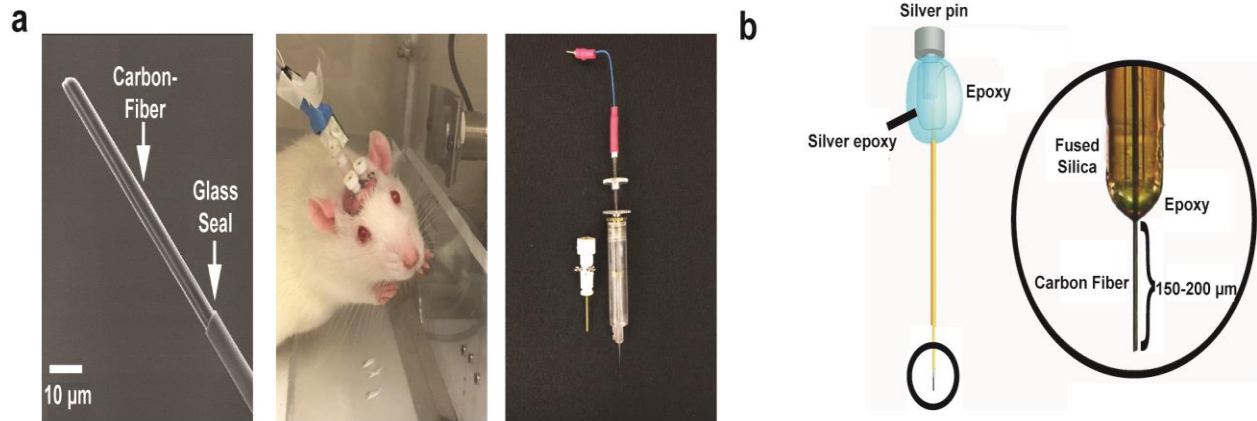


**Figure 5.1.** The designs of (a) borosilicate glass and (b) fused silica CFMs. a) Carbon-fibers are aspirated through borosilicate glass under vacuum. A seal is created by heating and pulling the capillary to a fine tip. The protruding fiber is then trimmed, typically between 75-125  $\mu\text{m}$ . For optimal electrochemical performance, epoxy resin is used to fill any leaks in the seal that occur during electrode fabrication. Left panel: Electron micrograph of CFM, generated with. Reprinted with permission from (Robinson et al., 2003). Copyright 2003 American Association for Clinical Chemistry. Middle panel: A rat with dual cannulas for later acute implantation of a CFM and reference electrode. The rat is tethered to a swivel and commutator via fastening of the headstage to an implanted stimulating electrode. Right panel: Side view of cannula for acute implantation of electrodes (left) and a micromanipulator for precise driving of the CFM during *in vivo* recordings (right). b) Carbon-fibers are threaded through a small diameter fused silica capillary under isopropyl alcohol. After drying, epoxy is placed on the fiber and wicked into the fused silica capillary to create a hemispherical seal (inset image). The protruding carbon-fiber is trimmed between 150-200  $\mu\text{m}$  long. Electrical connection is established between a silver pin and the fiber with silver epoxy, which is later insulated with clear epoxy. Reprinted with permission from (Clark, et al., 2010). Copyright 2010 Nature Publishing Group.

both their durability, and biocompatibility arising from their narrow diameter and polyimide coating (Hassler et al., 2011).

Not all electrodes are created equal. For glass electrodes, the structural integrity of the pulled seal is the most important determinant of electrode performance. Large cracks or gaps in the seal will lead to exposed fiber and/or increased fragility, which will impede electrochemical measurements. These problems can be alleviated by the use of epoxy to reinforce the seal (see above). For fused-silica encased CFMs, it is important that no epoxy remains on the fiber itself and that the seal forms a convex, rather than concave, seal (see Figure 5.1b for illustration). Electrochemical characteristics of either electrode design can be tested pre-experiment, either *in vitro* (i.e. in buffer) or *in vivo* (i.e. during surgical implantation of chronic CFMs before cementation, or after lowering the electrode for acute CFMs), to observe noise levels and ensure electrical connectivity.

### **Experimental design for FSCV recordings in freely-moving animals**

Measurements in freely-moving animals are conducted using head-mounted amplifiers (“headstages”), which connect to the CFM and reference electrodes and transduce the experimental current into voltages for downstream data collection and analysis (Phillips et al., 2003a; Takmakov et al., 2011). These headstages are anchored to the animal’s heads either directly via an electrical connector or at a separate point, such as the pedestal for the stimulating electrode assembly (Figure 5.1a, middle panel). The headstage is also connected to a swivel and commutator that permits movement within the behavioral chamber. Depending on the type of electrode used, cannulae may be affixed to the skull for later implantation of fresh CFM or reference electrodes (Figure 5.1a, middle panel) or fused-silica CFMs can be cemented directly to the skull.

The electrode design used influences both the type of experimental questions that can be answered and the overall success rate of recordings. The fragility of borosilicate glass

electrodes can lead to a lower yield of successful experiments with respect to fused-silica implantations. Moreover, tissue damage from repeated insertion limits the number of within-subject recordings (Phillips, et al., 2003a; Rebec, et al., 1993). Once successfully lowered, however, these electrodes tend to be stable over the course of individual measurement periods. Thus, these electrodes are best served for studies in which experimentally relevant manipulations occur during single recording sessions.

Conversely, the flexibility of fused-silica electrodes permits a higher success rate for implantation compared to glass electrodes. For chronic recordings, fused-silica electrodes are affixed to the skull with dental cement and left unused for at least a month to allow the immune response to these probes to dissipate (Clark, et al., 2010). Following this waiting period, it is possible to conduct many recordings at each electrode, increasing the data yield of chronic electrodes over acute electrodes. Longitudinal measurements permit the monitoring of dopamine over extended behavioral training and treatments. This is particularly relevant for models of disease states in which conditions develop slowly over time (Covey et al., 2016). These electrodes are routinely used for periods up to four months of recording. Naturally, there is some attrition of usable electrodes over that time. The majority of this attrition pertains to physical failures (e.g. separation of surgical implant from subject's head, loss of electrical continuity) and is much more infrequently due to altered electrochemical properties of the electrode (see Figure 3a, Supplementary Table 1 of (Clark, et al., 2010)).

### ***In vivo* electrode positioning**

For different applications, recording electrodes can either be fixed in the brain, or can be housed in a microdrive that allows their position to be adjusted (Figure 5.1a, right panel). The former is amenable to multiple electrodes in the same animal (Clark, et al., 2010), whereas the latter permits systematic mapping of heterogeneity of electrically or naturally evoked dopamine release along the dorsal-ventral axis (Wightman et al., 2007). Microdrives also allow selection of

a recording site within this heterogeneity by identifying 'hot spots' (i.e. areas with a high density of release sites) (Robinson, et al., 2002; Wightman, et al., 2007). Placement of fixed electrodes does not typically use this type of feedback-based selection. Therefore, positioning of these electrodes is more akin to random sampling of the tissue, and so signals converge upon the population average rather than local maxima. Consequently, signals measured with fixed electrodes tend to be smaller than those from drivable electrodes due to unbiased selection of recording sites (Figure 5.2) (Owesson-White et al., 2009; Willuhn et al., 2012). Dopamine signals in regions without release or uptake sites rely on diffusion from nearby terminals, and these sites exhibit both slower rises and decays compared to 'hot spots' (Venton et al., 2003b). As a result, electrodes not deliberately targeted at regions of high terminal density would be expected to have slower signals due to heterogeneity of release sites (Wightman, et al., 2007). For similar reasons, one would intuit that fixed electrodes should detect fewer spontaneous transients. However, most studies using chronic electrodes focus on the analysis of task-related events, and so spontaneous transients have seldom been reported. Nonetheless, on the rare occasion when they were quantified, they were comparable in detected frequency as those measured with drivable electrodes (Flagel, et al., 2010). Figure 5.3 demonstrates examples of pharmacologically and behaviorally evoked dopamine transients, as well as spontaneous transients, measured at chronically implanted CFMs.

Acute electrodes have the advantage of being drivable. However, in addition to the concerns with electrode fragility during repeated use mentioned above, electrode insertion imposes restraint stress on the animals. This could impact behavioral assays that study stress under controlled conditions (Wanat et al., 2013). Because chronic electrodes do not require repeated insertion, they do not share these issues. Although chronic electrodes are not drivable in regular use, chronically implanted electrode arrays have been used that permit independent movement of electrodes within the array (Howe et al., 2013).

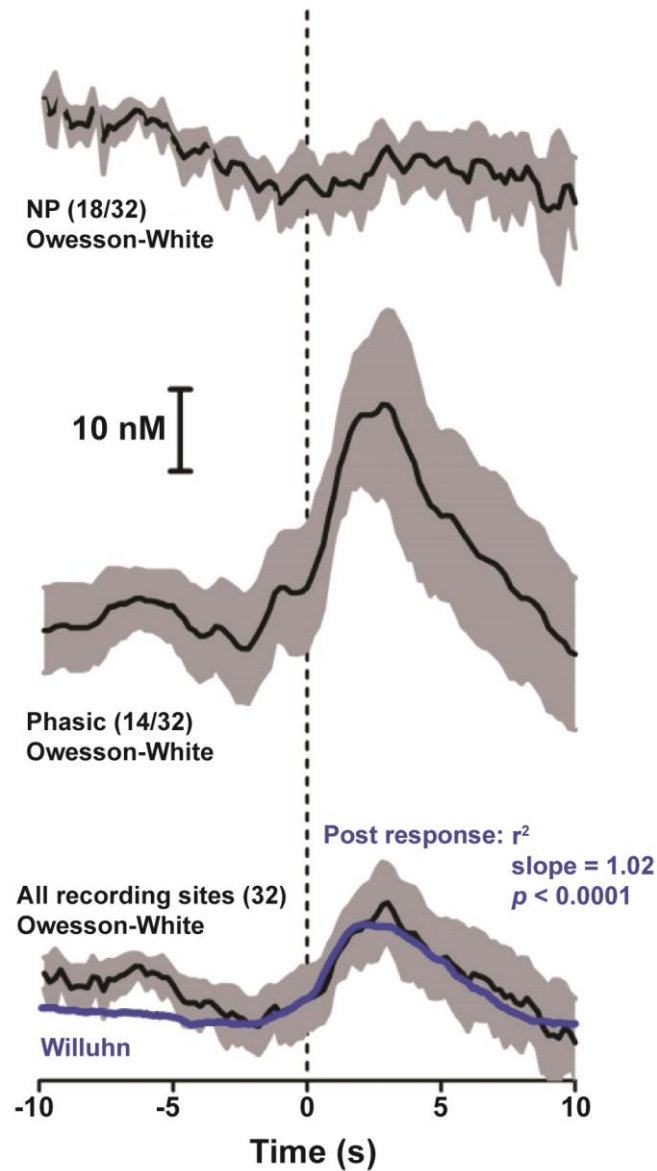


**Figure 5.2.** Comparison of concentrations measured at acute and chronic CFMs without optimization for dopamine release sites. In a study with acute CFMs (Owesson-White, et al., 2009) electrode placement was optimized for extracellular electrophysiological signals rather than dopamine release, resulting in recording locations without (top) and with (middle) phasic dopamine release. The average concentrations and concentration profile correspond well with values from chronically implanted CFMs that were not optimized for recording location (bottom), indicating the lower concentrations measured with chronic CFM may be an artifact of recording site selection. Reprinted with permissions from (Willuhn, et al., 2012). Copyright 2012 PNAS.

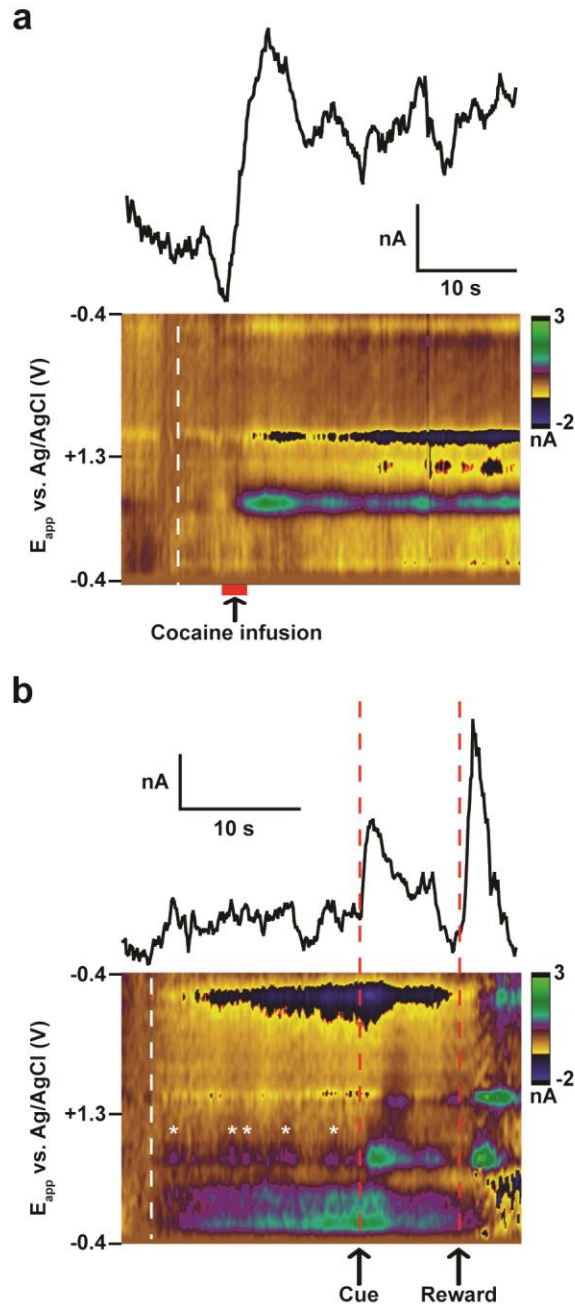


**Figure 5.3.** Dopamine transients at chronically implanted CFMs. (a) Pharmacologically induced dopamine transients at a chronic CFM in response to i.v. cocaine infusion (red bar, 1.5 s duration). Background subtraction is denoted by the white dashed line. (b) Measurements at a chronic CFM during a behavioral session of Pavlovian conditioning. Spontaneous dopamine transients are observed preceding cue onset (white asterisks). Moreover, both cue onset (left red dotted line) and reward delivery immediately following cue offset (right red dotted line) evoked phasic dopamine release. Background subtraction is denoted by the white dashed line. Dopamine traces were extracted with PCR using a standard training set. Both measurements were made in the nucleus accumbens core.

## Reference electrodes

Experiments using FSCV in freely moving animals generally use chronically implanted Ag/AgCl reference electrodes (Phillips, et al., 2003a). An issue with this approach is that half-cell reaction is not maintained over time, producing a shift in the reference potential and polarizing the reference electrode, most likely due to dechlorination (Moussy & Harrison, 1994). Further, fouling of the reference electrode would be expected upon insertion. This status is evident from an altered shape of the background current (Arnold et al., 2015). While the shift in reference potential can be compensated for by positive offsets to the applied potential, some non-linearity may be introduced by the polarization if voltage error persists (Roberts et al., 2013). Use of a polymer coating on the Ag/AgCl surface has been shown to delay dechlorination (Hashemi et al., 2011; Moussy & Harrison, 1994). Alternatively, reference electrodes can be implanted on the day of recordings through a guide cannula (Rodeberg, et al., 2016; Saddoris et al., 2015; Saddoris et al., 2016).

## Signal stability

During each voltage scan with FSCV, a cyclic voltammogram (CV) is generated that contains faradaic (redox) current from electroactive neurochemicals. In addition, there are other sources of current, primarily from the electrode itself, which produces both faradaic current from redox processes at its surface moieties, and non-faradaic current due to its resistive-capacitive properties. The 'background' current from the electrode is quantitatively much greater than the current produced by physiological levels of neurochemicals. For this reason, background subtraction is used with FSCV to measure changes in analyte concentration from a baseline reference point: CVs obtained during the baseline period are averaged and subtracted from each of the subsequent CVs in the time series. This approach allows the detection of bidirectional changes in the concentrations of electroactive neurochemicals from the baseline. However, any changes in the other components of the CV following the baseline period will

necessarily also contribute to background-subtracted CVs. The electrode background current described above is quite stable from scan to scan, but because it dominates the CV, even very small changes in the electrode's chemical or physical properties following the baseline period can contaminate background-subtracted CVs in the form of 'drift'.

The first type of drift that we will discuss is that relating to the chemical properties of the electrode surface. This type of drift is most prevalent when applying waveforms to the electrode that have anodic limits that exceed 1.0 V versus Ag/AgCl. Application of these waveforms in aqueous solutions such as the interstitial fluid in the brain, changes the surface chemistry of carbon fibers by introducing surface oxide groups (Roberts, et al., 2010), increasing the faradaic current in the CV. Until this 'activation' process reaches equilibrium, there will be progressive increase in the overall current in the background CV, as well as a net negative potential shift in the background peak.

To get to equilibrium more expediently, waveforms can be applied ('cycled') at a higher repetition rate than that used for data collection (typically 60 Hz). The required time to reach equilibrium differs across electrodes and implantations. In practice, acutely implanted electrodes are cycled for 15-30 min at 60 Hz before use. Chronically implanted electrodes are typically cycled more extensively, as much as two hours on the first use, followed by shorter durations (30-60 min) for each subsequent recording. As the necessary amount of cycling to reach equilibrium can vary between electrodes, however, it is more reliable to assess electrode stability via the background CV, which should remain relatively consistent in shape and amplitude following cycling. With either approach, additional cycling at the data-collection repetition rate (usually 10 Hz) for at least 10 min is required to re-establish equilibrium at this waveform application frequency. Nonetheless, even with extensive cycling of the electrode before the experiment, some drift may still persist.

Another type of background-current drift can be caused by etching of the carbon fiber during voltage scans. Etching drives evolution of the electrode surface and thereby affects both

the faradaic and non-faradaic currents. The extent that an applied waveform will produce etching of carbon fiber is dependent on its duration at higher potentials, specifically the period in which the applied potential remains greater than 1.0 V versus Ag/AgCl (Keithley et al., 2011). With the waveforms typically used in FSCV for *in vivo* dopamine detection, the excursion above 1.0 V is relatively short (1.5 ms/scan) and so, any etching that takes place is incremental over millions of scans ( $\sim 0.002 \text{ \AA}/\text{scan}$ ) (Keithley, et al., 2011). Therefore, drift attributable to this process occurs at a much lower rate than that from changes in surface chemistry. Thus, two main sources of background drift are augmented using voltage waveforms that have an anodic limit in excess of 1.0 V. This drift is a tradeoff with the increase in sensitivity afforded by these waveforms (Heien, et al., 2003).

The structural quality of the electrode and its connection to the headstage can also impact the stability of the signal. For example, if the seal between the carbon fiber and the insulating capillary is compromised then fluid can leak into the capillary increasing the background size (i.e., producing drift). The likelihood of this problem occurring can be reduced using epoxy to make, or reinforce, the seal. The integrity of electrical connections between the electrode and headstage are also important, especially with regard to movement artifacts. These types of problems are largely eliminated with practice in electrode fabrication, combined with robust quality control prior to implantation.

These instabilities in the signal can interfere with reliable signal analysis. While the reduction of noise can lessen this issue (e.g., with good electrode quality control), background drift poses a particular problem. Background drift, by definition, is an accumulative process where the level of interference in an analytical signal increases from the baseline (subtraction) period, limiting the effective window of analysis. Heien and colleagues suggested, as a guideline, that with standard parameters for FSCV in behaving animals, chemometric data analysis (see below) remains reliable for CVs taken up to 90 seconds from the baseline (Heien, et al., 2005). This window is sufficient for the routine use of peri-event histograms to test

changes in analyte concentration time locked to a stimulus or action. However, as discussed below, the exact size of a reliable analysis window will be dependent upon the quality of the data, and will be assessed as part of the data-analysis process. To attempt to remove the influence of drift, thereby increasing the analysis window, one strategy has been to incorporate CVs representing the drift in to the training sets used for analysis (Collins et al., 2016; Hermans et al., 2008).

When considering different types of electrode with respect to signal stability, a number of factors come into play. Glass-based electrodes are more fragile than fused-silica-based electrodes and are therefore more susceptible to noise from compromised seals or other structural damage. Fixed electrodes have a low profile with connectors cemented in place, reducing movement artifacts and overall noise due to the absence of pendulum effects from a microdrive, or movement of wires relative to the electrode and headstage. However, these electrodes cannot be easily replaced with a fresh electrode in the event of a failure. Drift relating to the surface chemistry of the electrode is dependent on the type of carbon fiber used and the waveform applied. These aspects are not systematically different between acute and chronic electrodes and so neither application appears to be more susceptible to this type of background drift. By the same rationale, the *rate* of background drift due to etching should not differ between acute and chronic electrodes.

However, because the cumulative duration of recording with chronic electrodes is substantially longer than for acute electrodes, it is likely that the *total* etching across the working lifetime of a chronic electrode will be greater. This may impact the sensitivity of the electrode. For this reason, it is advisable that positive controls are used to ensure that the sensitivity is not changing over the course of an experiment (e.g., Figure 2E of (Clark et al., 2013)).

## CHEMOMETRIC DATA ANALYSIS

Extracellular dopamine is detected via its oxidation and reduction at the carbon-fiber surface, producing a voltammetric current proportional to its local concentration. However, how to obtain this concentration has been a matter of considerable debate and development within the field. Original calibrations of *in vivo* voltammetric data directly converted the voltammetric current at the peak oxidation potential for dopamine into a concentration using an externally obtained calibration factor. However, various electroactive substances can interfere at the oxidative peak for dopamine, including ascorbic acid (Baur, et al., 1988; Ewing et al., 1982; Gerhardt, et al., 1984; Gonon et al., 1981), dopamine metabolites (Baur, et al., 1988; Garris et al., 1993; Gonon, et al., 1980; Gonon, et al., 1981), pH (Jones et al., 1994; Kawagoe et al., 1993; Rice & Nicholson, 1989; Runnels, et al., 1999; Takmakov et al., 2010), and other ions (Jones, et al., 1994; Rice & Nicholson, 1989). Because this method is univariate (i.e. only uses a single measurement point to predict concentration), it cannot separate out these interferences (Booksh & Kowalski, 1994; Olivieri, 2014). While anatomical and pharmacological criteria can increase confidence in the identity of the measured signal, univariate analysis will fail if interfering analytes significantly contribute.

To circumvent this problem, a method was developed to compare experimental cyclic voltammograms to electrically-evoked templates collected at the same electrode (Cheer et al., 2004; Heien, et al., 2003; Phillips, et al., 2003a; Phillips & Wightman, 2003; Robinson, et al., 2003; Troyer et al., 2002; Venton et al., 2003a). Cyclic voltammograms with a lower correlation coefficient than a user-defined value (typically  $r^2 < 0.75$ ) were considered to have significant contribution from other electroactive substances and were not used for univariate prediction. In some cases, current contributions from pH (Cheer, et al., 2004; Venton, et al., 2003a) and drift (Borland & Michael, 2004) were manually subtracted by using currents from a potential where dopamine did not contribute to predict current interference at the peak oxidation potential for

dopamine. However, this approach can miss dopamine events that are identified with more rigorous analysis (Heien, et al., 2005).

A more reliable calibration methodology is the use of chemometric multivariate analysis. Instead of using measurements at a single potential to predict concentration, multivariate analysis uses the entirety of the potential window to separate and quantitate multiple analytes, taking advantage of the chemical selectivity afforded FSCV (Figure 5.4a) (Bro, 2003; Kramer, 1998; Lavine & Workman, 2013). While there have been a few different multivariate methods implemented with *in vivo* FSCV data (Kishida et al., 2016; Yorgason et al., 2011), the most implemented and characterized method with FSCV data is principal component analysis (PCA) with inverse least-squares regression, also referred to as principal component regression (PCR) (Heien, et al., 2004; Heien, et al., 2005; Keithley et al., 2010; Keithley et al., 2009a; Keithley et al., 2009b; Keithley & Wightman, 2011). Therefore, the focus of this section of the review will be on the use of PCR for analysis of FSCV data. Nonetheless, the fundamental theory behind PCR is similar to other multivariate methods.

### **Principal Component Regression**

Data collected with FSCV tends to be complex. At high sample rates (>100 kHz), there are approximately 1000 data points per individual CV. One of the chief goals of PCR is to reduce the dimensionality of data. In this way, a large number of data points can be described by a handful of abstract vectors referred to as 'principal components' (PCs). Despite this reduction in dimensionality, PCR extracts more information from the data than univariate methods, and allows resolution of simultaneously varying analytes with overlapping signals (Heien, et al., 2005). PCR also functions as a noise removal technique, because PCs that represent non-deterministic variance (i.e. random noise) in the training set are discarded. This process improves the quality of its determinations and allows stronger confidence in the model. Lastly, this method provides objectivity and statistical validation of the measured signal.

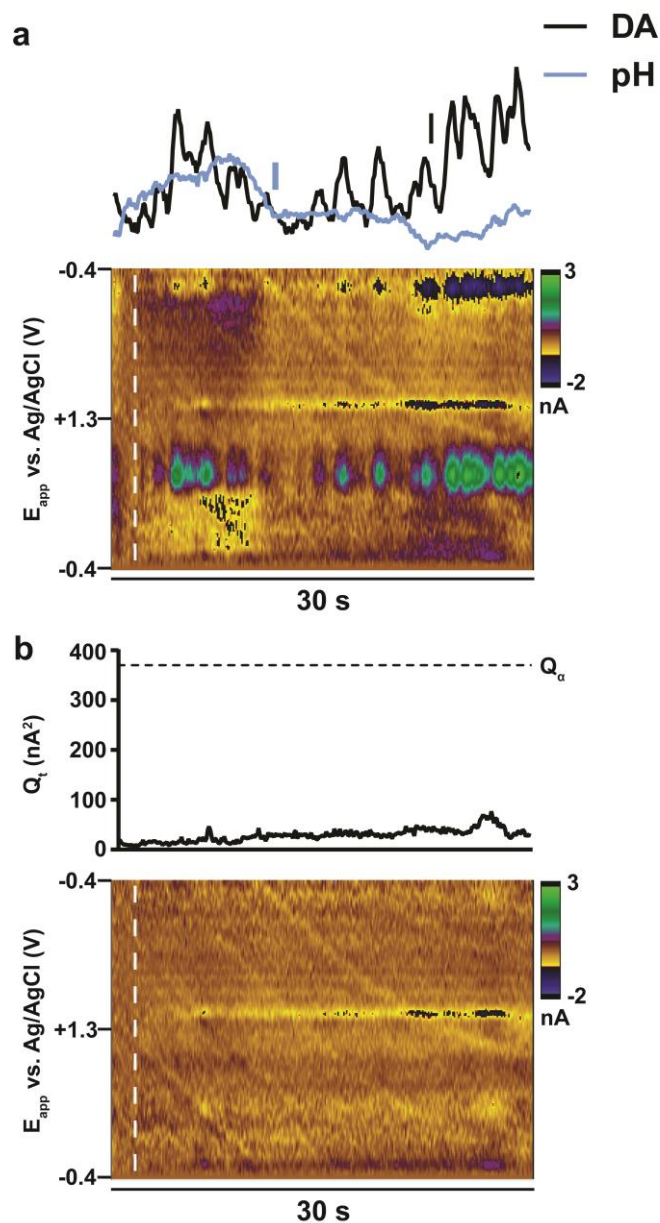


**Figure 5.4.** An example of the use of principal component analysis to analyze cocaine-induced dopamine transients. (a) A thirty second color plot following cocaine (20 mg/kg) administration in an awake rat shows overlapping dopamine and pH changes. The dopamine (black) and pH (blue) changes are separated by PCA, and quantitated using inverse-least squares regression. pH changes have a maximum contribution of +0.019 pH units (-0.76 nA) at 8.3 s, while dopamine maximizes at 262 nM (3.13 nA) at 28.9 s. (b) Residual analysis confirms that the PCA model is valid for analysis of this data.  $Q_t$  values (black) fall below the model specific tolerance level ( $Q_\alpha$ , 379  $nA^2$ ) for the data shown in panel (a). A residual color plot displays current uncaptured by the model.

Generally, the construction and application of a PCR model to predict concentrations from FSCV measurements consists of five steps: 1) training set construction, 2) generation of PCs, 3) discarding PCs that only represent noise (i.e. rank determination), 4) signal extraction, and 5) model validation. Importantly, free software (HDCV) is available that automatically carries out steps 2-5 and is compatible with data collected with TarHeel and other voltammetric software (Bucher et al., 2013). This software also includes additional diagnostics to assess training set quality. Nonetheless, it is important to understand the basic concepts of PCR to use it effectively. With this aim in mind, each step will be described briefly. More detailed discussion of PCR (Bro, 2003; Kramer, 1998; Lavine & Workman, 2013) and its use with FSCV is available elsewhere (Heien, et al., 2004; Heien, et al., 2005; Johnson et al., 2016; Keithley, et al., 2010; Keithley, et al., 2009a; Keithley, et al., 2009b; Keithley & Wightman, 2011; Rodeberg et al., 2015).

### *1) Training Set Construction*

The first step in building a PCR model is the collection of a group of CV standards known collectively as a 'training set'. Several guidelines for building training sets have been outlined previously (Johnson, et al., 2016; Keithley, et al., 2010; Keithley, et al., 2009a; Keithley, et al., 2009b; Keithley & Wightman, 2011; Kramer, 1998; Rodeberg, et al., 2015). First, the training set should comprise all expected contributions to the data. For measurements of striatal dopamine, this typically includes dopamine and pH changes, though background drift has also been included (Collins, et al., 2016; Hermans, et al., 2008). Second, the CV standards should span the expected current range in the data to be analyzed, which prevents model extrapolation (Kramer, 1998). Third, the training set should contain an adequate number of samples. While there is no strict consensus on the ideal number of standards, a minimum of three standards per analyte is needed to satisfy the requirements for regression (Kramer, 1998). The use of a larger number of standards is preferred however, and previous work has suggested that five CVs per

analyte is sufficient to provide reliable models (Heien, et al., 2005; Keithley, et al., 2010; Keithley & Wightman, 2011; Kramer, 1998). Fourth, to satisfy mutual independence, training set CVs should be selected from separate events, and not include CVs that will be analyzed by the final model. Finally, a training set should be generated in a recording environment that matches the experimental environment.

## *2) Principal component generation*

Next, the training set standards are used to generate the PCs. As such, the quality and representativeness of training set standards is of critical importance. Importantly, the largest amplitude standards in the training set dominate the appearance and quality of these PCs; this is because FSCV standards are not usually mean-centered which avoids giving undue influence to the smallest standards in training set CVs, which typically have the lowest signal-to-noise ratio (Kramer, 1998).

These PCs are determined by singular value decomposition (SVD), a process that is described in detail elsewhere (Johnson, et al., 2016). With SVD, each successive PC is calculated to span as much of the remaining variance in the training set standards as possible. The maximum number of PCs for a particular model is equal to the number of measurements being made (i.e. for CVs with 1000 data points, there could be a maximum of 1000 PCs). However, the use of SVD limits the number of PCs to the total number of standards in the training set. The PCs were created from the same dimensions as the data, and thus can be visualized in the form of CVs (Johnson, et al., 2016; Keithley, et al., 2010). However, it is important to understand that PCs are by definition abstract, and thus should not be viewed as representing individual analytes (Keithley, et al., 2009b). Indeed, it is extremely unlikely that PCs will precisely align to individual analytes because of the requirement of orthogonality between PCs in the PCA approach.

### 3) Rank determination

While several PCs are provided by SVD, only a subset has information that is relevant to concentration prediction (Keithley, et al., 2010; Malinowski, 1977). These are *primary PCs*, which represent analytically relevant variance in the standards, while *secondary PCs* reflect any remaining variance (i.e. noise). The number of primary PCs is referred to as the *rank* of the PCR model. The exclusion of secondary PCs is desirable, as it prevents the use of noise in concentration prediction and allows for an estimation of noise levels for model validation (see below).

Rank selection in FSCV is customarily done with Malinowski's F-test (Keithley, et al., 2010; Malinowski, 1977). This procedure is objective, statistically validated, and does not require pre-existing knowledge of noise levels in the data, which can be difficult to obtain. Moreover, it has been demonstrated to discard more noise than other methods (Keithley, et al., 2010). This process is most suitable for training sets with a signal-to-noise ratio larger than 10 (Malinowski, 2004). Rank tends to increase when there is more variability between training set standards (i.e. peak shifting and broadening). Therefore, while a rank of two may be desirable for a moderate training set size (e.g. 10 total standards) representing a two component system (i.e. dopamine and pH changes), the rank will vary both with the consistency of the CVs and the signal-to-noise of the training set (Johnson, et al., 2016; Keithley, et al., 2010).

### 4) Signal Extraction

The generated PCs are then used to extract concentrations of any analyte that was included in the training set. The first step is using the training set standards to generate 'scores', which are the dot products of each PC with each training set standard. Notably, CVs have higher score magnitudes with PCs they closely resemble in shape. Scores arising from secondary PCs are discarded, as these PCs describe only noise. The concentrations are then regressed against retained scores, producing a regression that defines the calibration model. To

predict the concentrations of experimental CVs, their scores are determined for the retained PCs and plugged into this regression equation. This entire process has been depicted visually (see (Johnson, et al., 2016)).

#### 5) Model validation

As Douglas Adams states in 'Hitchhiker's Guide to the Galaxy', "we demand rigidly defined areas of doubt and uncertainty" (Adams, 1980). Because multivariate calibrations are complex, it is important to verify that these models are of sufficient quality to capture experimental data and demonstrate what data remains uncaptured. This process is referred to as 'model validation'. In other fields (e.g. spectroscopy), validation is performed by running independent standards on the instrument to determine the accuracy of the model (Kramer, 1998). However, this is not possible when building an *in vivo* training set (see below), as the concentrations of analyte signals are not known. Therefore, a 'pseudo-validation' procedure is applied to PCR analysis of FSCV data in which the ability of the model to capture the experimental data is assessed (Jackson & Mudholkar, 1979; Keithley, et al., 2009a; Keithley, et al., 2009b). In other words, this validation procedures tests the *applicability*, rather than the accuracy, of the model. Nonetheless, if the model is considered 'invalid' (i.e. not applicable) for a particular experimental datum, the concentration value obtained is rejected.

One method for evaluating model validity relies on the 'first order advantage' of multivariate calibration, which allows for detection, but not removal, of interfering signals through residual analysis (Booksh & Kowalski, 1994; Olivieri, 2014). During PCR, primary PCs are used to reconstruct experimental CVs. However, it is rare for these PCs to fit the data perfectly, with remaining uncaptured current referred to as the 'residual'. Jackson & Muldholkar developed a procedure to statistically test residual values to validate the model (Jackson & Mudholkar, 1979). A significance threshold is determined using the secondary PCs that were discarded during rank selection at a user-defined confidence interval  $\alpha$  ( $Q_\alpha$ ), under which  $100*(1-\alpha)\%$  of

uncaptured random noise should fall (Keithley, et al., 2009a; Keithley, et al., 2009b). If the squared sum of the residual current for a particular CV ( $Q_t$ ) is greater than  $Q_\alpha$ , it is determined that a significant current source is present that cannot be captured by the model, which invalidates its use for analysis of this data. The concern with deterministic variance being present in the residual is that this variance may be the result of misattribution of dopamine to the residual rather than the dopamine vector (false negative). Alternatively, it could be an indicator that a signal that is not identical to dopamine is attributed to the dopamine vector (false positive) since the remainder of that signal (i.e., the difference between the CV for the signal and that for dopamine) would be attributed to the residual. However, the source of deterministic variance could be due to ancillary noise sources such as an unexpected electroactive neurochemical or movement artifacts in that absence of false positives or negatives. Therefore, the process is conservative inasmuch as the model will be rejected if  $Q_t$  exceeds  $Q_\alpha$  because of false-negative or false-positive errors, but also due to the presence of other components that cannot be accounted for by the model. Importantly, this process does not statistically confirm whether the collected data contains dopamine; this can only be confirmed with pharmacological and/or histological tests, or selective (i.e. optogenetic) stimulation.

The residual ( $Q_t$ ) is calculated for each cyclic voltammogram in any given set of data, and these values can be plotted along the same time scale as the data (Figure 5.4b, top). Residual color plots can be used to visualize uncaptured current, which could reveal the source of variance uncaptured by the training set (Figure 5.4b, bottom). Residual failure outside of the window in which concentrations are being predicted should not impair the ultimate success of the model. However,  $Q_t$  may cross  $Q_\alpha$  for multiple CVs within the prediction window (i.e. during prolonged dopamine and/or pH events). Any individual data point that fails residual analysis (i.e.  $Q_t > Q_\alpha$ ) is excluded from the data set. The omission can be executed by replacing the data point with a new value based on interpolation between adjacent data points, or by designating the data point as “NaN” (not a number). Additional *a priori* exclusion criteria are also utilized if

there are too many data points missing from a trace that represents the single unit of analysis (e.g. one trial around a task-related event). Any trial is removed from subsequent analysis if it fulfills *either* of the following two criteria: 1) a total of ten percent or more of the data points have been excluded, or 2) a string of contiguous data points have been excluded that amounts to more than five percent of the data points.

### **Additional diagnostics to test the quality of training sets**

Further procedures are available to assess the quality of training sets. One such tool is a Cook's distance plot, which displays the scores for each analyte of interest with respect to the primary PCs (Keithley & Wightman, 2011). For the sake of simplicity, these are typically depicted with the x- and y-axis representing the first two primary PCs, though for higher dimension models (i.e. training sets with a rank >2), it should be understood that more projections exist. The use of these plots, along with calculation of Cooks' Distances, also allows the identification of outliers in the training set, described elsewhere (Keithley & Wightman, 2011).

The robustness of a training set can also be assessed with the model k-vectors (sometimes referred to as a K-matrix). A k vector is typically calculated to represent the estimation of the CV for a pure unit analyte concentration change (i.e. 1  $\mu$ M dopamine or a full pH unit change) (Johnson, et al., 2016; Keithley & Wightman, 2011). A representative k vector indicates the success of the model in isolating analytes of interest from the training set standards. A k vector that does not resemble the desired species can arise from the poor quality of training set standards and/or significant differences between them (Johnson, et al., 2016; Keithley & Wightman, 2011; Rodeberg, et al., 2015). Notably, it has been shown that the quality of CVs for each analyte (i.e. DA and pH for typical training sets) can affect the predictions for the other analytes in the training set, making the quality of standards for each analyte in the

training set an important experimental aim (in particular, see Figure 1 of (Keithley & Wightman, 2011)).

### **PCR with residual analysis in practice**

The most controversial component of the chemometric PCR analysis for FSCV that is the construction of a training set (Johnson, et al., 2016; Rodeberg, et al., 2015). The standard procedure for constructing a training set for chemometric analysis is to use a series of known concentration standards applied to the instrument *in vitro*, for example in a flow cell. However, even when collected at the same electrode, *in vivo* and *in vitro* CVs differ (See Supplementary Figure 3 of (Clark, et al., 2010)). This is likely due to chemical and electrical (impedance) differences between the two environments (Heien, et al., 2005; Phillips, et al., 2003a) and has led to the practice of acquiring training sets *in vivo* by stimulation of an afferent dopamine pathway following the experiment (Heien, et al., 2005; Keithley & Wightman, 2011; Rodeberg, et al., 2015), which is an extensively characterized source of dopamine release *in vivo* (Ewing, et al., 1983; Garris et al., 1994; Heien, et al., 2005; Kuhr, et al., 1987). This stimulation evokes both dopamine release and a subsequent temporally resolved hemodynamic response, including a pH change (Venton, et al., 2003a). Notably, these pH changes are difficult to resolve from changes in other electroactive substances (e.g.  $\text{H}_2\text{O}_2/\text{O}_2$ , adenosine) that also occur in response to electrical stimulation. As a result, *in vivo* pH CVs typically include contributions from these substances, and are thus difficult to simulate *in vitro* (Dengler et al., 2015). Ultimately, with a series of stimulation intensities (e.g. current amplitude, pulse number, frequency), a training set can be constructed, which spans the range of signals from dopamine and pH observed under experimental conditions. This method produces CVs that match the electrochemical and biological environment of the data to be analyzed, which is important for PC generation, signal extraction, and residual analysis (see above).

However, unlike with a training set generated from exogenous standards, the analyte concentrations producing these *in vivo* signals are not inherently known. Therefore, to estimate the concentrations of analytes in the training set, an additional step is required. Common practice is to use *in vitro* standards to obtain a calibration factor to convert current to concentration. Thus, while the analyte identity is not determined from *in vitro* standards, the estimation of concentration is. As stated above, *in vitro* CVs do not perfectly map onto *in vivo* CVs and, as such, the mapping of a calibration factor also incorporates some level of inaccuracy. For this reason, it is important to recognize that analyte concentrations reported from *in vivo* FSCV experiments should be regarded as estimates.

An additional limitation of the use of *in vivo* training sets is that, rather than using chemical standards, biological signals of presumed chemical origin are employed. Therefore, under these conditions, the model extracts signals that are similar to those produced by the biological manipulation rather than signals that are necessarily similar to a specific chemical. This approach is tolerated as a proxy of a chemical signal when the signal evoked by the stimulus used to generate the training set has been well characterized (such as *in vivo* stimulation along the ascending dopaminergic pathway, discussed above).

Using the original incarnation of chemometric analysis of *in vivo* FSCV signals (Heien, et al., 2005), training sets and experimental data are collected from the same recording site (or sometimes at different recording sites from the same subject), and so they lack full statistical independence. In these cases, the model identifies signals at a recording site evoked by one stimulus that resembles signals at the same recording site evoked by a different stimulus; or even by the same stimulus when electrically evoked signals are analyzed using a training set generated from electrical stimulation at the same location (Cheer et al., 2007a; Owesson-White et al., 2008; Park et al., 2013; Rodeberg, et al., 2016). One means utilized to avoid this circularity, and obtain greater independence, has been to construct *in vivo* training sets in a different subject to that from which the experimental data will be collected. However, for

practical (and ethical) reasons, it is not always possible to take each electrode used in an experiment and collect a training set with it from another animal. Consequently, the use of 'standard' training sets has evolved where a model is built from a training set generated at one electrode and used to analyze data from another electrode in a different subject. This approach assumes generalization of signals across electrodes. Indeed, electrochemical detection is founded on the premise that molecules exhibit consistent faradaic properties on a particular substrate when conditions are reproduced. Therefore, the key to the success of this approach is to maintain reproducibility of electrode fabrication, a goal that may be more favorable for (non-pulled) fused-silica than for pulled borosilicate-glass based electrodes, which tend to have significant variation in their tapers. However, other sources of variability can also violate generalization across experiments, including reference electrode drift and electrochemical differences between different carbon-fibers.

There are some additional advantages to using standard training sets. Models no longer need to be built at each individual electrode, which results in reduced analysis time. In addition, the use of a single standard training set could avoid the variability between experimenters in training set construction that has been demonstrated previously (Keithley, et al., 2010). Finally, a stimulating electrode, which can perturb the tissue and ultimately affect behavior (Garris et al., 2003), does not need to be implanted in the experimental animal.

Nonetheless, there are limitations to this approach. The ultimate characteristics of any PCR model are dependent on the CVs provided for the training set, and not the data to which it is being applied. The primary PCs, those used for concentration prediction, will exhibit characteristics of the signals seen at whichever electrode was used for training set construction. If there are differences in CV shapes between the experimental data and the training set, primary PCs will prove less able to extract and attribute experimental currents to the desired analytes. A recent study demonstrated that CVs differ between electrodes and experiments and,

despite high correlation coefficients between k vectors, this lead to differences in predicted dopamine concentrations (Rodeberg, et al., 2015).

A more significant problem is the impact on the reliability of model validation. Differences between experimental and standard training set CVs may lead to the assignment of deterministic currents (i.e. signals arising from analytes in the training set) to  $Q_i$ , resulting in unrepresentative residual traces. In some cases, this can lead to data being discarded that would have been retained with a within-subject training set (i.e. a false negative) (Rodeberg, et al., 2015). Moreover, because  $Q_{\alpha}$  is determined from information in secondary PCs, it will be model-specific and invariant across different sets of data even when noise levels vary from experiment to experiment. Lower than expected  $Q_{\alpha}$  values could increase the rate of false negatives; however, unrepresentatively high  $Q_{\alpha}$  values are also possible, which could lead to the retention of data that should have been discarded (i.e. false positives). This is more concerning, as it would permit the retention of poor data.

Ultimately, standard training sets suffer from the disadvantage of being unrepresentative of the experimental data. Nonetheless, standard training sets could provide similar qualitative results to within-subject training sets. Previous work has demonstrated that replacing dopamine CVs in a within-subject training set with CVs from a separate electrode (leaving pH CVs unaltered) resulted in a qualitatively similar trace (Figure 5.5) (Keithley & Wightman, 2011), and comparisons of data from different experiments using within-subject and standard training sets, respectively, has yielded similar results (Figure 5.2). However, current standard training set methodology precludes the ability to test whether the quantitative or residual analysis failures outlined above occur for any given application. Thus, improvements to standard training set methodology to reflect these concerns are important. One method that has been adopted to provide a level of validation between the generalized model (standard training set) and the experimental data is to use positive controls at the start and end of the experiment to compare the evoked signals with those in the training set. Commonly for experiments where striatal

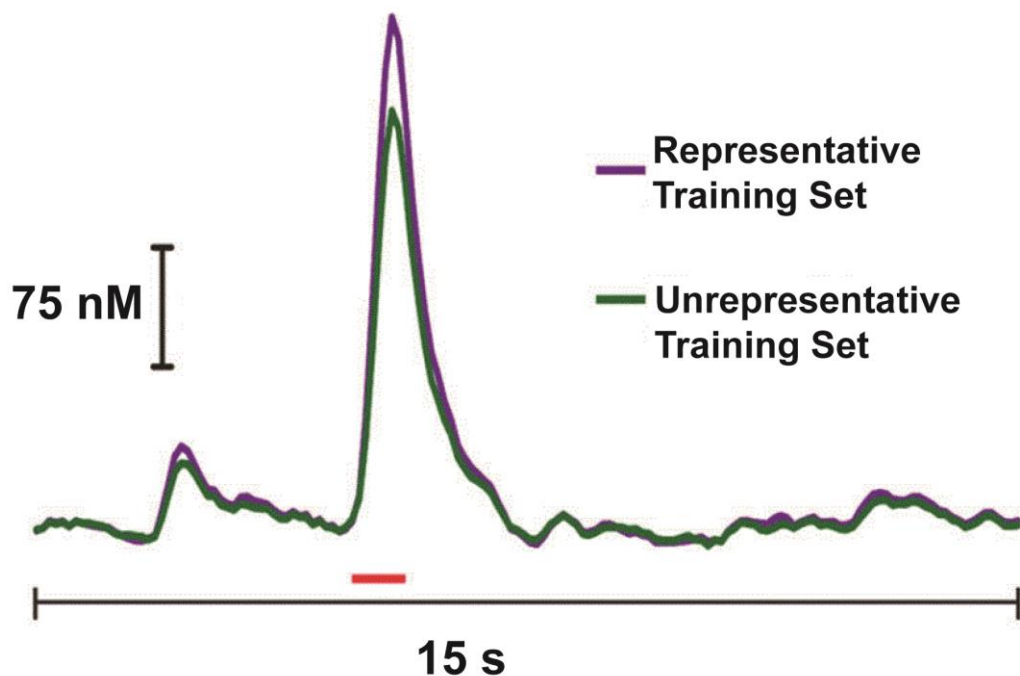


**Figure 5.5.** Training sets built with data from separate electrodes could capture qualitative information. Dopamine CVs from a training set built at the same electrode as the collected data were replaced with dopamine CVs from a separate electrode. pH CVs were left unaltered. Analysis with this composite training set resulted in underestimation of signal, but tracked qualitative information for this electrical stimulation (red bar). Figure reproduced with permissions from (Keithley & Wightman, 2011). Copyright 2011 American Chemical Society.

dopamine is being recorded, the unexpected delivery of a food reward is used to elicit an electrochemical signal (Clark, et al., 2013; Wanat et al., 2010). This signal is then compared to the CVs in the training set. If there is not close correlation between the positive-control signal and the training set, then either the signal is not predominantly dopamine, or the model will not generalize to the electrode being tested. While one could not easily discern these two scenarios, in either case it would not be fruitful to continue to collect and analyze experimental data under these conditions. However, this procedure does not address similarity of pH signals or noise levels between the data and training sets, both of which influence the predictions and success of the PCR model. Therefore, improving this verification process is a warranted area for progress in future investigations.

In addition, the methodology for constructing and/or implementing standard training sets could be improved. Notably, multivariate calibration transfer between instruments or electrodes is a significant area of inquiry within the field of chemometrics (De Noord, 1994; Feudale et al., 2002). These methods often require independent standards being run on each instrument (not possible with *in vivo* measurements) or use data from the new instrument to update the model. Further collaboration between chemometricians and users of FSCV could improve standard training set methodology by incorporating differences between electrodes and instrumentation to better match the experimental environment.

#### *Guidelines for Methods Presentation*

Because variability exists in procedures for PCR, a few basic guidelines for reporting these procedures are warranted. First, it is important to make clear what methods were used to construct training sets for the study. In particular, it should be elucidated which electrodes were used to generate the training sets (i.e. specific or standard training sets) so that readers can understand the procedure used to acquire and select standards. Second, because these chemometric models will be used to analyze large amounts of data, it is important to report their

general characteristics. This would include the analytes that comprise the training set,  $Q_{\alpha}$  values, and rank. The use of k-matrices could also illustrate the quality of these training sets. Third, the criteria for exclusion of data (i.e. residual analysis) should be made clear. Lastly, the use of additional methods to increase confidence in the acquired signal (e.g. the use of positive controls to verify the applicability of the model to experimental conditions (Clark, et al., 2013; Wanat, et al., 2010)) should be reported.

## **CONCLUSIONS AND PERSPECTIVES**

The authors of this review are in general agreement that, when appropriate caution is observed, both acute and chronic CFMs can be used for detection of behaviorally evoked dopamine release in regions of the striatum using FSCV. In support of the reliability of these measurements, there is generally high concordance between results from FSCV of dopamine concentration fluctuations in the striatum with either acute or chronic electrodes, and electrophysiological recordings of dopamine neurons in the midbrain, with many key findings reproduced across approaches. These replications include the characterization of reward prediction-error signals (Day, et al., 2007; Flagel, et al., 2011; Schultz et al., 1997) that convey quantitative information (Bayer et al., 2007; Hart, et al., 2014). They include demonstrations that dopamine signals to reward-related cues are sensitive to factors that influence subjective value such as delayed reward delivery (temporal discounting) (Day, et al., 2007; Fiorillo et al., 2008; Kobayashi & Schultz, 2008) or subjective risk preference (Lak et al., 2014; Nasrallah et al., 2011; Sugam et al., 2012), and concur that there is stronger encoding of reward size than effort-based response cost by dopamine signals (Gan et al., 2010; Pasquereau & Turner, 2013). An uncertainty-like signal following presentation of a Pavlovian stimulus predicting probabilistic reward has been identified and replicated across methodologies (Fiorillo et al., 2003; Hart et al., 2015) as have observations of partial generalization between sensory stimuli that are associated with different economic values (Day, et al., 2007; Waelti et al., 2001), which can

come in the form of a presumed sensory signal, temporally separated from a value signal (Hart, et al., 2014; Lak, et al., 2014; Sadoris et al., 2017). The success of chronic electrodes is notable, as it has long been held that chronically implanted electrodes are prone to failure. A recent review of glucose biosensors documents the importance of chronic sensors for monitoring in diabetes. The chief problem to their use is the foreign body response that impairs sensor performance (Soto et al., 2017). It may be that the finding that very small electrodes remain functional will be very useful to other health related fields involving biosensors.

The chief remaining disagreement between the authors is the standard training set methodology (discussed in **PCR with Residual Analysis in Practice**). In its current design, the use of PCR to analyze *in vivo* voltammetry data results in a tradeoff between two separate guidelines for PCR: 1) matching instrumental and environmental conditions when generating calibration models and 2) independence between training set standards and data. Phillips and colleagues value the use of a training set that is generated from an independent source to that from which experimental data is collected. However, Wightman and colleagues maintain that the use of training sets obtained under unrepresentative conditions prevents definitive statements regarding statistical validation of PCR models when analyzing FSCV data, and has practical implications for signal extraction. Notably, this is true for training sets generated *in vitro*, in which it can be difficult to simulate the chemical environment of *in vivo* measurements, which is of particular importance for generating pH standards.

While the robustness of detection of striatal dopamine by FSCV in awake animals should inspire confidence, some of the greatest promise is beyond dopamine in the striatum. For detection of other electroactive neurochemicals in other brain regions (Dankoski & Wightman, 2013; Fox et al., 2015; Spanos et al., 2013; Swamy & Venton, 2007b), sensitivity and selectivity are more serious concerns because of lower analyte concentrations and greater number of possible interferents. With this in mind, we believe that many of the caveats we have described in this review will pose much greater challenges for these new applications. Specifically, key

hardware changes could be more widespread use of chronically implanted electrode arrays that have moveable probes, and the use of stable polymer coatings on Ag/AgCl reference electrodes.

## REFERENCES

- Adams, D. (1980). *The hitchhiker's guide to the galaxy*. New York: Harmony Books.
- Aragona, B. J., Cleaveland, N. A., Stuber, G. D., Day, J. J., Carelli, R. M., & Wightman, R. M. (2008). Preferential enhancement of dopamine transmission within the nucleus accumbens shell by cocaine is attributable to a direct increase in phasic dopamine release events. *J Neurosci*, *28*(35), 8821-8831.
- Armstrong-James, M., & Millar, J. (1979). Carbon fibre microelectrodes. *J Neurosci Methods*, *1*(3), 279-287.
- Armstrong-James, M., Millar, J., & Kruk, Z. L. (1980). Quantification of noradrenaline iontophoresis. *Nature*, *288*(5787), 181-183.
- Arnold, M. M., Burgeno, L. M., & Phillips, P. E. (2015). Fast-Scan Cyclic Voltammetry in Behaving Animals. *Basic Electrophysiological Methods*, 108.
- Baur, J. E., Kristensen, E. W., May, L. J., Wiedemann, D. J., & Wightman, R. M. (1988). Fast-scan voltammetry of biogenic amines. *Anal Chem*, *60*(13), 1268-1272.
- Bayer, H. M., Lau, B., & Glimcher, P. W. (2007). Statistics of midbrain dopamine neuron spike trains in the awake primate. *J Neurophysiol*, *98*(3), 1428-1439.
- Belle, A. M., Owesson-White, C., Herr, N. R., Carelli, R. M., & Wightman, R. M. (2013). Controlled iontophoresis coupled with fast-scan cyclic voltammetry/electrophysiology in awake, freely moving animals. *ACS Chem Neurosci*, *4*(5), 761-771.
- Booksh, K. S., & Kowalski, B. R. (1994). Theory of Analytical-Chemistry. *Anal Chem*, *66*(15), A782-A791.
- Borland, L. M., & Michael, A. C. (2004). Voltammetric study of the control of striatal dopamine release by glutamate. *J Neurochem*, *91*(1), 220-229.
- Bro, R. (2003). Multivariate calibration - What is in chemometrics for the analytical chemist? *Analytica Chimica Acta*, *500*(1-2), 185-194.
- Bucher, E. S., et al. (2013). Flexible software platform for fast-scan cyclic voltammetry data acquisition and analysis. *Anal Chem*, *85*(21), 10344-10353.
- Cheer, J. F., Aragona, B. J., Heien, M. L., Seipel, A. T., Carelli, R. M., & Wightman, R. M. (2007a). Coordinated accumbal dopamine release and neural activity drive goal-directed behavior. *Neuron*, *54*(2), 237-244.
- Cheer, J. F., Heien, M. L., Garris, P. A., Carelli, R. M., & Wightman, R. M. (2005). Simultaneous dopamine and single-unit recordings reveal accumbens GABAergic responses: implications for intracranial self-stimulation. *Proc Natl Acad Sci U S A*, *102*(52), 19150-19155.

- Cheer, J. F., Wassum, K. M., Heien, M. L., Phillips, P. E., & Wightman, R. M. (2004). Cannabinoids enhance subsecond dopamine release in the nucleus accumbens of awake rats. *J Neurosci*, *24*(18), 4393-4400.
- Cheer, J. F., et al. (2007b). Phasic dopamine release evoked by abused substances requires cannabinoid receptor activation. *J Neurosci*, *27*(4), 791-795.
- Cheramy, A., Leviel, V., & Glowinski, J. (1981). Dendritic release of dopamine in the substantia nigra. *Nature*, *289*(5798), 537-542.
- Clark, J. J., Collins, A. L., Sanford, C. A., & Phillips, P. E. (2013). Dopamine encoding of Pavlovian incentive stimuli diminishes with extended training. *J Neurosci*, *33*(8), 3526-3532.
- Clark, J. J., et al. (2010). Chronic microsensors for longitudinal, subsecond dopamine detection in behaving animals. *Nat Methods*, *7*(2), 126-129.
- Collins, A. L., Greenfield, V. Y., Bye, J. K., Linker, K. E., Wang, A. S., & Wassum, K. M. (2016). Dynamic mesolimbic dopamine signaling during action sequence learning and expectation violation. *Sci Rep*, *6*, 20231.
- Conti, J. C., Strobe, E., Adams, R. N., & Marsden, C. A. (1978). Voltammetry in brain tissue: chronic recording of stimulated dopamine and 5-hydroxytryptamine release. *Life Sci*, *23*(27-28), 2705-2715.
- Covey, D. P., Dantrassy, H. M., Zlebnik, N. E., Gildish, I., & Cheer, J. F. (2016). Compromised Dopaminergic Encoding of Reward Accompanying Suppressed Willingness to Overcome High Effort Costs Is a Prominent Prodromal Characteristic of the Q175 Mouse Model of Huntington's Disease. *J Neurosci*, *36*(18), 4993-5002.
- Dankoski, E. C., & Wightman, R. M. (2013). Monitoring serotonin signaling on a subsecond time scale. *Front Integr Neurosci*, *7*, 44.
- Day, J. J., Roitman, M. F., Wightman, R. M., & Carelli, R. M. (2007). Associative learning mediates dynamic shifts in dopamine signaling in the nucleus accumbens. *Nat Neurosci*, *10*(8), 1020-1028.
- De Noord, O. E. (1994). Multivariate calibration standardization. *Chemometrics and Intelligent Laboratory Systems*, *25*(2), 85-97.
- Delgado, J. M., DeFeudis, F. V., Roth, R. H., Ryugo, D. K., & Mitruka, B. M. (1972). Dialytrode for long term intracerebral perfusion in awake monkeys. *Arch Int Pharmacodyn Ther*, *198*(1), 9-21.
- Dengler, A. K., Wightman, R. M., & McCarty, G. S. (2015). Microfabricated Collector-Generator Electrode Sensor for Measuring Absolute pH and Oxygen Concentrations. *Anal Chem*, *87*(20), 10556-10564.
- Ewing, A. G., Bigelow, J. C., & Wightman, R. M. (1983). Direct in vivo monitoring of dopamine released from two striatal compartments in the rat. *Science*, *221*(4606), 169-171.

- Ewing, A. G., Wightman, R. M., & Dayton, M. A. (1982). In vivo voltammetry with electrodes that discriminate between dopamine and ascorbate. *Brain Res*, 249(2), 361-370.
- Feudale, R. N., Woody, N. A., Tan, H., Myles, A. J., Brown, S. D., & Ferré, J. (2002). Transfer of multivariate calibration models: a review. *Chemometrics and Intelligent Laboratory Systems*, 64(2), 181-192.
- Fiorillo, C. D., Newsome, W. T., & Schultz, W. (2008). The temporal precision of reward prediction in dopamine neurons. *Nat Neurosci*, 11(8), 966-973.
- Fiorillo, C. D., Tobler, P. N., & Schultz, W. (2003). Discrete coding of reward probability and uncertainty by dopamine neurons. *Science*, 299(5614), 1898-1902.
- Flagel, S. B., et al. (2011). A selective role for dopamine in stimulus-reward learning. *Nature*, 469(7328), 53-57.
- Flagel, S. B., et al. (2010). An animal model of genetic vulnerability to behavioral disinhibition and responsiveness to reward-related cues: implications for addiction. *Neuropsychopharmacology*, 35(2), 388-400.
- Fox, M. E., Rodeberg, N. T., & Wightman, R. M. (2017). Reciprocal Catecholamine Changes during Opiate Exposure and Withdrawal. *Neuropsychopharmacology*, 42(3), 671-681.
- Fox, M. E., Studebaker, R. I., Swofford, N. J., & Wightman, R. M. (2015). Stress and Drug Dependence Differentially Modulate Norepinephrine Signaling in Animals with Varied HPA Axis Function. *Neuropsychopharmacology*, 40(7), 1752-1761.
- Gan, J. O., Walton, M. E., & Phillips, P. E. (2010). Dissociable cost and benefit encoding of future rewards by mesolimbic dopamine. *Nat Neurosci*, 13(1), 25-27.
- Garris, P. A., et al. (2003). A role for presynaptic mechanisms in the actions of nomifensine and haloperidol. *Neuroscience*, 118(3), 819-829.
- Garris, P. A., Christensen, J. R., Rebec, G. V., & Wightman, R. M. (1997). Real-time measurement of electrically evoked extracellular dopamine in the striatum of freely moving rats. *J Neurochem*, 68(1), 152-161.
- Garris, P. A., Ciolkowski, E. L., Pastore, P., & Wightman, R. M. (1994). Efflux of dopamine from the synaptic cleft in the nucleus accumbens of the rat brain. *J Neurosci*, 14(10), 6084-6093.
- Garris, P. A., Collins, L. B., Jones, S. R., & Wightman, R. M. (1993). Evoked extracellular dopamine in vivo in the medial prefrontal cortex. *J Neurochem*, 61(2), 637-647.
- Gerhardt, G. A., Oke, A. F., Nagy, G., Moghaddam, B., & Adams, R. N. (1984). Nafion-coated electrodes with high selectivity for CNS electrochemistry. *Brain Res*, 290(2), 390-395.
- Gonon, F., Buda, M., Cespuglio, R., Jouvét, M., & Pujol, J. F. (1980). In vivo electrochemical detection of catechols in the neostriatum of anaesthetized rats: dopamine or DOPAC? *Nature*, 286(5776), 902-904.

- Gonon, F., Buda, M., Cespuoglio, R., Jouvet, M., & Pujol, J. F. (1981). Voltammetry in the striatum of chronic freely moving rats: detection of catechols and ascorbic acid. *Brain Res*, 223(1), 69-80.
- Gratton, A., & Wise, R. A. (1994). Drug- and behavior-associated changes in dopamine-related electrochemical signals during intravenous cocaine self-administration in rats. *J Neurosci*, 14(7), 4130-4146.
- Hafizi, S., Kruk, Z. L., & Stamford, J. A. (1990). Fast cyclic voltammetry: improved sensitivity to dopamine with extended oxidation scan limits. *J Neurosci Methods*, 33(1), 41-49.
- Harstad, R. K., & Bowser, M. T. (2016). High-Speed Microdialysis-Capillary Electrophoresis Assays for Measuring Branched Chain Amino Acid Uptake in 3T3-L1 cells. *Anal Chem*.
- Hart, A. S., Clark, J. J., & Phillips, P. E. (2015). Dynamic shaping of dopamine signals during probabilistic Pavlovian conditioning. *Neurobiol Learn Mem*, 117, 84-92.
- Hart, A. S., Rutledge, R. B., Glimcher, P. W., & Phillips, P. E. (2014). Phasic dopamine release in the rat nucleus accumbens symmetrically encodes a reward prediction error term. *J Neurosci*, 34(3), 698-704.
- Hashemi, P., et al. (2011). Chronically Implanted, Nafion-Coated Ag/AgCl Reference Electrodes for Neurochemical Applications. *ACS Chem Neurosci*, 2(11), 658-666.
- Hassler, C., Boretius, T., & Stieglitz, T. (2011). Polymers for neural implants. *J. Polym. Sci., Part B.: Polym. Phys.*, 49(1), 18-33.
- Hawley, M. D., Tatawawadi, S. V., Piekarski, S., & Adams, R. N. (1967). Electrochemical studies of the oxidation pathways of catecholamines. *J Am Chem Soc*, 89(2), 447-450.
- Heien, M. L., Johnson, M. A., & Wightman, R. M. (2004). Resolving neurotransmitters detected by fast-scan cyclic voltammetry. *Anal Chem*, 76(19), 5697-5704.
- Heien, M. L., et al. (2005). Real-time measurement of dopamine fluctuations after cocaine in the brain of behaving rats. *Proc Natl Acad Sci U S A*, 102(29), 10023-10028.
- Heien, M. L., Phillips, P. E., Stuber, G. D., Seipel, A. T., & Wightman, R. M. (2003). Overoxidation of carbon-fiber microelectrodes enhances dopamine adsorption and increases sensitivity. *Analyst*, 128(12), 1413-1419.
- Hermans, A., Keithley, R. B., Kita, J. M., Sombers, L. A., & Wightman, R. M. (2008). Dopamine detection with fast-scan cyclic voltammetry used with analog background subtraction. *Anal Chem*, 80(11), 4040-4048.
- Herr, N. R., Daniel, K. B., Belle, A. M., Carelli, R. M., & Wightman, R. M. (2010). Probing presynaptic regulation of extracellular dopamine with iontophoresis. *ACS Chem Neurosci*, 1(9), 627-638.
- Howe, M. W., Tierney, P. L., Sandberg, S. G., Phillips, P. E., & Graybiel, A. M. (2013). Prolonged dopamine signalling in striatum signals proximity and value of distant rewards. *Nature*, 500(7464), 575-579.

- Huff, R., Adams, R. N., & Rutledge, C. O. (1979). Amphetamine dose-dependent changes of in vivo electrochemical signals in rat caudate. *Brain Res*, 173(2), 369-372.
- Jackson, J. E., & Mudholkar, G. S. (1979). Control procedures for residuals associated with principal component analysis. *Technometrics*, 21(3), 341-349.
- Johnson, J. A., Rodeberg, N. T., & Wightman, R. M. (2016). Failure of Standard Training Sets in the Analysis of Fast-Scan Cyclic Voltammetry Data. *ACS Chem Neurosci*, 7(3), 349-359.
- Jones, S. R., Mickelson, G. E., Collins, L. B., Kawagoe, K. T., & Wightman, R. M. (1994). Interference by pH and Ca<sup>2+</sup> ions during measurements of catecholamine release in slices of rat amygdala with fast-scan cyclic voltammetry. *J Neurosci Methods*, 52(1), 1-10.
- Kawagoe, K. T., Garris, P. A., & Wightman, R. M. (1993). Ph-Dependent Processes at Nafion(R)-Coated Carbon-Fiber Microelectrodes. *Journal of Electroanalytical Chemistry*, 359(1-2), 193-207.
- Keithley, R. B., Carelli, R. M., & Wightman, R. M. (2010). Rank estimation and the multivariate analysis of in vivo fast-scan cyclic voltammetric data. *Anal Chem*, 82(13), 5541-5551.
- Keithley, R. B., Heien, M. L., & Wightman, R. M. (2009a). Erratum to "Multivariate concentration determination using principal component regression with residual analysis". *Trends Analyt Chem*, 29(1), 110-110.
- Keithley, R. B., Heien, M. L., & Wightman, R. M. (2009b). Multivariate concentration determination using principal component regression with residual analysis. *Trends Analyt Chem*, 28(9), 1127-1136.
- Keithley, R. B., et al. (2011). Higher sensitivity dopamine measurements with faster-scan cyclic voltammetry. *Anal Chem*, 83(9), 3563-3571.
- Keithley, R. B., & Wightman, R. M. (2011). Assessing principal component regression prediction of neurochemicals detected with fast-scan cyclic voltammetry. *ACS Chem Neurosci*, 2(9), 514-525.
- Kirkpatrick, D. C., McKinney, C. J., Manis, P. B., & Wightman, R. M. (2016). Expanding neurochemical investigations with multi-modal recording: simultaneous fast-scan cyclic voltammetry, iontophoresis, and patch clamp measurements. *Analyst*, 141(16), 4902-4911.
- Kishida, K. T., et al. (2016). Subsecond dopamine fluctuations in human striatum encode superposed error signals about actual and counterfactual reward. *Proc Natl Acad Sci U S A*, 113(1), 200-205.
- Kissinger, P. T., Hart, J. B., & Adams, R. N. (1973). Voltammetry in brain tissue--a new neurophysiological measurement. *Brain Res*, 55(1), 209-213.
- Kobayashi, S., & Schultz, W. (2008). Influence of reward delays on responses of dopamine neurons. *J Neurosci*, 28(31), 7837-7846.

- Kozai, T. D., Jaquins-Gerstl, A. S., Vazquez, A. L., Michael, A. C., & Cui, X. T. (2015). Brain tissue responses to neural implants impact signal sensitivity and intervention strategies. *ACS Chem Neurosci*, 6(1), 48-67.
- Kozai, T. D., et al. (2012). Ultrasmall implantable composite microelectrodes with bioactive surfaces for chronic neural interfaces. *Nat Mater*, 11(12), 1065-1073.
- Kramer, R. (1998). *Chemometric techniques for quantitative analysis*. New York: Marcel Dekker, Inc.
- Kruk, Z. L., Cheeta, S., Milla, J., Muscat, R., Williams, J. E., & Willner, P. (1998). Real time measurement of stimulated dopamine release in the conscious rat using fast cyclic voltammetry: dopamine release is not observed during intracranial self stimulation. *J Neurosci Methods*, 79(1), 9-19.
- Kuhr, W. G., Ewing, A. G., Caudill, W. L., & Wightman, R. M. (1984). Monitoring the stimulated release of dopamine with in vivo voltammetry. I: Characterization of the response observed in the caudate nucleus of the rat. *J Neurochem*, 43(2), 560-569.
- Kuhr, W. G., Wightman, R. M., & Rebec, G. V. (1987). Dopaminergic neurons: simultaneous measurements of dopamine release and single-unit activity during stimulation of the medial forebrain bundle. *Brain Res*, 418(1), 122-128.
- Lak, A., Stauffer, W. R., & Schultz, W. (2014). Dopamine prediction error responses integrate subjective value from different reward dimensions. *Proc Natl Acad Sci U S A*, 111(6), 2343-2348.
- Lavine, B. K., & Workman, J., Jr. (2013). Chemometrics. *Anal Chem*, 85(2), 705-714.
- Malinowski, E. R. (1977). Determination of Number of Factors and Experimental Error in a Data Matrix. *Anal Chem*, 49(4), 612-617.
- Malinowski, E. R. (2004). Adaptation of the Vogt-Mizaikoff F-test to determine the number of principal factors responsible for a data matrix and comparison with other popular methods. *J. Chemom.*, 18(9), 387-392.
- Marsden, C. A., et al. (1988). In vivo voltammetry--present electrodes and methods. *Neuroscience*, 25(2), 389-400.
- McCreery, R. L. (1995). Carbon Electrode Surface Chemistry. In A. A. Boulton, G. B. Baker & R. N. Adams (Eds.), *Voltammetric Methods in Brain Systems* (pp. 1-26). Totowa, NJ: Humana Press.
- Michael, D. J., Joseph, J. D., Kilpatrick, M. R., Travis, E. R., & Wightman, R. M. (1999). Improving data acquisition for fast-scan cyclic voltammetry. *Anal Chem*, 71(18), 3941-3947.
- Moussy, F., & Harrison, D. J. (1994). Prevention of the rapid degradation of subcutaneously implanted Ag/AgCl reference electrodes using polymer coatings. *Anal Chem*, 66(5), 674-679.

- Nasrallah, N. A., Clark, J. J., Collins, A. L., Akers, C. A., Phillips, P. E., & Bernstein, I. L. (2011). Risk preference following adolescent alcohol use is associated with corrupted encoding of costs but not rewards by mesolimbic dopamine. *Proc Natl Acad Sci U S A*, *108*(13), 5466-5471.
- Nieoullon, A., Cheramy, A., & Glowinski, J. (1977). Nigral and striatal dopamine release under sensory stimuli. *Nature*, *269*(5626), 340-342.
- O'Neill, R. D., Fillenz, M., Albery, W. J., & Goddard, N. J. (1983). The monitoring of ascorbate and monoamine transmitter metabolites in the striatum of unanaesthetised rats using microprocessor-based voltammetry. *Neuroscience*, *9*(1), 87-93.
- Olivieri, A. C. (2014). Analytical figures of merit: from univariate to multiway calibration. *Chem Rev*, *114*(10), 5358-5378.
- Owesson-White, C., et al. (2016). Cue-Evoked Dopamine Release Rapidly Modulates D2 Neurons in the Nucleus Accumbens During Motivated Behavior. *J Neurosci*, *36*(22), 6011-6021.
- Owesson-White, C. A., et al. (2009). Neural encoding of cocaine-seeking behavior is coincident with phasic dopamine release in the accumbens core and shell. *Eur J Neurosci*, *30*(6), 1117-1127.
- Owesson-White, C. A., Cheer, J. F., Beyene, M., Carelli, R. M., & Wightman, R. M. (2008). Dynamic changes in accumbens dopamine correlate with learning during intracranial self-stimulation. *Proc Natl Acad Sci U S A*, *105*(33), 11957-11962.
- Owesson-White, C. A., et al. (2012). Sources contributing to the average extracellular concentration of dopamine in the nucleus accumbens. *J Neurochem*, *121*(2), 252-262.
- Park, J., et al. (2013). Opposing catecholamine changes in the bed nucleus of the stria terminalis during intracranial self-stimulation and its extinction. *Biol Psychiatry*, *74*(1), 69-76.
- Pasquereau, B., & Turner, R. S. (2013). Limited encoding of effort by dopamine neurons in a cost-benefit trade-off task. *J Neurosci*, *33*(19), 8288-8300.
- Peters, J. L., Miner, L. H., Michael, A. C., & Sesack, S. R. (2004). Ultrastructure at carbon fiber microelectrode implantation sites after acute voltammetric measurements in the striatum of anesthetized rats. *J Neurosci Methods*, *137*(1), 9-23.
- Pettit, H. O., & Justice, J. B., Jr. (1989). Dopamine in the nucleus accumbens during cocaine self-administration as studied by in vivo microdialysis. *Pharmacol Biochem Behav*, *34*(4), 899-904.
- Phillips, P. E., Robinson, D. L., Stuber, G. D., Carelli, R. M., & Wightman, R. M. (2003a). Real-time measurements of phasic changes in extracellular dopamine concentration in freely moving rats by fast-scan cyclic voltammetry. *Methods Mol Med*, *79*, 443-464.
- Phillips, P. E., Stuber, G. D., Heien, M. L., Wightman, R. M., & Carelli, R. M. (2003b). Subsecond dopamine release promotes cocaine seeking. *Nature*, *422*(6932), 614-618.

- Phillips, P. E. M., & Wightman, R. M. (2003). Critical guidelines for validation of the selectivity of in-vivo chemical microsensors. *Trac-Trends in Analytical Chemistry*, 22(9), 509-514.
- Ponchon, J. L., Cespuoglio, R., Gonon, F., Jouvret, M., & Pujol, J. F. (1979). Normal pulse polarography with carbon fiber electrodes for in vitro and in vivo determination of catecholamines. *Anal Chem*, 51(9), 1483-1486.
- Rebec, G. V., Christensen, J. R., Guerra, C., & Bardo, M. T. (1997). Regional and temporal differences in real-time dopamine efflux in the nucleus accumbens during free-choice novelty. *Brain Res*, 776(1-2), 61-67.
- Rebec, G. V., Langley, P. E., Pierce, R. C., Wang, Z. R., & Heidenreich, B. A. (1993). A Simple Micromanipulator for Multiple Uses in Freely Moving Rats - Electrophysiology, Voltammetry, and Simultaneous Intracerebral Infusions. *Journal of Neuroscience Methods*, 47(1-2), 53-59.
- Refshauge, C., Kissinger, P. T., Dreiling, R., Blank, L., Freeman, R., & Adams, R. N. (1974). New high performance liquid chromatographic analysis of brain catecholamines. *Life Sci*, 14(2), 311-322.
- Rice, M. E., & Nicholson, C. (1989). Measurement of nanomolar dopamine diffusion using low-noise perfluorinated ionomer coated carbon fiber microelectrodes and high-speed cyclic voltammetry. *Anal Chem*, 61(17), 1805-1810.
- Roberts, J. G., Moody, B. P., McCarty, G. S., & Sombers, L. A. (2010). Specific oxygen-containing functional groups on the carbon surface underlie an enhanced sensitivity to dopamine at electrochemically pretreated carbon fiber microelectrodes. *Langmuir : the ACS journal of surfaces and colloids*, 26(11), 9116-9122.
- Roberts, J. G., Toups, J. V., Eyuaem, E., McCarty, G. S., & Sombers, L. A. (2013). In situ electrode calibration strategy for voltammetric measurements in vivo. *Anal Chem*, 85(23), 11568-11575.
- Robinson, D. L., Heien, M. L., & Wightman, R. M. (2002). Frequency of dopamine concentration transients increases in dorsal and ventral striatum of male rats during introduction of conspecifics. *J Neurosci*, 22(23), 10477-10486.
- Robinson, D. L., Phillips, P. E., Budygin, E. A., Trafton, B. J., Garris, P. A., & Wightman, R. M. (2001). Sub-second changes in accumbal dopamine during sexual behavior in male rats. *Neuroreport*, 12(11), 2549-2552.
- Robinson, D. L., Venton, B. J., Heien, M. L., & Wightman, R. M. (2003). Detecting subsecond dopamine release with fast-scan cyclic voltammetry in vivo. *Clin Chem*, 49(10), 1763-1773.
- Rodeberg, N. T., Johnson, J. A., Bucher, E. S., & Wightman, R. M. (2016). Dopamine Dynamics during Continuous Intracranial Self-Stimulation: Effect of Waveform on Fast-Scan Cyclic Voltammetry Data. *ACS Chem Neurosci*, 7(11), 1508-1518.

- Rodeberg, N. T., Johnson, J. A., Cameron, C. M., Saddoris, M. P., Carelli, R. M., & Wightman, R. M. (2015). Construction of Training Sets for Valid Calibration of in Vivo Cyclic Voltammetric Data by Principal Component Analysis. *Anal Chem*, *87*(22), 11484-11491.
- Roitman, M. F., Stuber, G. D., Phillips, P. E., Wightman, R. M., & Carelli, R. M. (2004). Dopamine operates as a subsecond modulator of food seeking. *J Neurosci*, *24*(6), 1265-1271.
- Runnels, P. L., Joseph, J. D., Logman, M. J., & Wightman, R. M. (1999). Effect of pH and surface functionalities on the cyclic voltammetric responses of carbon-fiber microelectrodes. *Anal Chem*, *71*(14), 2782-2789.
- Saddoris, M. P., Cacciapaglia, F., Wightman, R. M., & Carelli, R. M. (2015). Differential Dopamine Release Dynamics in the Nucleus Accumbens Core and Shell Reveal Complementary Signals for Error Prediction and Incentive Motivation. *J Neurosci*, *35*(33), 11572-11582.
- Saddoris, M. P., Sugam, J. A., & Carelli, R. M. (2017). Prior Cocaine Experience Impairs Normal Phasic Dopamine Signals of Reward Value in Accumbens Shell. *Neuropsychopharmacology*, *42*(3), 766-773.
- Saddoris, M. P., Wang, X., Sugam, J. A., & Carelli, R. M. (2016). Cocaine Self-Administration Experience Induces Pathological Phasic Accumbens Dopamine Signals and Abnormal Incentive Behaviors in Drug-Abstinent Rats. *J Neurosci*, *36*(1), 235-250.
- Saylor, R. A., & Lunte, S. M. (2015). A review of microdialysis coupled to microchip electrophoresis for monitoring biological events. *J Chromatogr A*, *1382*, 48-64.
- Schenk, J. O., Miller, E., Rice, M. E., & Adams, R. N. (1983). Chronoamperometry in brain slices: quantitative evaluations of in vivo electrochemistry. *Brain Res*, *277*(1), 1-8.
- Schmidt, A. C., Wang, X., Zhu, Y., & Sombers, L. A. (2013). Carbon nanotube yarn electrodes for enhanced detection of neurotransmitter dynamics in live brain tissue. *ACS Nano*, *7*(9), 7864-7873.
- Schultz, W., Dayan, P., & Montague, P. R. (1997). A neural substrate of prediction and reward. *Science (New York, N Y)*, *275*(5306), 1593-1599.
- Sharp, T., Zetterstrom, T., & Ungerstedt, U. (1986). An in vivo study of dopamine release and metabolism in rat brain regions using intracerebral dialysis. *J Neurochem*, *47*(1), 113-122.
- Singh, Y. S., Sawarynski, L. E., Dabiri, P. D., Choi, W. R., & Andrews, A. M. (2011). Head-to-head comparisons of carbon fiber microelectrode coatings for sensitive and selective neurotransmitter detection by voltammetry. *Anal Chem*, *83*(17), 6658-6666.
- Sombers, L. A., Beyene, M., Carelli, R. M., & Wightman, R. M. (2009). Synaptic overflow of dopamine in the nucleus accumbens arises from neuronal activity in the ventral tegmental area. *J Neurosci*, *29*(6), 1735-1742.

- Soto, R. J., Hall, J. R., Brown, M. D., Taylor, J. B., & Schoenfisch, M. H. (2017). In Vivo Chemical Sensors: Role of Biocompatibility on Performance and Utility. *Anal Chem*, *89*(1), 276-299.
- Spanos, M., Gras-Najjar, J., Letchworth, J. M., Sanford, A. L., Toups, J. V., & Sombers, L. A. (2013). Quantitation of hydrogen peroxide fluctuations and their modulation of dopamine dynamics in the rat dorsal striatum using fast-scan cyclic voltammetry. *ACS Chem Neurosci*, *4*(5), 782-789.
- Stamford, J. A., Kruk, Z. L., Millar, J., & Wightman, R. M. (1984). Striatal dopamine uptake in the rat: in vivo analysis by fast cyclic voltammetry. *Neurosci Lett*, *51*(1), 133-138.
- Stamford, J. A., Palij, P., Davidson, C., Jorm, C. M., & Millar, J. (1993). Simultaneous Real-Time Electrochemical and Electrophysiological Recording in Brain-Slices with a Single Carbon-Fiber Microelectrode. *Journal of Neuroscience Methods*, *50*(3), 279-290.
- Strand, A. M., & Venton, B. J. (2008). Flame etching enhances the sensitivity of carbon-fiber microelectrodes. *Anal Chem*, *80*(10), 3708-3715.
- Stuber, G. D., Roitman, M. F., Phillips, P. E., Carelli, R. M., & Wightman, R. M. (2005). Rapid dopamine signaling in the nucleus accumbens during contingent and noncontingent cocaine administration. *Neuropsychopharmacology*, *30*(5), 853-863.
- Suaud-Chagny, M. F., Steinberg, R., Mermut, C., Biziere, K., & Gonon, F. (1986). In vivo voltammetric monitoring of catecholamine metabolism in the A1 and A2 regions of the rat medulla oblongata. *J Neurochem*, *47*(4), 1141-1147.
- Sugam, J. A., Day, J. J., Wightman, R. M., & Carelli, R. M. (2012). Phasic nucleus accumbens dopamine encodes risk-based decision-making behavior. *Biol Psychiatry*, *71*(3), 199-205.
- Swamy, B. E., & Venton, B. J. (2007a). Carbon nanotube-modified microelectrodes for simultaneous detection of dopamine and serotonin in vivo. *Analyst*, *132*(9), 876-884.
- Swamy, B. E., & Venton, B. J. (2007b). Subsecond detection of physiological adenosine concentrations using fast-scan cyclic voltammetry. *Anal Chem*, *79*(2), 744-750.
- Takmakov, P., McKinney, C. J., Carelli, R. M., & Wightman, R. M. (2011). Instrumentation for fast-scan cyclic voltammetry combined with electrophysiology for behavioral experiments in freely moving animals. *Rev Sci Instrum*, *82*(7), 074302.
- Takmakov, P., Zachek, M. K., Keithley, R. B., Bucher, E. S., McCarty, G. S., & Wightman, R. M. (2010). Characterization of local pH changes in brain using fast-scan cyclic voltammetry with carbon microelectrodes. *Anal Chem*, *82*(23), 9892-9900.
- Troyer, K. P., Heien, M. L., Venton, B. J., & Wightman, R. M. (2002). Neurochemistry and electroanalytical probes. *Curr Opin Chem Biol*, *6*(5), 696-703.
- Ungerstedt, U., & Pycock, C. (1974). Functional correlates of dopamine neurotransmission. *Bull Schweiz Akad Med Wiss*, *30*(1-3), 44-55.

- Vander Weele, C. M., et al. (2014). Rapid dopamine transmission within the nucleus accumbens: dramatic difference between morphine and oxycodone delivery. *Eur J Neurosci*, 40(7), 3041-3054.
- Venton, B. J., Michael, D. J., & Wightman, R. M. (2003a). Correlation of local changes in extracellular oxygen and pH that accompany dopaminergic terminal activity in the rat caudate-putamen. *J Neurochem*, 84(2), 373-381.
- Venton, B. J., Zhang, H., Garris, P. A., Phillips, P. E., Sulzer, D., & Wightman, R. M. (2003b). Real-time decoding of dopamine concentration changes in the caudate-putamen during tonic and phasic firing. *J Neurochem*, 87(5), 1284-1295.
- Vreeland, R. F., et al. (2015). Biocompatible PEDOT:Nafion composite electrode coatings for selective detection of neurotransmitters in vivo. *Anal Chem*, 87(5), 2600-2607.
- Waelti, P., Dickinson, A., & Schultz, W. (2001). Dopamine responses comply with basic assumptions of formal learning theory. *Nature*, 412(6842), 43-48.
- Wanat, M. J., Bonci, A., & Phillips, P. E. (2013). CRF acts in the midbrain to attenuate accumbens dopamine release to rewards but not their predictors. *Nat Neurosci*, 16(4), 383-385.
- Wanat, M. J., Kuhnen, C. M., & Phillips, P. E. (2010). Delays conferred by escalating costs modulate dopamine release to rewards but not their predictors. *J Neurosci*, 30(36), 12020-12027.
- Wang, M., Roman, G. T., Schultz, K., Jennings, C., & Kennedy, R. T. (2008). Improved temporal resolution for in vivo microdialysis by using segmented flow. *Anal Chem*, 80(14), 5607-5615.
- Wang, M., Slaney, T., Mabrouk, O., & Kennedy, R. T. (2010). Collection of nanoliter microdialysate fractions in plugs for off-line in vivo chemical monitoring with up to 2 s temporal resolution. *J Neurosci Methods*, 190(1), 39-48.
- Wightman, R. M. (1981). Microvoltammetric Electrodes. *Anal Chem*, 53(9), 1125-&.
- Wightman, R. M., et al. (1988a). Real-time characterization of dopamine overflow and uptake in the rat striatum. *Neuroscience*, 25(2), 513-523.
- Wightman, R. M., et al. (2007). Dopamine release is heterogeneous within microenvironments of the rat nucleus accumbens. *Eur J Neurosci*, 26(7), 2046-2054.
- Wightman, R. M., May, L. J., & Michael, A. C. (1988b). Detection of dopamine dynamics in the brain. *Anal Chem*, 60(13), 769A-779A.
- Willuhn, I., Burgeno, L. M., Everitt, B. J., & Phillips, P. E. (2012). Hierarchical recruitment of phasic dopamine signaling in the striatum during the progression of cocaine use. *Proc Natl Acad Sci U S A*, 109(50), 20703-20708.

- Yamamoto, B. K., & Spanos, L. J. (1988). The acute effects of methylenedioxymethamphetamine on dopamine release in the awake-behaving rat. *Eur J Pharmacol*, 148(2), 195-203.
- Yorgason, J. T., Espana, R. A., & Jones, S. R. (2011). Demon voltammetry and analysis software: analysis of cocaine-induced alterations in dopamine signaling using multiple kinetic measures. *J Neurosci Methods*, 202(2), 158-164.
- Zetterstrom, T., et al. (1986). In vivo measurement of spontaneous release and metabolism of dopamine from intrastriatal nigral grafts using intracerebral dialysis. *Brain Res*, 362(2), 344-349.
- Zetterstrom, T., Sharp, T., Marsden, C. A., & Ungerstedt, U. (1983). In vivo measurement of dopamine and its metabolites by intracerebral dialysis: changes after d-amphetamine. *J Neurochem*, 41(6), 1769-1773.

## CHAPTER 6: CHARACTERIZATION OF FUSED-SILICA ELECTRODES FOR LONGITUDINAL MEASUREMENTS OF STRIATAL DOPAMINE RELEASE

### INTRODUCTION

The neurotransmitter dopamine plays vital roles in reward-seeking behavior (Ikemoto & Panksepp, 1999; Schultz et al., 1997) and the effects of drugs of abuse (Covey et al., 2014; Sulzer, 2011), and its dysfunction is associated with several different diseases and disorders, including Parkinson disease (Lohr et al., 2014; Lotharius & Brundin, 2002) and schizophrenia (Stone et al., 2007; Urs et al., 2017). Study of the role of dopamine in complex behavior is bolstered by the ability to monitor its release on a time scale relevant to behavioral responses. This aim can be accomplished with fast-scan cyclic voltammetry (FSCV), which utilizes the electroactive nature of dopamine to study its release in real time. FSCV measurements with carbon-fiber microelectrodes (CFMs) have been adapted to monitor rapid dopamine release in freely-moving animals (Phillips et al., 2003a; Rebec et al., 1997). These advances have allowed many unique insights into the role of dopamine release in a variety of behaviors (Day et al., 2007; Owesson-White et al., 2016; Phillips et al., 2003b; Roitman et al., 2004).

However, the growth of FSCV as a widespread technique has been hindered by a few limitations. The borosilicate glass (BSG) electrodes conventionally used for FSCV measurements in awake animals are fragile, and brain tissue damage from repeated insertion of electrodes can prevent multiple measurements in the same animal (Phillips, et al., 2003a; Rodeberg et al., 2017). As a result, FSCV measurements with BSG electrodes are typically limited to a small number of measurements in any given animal. Consequently, it is common for several rats to be needed to assay different behavioral time points when studying dopamine release during progression of more complex behaviors. Alternatively, FSCV studies can make

use of more simple behaviors that can be learned within single recording sessions (Owesson-White et al., 2008). A new method for FSCV measurements was introduced with the development of fused silica (FS)-based electrodes, which can be cemented into individual recording locations for longitudinal measurements of dopamine release at the same recording site (Clark et al., 2010). This reduces the number of animals needed to track long-term changes in dopamine release, and the flexibility of these electrodes reduces concerns with electrode fragility. Since their inception, the use of chronically implanted CFMs has grown significantly (Ferguson et al., 2011; Flagel et al., 2011; Howe et al., 2013; Rodeberg, et al., 2017; Willuhn et al., 2014).

The ability of implanted CFMs to track long-term changes in dopamine release depends on both the stability of the recording environment and the sensor itself. The former has been demonstrated for through immunohistochemical experiments for acute (Peters et al., 2004) and chronic (Clark, et al., 2010) implantation of CFMs; these studies found that the small size of the implanted carbon fiber (~5-7  $\mu\text{m}$  in diameter) allows it to evade the progressive immune response and corresponding insulation that impedes larger implanted devices (Polikov et al., 2005). In particular, chronically-implanted CFMs have proven to be capable of monitoring dopamine over extended durations (i.e. up to 4 months), and their long-term presence in brain tissue does not appear to, in and of itself, alter sensitivity as assessed by post-implantation calibration (Clark, et al., 2010). However, it is unknown whether repeated use of CFMs significantly alters their sensitivity over time, as application of voltammetric waveforms with extended anodic limits ( $>+1.0$  V) have been shown to condition the electrode surface (Heien et al., 2003; Takmakov et al., 2010). Thus, further investigation into the stability of these electrodes over time is warranted.

A significant area of debate with respect to the use of chronic CFMs is their calibration (Johnson et al., 2016; Rodeberg et al., 2015; Rodeberg, et al., 2017). Data collected with FSCV consists of complex overlapping currents when multiple electroactive species are present during

measurements. Principal component regression (PCR), a multivariate analysis technique, has been introduced to separate and quantitate multiple analytes of interest during FSCV measurements (Heien et al., 2004; Heien et al., 2005). This approach requires several isolated standards for each analyte to build reliable PCR models. For measurements of striatal dopamine release, this is typically achieved with electrical stimulation of afferent dopamine neurons to evoke release at the recording site, in addition to alkaline pH changes that lag temporally behind electrically-evoked dopamine transients (Heien, et al., 2005; Venton et al., 2003). However, most studies that have utilized chronic CFMs have been performed without stimulating electrodes, which has precluded building PCR models at the same electrode as FSCV measurements. Instead, a 'standard training set' built from dopamine and pH standards acquired at one (or several) separate CFMs has been used to calibrate all acquired data. We have previously demonstrated that this approach can lead to difficulties with reliable quantitation and PCR quality control (i.e. residual analysis) (Johnson, et al., 2016; Rodeberg, et al., 2015), though this approach may capture qualitative information (Rodeberg, et al., 2017). The limitations of this approach arise from differences in dopamine and pH cyclic voltammograms (CVs) between CFMs, which can impede reliable extraction of analyte-specific current from complex FSCV data. It has been suggested that the more robust construction method of FS electrodes, compared to BSG electrodes, could result in more desirable electrochemical characteristics, including more consistent dopamine CVs across electrodes (Rodeberg, et al., 2017). If this is the case, the use of 'standard training sets' at FS electrodes may encounter less problems than those seen in previous studies that used BSG electrodes (Johnson, et al., 2016; Rodeberg, et al., 2015).

This study first compared the electrochemical performance of BSG and FS electrodes *in vitro*, and demonstrated that FS electrodes have lower noise and stray impedance than their BSG counterparts. The use of epoxy resin to treat BSG electrodes abolished these differences. However, no significant differences in the variance of dopamine CVs were seen between

electrode designs. This suggests that the principal source of variability in dopamine CVs across experiments arises from the carbon fibers themselves. Moreover, we found that repeated cycling of CFMs *in vitro* has dynamic effects on their sensitivity, which has implications for their long-term use. Next, we investigated the performance of chronic CFMs *in vivo*. BSG and FS electrodes performed similarly during acute *in vivo* recordings, though FS electrodes show diminished temporal resolution following implantation. Last, stimulating electrodes were found to be insufficient to reliably evoke dopamine release following weeks of implantation, which prevented their use to track sensitivity at chronically-implanted CFMs. Instead, we used drug cocktail to evoke phasic dopamine release under anesthesia during and following electrode implantation. This study revealed that, while chronic CFMs are capable of stable monitoring of dopamine release over time, results can be variable. Altogether, these results emphasize the need for positive controls in experiments using chronically-implanted microelectrodes.

## **EXPERIMENTAL**

### **Animals**

Male Sprague Dawley rats (250 – 400 g, Charles River, Wilmington, MA) were housed (paired before surgery, singly-housed post-surgery) on a 12:12 hr light-dark cycle in a temperature and humidity controlled environment. Rat chow and water was available *ad libitum*. All animal procedures were approved by the Institutional Animal Care and Use Committee (IACUC) at UNC Chapel Hill.

### **Electrode Construction**

#### *Borosilicate glass electrodes*

Carbon fiber (T-650, Amoco, Greenville, SC) were aspirated into borosilicate glass (BSG) capillaries (600  $\mu\text{m}$  outer diameter, 400  $\mu\text{m}$  inner diameter) under vacuum. Capillaries

were pulled using a micropipette puller (Narishige, East Meadow, NY) to produce two tapered capillaries of approximately equal length. The exposed carbon fiber was trimmed to 150 to 200  $\mu\text{m}$  in length. For epoxy-BSG electrodes, the electrodes were then dipped in heated epoxy resin (Epon 828, Miller Stephenson Chemical Co., Inc., Danbury, CT) mixed with 15% hardener m/m (m-phenylenediamine, Sigma, St. Louis, MO) for 30 s, followed by a brief rinse ( $\sim 5$  s) in warm acetone to remove residual epoxy from the carbon-fiber surface. Following air drying overnight, epoxy-BSG electrodes were cured in an oven ( $100^\circ\text{C}$  for 4 hr,  $150^\circ\text{C}$  overnight). For both BSG and epoxy-BSG electrodes, electrical connection was created by insertion of silver wires (Squires Electronics Inc., Cornelius, OR) coated in conductive silver paint into the glass capillaries to make electrical contact with the insulated carbon fiber. BSG electrodes with obvious cracks under an optical microscope were discarded before use.

#### *Fused silica electrodes*

First, polyimide-coated fused silica (FS) tubing (90  $\mu\text{m}$  outer diameter, 20  $\mu\text{m}$  inner diameter) was cut into approximately 10 mm segments with a scalpel blade. Carbon fibers were threaded through capillaries submerged in ethanol with use of cotton applicators under a stereoscope (Wild M3Z, Leica, Buffalo Grove, IL) until exposed carbon fiber was visible on both ends of the capillary. Following overnight drying, each FS capillary was suspended above wax paper with arched tape. A small bead of epoxy (TQS-2, Super Glue Corp., Rancho Cucamonga, CA) was applied onto one end of the carbon fiber, and this bubble was pulled backwards by hand via the exposed fiber at the opposite end of the FS capillary. This process was considered successful if epoxy had wicked several mm into the FS capillary, and if the exposed epoxy formed a hemispherical seal around the remaining exposed fiber. Electrodes with obvious defects in the seal (i.e. flat, incomplete) or residual epoxy on the exposed fiber visible under an optical microscope, were discarded.

After the epoxy was allowed to harden overnight, exposed carbon fiber at the epoxy-sealed end of the FS capillary was trimmed to 150-200  $\mu\text{m}$  in length. The open end of each FS capillary (and its corresponding exposed fiber) was placed in a patch of silver epoxy (8331-14-G, MG Chemicals, Surrey, B.C., Canada) dabbed on Parafilm. The silver connector pin (Mill Max Mfg. Corp., Oyster Bay, NY) was placed on top of the silver epoxy/ FS capillary junction, and the complex was allowed to dry overnight. Last, the epoxy-capillary-pin junction was secured and insulated with epoxy (same as above). Following a final night of drying, the FS electrodes were ready for use.

## **FSCV**

FSCV measurements were conducted with locally designed equipment (UEI, UNC Electronics Facility, Chapel Hill, NC) and software (flow cell analysis with Tarheel CV, *in vivo* recordings with HDCV, both built in LabVIEW, National Instruments, Austin, TX). All measurements were made with a triangular waveform sweeping from a holding potential of -0.4 V to an anodic limit of +1.3 V (vs. Ag/AgCl) and back at 400 V/s. Ag/AgCl electrodes were constructed by applying +5 V to sanded silver wire for 30 s in 0.1 N HCl. For measurements in freely-moving animals with chronically-implanted Ag/AgCl reference electrodes, an offset of 200 mV was applied to the waveform to account for reference potential drift that occurs over long-term implantation (Hashemi et al., 2011). All data was filtered with a low-pass Bessel filter (cutoff frequency = 2KHz).

## **Flow-Cell Analysis**

All flow cell measurements were made in TRIS buffer (15 mM Trizma HCl, 126 mM NaCl, 2.5 mM KCl, 25 mM  $\text{NaHCO}_3$ , 2.4 mM  $\text{CaCl}_2$ , 1.2 mM  $\text{NaH}_2\text{PO}_4$ , 1.2 mM  $\text{MgCl}_2$ , 2.0 mM

Na<sub>2</sub>SO<sub>4</sub>), with an adjusted pH of 7.4. Dopamine standards were prepared in TRIS buffer, and bubbled under N<sub>2</sub> to prevent oxidative degradation during measurements. All dopamine injections were 5 s in duration at a flow rate of 2 mL/min. The Ag/AgCl reference electrode was rechlorinated for each day of use. The current at the peak oxidative potential for dopamine (E<sub>p,a</sub>) was used for calibration. For measurement of background currents, no dopamine injections were made, and the RMS noise was defined as the 3 \* standard deviation of current at the approximate peak potential for dopamine (~620 mV) for a 30 s file following cycling (30 min 60 Hz, 10 min 60 Hz) of the electrode. For the series of dopamine calibration curves, noise was assessed in the 5 s window preceding injection of dopamine standards. The temporal response of the electrodes over time was assessed with the rise time (10-90% max signal) in response to the dopamine boluses.

## **Surgery**

### *Acute recordings*

Rats were anesthetized with urethane (1.5 mg/kg) and placed in a stereotaxic frame. Both BSG and FS electrodes were lowered into the dorsal striatum (AP +1.2 mm, ML +2.0 mm, DV -4.0, with respect to skull landmark bregma). A Ag/AgCl reference electrode was lowered in the contralateral hemisphere and secured in place by wrapping it around a skull-imbedded screw. A bipolar stimulating electrode was lowered into the substantia nigra / ventral tegmental area (SN/VTA) (AP -5.2 mm, ML +1.0 mm, DV -7.0 mm). Electrical stimulation (300 µA, 60 Hz, 60 biphasic pulses, 2 ms pulse duration) was applied through optically isolated equipment (NL 800 A, Neurolog, Digitimer, Hertfordshire, UK) in 0.2 mm intervals until dopamine release was observed at the working electrode. The stimulating electrode was then lowered in 0.1 mm increments until stimulated release maximized in the dorsal striatum. Next, the working electrodes were optimized for recording location (lowered in 0.1 mm increments) until no further increases in dopamine release were seen.

Following signal optimization, short electrical stimulation was applied (24 pulses) to determine temporal response ( $t_{1/2}$ , rise time), later determined with ClampFit software (Molecular Devices LLC, Sunnyvale, CA). Next, prolonged electrical stimulation (120 p) was applied at 30, 40, 50, and 60 Hz ( $n = 5$  stimulations at each frequency). The peak evoked current for dopamine was compared between frequencies.

### *Chronic Implantation of FS Electrodes*

For long-term implantation FS electrodes, animals were prepared surgically in a similar manner to above, with a few exceptions. The same signal optimization procedure was used under isoflurane anesthesia (4% induction, 1.5-2.5% maintenance). However, once electrically-evoked dopamine release was optimized, all three electrodes (FS, Ag/AgCl reference electrode, stimulating electrode) were affixed with dental cement. For electrical stimulation experiments, short electrical stimulation (300  $\mu$ A, 60 Hz, 24 or 60 biphasic pulses, 2 ms pulse duration) was applied after the cement hardened for later comparisons to post-recovery release. Animals were allowed to recover in their cage (singly-housed) for 1 week (first electrical stimulation experiment) or 4 weeks (for subsequent experiment).

For the pharmacologically-induced dopamine transients experiment, animals were administered a drug cocktail of cocaine (20 mg/kg, i.p.) and haloperidol (0.5 mg/kg, i.p.) dissolved in 0.9% saline. Drugs were administered in consecutive injections after the cement had hardened. Following 1 hr of measurements of drug-evoked dopamine transients, electrical stimulation was applied to collect standards for construction of training sets for PCR analysis, as described previously (Rodeberg, et al., 2015).

### ***In vivo recordings***

Following recovery, implanted CFMs were extensively cycled (2 hr at 60 Hz, 30 min at 10 Hz) before first use, and cycled (1 hr at 60 Hz, 30 min at 10 Hz) before each subsequent

measurement to minimize the effects of electrode drift. FSCV recordings were made a maximum of once a week. For awake measurements, electrical stimulation was applied (60 Hz, 24 p, 2 ms pulses) at stimulation frequencies (75 – 150  $\mu$ A) that evoked minimal motor effects (i.e. head bucking); the stimulation current was determined on an individual rat basis. Next, multiple stimulations (n = 6) were applied to test for electrically-evoked dopamine and pH changes. Animals with electrically-evoked dopamine release were anesthetized with isoflurane and administered electrical stimulation at surgical parameters (300  $\mu$ A, 24 or 60 pulses) for comparison to original measurements during surgery.

Animals that had received a cocaine-haloperidol injection during surgery were again anesthetized with isoflurane, and the cocktail experiment was repeated. Following 1 hr of FSCV recordings, electrical stimulation was administered to build a within-subject training set. Animals were then allowed to fully recover from isoflurane under O<sub>2</sub> and returned to their cages.

## **Data analysis**

Electrically-evoked dopamine transients measured in freely-moving animals and isoflurane-anesthetized rats were isolated using principal component analysis as described previously (Heien, et al., 2005; Rodeberg, et al., 2015). Briefly, stimulation currents were applied at a range of parameters (varied current intensity and pulse number) to evoke a range of dopamine and pH changes for subsequent construction of a training set to analyze experimental data collected at the same electrode. However, a calibration factor was not used to convert extracted current into concentration, as the post-implantation calibration factor was not inherently known. Therefore, all dopamine measurements are reflected in current, despite signal extraction with principal component analysis (PCA).

For analysis of drug-evoked transients, dopamine transients were similarly isolated with PCR using previously described protocol (Fox et al., 2017). 10 min following drug administration, data was broken into 30 s segments with local background subtraction to

minimize the influence of drift. Deflections in PCA-isolated dopamine currents were considered transients if they exceeded 3 times the noise in the traces. The average isolated current and total number of transients per measurement time (i.e. transient frequency) was compared across drug administrations within each animal.

## **Statistics**

All statistical test were performed in GraphPad Prism, with a user-defined significance level of  $p < 0.05$ . One-way ANOVAs were used to compare electrochemical characteristics of the three different electrode designs (BSG, epoxy-BSG, FS). Two outliers were removed from the 'noise' measurements, following the ROUT test provided by GraphPad Prism (Q = 1%). A two-way ANOVA was used to determine the effects of two independent variables (time, electrode design) on a dependent variable (dopamine peak oxidation potential). For significant ANOVA results, Tukey's post hoc test for multiple comparisons was used when sample sizes were equal, and Bonferroni's post hoc test was use for unequal sample sizes. Paired t-tests was used to compare the amplitude and time course ( $t_{1/2}$ ) of electrically-evoked dopamine transients during and after implantation of chronically-implanted CFMs. Unpaired t-test were used to compare the average magnitude (in nA) of dopamine transients following drug administration during and after implantation.

## **RESULTS**

### ***In vitro* comparison of electrode designs**

The difference in outer diameters for borosilicate-glass (BSG) and fused-silica (FS) capillaries (600  $\mu\text{m}$  and 90  $\mu\text{m}$ , respectively) necessitates different construction methods for the

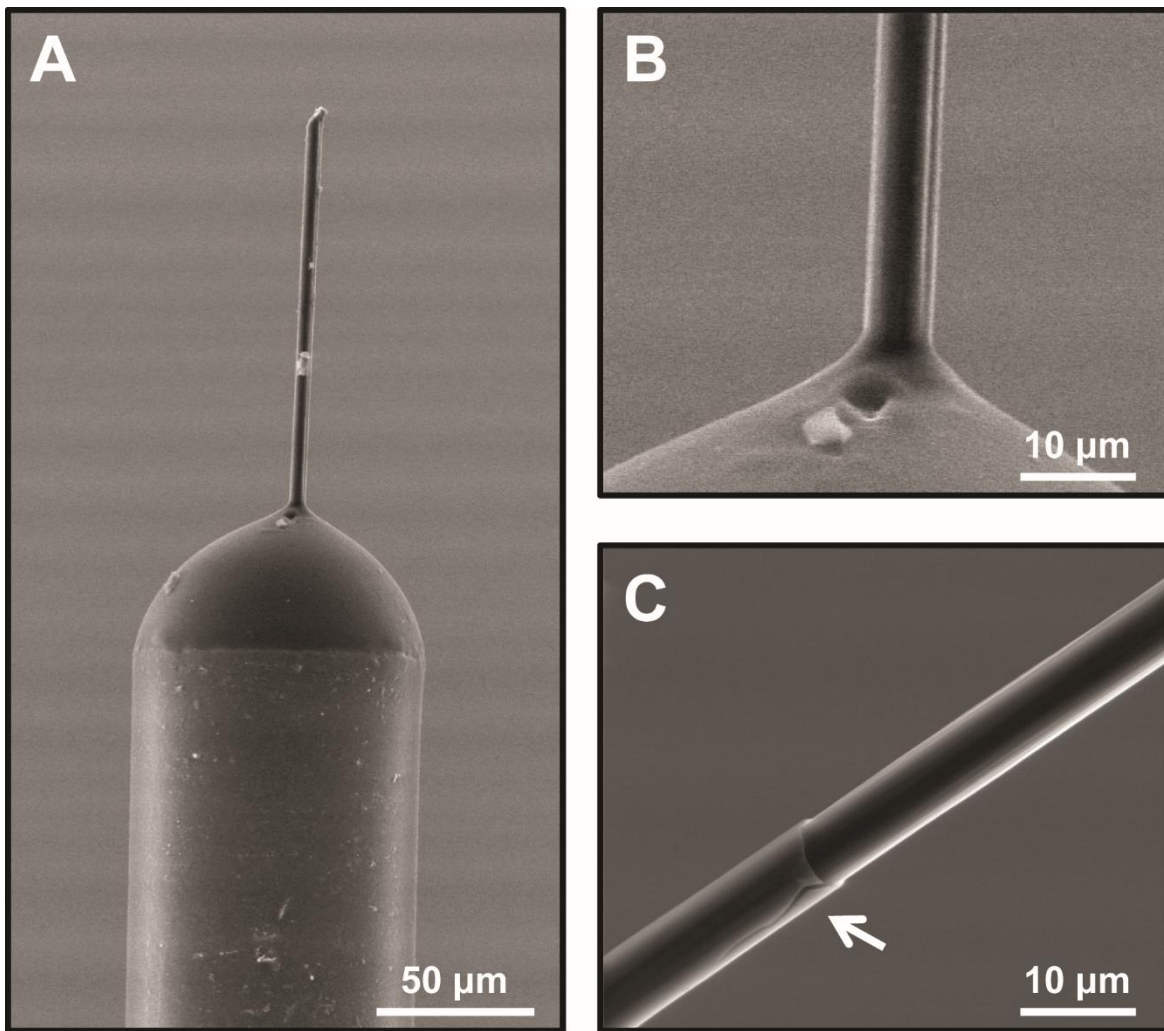


**Figure 6.1.** Environmental scanning electron micrographs of fused-silica (FS) (a-b) and borosilicate glass (BSG) (c) carbon-fiber microelectrodes. a-b) The seal of FS electrodes is created by wicking epoxy beads dropped onto exposed fiber back into the 90  $\mu\text{m}$  diameter FS capillary. This process creates hemispherical seals. C) For construction of BSG electrodes, glass capillaries filled with carbon fiber are pulled under heat in a gravity-assisted puller, which produces a fine glass taper seal around the carbon-fiber. This process can introduce defects (i.e. leaks, cracks) in the seal (white arrow).

two CFM designs. For BSG electrodes, the electrochemical seal is formed with a micropipette puller, which produces a fine glass taper around the unexposed carbon-fiber. As FS capillaries are not compatible with heat-pulling, seals are instead formed by back capillary action with epoxy resin. This process creates hemispherical seals that insulate retracted carbon fiber from the surrounding environment (Figure 6.1a-b). The lack of pronounced 'tapers' brings the full diameter of FS capillaries in closer proximity to the exposed carbon-fiber compared to BSG designs. While the taper of BSG electrodes may result in less tissue damage around the sensing element of the microelectrode, the heat-pulling process can introduce imperfections (i.e. cracks, leaks) into the seal of BSG electrodes (Figure 6.1c). The resulting shunt capacitance can result in undesirable electrochemical properties. A common practice to alleviate this concern is the use of epoxy resin to fill in potential cracks in the BSG seal.

To test whether differences in electrode construction causes differences in electrochemical performance, we made *in vitro* comparisons between BSG (with and without epoxy treatment) and FS electrodes. First, the background currents and noise levels in TRIS buffer were compared (Figure 6.2). Application of the standard waveform used for *in vivo* measurements of dopamine (voltage sweep at 400 V/s from holding potential of -400 mV to a 1300 mV switching potential before return to -400 mV against Ag/AgCl) in TRIS buffer (pH = 7.4) results in a cyclic voltammogram that is composed of non-faradaic processes (i.e. charging of the double layer) and redox of surface functional groups on the carbon fiber (Figure 6.2a). This background current can be characterized by its peak amplitude, which is a function of the surface area of the exposed carbon fiber, and the location of the background peak ( $E_{BG}$ ), which can vary as a function of the impedance of the electrochemical circuit (Meunier et al., 2017) and the integrity of the carbon-fiber seal. To test whether these background currents varied systematically between different CFM designs, electrodes (n = 20 for each design, trimmed to 150-200  $\mu\text{m}$  in length) were first cycled in TRIS buffer (30 min at 60 Hz, 30 min at 10 Hz) to equilibrate the CFM surface in the TRIS environment. Next, the amplitude and peak position

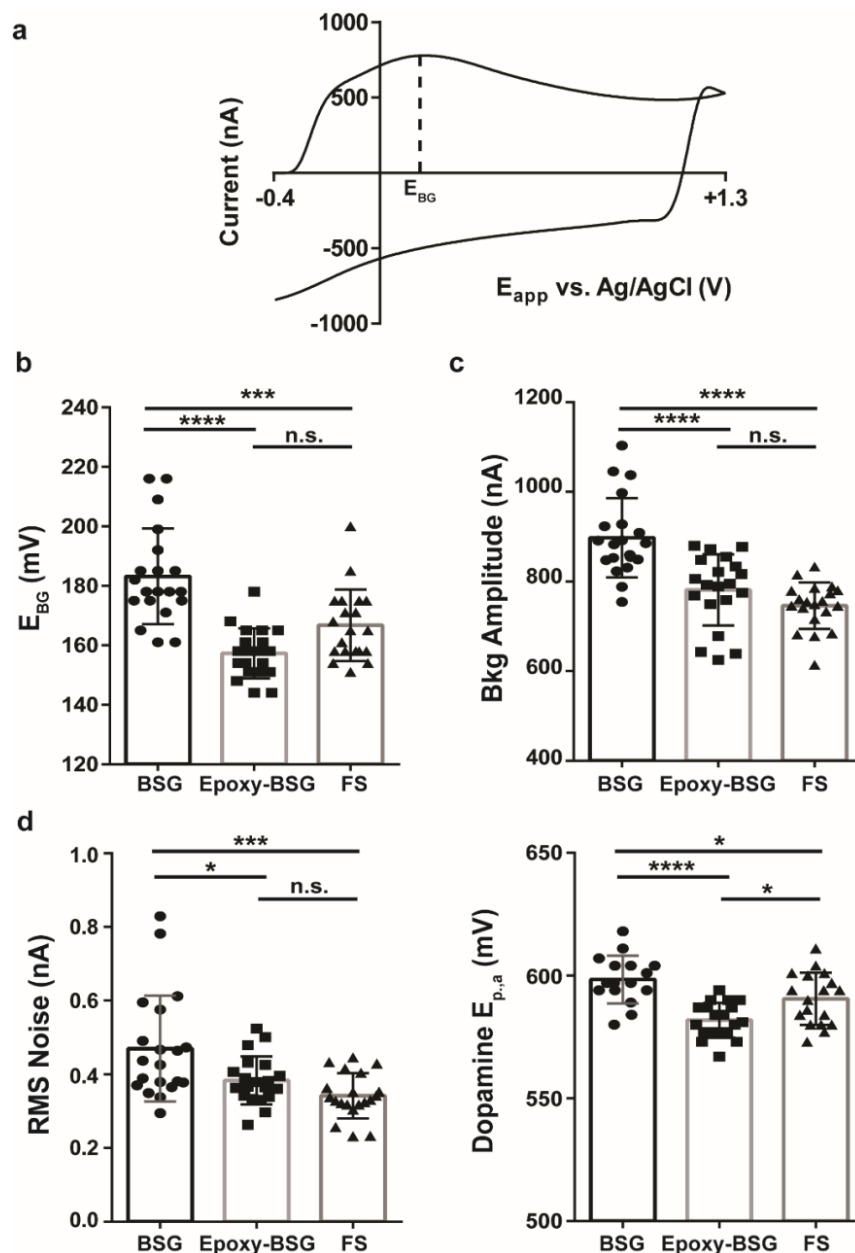


**Figure 6.2.** *In vitro* characterization of FS and BSG electrodes (with and without epoxy). a) A characteristic cyclic voltammogram for the background current of a CFM electrode in TRIS buffer (pH = 7.4). These backgrounds can be characterized by their amplitude (in nA) and the position of the background peak ( $E_{BG}$ ). b-d) The position of the peak potential for the background current ( $E_{BG}$ ) (b), the background amplitude (c), and noise levels (d) were significantly different between BSG and FS electrodes, and between epoxy-BSG and BSG electrodes, but not between FS and epoxy BSG electrodes. This suggests improper insulation of unexposed carbon fiber drives these electrochemical differences. e) When measured against the same reference electrode, all three designs had significantly different peak oxidation potentials for dopamine ( $E_{p,a}$ ) but similar spreads of peak potentials (~40 mV). This suggests that the carbon fiber itself is the major source of variability between CFMs.

of the background CVs were compared between groups (Figure 6.2b-c). Significant differences in peak location were seen between electrode designs ( $F_{2,57} = 21.72$ ,  $p < 0.0001$ ), and Tukey's post hoc test revealed that non-epoxied BSG had significantly more positive  $E_{BG}$  values than epoxied BSG ( $p < 0.0001$ ) and FS ( $p < 0.001$ ), while no differences were seen between epoxy-BSG and FS electrodes ( $p > 0.05$ ). Significant differences in background amplitude were also found between designs (one-way ANOVA,  $F_{2,57} = 22.59$ ,  $p < 0.0001$ ), specifically between BSG and epoxy-BSG ( $p < 0.0001$ ) and FS ( $p < 0.0001$ ) electrodes. This was likely due to unintended exposure of carbon fiber via leaks in BSG seals, as there was no significant difference between fiber lengths of the three electrode groups ( $F_{2,57} = 0.493$ ,  $p = 0.6134$ ).

These leaks may also impact the fidelity of FSCV recordings. To investigate this, the noise levels of each electrode design were assessed by determining RMS noise levels in measured current at the approximate peak potential for dopamine over a 30 s period. The average noise level varied significantly across designs ( $F_{2,57} = 8.885$ ,  $p = 0.0004$ ), and Tukey's multiple comparisons post hoc test revealed significant differences between BSG and epoxy-BSG ( $p < 0.05$ ) and FS ( $p < 0.001$ ), but no difference between epoxy-BSG and FS electrodes. We also found significant differences in variance of noise levels between electrode populations (Brown-Forsythe test,  $F(2,57) = 4.321$ ,  $p = 0.0179$ ). To test whether this was the effect of outliers in the data, the ROUT method (GraphPad Prism) was selected for its ability to detect multiple outliers. ROUT ( $Q = 1\%$ ) revealed two outliers in the BSG group (top two data points in Figure 6.2d, left bar). Upon removal of outliers, significant differences in noise levels remained between BSG and FS electrodes (one-way ANOVA,  $F(2,55) = 0.0016$ ,  $p = 0.0016$ ; Tukey's post-hoc,  $p < 0.001$ ), but no differences were seen between the other pairings ( $p > 0.05$ ). This data suggests that FS electrodes are significantly less noisy than the BSG design, which is likely due to more robust electrochemical seals.

The consistency of dopamine CVs across electrodes is an important experimental consideration, as it could define the success of the use of standard calibration models to

measure FSCV data acquired different electrodes (Johnson, et al., 2016; Rodeberg, et al., 2015; Rodeberg, et al., 2017). To test whether the more desirable electrochemical characteristics of epoxy-BSG and FS electrodes results in more reproducible dopamine CVs, each group of electrode designs was tested with injections of dopamine ([DA] = 2  $\mu$ M) via flow-injection analysis, and the peak oxidative potential of dopamine ( $E_{DA,ox}$ ) was measured. To avoid variability in the potential of the Ag/AgCl reference electrode that could affect dopamine measurements, all electrodes were measured against the same reference electrode on the same recording day. We counterbalanced electrodes of each type over time (in four time bins) to test for the possible effect of reference potential drift on measurements. A two-way ANOVA revealed no interaction between time and electrode design ( $F_{6,41} = 1.439$ ,  $p = 0.2234$ ) or main effect of time ( $F_{3,41} = 0.531$ ,  $p = 0.664$ ). However, a main effect of electrode design ( $F_{2,41} = 15.00$ ,  $p < 0.0001$ ) was found. Bonferroni's post-hoc test for multiple comparisons found significant differences in the mean value of the peak anodic potential for dopamine ( $E_{DA,a}$ ) between each electrode design (Figure 6.2e). All electrode designs, however, showed a similar range of peak potentials (~40 mV) and similar coefficients of variation (BSG: 1.62%, epoxy-BSG: 1.23%, FS: 1.80%), with a Brown-Forsythe test revealing no significant differences in deviations between groups ( $F_{2,50} = 1.644$ ,  $p = 2.036$ ). Due to all electrodes being tested against the same reference electrode, the deviation within populations reflects differences between individual CFMs.

### **Acute *in vivo* comparison of electrode designs**

As differences in electrode construction led to differences in electrochemical performance, we tested next whether these differences could also impact *in vivo* recordings of dopamine release. The geometry of the FS electrodes brings the full capillary diameter in close proximity to the exposed carbon fiber, and this may act as a diffusional barrier to measuring dopamine efflux in the brain. Notably, it has been suggested in literature that chronically

implanted FS electrodes appear to have more temporal distortion than acutely implanted BSG electrodes in measurements of electrically-evoked dopamine release (Clark, et al., 2010). It is possible that differences in geometry between these two electrodes could explain some of this variation.

To investigate this possibility, we used short electrical stimulation of the SN/VTA (300  $\mu$ A, 60 Hz, 24 pulses) to evoke dopamine release in the dorsal striatum (Figure 6.3a), which was measured with BS and FS electrodes ( $n = 6$  for each design). Each transient was temporally defined by its rise time (10-90% max signal) and  $t_{1/2}$  value (100-50% max signal on decaying portion of the transient). No significant differences were seen between BSG and FS designs in either rise time ( $t_{10} = 0.5423$ ,  $p = 0.5995$ ) or  $t_{1/2}$  ( $t_{10} = 0.2774$ ,  $p = 0.7872$ ) (Figure 6.3b). This suggests these two electrodes do not differ in responses to stimulation responses that mimic short, burst firing of dopamine neurons.

The comparative responses of these two electrode designs were also tested across a range of different stimulation frequencies. It has been demonstrated previously that when the number of stimulation pulses is kept constant, maximally evoked dopamine release in the dorsal striatum is a linear function of stimulation frequency between 30 and 60 Hz (Wightman et al., 1988). This is because dopamine efflux depends on the competing processes of release and uptake; slower stimulation frequencies allow more time for reuptake of dopamine between subsequent pulses, and thus result in lower amplitudes of dopamine release. Consistent with previous results, the amplitude of electrically-evoked dopamine release events increased with stimulation frequency when the number of pulses (120) was kept constant (Figure 6.3c). To control for variations in overall release magnitude between animals, the value of release events was normalized against the maximal response (i.e. 60 Hz, 120 pulse stimulation) for each recording location. Consistent with previous results, both FS and BSG electrodes exhibited a strong linear trend between peak release magnitude and stimulation frequency (BSG:  $r^2 = 0.999$ ,  $p = 0.0005$ ; FS:  $r^2 = 0.996$ ,  $p = 0.0022$ ) (Figure 6.3d). There was no significant difference

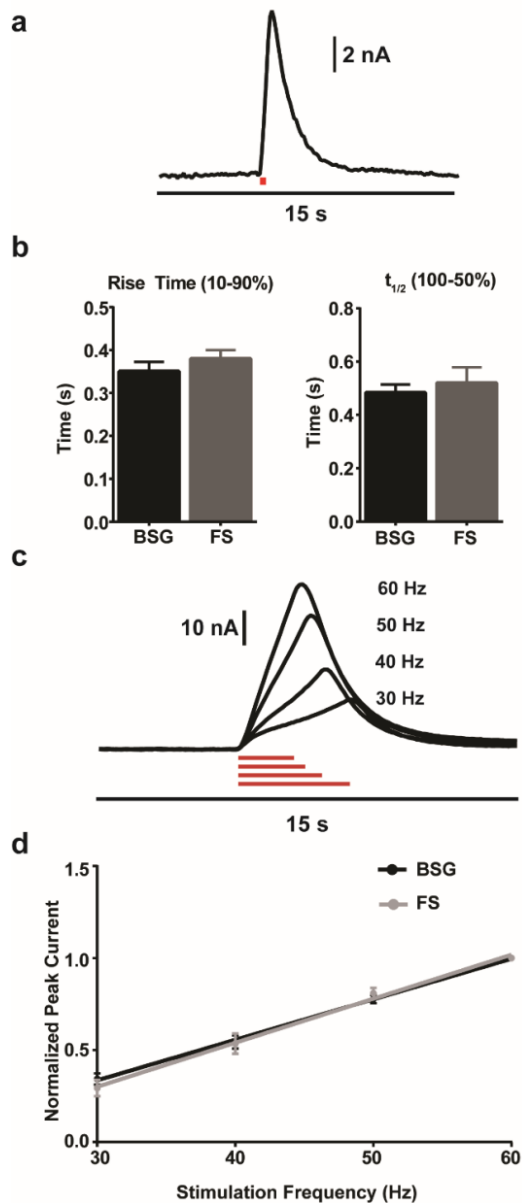


**Figure 6.3.** Acute *in vivo* comparison of BSG and FS electrodes. a) A representative electrically-evoked dopamine transient in the dorsal striatum response to short (24 pulse) electrical stimulation of the SN/VTA. b) No significant differences were seen in the temporal response of BSG and FS electrodes, as assessed by average rise time (10-90%, left) and decay time ( $t_{1/2}$ , 100-50%, right) of electrically-evoked transients at each electrode type. c) Representative dopamine events in response to prolonged stimulation (120 p) at four different frequencies (30, 40, 50, and 60 Hz). The peak dopamine amplitude increases as a function of stimulation frequency. d) No differences were seen in the relationship between stimulation frequency and peak amplitude for BSG and FS electrodes, which suggests that these electrodes respond similarly to dopamine release events with a range of different durations.

between slopes for BSG and FS groups ( $p = 0.1971$ ). Ultimately, BSG and FS electrodes performed very similarly during acute *in vivo* implantation, and showed no systematic differences in their responses to dopamine release over a wide range of different durations. Therefore, any noted differences in temporal distortion between acutely implanted BSG electrodes and chronically implanted FS electrodes are due to the duration of implantation.

### **Effect of prolonged use of carbon-fibers on electrode sensitivity**

While both electrode designs can be used for acute implantations, only FS electrodes are compatible with chronic recordings due to their enhanced flexibility and durability (Clark, et al., 2010; Rodeberg, et al., 2017). The use of CFMs over several recording sessions emphasizes the need for stable sensitivity over time. It has been shown that long-term implantation of CFMs does not in itself systematically alter sensitivity, as assessed by post-calibration following 1, 2, and 4 months of stagnant implantation (Clark, et al., 2010). This is consistent with evidence that the majority of CFM sensitivity loss occurs immediately upon implantation (Ewing et al., 1981; Michael et al., 1987; Singh et al., 2011). However, it is known that repeated cycling of application of voltammetric waveforms with high anodic limits (i.e. +1.3-1.4 V) etches the CFM surface (Takmakov, et al., 2010) and enhances sensitivity towards dopamine due to generation of surface oxide groups (Heien, et al., 2003; Roberts et al., 2010). Therefore, repeated waveform application during extended use could dynamically tune sensitivity over time.

We cycled FS electrodes at a high repetition frequency (60 Hz) to simulate long term use at the standard application frequency (10 Hz) during *in vivo* measurements (i.e. 2 hr cycling at 60 Hz was assumed to mimic 12 hr at 10 Hz, due to an equivalent number of waveform repetitions). After each 12 hr equivalent, we tested the sensitivity of each electrode towards dopamine (Figure 6.4). The sensitivity of FS electrodes towards dopamine increased following

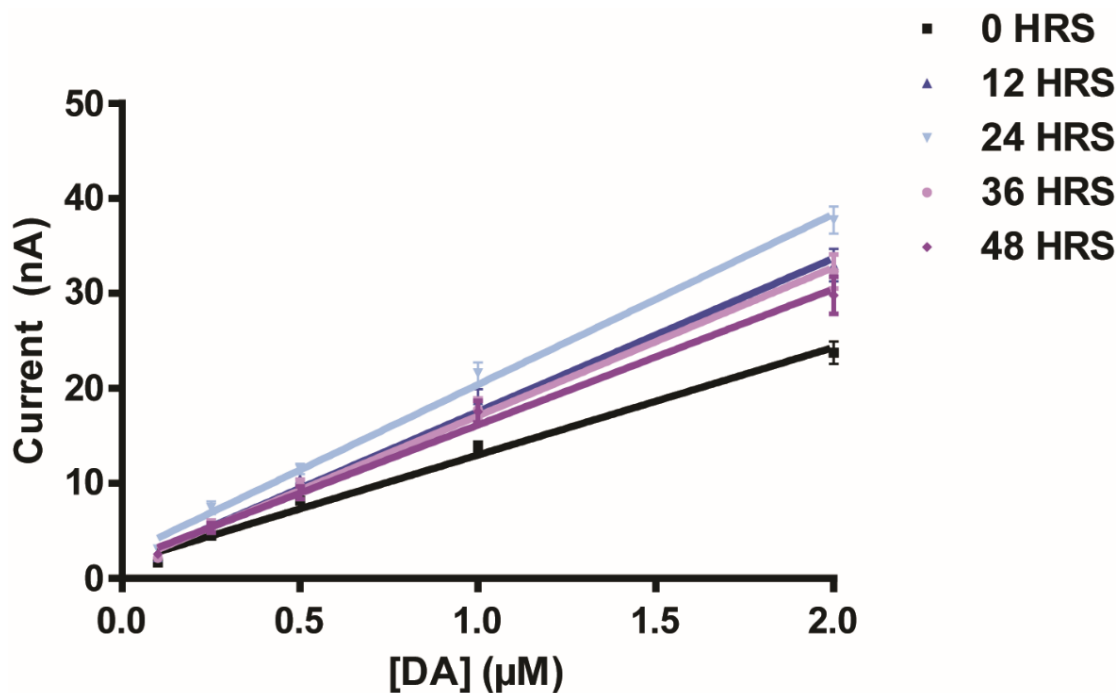


**Figure 6.4.** The effect of prolonged cycling of CFMs on sensitivity towards dopamine. FS electrodes were cycled at a high repetition frequency (60 Hz) to imitate long-term use of CFMs at the standard application frequency *in vivo* (10 Hz). 60 Hz cycling for 2 hr was assumed to mimic 12 hr of use at 10 Hz. Repeated cycling of FS CFMs resulted in a significant increase in sensitivity, followed by progressive decreases in sensitivity, when assessed over five different time points.

n	Cycle Time (hr)	Sensitivity (nA/ $\mu$ M)	RMS noise (nA)	Rise Time (s)
22	0	11.3 $\pm$ 0.4	0.16 $\pm$ 0.10	1.0 $\pm$ 0.3
14	12	16.2 $\pm$ 0.7	0.18 $\pm$ 0.16	0.9 $\pm$ 0.5
12	24	18.0 $\pm$ 0.6	0.18 $\pm$ 0.10	0.8 $\pm$ 0.4
12	36	15.6 $\pm$ 0.7	0.15 $\pm$ 0.05	0.9 $\pm$ 0.4
12	48	14.3 $\pm$ 0.7	0.16 $\pm$ 0.05	0.9 $\pm$ 0.2

**Table 6.1.** The sensitivity, noise levels, and temporal response over repeated cycling of FS CFMs. Repeated use of chronic CFMs resulted in significant increases followed by decreases over time, without any significant changes in noise levels or the rise time (10-90%) during measurements of flow cell. One outlier was removed from RMS noise calculations following Grubb's test.

early use, followed by a decrease in sensitivity at later time points (Table 6.1). A one-way ANOVA revealed significant differences in sensitivity between time points ( $F_{4,67} = 292.4$ ,  $p < 0.0001$ ). Bonferroni's post-hoc test for multiple comparisons revealed significant differences in average calibration factor between every time point ( $p < 0.0001$ ), aside from between 12 and 36 hr ( $p > 0.05$ ). To test whether repeated cycling altered noise levels, the RMS noise was calculated from current fluctuations at the peak oxidation potential for dopamine in the 5 s preceding injection. No significant differences in noise levels between time points ( $F_{4,66} = 0.2644$ ,  $p = 0.8998$ , following one outlier removal from 48 hr time following Grubb's test). Similarly, a one-way ANOVA revealed no significant difference in the temporal response (assessed by the rise time, 10-90%) between time points ( $F_{4,67} = 0.6003$ ,  $p = 0.6637$ ). Altogether, this data suggests that long-term use of CFMs *in vivo* could alter their sensitivity following repetitive conditioning and etching of the CFM surface.

### **Failure of electrical stimulation to track potential sensitivity changes *in vivo***

Methods to track prospective changes in CFM sensitivity *in vivo* are less straightforward than *in vitro* conditions, as introduction of dopamine standards to probe electrode responses over time is difficult *in vivo*. One possible approach is the use of electrical stimulation to evoke dopamine release at the implanted CFM to test its sensitivity over subsequent recording sessions (and cycling). Electrical stimulation would provide distinct benefits, as its magnitude (i.e. current intensity, pulse number, frequency) can be precisely controlled and it can produce robust, time-locked dopamine release events.

This tactic was first attempted for FS electrodes implanted in the dorsolateral striatum. A bipolar stimulating electrode was lowered into the SN/VTA region and optimized for placement by administering electrical stimulation (300  $\mu$ A, 60 p) and measuring dopamine release at the FS electrode. Once the signal was optimized for amplitude, we cemented the FS and stimulating electrodes in place and allowed animals to recover for one week. Administration of electrical

stimulation (60 Hz, 24p) after one week of implantation failed to elicit measurable dopamine release in any tested subjects ( $n = 5$ ). This was not due to failure of the stimulating electrode, as successful FSCV measurements of dopamine release during intracranial self-stimulation (ICSS) over this time interval can be performed (Garris et al., 1999; Rodeberg et al., 2016) and electrical stimulation evoked pH changes at chronically implanted FS electrodes in all five subjects (data not shown). Therefore, this was likely due to impediments at the FS electrode. Indeed, it has been suggested to wait a minimum of four weeks before FSCV measurements at chronically-implanted CFMs to allow the brain immune response to dissipate (Clark, et al., 2010). Therefore, all future recordings were done after a minimum of four weeks of recovery post-surgery.

Following a minimum of four weeks of recovery, the occurrence of stimulated dopamine release was variable amongst subjects. Amongst tested subjects ( $n = 7$ ), only four subjects exhibited stimulated dopamine release, though pH changes following electrical stimulation occurred in all subjects (data not shown). Administration of cocaine (10 mg/kg, i.p.) in the three subjects without electrically-evoked release resulted in observable, spontaneous dopamine transients, which indicates that the absence of stimulated release is at least in part due to failure of the stimulating electrode, rather than inability of the chronic CFM to measure phasic dopamine release. Repeating electrical stimulation under identical conditions (i.e. same stimulation parameters, isoflurane anesthesia) in subjects that exhibited stimulated release revealed the dopamine signal had significantly attenuated in amplitude compared to release evoked during surgery (avg % recovery of signal amplitude:  $17.8 \pm 8.2$  %; paired t test,  $t_3 = 10.00$ ,  $p = 0.0021$ ). Moreover, electrically-evoked dopamine transients were more temporally distorted following implantation (Figure 6.5). Comparison of  $t_{1/2}$  values before and after implantation revealed that electrically-evoked transients were significantly broader post-implantation (surgery:  $0.6 \pm 0.2$  s, post-implant:  $1.8 \pm 0.4$  s;  $t_3 = 3.651$ ,  $p = 0.0355$ ). The temporal distortion of the dopamine signal following implantation cannot be attributed to failure

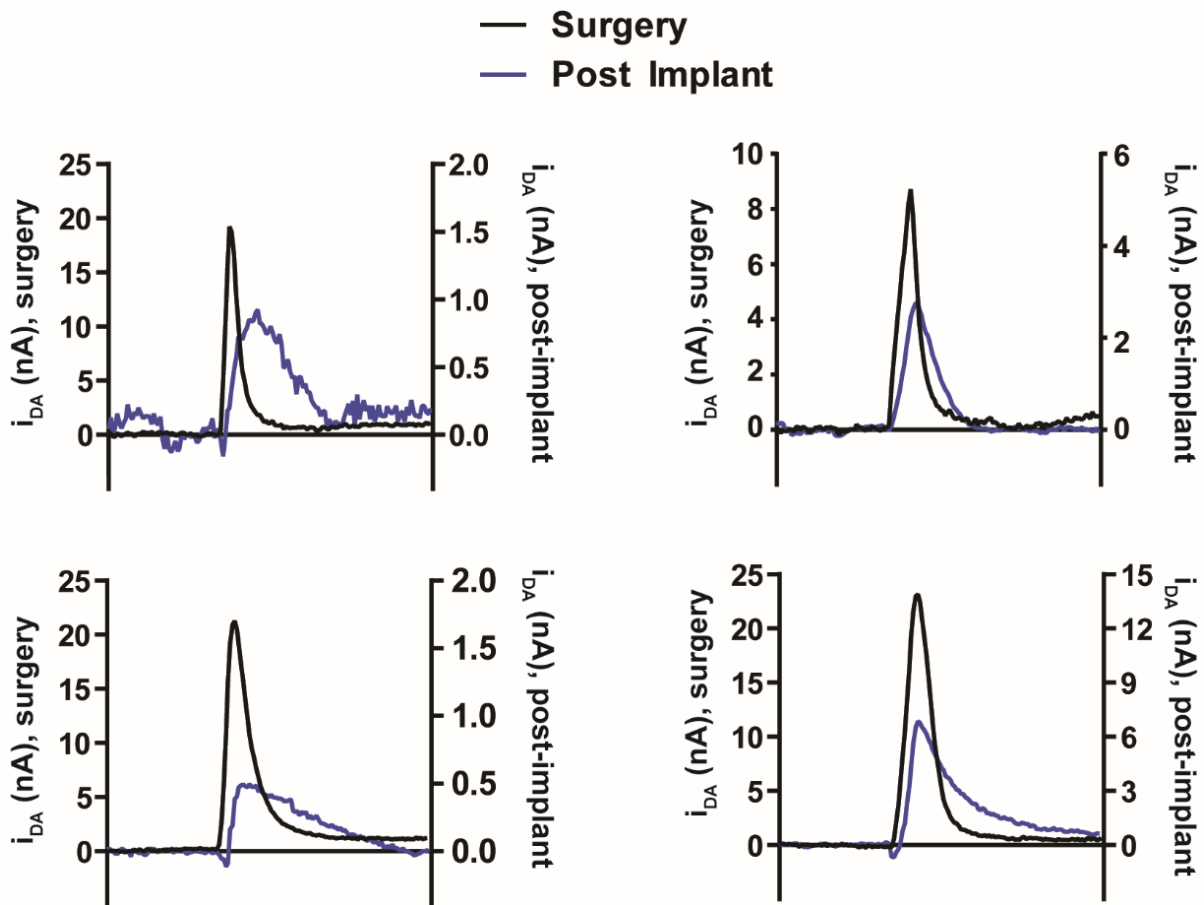


**Figure 6.5.** Temporal distortion in the electrically-evoked dopamine signal at chronically-implanted CFMs. All electrodes with measurable dopamine release under conditions identical to surgical measurements (isoflurane anesthesia, matched stimulation parameters) ( $n = 4$ ) exhibited temporal distortion following implantation. While changes in the electrically-evoked amplitude could be due to changes surrounding either the working or stimulating electrode, temporal distortion can only be attributed to changes at the chronic CFM.

of the stimulating electrode, as action potentials evoked by electrical stimulation stop immediately upon cessation of the stimulus (Kuhr et al., 1987). These results suggest changes in the recording environment around the FS electrode following implantation. However, the diminished amplitude could be due to occlusion of the stimulating electrode, which compared to implanted CFMs (Clark, et al., 2010), is unlikely to avoid the progressive immune response that impedes other brain-implanted devices due to its larger size (Polikov, et al., 2005). Ultimately, these data show the use of stimulating electrodes is insufficient to track changes in CFM sensitivity over time, and is an unreliable tactic to acquire clean dopamine CVs for within-subject calibration (Rodeberg, et al., 2015).

### **Alternate methods for tracking sensitivity of chronically implanted CFMs**

An alternative method for tracking sensitivity of implanted CFMs is through pharmacological manipulations that evoke dopamine release. Ideally, drug-evoked dopamine transients could be compared (i.e. frequency, magnitude) to surgical recordings to test whether long-term dwelling of the CFM in brain tissue alters its sensitivity over time *in situ*, which is difficult to assess with post-*vitro* calibration alone. Previous work has shown that a mixture of dopamine transporter blockade and autoreceptor inhibition can induce dopamine transients in the dorsal striatum of anesthetized rats (Venton & Wightman, 2007). Using a similar protocol, we induced dopamine transients in isoflurane-anesthetized rats during surgery and following implantation with co-injection of cocaine (20 mg/kg, i.p.) and haloperidol (0.5 mg/kg, i.p.). Dopamine transients were isolated and quantitated using PCR following previous protocol (Fox, et al., 2017). Although electrical stimulation was often unsuccessful in evoking dopamine release in the previous experiment, the combined effects of cocaine and haloperidol sufficiently elevated electrically-stimulated dopamine release that training sets could be built at every electrode/subject (n = 4) for each individual recording. The average amplitude and overall

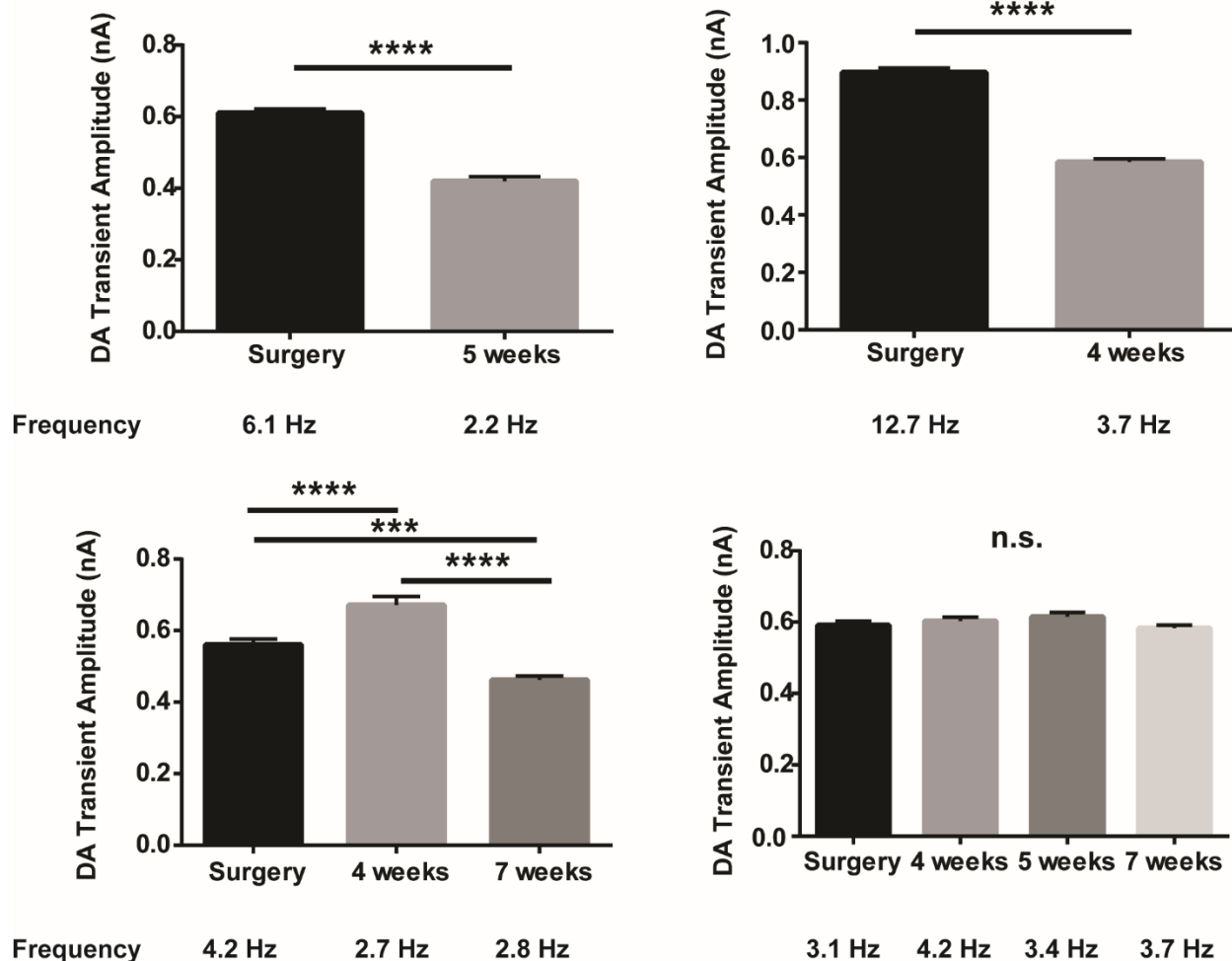


**Figure 6.6.** The amplitude and frequency of dopamine transients evoked by a drug cocktail of cocaine and haloperidol before and after CFM implantation. Two subjects (top) showed decreases in the amplitude and frequency of dopamine transients following 4 weeks of chronic implantation. However, one subject (bottom left) showed a significant increase in transient amplitude in the first post-implantation measurement, followed by a significant decrease in amplitude. Lastly, one subject showed no significant changes in transient amplitude across recording sessions. This indicates that, while chronic CFMs are capable of consistent, stable measurements of striatal dopamine, results can be variable. This emphasizes the need for positive controls during FSCV recordings at chronically implanted CFMs.

frequency of transients following drug cocktail administration were compared between time points.

Changes in dopamine transient magnitude and frequency were variable amongst the four subjects tested (Figure 6.6). Two subjects exhibited a decrease in dopamine transient frequency for the first drug administration following implantation (top panels). A third subject showed an increase in transient amplitude, but not frequency, following drug administration 4 weeks post-surgery, but a significant decrease in magnitude during a second measurement at 7 weeks post-implantation (bottom left panel). However, a fourth subject had stable dopamine transient magnitudes across three separate post-implantation drug administrations (bottom right panel). While this subject demonstrates the possibility of high fidelity dopamine recordings over time at chronically-implanted CFMs, the variability in recovery of the dopamine signal between subjects emphasizes the need for 'positive controls' (i.e. independent measures to elicit stable dopamine release) to assay dopamine sensitivity over long-scale use of chronically implanted CFMs. The decreased frequency of dopamine transients following implantation in three out of four subjects demonstrates a diminished ability to monitor dopamine transients, and suggests that the use of an average post-calibration factor based on removal of the electrode from tissue may not be representative of the post-implantation environment *in situ*.

### **Changes in background current following long-term implantation**

It has been demonstrated that the background current amplitudes of CFMs correlate strongly with their sensitivity towards dopamine, as both measures increase linearly with surface area (Roberts et al., 2013). Therefore, tracking the amplitude of the background current over consecutive recording sessions may serve as an indirect method of tracking CFM sensitivity. Background currents during surgery were compared before and after implantation at different time points, grouping animals from the electrical stimulation and the drug treatment experiments (Table 6.2). Background currents increased by approximately 40% upon first use following four

n	Timepoint	Bkg Current Amplitude (nA)	Normalized Amplitude
11	Surgery	723 ± 21	100
11	4 wks	1010 ± 98	140 ± 16
8	5 wks	1015 ± 103	146 ± 16
7	6 wks	1044 ± 124	145 ± 25
7	7 wks	1012 ± 130	142 ± 21

**Table 6.2.** The background amplitudes at chronically-implanted CFMs before and after long-term implantation. A significant increase in background amplitude was seen upon first use 4 wks following implantation, but no significant changes were seen between subsequent measurements. Data expressed as mean ± SD.

n	Cycle Time (hr)	Bkg Current Amplitude (nA)	Normalized Amplitude
22	0	481 ± 87	100
14	12	703 ± 97	146 ± 20
12	24	719 ± 109	153 ± 16
12	36	688 ± 90	147 ± 17
12	48	676 ± 107	144 ± 17

**Table 6.3.** Changes in background amplitude over repeated cycling of FS CFMs *in vitro*. Background currents significantly increased following the first extensive cycling period. However, no significant changes were seen for subsequent measurements despite significant changes in sensitivity. This suggests that the use of background amplitude alone to track electrode performance *in vivo* may mask underlying changes in sensitivity.

weeks of implantation. Significant differences were seen between time points ( $F_{3,33} = 18.62$ ,  $p < 0.0001$ ), with Bonferroni's post-hoc test revealing significance differences between the background amplitude during surgery and each other time point ( $p < 0.0001$ ), but not between any time points post-implantation ( $p > 0.05$ ). Based off previous work (Roberts, et al., 2013), this would suggest that there should be minimal changes in sensitivity following first use of the CFM post-implantation.

Interestingly, the trend between surgery and the first measurements following implantation mirror the increases in sensitivity seen upon first extensive cycling *in vitro* (Figure 6.4, Table 1), which suggests the increase in background current may be an effect of the extensive cycling (2 hr at 60 Hz) performed before the first measurement with each chronically implanted CFM. To further investigate the relationship between the *in vivo* and *in vitro* findings, we compared the magnitude of background currents for the calibration data represented in Table 6.1 between time points (Table 6.3). The relative changes in background currents *in vitro* closely matched the trends found *in vivo*. Background current varied over time ( $F_{4,67} = 19.47$ ,  $p < 0.0001$ ), and significant differences were found between the first time point and each later measurement (Bonferroni's post-hoc,  $p < 0.0001$ ). However, there were no significant differences in background currents between later time points ( $p > 0.05$ ), despite the significant changes in sensitivity described above (Figure 4, Table 1). This suggests that tracking the amplitude of background currents at individual electrodes *in vivo* may be inadequate for the reliable determination of changes in sensitivity between subsequent recordings.

## DISCUSSION

This work represents the first detailed characterization of fused silica CFMs with respect to borosilicate glass electrodes. We found that FS electrodes behaved more favorably than BSG electrodes *in vitro*, as evidenced by lower stray impedance and noise, though epoxy treatment of BSG electrodes alleviated these differences. Despite these findings, dopamine CVs varied

similarly across electrode designs, which suggests that the carbon fiber itself is a major source of variability between electrodes. *In vivo* comparison of BSG and FS electrodes revealed that these two electrode designs behave identically during acute use, which suggests that any noted differences in literature between these two electrodes are due to different implantation durations. Lastly, we found that repeated cycling of CFMs *in vitro* significantly alters their sensitivity significantly over time. To test whether these effects persisted *in vivo*, we administered drug cocktails to evoke dopamine transients under anesthesia before and after implantation. We found that the changes in dopamine amplitudes and frequencies following implantation varied between subjects. This finding emphasizes the need for positive controls in studies with chronically-implanted CFMs.

We found that the peak oxidation potential for dopamine CVs varies similarly across all electrode designs, even when measuring against the same Ag/AgCl reference electrode. This suggests that the heterogeneity of carbon-fiber surfaces drives much of the previously reported differences in CVs across different CFMs (Johnson, et al., 2016; Rodeberg, et al., 2015). Interestingly, FS electrodes were found to have significantly more positive dopamine peak potentials than epoxy-BSG electrodes, despite having very similar electrochemical characteristics. This may be due to differences in the internal resistance of the two designs. Electrical connection with BSG electrodes is generated via insertion of a silver wire coated in conductive silver paint into the BSG capillary, where it makes contact with the unexposed carbon fiber. In contrast, electrical connection to the connector pin at FS electrodes is made only at the very end of the FS capillary via silver epoxy. Thus, the carbon fiber carries the current for the length of the fused silica capillary, which would increase the internal resistance of the electrode. Regardless of the mechanism, the ~40 mV range of peak potentials at each design under ideal conditions (i.e. low impedance *in vitro* environment, same reference electrode) suggests that the variability in experimental CVs is inherent to the use of CFMs. This suggests that the previous concerns with 'standard' calibration models (Johnson, et al., 2016;

Rodeberg, et al., 2015) may be difficult to avoid even with more robust CFM construction methods. However, the method for collecting dopamine and pH standards at acutely implanted BSG electrodes for within-subject PCR models (i.e. electrical stimulation of afferent dopamine neurons) is not appropriate for experiments with chronically-implanted CFMs, as stimulating electrodes appeared to fail over long-term implantation. Moreover, the other method used in this study to evoke dopamine transients at chronic CFMs (i.e. injection of a cocaine-haloperidol cocktail) is infeasible for routine studies, as these injections would likely alter behavior. Therefore, the best approach to improve generalized calibration at chronic CFMs may be adaptation of multivariate calibration to control for differences in CVs across electrodes (or differences in CVs over time at the same electrode).

We found that repeated cycling of CFMs *in vitro* significantly changes their sensitivity over time. This finding was not unanticipated, as previous studies have shown that repeated application of waveforms with extended anodic limits etches the surface and generates surface oxides, which facilitate sensitivity towards dopamine (Heien, et al., 2003; Roberts, et al., 2010; Takmakov, et al., 2010). This would explain the two trends in sensitivity seen during repeated use; the early increases in sensitivity would likely be due to generation of surface oxide groups on the CFM surface, while the diminished sensitivity at later time points would be due to active etching (and reduction) of the carbon-fiber surface. However, it is difficult to determine whether these same effects persist in an *in vivo* environment. While previous studies have shown that background current amplitudes can predict differential sensitivity towards dopamine across different electrodes and anodic limits (Roberts, et al., 2013), our findings here suggest that significant changes in sensitivity over time at the same CFM are unpaired from significant alterations in background current amplitude. Therefore, while background currents *in vivo* appear stable following first use post-implantation, this metric alone may be insufficient to guarantee stable sensitivity over time.

Due to failure of the stimulating electrode, we used a drug cocktail to evoke dopamine transients at FS CFMs before and after implantation to track their sensitivity. We found that changes in average dopamine transient amplitude differed across electrodes. Notably, there was a minimum interval of one week between injections in this study. It is possible that a more rapid dosing paradigm, which would mirror more consistent use of chronic CFMs, would result in plasticity and/or sensitization of dopamine release that would confound results (Singer et al., 2017). Therefore, systematic tests of the relationship between chronic CFM use and sensitivity may be infeasible with this method. One possible alternative is selective optogenetic stimulation of dopamine neurons, which evokes dopamine release in the dorsal and ventral striatum (Bass et al., 2010; Tsai et al., 2009). If optical fibers avoid the problems that plague bipolar stimulating electrodes during chronic implantation, optogenetic stimulation could be used to test the sensitivity of chronic CFMs using precisely controlled stimulation parameters. With this method, it could be tested whether (possible) changes in sensitivity of chronically-implanted CFMs are a function of the frequency and duration of their use. As it stands, the best current practice for positive controls at chronic CFMs is the use of unexpected food reward to elicit dopamine release. A previous study showed that dopamine release to this stimulus remained relatively consistent over fifteen sessions of measurements, despite dynamic changes in dopamine release to other conditioned and unconditioned stimuli (Clark et al., 2013). Alternatively, experimental design that ensures both increases *and* decreases in dopamine could ensure that chronically-implanted CFMs aren't being systematically altered over repeated use.

## REFERENCES

- Bass, C. E., Grinevich, V. P., Vance, Z. B., Sullivan, R. P., Bonin, K. D., & Budygin, E. A. (2010). Optogenetic control of striatal dopamine release in rats. *J Neurochem*, *114*(5), 1344-1352.
- Clark, J. J., Collins, A. L., Sanford, C. A., & Phillips, P. E. (2013). Dopamine encoding of Pavlovian incentive stimuli diminishes with extended training. *J Neurosci*, *33*(8), 3526-3532.
- Clark, J. J., et al. (2010). Chronic microsensors for longitudinal, subsecond dopamine detection in behaving animals. *Nat Methods*, *7*(2), 126-129.
- Covey, D. P., Roitman, M. F., & Garris, P. A. (2014). Illicit dopamine transients: reconciling actions of abused drugs. *Trends Neurosci*, *37*(4), 200-210.
- Day, J. J., Roitman, M. F., Wightman, R. M., & Carelli, R. M. (2007). Associative learning mediates dynamic shifts in dopamine signaling in the nucleus accumbens. *Nat Neurosci*, *10*(8), 1020-1028.
- Ewing, A. G., Dayton, M. A., & Wightman, R. M. (1981). Pulse voltammetry with microvoltammetric electrodes. *Anal Chem*, *53*(12), 1842-1847.
- Ferguson, S. M., et al. (2011). Transient neuronal inhibition reveals opposing roles of indirect and direct pathways in sensitization. *Nat Neurosci*, *14*(1), 22-24.
- Flagel, S. B., et al. (2011). A selective role for dopamine in stimulus-reward learning. *Nature*, *469*(7328), 53-57.
- Fox, M. E., Rodeberg, N. T., & Wightman, R. M. (2017). Reciprocal Catecholamine Changes during Opiate Exposure and Withdrawal. *Neuropsychopharmacology*, *42*(3), 671-681.
- Garris, P. A., Kilpatrick, M., Bunin, M. A., Michael, D., Walker, Q. D., & Wightman, R. M. (1999). Dissociation of dopamine release in the nucleus accumbens from intracranial self-stimulation. *Nature*, *398*(6722), 67-69.
- Hashemi, P., et al. (2011). Chronically Implanted, Nafion-Coated Ag/AgCl Reference Electrodes for Neurochemical Applications. *ACS Chem Neurosci*, *2*(11), 658-666.
- Heien, M. L., Johnson, M. A., & Wightman, R. M. (2004). Resolving neurotransmitters detected by fast-scan cyclic voltammetry. *Anal Chem*, *76*(19), 5697-5704.
- Heien, M. L., et al. (2005). Real-time measurement of dopamine fluctuations after cocaine in the brain of behaving rats. *Proc Natl Acad Sci U S A*, *102*(29), 10023-10028.
- Heien, M. L., Phillips, P. E., Stuber, G. D., Seipel, A. T., & Wightman, R. M. (2003). Overoxidation of carbon-fiber microelectrodes enhances dopamine adsorption and increases sensitivity. *Analyst*, *128*(12), 1413-1419.

- Howe, M. W., Tierney, P. L., Sandberg, S. G., Phillips, P. E., & Graybiel, A. M. (2013). Prolonged dopamine signalling in striatum signals proximity and value of distant rewards. *Nature*, *500*(7464), 575-579.
- Ikemoto, S., & Panksepp, J. (1999). The role of nucleus accumbens dopamine in motivated behavior: a unifying interpretation with special reference to reward-seeking. *Brain Res Rev*, *31*(1), 6-41.
- Johnson, J. A., Rodeberg, N. T., & Wightman, R. M. (2016). Failure of Standard Training Sets in the Analysis of Fast-Scan Cyclic Voltammetry Data. *ACS Chem Neurosci*, *7*(3), 349-359.
- Kuhr, W. G., Wightman, R. M., & Rebec, G. V. (1987). Dopaminergic neurons: simultaneous measurements of dopamine release and single-unit activity during stimulation of the medial forebrain bundle. *Brain Res*, *418*(1), 122-128.
- Lohr, K. M., et al. (2014). Increased vesicular monoamine transporter enhances dopamine release and opposes Parkinson disease-related neurodegeneration in vivo. *Proc Natl Acad Sci U S A*, *111*(27), 9977-9982.
- Lotharius, J., & Brundin, P. (2002). Pathogenesis of Parkinson's disease: dopamine, vesicles and alpha-synuclein. *Nat Rev Neurosci*, *3*(12), 932-942.
- Meunier, C. J., Roberts, J. G., McCarty, G. S., & Sombers, L. A. (2017). Background Signal as an in Situ Predictor of Dopamine Oxidation Potential: Improving Interpretation of Fast-Scan Cyclic Voltammetry Data. *ACS Chem Neurosci*, *8*(2), 411-419.
- Michael, A. C., Ikeda, M., & Justice, J. B., Jr. (1987). Mechanisms contributing to the recovery of striatal releasable dopamine following MFB stimulation. *Brain Res*, *421*(1-2), 325-335.
- Owesson-White, C., et al. (2016). Cue-Evoked Dopamine Release Rapidly Modulates D2 Neurons in the Nucleus Accumbens During Motivated Behavior. *J Neurosci*, *36*(22), 6011-6021.
- Owesson-White, C. A., Cheer, J. F., Beyene, M., Carelli, R. M., & Wightman, R. M. (2008). Dynamic changes in accumbens dopamine correlate with learning during intracranial self-stimulation. *Proc Natl Acad Sci U S A*, *105*(33), 11957-11962.
- Peters, J. L., Miner, L. H., Michael, A. C., & Sesack, S. R. (2004). Ultrastructure at carbon fiber microelectrode implantation sites after acute voltammetric measurements in the striatum of anesthetized rats. *J Neurosci Methods*, *137*(1), 9-23.
- Phillips, P. E., Robinson, D. L., Stuber, G. D., Carelli, R. M., & Wightman, R. M. (2003a). Real-time measurements of phasic changes in extracellular dopamine concentration in freely moving rats by fast-scan cyclic voltammetry. *Methods Mol Med*, *79*, 443-464.
- Phillips, P. E., Stuber, G. D., Heien, M. L., Wightman, R. M., & Carelli, R. M. (2003b). Subsecond dopamine release promotes cocaine seeking. *Nature*, *422*(6932), 614-618.
- Polikov, V. S., Tresco, P. A., & Reichert, W. M. (2005). Response of brain tissue to chronically implanted neural electrodes. *J Neurosci Methods*, *148*(1), 1-18.

- Rebec, G. V., Christensen, J. R., Guerra, C., & Bardo, M. T. (1997). Regional and temporal differences in real-time dopamine efflux in the nucleus accumbens during free-choice novelty. *Brain Res*, 776(1-2), 61-67.
- Roberts, J. G., Moody, B. P., McCarty, G. S., & Sombers, L. A. (2010). Specific oxygen-containing functional groups on the carbon surface underlie an enhanced sensitivity to dopamine at electrochemically pretreated carbon fiber microelectrodes. *Langmuir*, 26(11), 9116-9122.
- Roberts, J. G., Toups, J. V., Eyualem, E., McCarty, G. S., & Sombers, L. A. (2013). In situ electrode calibration strategy for voltammetric measurements in vivo. *Anal Chem*, 85(23), 11568-11575.
- Rodeberg, N. T., Johnson, J. A., Bucher, E. S., & Wightman, R. M. (2016). Dopamine Dynamics during Continuous Intracranial Self-Stimulation: Effect of Waveform on Fast-Scan Cyclic Voltammetry Data. *ACS Chem Neurosci*, 7(11), 1508-1518.
- Rodeberg, N. T., Johnson, J. A., Cameron, C. M., Saddoris, M. P., Carelli, R. M., & Wightman, R. M. (2015). Construction of Training Sets for Valid Calibration of in Vivo Cyclic Voltammetric Data by Principal Component Analysis. *Anal Chem*, 87(22), 11484-11491.
- Rodeberg, N. T., Sandberg, S. G., Johnson, J. A., Phillips, P. E., & Wightman, R. M. (2017). Hitchhiker's Guide to Voltammetry: Acute and Chronic Electrodes for in Vivo Fast-Scan Cyclic Voltammetry. *ACS Chem Neurosci*, 8(2), 221-234.
- Roitman, M. F., Stuber, G. D., Phillips, P. E., Wightman, R. M., & Carelli, R. M. (2004). Dopamine operates as a subsecond modulator of food seeking. *J Neurosci*, 24(6), 1265-1271.
- Schultz, W., Dayan, P., & Montague, P. R. (1997). A neural substrate of prediction and reward. *Science (New York, N Y)*, 275(5306), 1593-1599.
- Singer, B. F., Bryan, M. A., Popov, P., Robinson, T. E., & Aragona, B. J. (2017). Rapid induction of dopamine sensitization in the nucleus accumbens shell induced by a single injection of cocaine. *Behav Brain Res*, 324, 66-70.
- Singh, Y. S., Sawarynski, L. E., Dabiri, P. D., Choi, W. R., & Andrews, A. M. (2011). Head-to-head comparisons of carbon fiber microelectrode coatings for sensitive and selective neurotransmitter detection by voltammetry. *Anal Chem*, 83(17), 6658-6666.
- Stone, J. M., Morrison, P. D., & Pilowsky, L. S. (2007). Glutamate and dopamine dysregulation in schizophrenia--a synthesis and selective review. *J Psychopharmacol*, 21(4), 440-452.
- Sulzer, D. (2011). How addictive drugs disrupt presynaptic dopamine neurotransmission. *Neuron*, 69(4), 628-649.
- Takmakov, P., et al. (2010). Carbon microelectrodes with a renewable surface. *Anal Chem*, 82(5), 2020-2028.
- Tsai, H. C., et al. (2009). Phasic firing in dopaminergic neurons is sufficient for behavioral conditioning. *Science*, 324(5930), 1080-1084.

- Urs, N. M., Peterson, S. M., & Caron, M. G. (2017). New Concepts in Dopamine D2 Receptor Biased Signaling and Implications for Schizophrenia Therapy. *Biol Psychiatry*, *81*(1), 78-85.
- Venton, B. J., Michael, D. J., & Wightman, R. M. (2003). Correlation of local changes in extracellular oxygen and pH that accompany dopaminergic terminal activity in the rat caudate-putamen. *J Neurochem*, *84*(2), 373-381.
- Venton, B. J., & Wightman, R. M. (2007). Pharmacologically induced, subsecond dopamine transients in the caudate-putamen of the anesthetized rat. *Synapse*, *61*(1), 37-39.
- Wightman, R. M., et al. (1988). Real-time characterization of dopamine overflow and uptake in the rat striatum. *Neuroscience*, *25*(2), 513-523.
- Willuhn, I., Burgeno, L. M., Groblewski, P. A., & Phillips, P. E. (2014). Excessive cocaine use results from decreased phasic dopamine signaling in the striatum. *Nat Neurosci*, *17*(5), 704-709.